

TALLINN UNIVERSITY OF TECHNOLOGY  
DOCTORAL THESIS  
54/2018

**Toxicological Profiling of Silver and Copper  
Oxide Nanoparticles on *Saccharomyces  
cerevisiae* BY4741 Wild-Type and its  
Single-Gene Deletion Mutants**

SANDRA KÄOSAAR



TALLINN UNIVERSITY OF TECHNOLOGY  
School of Engineering  
Department of Materials and Environmental Technology

NATIONAL INSTITUTE OF CHEMICAL PHYSICS AND BIOPHYSICS  
Laboratory of Environmental Toxicology

This dissertation was accepted for the defence of the degree of Doctor of Philosophy in Chemical and Materials Technology on June 28th, 2018.

**Supervisors:** Dr. Kaja Kasemets, Laboratory of Environmental Toxicology, National Institute of Chemical Physics and Biophysics, Tallinn, Estonia

Dr. Anne Kahru, Laboratory of Environmental Toxicology, National Institute of Chemical Physics and Biophysics, Tallinn, Estonia

**Co-supervisor:** Prof. Andres Õpik, Department of Materials and Environmental Technology, Tallinn University of Technology, Tallinn, Estonia

**Opponents:** Dr. Olga Muter, Laboratory of Environmental Microbiology, Institute of Microbiology and Biotechnology, University of Latvia, Riga, Latvia

Prof. Maia Kivisaar, Institute of Molecular and Cell Biology, Faculty of Science and Technology, University of Tartu, Tartu, Estonia

**Defence of the thesis:** September 14th, 2018

**Declaration:**

Hereby I declare that this doctoral thesis, my original investigation and achievement, submitted for the doctoral degree at Tallinn University of Technology has not been submitted for doctoral or equivalent academic degree.

Sandra Käosaar



European Union  
European Regional  
Development Fund



Investing  
in your future

Copyright: Sandra Käosaar, 2018

ISSN 2585-6898 (publication)

ISBN 978-9949-83-304-7 (publication)

ISSN 2585-6901 (PDF)

ISBN 978-9949-83-305-4 (PDF)

TALLINNA TEHNIKAÜLIKOOL  
DOKTORITÖÖ  
54/2018

**Hõbeda ja vaskoksiidi nanoosakeste  
toksilisuse iseloomustamine pärmi  
*Saccharomyces cerevisiae* BY4741  
metsiktüvele ning geenikatkestus-  
mutantidele**

SANDRA KÄOSAAR



# CONTENTS

LIST OF PUBLICATIONS .....	7
AUTHOR'S CONTRIBUTION TO THE PUBLICATIONS .....	8
OTHER PUBLICATIONS IN PEER-REVIEWED JOURNALS .....	10
INTRODUCTION .....	11
ABBREVIATIONS .....	12
1. REVIEW OF THE LITERATURE .....	13
1.1 The emergence of engineered nanoparticles.....	13
1.1.1 Commercial applications of engineered nanoparticles.....	13
1.1.2 Antibacterial and antifungal applications of metal-based nanoparticles.....	13
1.1.3 Human and environmental exposure to engineered nanoparticles .....	14
1.2 The toxicological and ecotoxicological testing of engineered nanoparticles .....	15
1.2.1 Characterization of the physicochemical properties of nanoparticles.....	16
1.2.2 Influence of test medium on the properties of Ag and CuO nanoparticles ..	17
1.3 The adverse effects and cytotoxicity of engineered nanoparticles .....	18
1.3.1 Toxicity mechanisms of metal-based nanoparticles .....	19
1.4 <i>Saccharomyces cerevisiae</i> as a unicellular eukaryotic model organism in toxicology ...	23
1.4.1 The response of <i>Saccharomyces cerevisiae</i> cells to oxidative stress .....	25
1.4.2 The response of <i>Saccharomyces cerevisiae</i> cells to Ag and Cu ions.....	25
1.4.3 Endocytosis in <i>Saccharomyces cerevisiae</i> cells .....	26
1.4.4 The toxicity of metal-based nanoparticles to yeast cells .....	26
AIMS OF THE STUDY.....	29
2. MATERIALS AND METHODS .....	30
2.1 The nanoparticles used in this study .....	30
2.1.1 Preparation of nanoparticle suspensions.....	30
2.1.2 The characterization of nanoparticles.....	31
2.2 The <i>Saccharomyces cerevisiae</i> BY4741 strains .....	31
2.3 Toxicity tests .....	33
2.3.1 <i>Saccharomyces cerevisiae</i> growth inhibition assay .....	33
2.3.2 <i>Saccharomyces cerevisiae</i> cell viability test .....	34
2.3.3 The 'Spot test' .....	34
3. RESULTS AND DISCUSSION.....	35

3.1 Characterization of Ag and CuO NPs (Publications I and IV).....	35
3.2 Toxicity of CuO NPs to <i>Saccharomyces cerevisiae</i> BY4741 (Publication IV).....	36
3.2.1 Toxicity of CuO nano- and micro-sized (bulk) particles to <i>Saccharomyces cerevisiae</i> BY4741 wild-type cells.....	37
3.2.2 Toxicity of CuO NPs to <i>Saccharomyces cerevisiae</i> BY4741 mutant strains: revealing the mechanisms of toxic action.....	38
3.2.3 Analysis of dissolved copper in the toxicity tests.....	38
3.3 Toxicity of Ag NPs to <i>Saccharomyces cerevisiae</i> BY4741 (Publication I) .....	39
3.3.1 Toxicity of coated and uncoated Ag NPs to <i>Saccharomyces cerevisiae</i> wild type cells.....	40
3.3.2 Toxicity of coated and uncoated Ag NPs to <i>Saccharomyces cerevisiae</i> BY4741 single-gene deletion mutants.....	40
3.3.3 Assessment of intracellular ROS.....	42
3.3.4 Assessment of the uptake of endocytosis marker Lucifer Yellow and AgNPs into yeast cells using confocal laser scanning microscopy.....	43
3.4 Size-dependent toxicity of Ag NPs to <i>Saccharomyces cerevisiae</i> BY4741 (Publication III).....	46
3.5 A novel method for the comparison of biocidal effects of metal-based nanoparticles to unicellular organisms bacteria, yeast and algae (Publication II) .....	46
3.5.1 Viability of cells in deionized water during toxicity test.....	47
3.5.2 Biocidal potency of nanomaterials in deionized water and comparison with standard biocidal chemicals.....	49
CONCLUSIONS.....	51
ACKNOWLEDGEMENTS.....	52
ABSTRACT.....	53
KOKKUVÕTE .....	54
Literature references .....	56
APPENDIX.....	67
PUBLICATION I.....	67
PUBLICATION II.....	95
PUBLICATION III.....	117
PUBLICATION IV .....	133
CURRICULUM VITAE.....	153
ELULOOKIRJELDUS .....	155

## LIST OF PUBLICATIONS

This thesis is based on the following publications referred to by their Roman numerals in the text.

- I. **Käosaar, S.**, Kahru, A., Mantecca, P., Kasemets, K. (2016). Profiling of the toxicity mechanisms of coated and uncoated silver nanoparticles to yeast *Saccharomyces cerevisiae* BY4741 using a set of its 9 single-gene deletion mutants defective in oxidative stress response, cell wall or membrane integrity and endocytosis. *Toxicology in Vitro*, 35, 149–162.
- II. **Suppi, S.**, Kasemets, K., Ivask, A., Künnis-Beres, K., Sihtmäe, M., Kurvet, I., Aruoja, V., Kahru, A. (2015). A novel method for comparison of biocidal properties of nanomaterials to bacteria, yeasts and algae. *Journal of Hazardous Materials*, 286, 75–84.
- III. Ivask, A., Kurvet, I., Kasemets, K., Blinova, I., Aruoja, V., **Suppi, S.**, Vija, H., Käkinen, A., Titma, T., Heinlaan, M., Visnapuu, M., Koller, D., Kisand, V., Kahru, A. (2014). Size-dependent toxicity of silver nanoparticles to bacteria, yeast, algae, crustaceans and mammalian cells in vitro. *PLoS One*, 9, e102108.
- IV. Kasemets, K., **Suppi, S.**, Künnis-Beres, K., Kahru, A. (2013). Toxicity of CuO nanoparticles to yeast *Saccharomyces cerevisiae* BY4741 wild-type and its nine isogenic single-gene deletion mutants. *Chemical Research in Toxicology*, 26, 356–367.

## AUTHOR`S CONTRIBUTION TO THE PUBLICATIONS

- I. The author participated in the design of the experimental work and selection of the test chemicals and silver nanoparticles (Ag NPs), performed the toxicity testing with *Saccharomyces cerevisiae* BY4741 wild-type and its single-gene deletion mutants, quantified dissolution of Ag NPs, detected the intracellular ROS, and cellular uptake of endocytosis marker Lucifer Yellow by confocal laser scanning microscopy, and assessed the role of endocytosis in the cellular uptake of the nanoparticles. She was the major interpreter of the data and was responsible for the preparation of the manuscript.
- II. The author contributed to the design of the study, performed the preparation and characterization of nanomaterials' aqueous dispersions and the toxicity assays with *Saccharomyces cerevisiae* BY4741 wild-type cells. She was the major interpreter of the data and was responsible for the preparation of the manuscript.
- III. The author was responsible for the toxicity testing of the differently sized citrate-coated Ag NPs and AgNO<sub>3</sub> with the yeast *Saccharomyces cerevisiae* BY4741 wild-type cells. She interpreted the data and participated in the preparation of the manuscript.
- IV. The author participated in performing the toxicity assays with the CuO nano- and microsized particles, CuSO<sub>4</sub> and the yeast *Saccharomyces cerevisiae* BY4741 wild-type and single-gene deletion mutants. She participated in data analysis and the preparation of the manuscript.

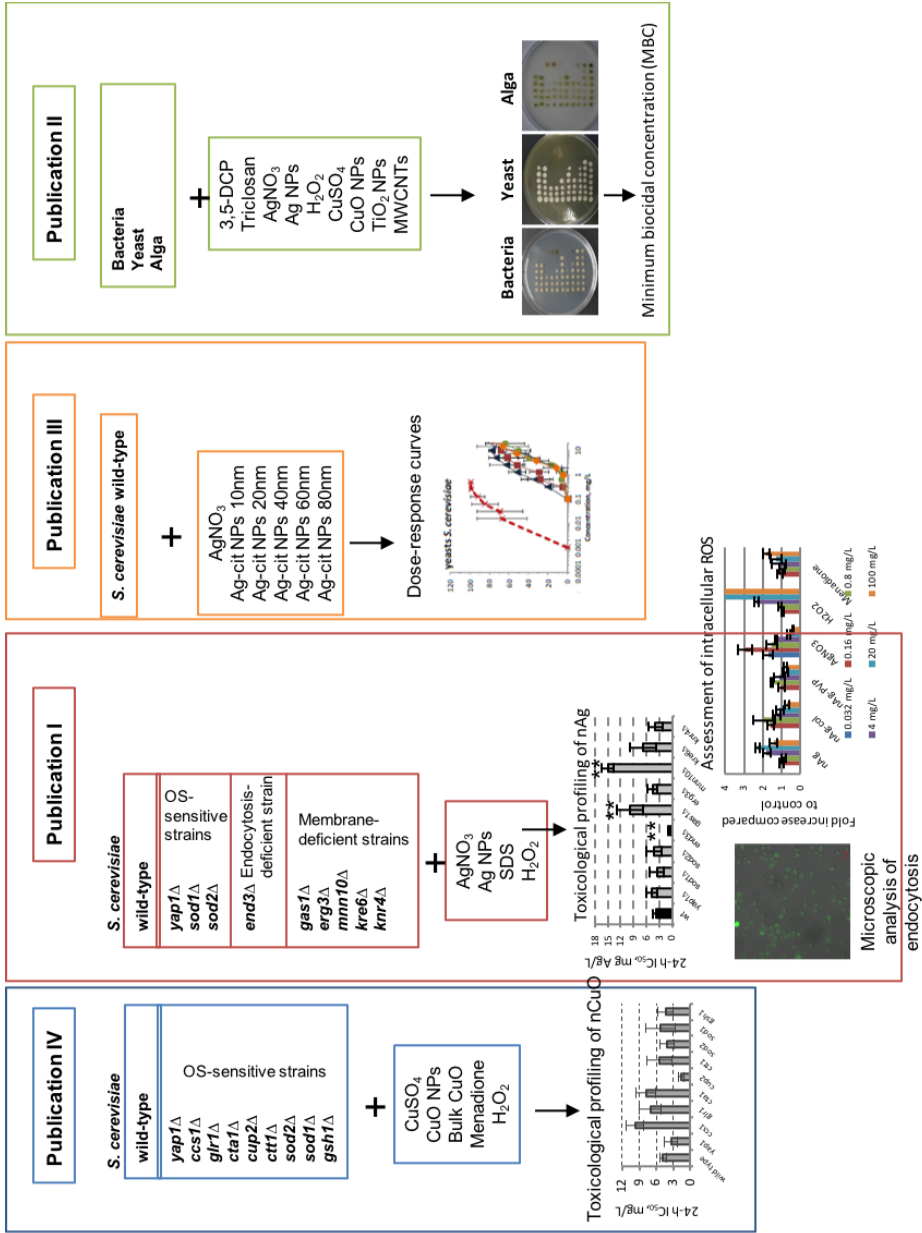


Figure 1. Graphical representation of the publications presented in this thesis and author's contribution.

## OTHER PUBLICATIONS IN PEER-REVIEWED JOURNALS

Uudeküll, P., Kozlova, J., Mändar, H., Link, J., Sihtmäe, M., **Käosaar, S.**, Blinova, I., Kasemets, K., Kahru, A., Stern, R., Tätte, T., Kukli, K., Tamm, A. (2017). Atomic layer deposition of titanium oxide films on As-synthesized magnetic Ni particles: Magnetic and safety properties. *Journal of Magnetism and Magnetic Materials* 429, 299–304.10.1016/j.jmmm.2017.01.045

**Suppi, S.**, Michelson, T., Viigand, K., Alamäe, T. (2013). Repression vs. activation of MOX, FMD, MPP1 and MAL1 promoters by sugars in *Hansenula polymorpha*: the outcome depends on cell's ability to phosphorylate sugar. *FEMS Yeast Research*, 13 (2), 219–232.10.1111/1567-1364.12023

## INTRODUCTION

The wide use of various engineered nanoparticles in consumer, medical as well as industrial products has raised concerns over the safety of these materials to the environment and human health. Nanoparticles (less than 100 nm in size) have novel physical-chemical properties and their small size and high reactivity allows unique interactions with living organisms which is both, the reason for their applications but also a cause for concern. The ongoing research initiative is aimed at understanding the effects that nanoparticles may have on living cells.

Silver and copper are well known for their antimicrobial properties and recently, Ag and CuO nanoparticles have gained interest in relation to the development of novel antibacterial, antifungal, antiviral and algacidal products to relieve the growing microbial antibiotics-resistance and in search of antimicrobial treatment with reduced toxicity to patients compared to the commonly used drugs. Ag and CuO nanoparticles have shown promise in the more efficient delivery of antimicrobial effects toward a wide spectrum of microbes compared to the respective ionic preparations. However, the mechanisms of action of the nanoparticles against microbial cells are not completely understood and at the same time, possible adverse effects to other organisms must be minimized in the process of material development.

The purpose of the current study was to elucidate the toxicity mechanisms of Ag and CuO NPs, using the unicellular yeast *Saccharomyces cerevisiae*. *S. cerevisiae* is a widely used model organism in cellular biology with similarities to higher eukaryotic organisms in cellular and genetic processes but is simply cultivated in the laboratory with the genome sequenced and genetic tools available. Also, *S. cerevisiae* is closely related to the opportunistic pathogenic yeast *Candida albicans*, making it a suitable model organism for the study of antifungal effects as well.

The unique approach in this study was the use of commercially available specifically selected single-gene deletion mutants for the toxicological profiling of Ag and CuO NPs. The mutant strains were selected according to the hypotheses in the literature on the main toxicity mechanisms of Ag and CuO NPs to test the importance of oxidative stress, metal ion stress, membrane damage and uptake in the toxic action. In addition, a novel test method was proposed for the testing of the biocidal potency of nanoparticles towards the unicellular organisms - bacteria, yeast and algae - in a test environment that is least affecting the speciation of solubilized metal ions, i.e. in the deionized water. Altogether, the methods used in this study aim to provide relevant test approaches and for the better understanding of the toxicological effects of metal-based nanoparticles.

## ABBREVIATIONS

3R's	strategy to reduce, replace and refine animal testing
CME	clathrin-mediated endocytosis
D <sub>h</sub>	hydrodynamic diameter
DI	deionized water
EC <sub>50</sub>	half-effective concentration, refers to the concentration of the test substance that causes the studied adverse effect to 50% of the test organisms after a specified exposure time
ENMs	engineered nanomaterials
IC <sub>50</sub>	half-inhibitory concentration, refers to the concentration of the test substance that causes the inhibition of the studied process (e. g. growth, viability etc.) by 50%
ISO	The International Standardization Organisation
LB	Luria-Bertani broth
MBC	minimal biocidal concentration
MIC	minimal inhibitory concentration
MWCNT	multi-wall carbon nanotube
NMs	nanomaterials
NPs	nanoparticles
OD	optical density
OECD	The Organization for Economic Co-operation and Development
OS	oxidative stress
PVP	polyvinylpyrrolidone
ROS	reactive oxygen species
SDS	sodium dodecyl sulfate
UV-Vis	ultraviolet-visible light
WT	wild-type
YPD	yeast extract-peptone-dextrose broth for yeast growth
YPD <sub>mod</sub>	modified (diluted) YPD medium used in this study

# **1. REVIEW OF THE LITERATURE**

## **1.1 The emergence of engineered nanoparticles**

### **1.1.1 Commercial applications of engineered nanoparticles**

Engineered nanomaterials (ENMs) are materials designed for specific purpose or function that have any external dimension in the nanoscale (1 to 100 nm), as defined by The International Organization for Standardization (ISO) (ISO 2015). There are naturally occurring nanosized materials, for example, originating from combustion processes, but recent technological progress has enabled the development of engineered nanoparticles (NPs) that have novel properties and an enormous potential for extensive benefits in industrial fields as well as consumer and medicinal products. NPs are desirable for so many promising technologies due to their small size, corresponding large specific surface area and unique properties and specific interactions that do not occur with the bulk materials. NPs may have enhanced electrical, optical, mechanical or catalytic activity (Oberdorster et al. 2005b).

Engineered nanoparticles are used in a range of commercial applications, in medicine and cosmetics, domestic consumables, electronics, energy production, agriculture etc (Tolaymat et al. 2017, Piccinno et al. 2012). Recently, metal-based NPs, and especially silver NPs have gained more interest for medical applications and the treatment of microbial infections and biofilms (Lara et al. 2015). Silver NPs are included in the biggest number of consumer products intended for various purposes such as personal care, clothing, cosmetics etc. ([www.nanotechproject.org](http://www.nanotechproject.org)).

### **1.1.2 Antibacterial and antifungal applications of metal-based nanoparticles**

Some metals like silver and copper have been used as antimicrobial agents since ancient times as they have microbicidal effects already at very low concentrations (Lemire et al. 2013). The use of antiseptics containing silver in soluble or colloidal form was common up until the discovery of antibiotics in the 1940s (Alexander 2009). Since the emergence of increasing antibiotic resistance in bacteria in the 1960s and the advent of nanotechnologies in the 1990s, Ag NPs have been developed as antibacterial substances for the control of bacterial infections and sterilization of instruments and surfaces (Ahonen et al. 2017, Massarsky et al. 2014, Neal 2008). Silver ions have some toxicity to humans, but the development of silver nanoparticle-based therapeutics has shown promise of slow release of ionic silver and therefore lower toxicity (Chaloupka et al. 2010, Maillard and Hartemann 2013). While silver nanoparticles are the most prominent antimicrobial agents, other metallic nanoparticles such as CuO NPs, TiO<sub>2</sub> NPs and ZnO NPs also exhibit antimicrobial effects (Seil and Webster 2012). Many studies have reported the high potency of silver NPs to environmental organisms (Bondarenko et al. 2013b, Blinova et al. 2013), therefore CuO and ZnO NPs have been proposed as less toxic and more available alternatives for antimicrobial applications (Mantecca et al. 2017). Silver has no essential function in cells, yet copper in trace amounts is an essential micronutrient, involved as a co-factor in enzymatic systems and has a critical role in human metabolism as well as fungal cells, but is toxic above certain concentration, depending on the organism (Gadd 1993, Slavin et al. 2017). There are

mechanisms to maintain copper homeostasis in eukaryotic as well as prokaryotic cells, including transporters for the export of excess copper (Slavin et al. 2017, Usman et al. 2013).

The search for novel and more efficient antibiotic therapeutic agents has been driven by the rise of pathogenic antibiotic-resistant microbes and systemic toxicity of many drugs, which are important obstacles to the use of traditional antibiotics in public healthcare (Lee et al. 2013, Seil and Webster 2012). Metal-based nanoparticles such as Ag NPs and CuO NPs are developed and used as efficient antimicrobial agents, active against Gram-negative and Gram-positive bacteria, fungi and even viruses (Neal 2008). The use of silver nanoparticles *in vitro* as antibiotics has proven to be effective against multidrug resistant bacteria (Cavassin et al. 2015) and pathogenic yeast *Candida albicans* at low concentration, which is not toxic to human cells *in vitro* (Panacek et al. 2009). At the same time, due to the wide use of silver as disinfectant, Ag-resistant bacterial strains have also been identified (Neal 2008).

Silver nanoparticles are incorporated into medical products such as wound dressings, bandages and ointments but also textiles, domestic appliances, food containers and functionalized plastics, paints, water filters etc. (McGillicuddy et al. 2017, Chaloupka et al. 2010). However, the use of nanoparticles in therapeutic applications is still limited due to considerations of the potential toxicity of nanoparticles to humans. There is a shortage of information about products on the market containing NPs because current regulations (with some exceptions of cosmetic products and food packaging) do not require labelling NPs as components (McGillicuddy et al. 2017).

### **1.1.3 Human and environmental exposure to engineered nanoparticles**

Due to large production volumes and the range of applications, the release of synthetic nanomaterials to the environment from anthropogenic sources is inevitable and is expected to increase dramatically. The possible sources of NPs in the environment are the sites of production, dissipation from product use and disposal, but also accidental spills (Lai et al. 2018). Pollution by NPs can be expected especially in the aquatic environment and associated sediment where metal-based NPs are expected to persist because they are essentially indegradable (von Moos and Slaveykova 2014). The likely human exposure can potentially occur during manufacturing or use of nano-based products via inhalation, or dermal or gastrointestinal route (Schrand et al. 2010).

There is little adequate information on the global production and application quantities, and very little data exists on measured environmental concentrations of NPs (Coll et al. 2016). In terms of mass flow, silica, titania, alumina, iron oxide and zinc oxide dominate the world NPs market (Keller et al. 2013). Piccinno et al. estimated the Ag NPs worldwide production to be between 5.5-550 t/a and according to the predictions of Massarsky et al., could reach 12.2-1216 t/a by 2020 (Piccinno et al. 2012, Massarsky et al. 2014). It is estimated that annually, the worldwide Cu-based nanoparticles production is a few hundred tons of the 18.7 million tons of total copper production and the majority of the environmental release is attributed to their use in marine antifouling paints (Keller et al. 2017).

Efforts have been made to evaluate the emissions of NPs during manufacturing, product use or waste management. The most widely studied metal-based NPs in regard to emissions are nanosilver and TiO<sub>2</sub>. The lack of appropriate analytical methods

hinders the relevant detecting, characterizing and quantifying of NPs in natural samples (Gottschalk et al. 2013). Experimental assessments of nanosilver emission in production facilities have obtained varying concentrations for air-emissions ranging from  $6.0 \times 10^{-8}$  to  $> 6.9 \times 10^{-4}$  mg/L<sub>air</sub>, which cover the ranges below and above current occupational exposure limits of  $2 \times 10^{-6}$  mg/L<sub>air</sub> (Tolaymat et al. 2017). The release of Ag (nanoparticles) have also been evaluated during the use and washing of Ag nanoparticles-containing textile products, food containers, spray applications and coated surfaces and the emission of Ag (nanoparticles) have been assessed in wastewater (Gottschalk et al. 2013, Tolaymat et al. 2017). Keller et al. used computational modeling to assess the global ENM emissions and estimated that 63–91% of the ENM emissions ended up in landfills, 8–28% reached soils, 0.4–7% water bodies and 0.2–1.5% to the atmosphere. The highest release was estimated for titanium dioxide, followed by zinc oxide, iron oxide, aluminum oxide, then copper oxide (Keller et al. 2013). Using the predicted environmental concentrations of NPs and predicted no effect concentrations from ecotoxicological studies, Coll et al. assessed the current environmental risk of nano-Ag to be low, despite being the most toxic of NPs. This was due to the low modeled environmental concentration which is reduced by the environmental transformation of nano-Ag to silver sulfide (Coll et al. 2016).

Although the nanotechnology market has been rapidly growing, the regulations on the labelling and specification of NPs, risk evaluation and pre-market registration or evaluation of products containing NPs are still limited. The current regulations and guidelines for material safety have been created for the bulk counterparts and therefore need reassessment in the light of research in the nanotoxicology field. The focus of this worldwide research is to ensure safe manufacture and marketing of nanomaterials.

## **1.2 The toxicological and ecotoxicological testing of engineered nanoparticles**

The unique properties of NPs that are designed for their intended functions also raise concerns about their biosafety (Nel et al. 2006). The first nanotoxicology papers were published in the 1990s, and the first nanoecotoxicology papers emerged since 2006 whereas approximately for a thousand papers on certain nanomaterial there are just 10 papers on human safety aspects and only 1 on ecotoxicological aspects (Kahru and Ivask 2013). The study of potential toxic effects of nanoparticles is important to create safety guidelines of nanoparticles production and for human use, for example in developing new efficient nanoantibiotics with microbial specificity and low toxicity to human cells, but also to evaluate their potential hazards to environmental species and microorganisms required for normal ecosystem functioning and production to prevent unnecessary ecotoxic effects. In the development of nanoantibiotics, their efficiency is aimed at the microbes who are the “target organisms”, while the organisms who might accidentally be exposed to the NPs, are the “non-target-organisms” (Bondarenko et al. 2013b). It has been reported that aquatic organisms such as algae and crustaceans are the most sensitive to many nanoparticles (Djurisic et al. 2015). Data from toxicological studies helps to understand the possible risks and allow for risk-benefit analysis and for the development of safe-by-design products (Dunne et al. 2017).

The toxicity of nanoparticles has been studied *in vivo* and *in vitro*, however the 3Rs policy recommends that “scientists reduce, refine and replace (3Rs) the use of animals in research” (Hartung and Sabbioni 2011). Therefore, we need relevant and simple, cost-effective, standardized *in vitro* systems and test strategies to allow for high-throughput toxicological screening of nanoparticles and further identifying the toxicity mechanisms of nanoparticles. A promising approach is the use of unicellular eukaryotic test organisms such as the yeast *Saccharomyces cerevisiae*, which allows for high-throughput screening using the available genetic tools.

Most studies on the impact of nanoparticles to human health use *in vitro* cell cultures of homogeneous, immortal cell types which reflects the possible exposure routes of nanoparticles such as ingestion, injection, transdermal delivery, or inhalation. Among the most widely-used *in vitro* cell cultures are the human lung cell epithelial line A549, human intestinal epithelial cell line Caco-2 and human keratinocyte cell line HaCaT (Love et al. 2012). The ecotoxicological research is mainly conducted with aquatic organisms required by the The Organization for Economic Co-operation and Development (OECD) such as the freshwater algae *Pseudokirchneriella subcapitata* or aquatic crustacean *Daphnia magna*, but the marine bacterium *Vibrio fischeri* luminescence inhibition assay has also been successfully used for ecotoxicological screening of turbid suspensions of NPs (Kahru and Dubourguier 2010).

There are specific challenges in testing nano-sized particles such as the preparation of relevant suspensions and accurate characterization of the particles in tests and the interference of nanoparticles with test medium components. The exposure conditions vary from standard organics-rich laboratory growth media to environmentally more relevant natural waters.

### **1.2.1 Characterization of the physicochemical properties of nanoparticles**

The biological effects of nanoparticles depend on the particles` chemical composition but critically also on their other parameters such as size, shape, surface functionalization etc. which make up the particles` intrinsic physicochemical properties or „the synthetic identity” (Fadeel et al. 2015). Upon introduction of nanoparticles to biological environments (e.g. for medical application or toxicity testing) they interact with the surrounding biomolecules and the characteristics of the suspension medium influence other particle properties such as effective surface charge (zeta potential), particle aggregation, dispersion stability and dissolution (Nel et al. 2009). Therefore, it is essential to determine and describe the nanoparticles used in any given test scenario to compare toxicity results from different studies (Djurisic et al. 2015).

Oberdörster et al. have suggested that toxicological studies should include information about the nanoparticle size and size distribution, agglomeration state, particle shape, crystal structure, chemical composition, surface area, surface chemistry, surface charge, and porosity (Oberdorster et al. 2005a). But it is important to note that the „as-synthesized” characteristics of nanomaterials in the dry phase are not always relevant for the toxicological studies in the wet phase in different biological environments, therefore the necessity of defining the nanoparticles metrics depends on each study (Fadeel et al. 2015).

The nanoparticles average primary size and size distribution are important features to determine for their impact to both toxicity and the fate of NPs (McGillicuddy et al. 2017).

The shape of nanoparticles is also important for their toxicological effects, as the shape of nanoparticles determines their exposed crystal planes and reactivity (Slavin et al. 2017). For example, triangular Ag NPs were found more toxic than spherical and rod-shaped Ag NPs (Pal et al. 2007). The size of nanoparticles is indeed a key factor in their toxicity, as a size-dependent trend in antibacterial activity has been shown for ~10-700 nm TiO<sub>2</sub> NPs (Simon-Deckers et al. 2009), ~8-1000 nm ZnO NPs (Jones et al. 2008), ~20-90 nm Ag NPs (Martinez-Gutierrez et al. 2010), i.e. the higher toxicity of smaller nanoparticles.

The surface charge of nanoparticles has been proposed to directly effect the particles' interactions with cells and can be altered with the reactants used in the NPs synthesis process or capping/coating agents (Slavin et al. 2017). Organic compounds such as carboxylic acids, polymers, polysaccharides and surfactants are often added as stabilizing agents to Ag NPs through adsorption or covalent attachment to increase their stability by providing electrostatic or steric repulsion or to reduce the release of ions (Levard et al. 2012). Electrostatic potential at the electrical double layer surrounding a nanoparticle in solution is the zeta potential and can be considered as an indicator of the particle's stability in suspension, whereas the surface charge >30 mV or <-30 mV is considered to provide the NPs with colloidal stability (Hartig et al. 2007). Silver and copper are prone to oxidation and therefore Ag and CuO NPs release Ag<sup>+</sup> and Cu<sup>2+</sup> ions during preparation and storage. Hence, polymers or surfactants are added in their synthesis as stabilizers (Usman et al. 2013).

The intrinsic properties of NPs determine some of the modifications that the particles are subject to in biological media. Of those modifications, perhaps toxicologically the most influential is the solubility and release of ions from metal-based NPs (Heinlaan et al. 2008, Kahru and Dubourguier 2010), which should be assessed in the test media as metal ions are prone to speciation (Käkinen et al. 2011, Bondarenko et al. 2013b). Smaller-sized nanoparticles have a higher dissolution property due to their higher specific surface area, but surface coatings and stabilizing agents can strongly influence the dispersion and solubility. The inverse relation of NPs size and dissolution has been experimentally shown in the case of Ag NPs and CuO NPs for example, and with CuO NPs, higher solubility of spherical NPs compared to rod-shaped NPs was reported as well (Misra et al. 2012).

Also, chemical residues from production and precursors such as metal impurities or organic compounds in carbon nanotubes or fullerenes and also endotoxin contamination can cause artifacts in toxicity tests (Petersen et al. 2014).

### **1.2.2 Influence of test medium on the properties of Ag and CuO nanoparticles**

The test conditions of metal-based nanoparticles can have a notable effect on the toxicological outcome because metal-based nanoparticles are susceptible to environmental influences. Results from toxicity testing of nanoparticles in a specific environment may not be reproducible under different conditions and the influences of test media must be considered to avoid misinterpretation (Petersen et al. 2014). In aquatic and biological systems, metal-based nanoparticles may undergo a series of transformations, the most important of which being the dissolution of metallic and metal-oxide nanoparticles, but also aggregation/agglomeration, sedimentation, adsorption, sulfidation and redox reactions (Figure 2) (Amde et al. 2017, Levard et al. 2012).

The surface of Ag NPs will readily oxidize or react with ligands, for example, silver reacts strongly with sulfide, chloride and organic matter (Levard et al. 2012).

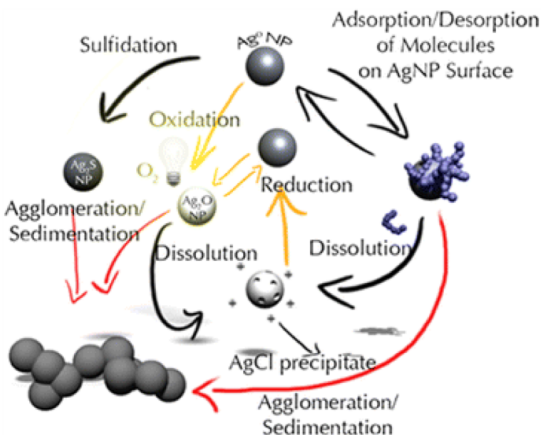


Figure 2. Schematic representation of the possible physicochemical transformations of silver nanoparticles during storage or ecotoxicology testing with aquatic organisms (modified from Petersen et al. 2014). Red lines indicate transformations that remove the AgNPs from the aqueous phase. Yellow lines indicate transformations that can occur as a result of illumination with laboratory light. Black lines describe transformations that can occur in the aqueous phase in the dark.

Aggregation of nanoparticles to larger clusters can decrease the mobility and reactivity of nanoparticles and lower their bioavailability and toxicity. Aggregation process depends on the size and shape of nanoparticles and their coating or surface functionalization, and on the other hand, on the pH, ionic strength and the presence of natural organic matter in the suspension medium (Amde et al. 2017).

Dissolution of metal-based nanoparticles is dependent on the intrinsic properties but in the same extent also on the surrounding medium, the presence of complexing ligands and may significantly effect the toxicity of nanoparticles. The pH, ionic strength, temperature and presence of organic components (natural organic matter, proteins, polysaccharides) influence dissolution of metallic nanoparticles (Amde et al. 2017). Tryptone and yeast extract have been shown to enhance the dissolution of CuO NPs and cysteine increases the dissolution of Ag NPs (Misra et al. 2012). However, the organic (proteins) and inorganic (salts) components present in the environment can also affect the bioavailability, uptake and toxicity of metals by binding, complexing and precipitating the free ions produced by dissolution (Misra et al. 2012).

### 1.3 The adverse effects and cytotoxicity of engineered nanoparticles

Considering the novel properties and enhanced reactivity and also the potential exposure to nanoparticles it is important to assess the biosafety of these materials. Due to their extremely small size nanoparticles are able to interact with living cells at the biomolecular level and cause hazardous effects. Despite extensive research over the last decades on the toxicity mechanisms of nanoparticles to humans and environmental

organisms, the results are often contradictory, and our understanding of toxicity mechanisms is still incomplete.

The science of particle toxicology has already previously investigated the toxic effects of ambient ultrafine particles (with sizes over 100 nm) such as mineral dust, asbestos fibres and carbon black. These materials induce oxidative injury and inflammation in lung tissue and cell culture analysis (Nel et al. 2006).

One of the most worrying features of nanoparticles is their capacity to cross biological barriers and enter cells (Pietrojusti et al. 2013).

### **1.3.1 Toxicity mechanisms of metal-based nanoparticles**

Nanoparticles can exert toxic effects in both eukaryotic and prokaryotic cells (Bondarenko et al. 2013b). The toxicity depends on the NPs characteristics like chemical composition, size, shape, surface characteristics (charge, crystal planes), which may determine the production of reactive oxygen species (ROS) or the dissolution of metallic NPs (Nel et al. 2006, Schrand et al. 2010, Slavin et al. 2017). In fact, in the case of metal-based NPs such as Ag, CuO and ZnO, the dissolution and release of metal ions is often considered as the main source of toxicity (Ivask et al. 2014b). The route to nanoparticle-specific toxicity to eukaryotic cells as well as antibacterial effects requires direct contact between the cells and nanoparticles, whereas the entry into cells is not a prerequisite (Wang et al. 2017). According to available research, the major processes in the antibacterial effects of NPs are the disruption of the bacterial cell membrane, induction of oxidative stress by the generation of ROS, penetration of the bacterial cell membrane, and intracellular toxic effects, including interactions with DNA and proteins (Wang et al. 2017). Both, Ag- and Cu-based nanoparticles have been reported to cause toxicity *in vitro* in various mammalian cell lines and also *in vivo* in rodents and zebrafish (Schrand et al. 2010). However, the most sensitive test organisms to Ag NPs are crustaceans and algae, followed by fish, nematodes and bacteria, whereas yeast and mammalian cells *in vitro* are the least sensitive (Bondarenko et al. 2013b). The median toxic concentrations (L(E)C<sub>50</sub> or MIC) of Ag and CuO NPs based on the literature search to yeast cells and mammalian cells *in vitro* are 7.9 and 11 mg/L, and 17 and 25 mg/L, respectively (Ivask et al. 2014b).

For mammalian cell lines, the majority of NPs toxicity mechanisms reported have been related to reactive oxygen species. The intracellular ROS induced by Ag and CuO NPs can cause DNA damage, the production of inflammation promoting cytokines, or cellular damage such as the degradation of mitochondrial membrane integrity which may lead to cell death (Schrand et al. 2010, Ivask et al. 2014b).

The inhibition of fungal cell growth and viability by Ag and CuO NPs has been suggested to be caused by cell wall damage, the generation of ROS or DNA damage (Lara et al. 2015, Hwang et al. 2012, Bayat et al. 2014).

#### **1.3.1.1 Contribution of dissolved metal ions to the toxicity of metal-based nanoparticles**

The cytotoxic effects of metal-based nanoparticles result from a combination of the release of toxic metal ions and intrinsic nanoparticle effects, whereas the dissolution status of the NPs in exposure media determines the uptake and toxicity pathways (Misra et al. 2012). Differentiating between the effects of the NPs and dissolved metal

ions is experimentally complicated, i.e. the separation of the particulate or partially dissolved NPs, free and complexed ions and adsorbed ions on the NPs surfaces (Ivask et al. 2014b). The oxidized surface of Ag NPs and chemisorbed Ag<sup>+</sup> on the particles' surface has been proposed to be responsible for the antibacterial activity, whereas optimal particle dispersion is the key factor (Lok et al. 2007).

Heavy metal ions like Ag<sup>+</sup> or Hg<sup>2+</sup> but also essential metals like Cu and Zn have high affinities to sulphur and they strongly bind to amino acid residues containing thiol groups (R-SH) (Slavin et al. 2017). While this interaction is biologically important in the functioning of many enzymes via binding essential metals, it also leads to toxicities of excessive metal concentrations when inhibiting vital enzyme functions (Waldron et al. 2009, Wysocki and Tamas 2010). The toxic effects of metal ions at the cellular level include oxidative stress, alteration of enzyme and protein function by blocking functional groups or the substitution of essential metal ions from biomolecules, denaturation of enzymes, lipid peroxidation, interfering with DNA repair and disruption of membrane integrity (Gadd 1993, Hosiner et al. 2014). Dissolved Ag<sup>+</sup> ions are recognized as powerful antibacterials due to poisoning of respiratory electron transport chains and components of DNA replication (Neal 2008). Many metals such as Fe, Cu, Zn, Se, Cr, Cd, Hg and Pb influence membrane fluidity (Wysocki and Tamas 2010).

While several studies have concluded that the dissolution of metal oxide nanoparticles is the main determinant of the toxicity to bacterial or mammalian cells, others have been able to show the dependence of toxicity on the surface charge of the nanoparticles, or the nanoparticles conduction band energy (Ivask et al. 2015). In a large study of 24 metal oxide nanoparticles, the toxic effects of nanoparticles of ZnO, CuO, NiO, MgO, and WO<sub>3</sub> to human lung cells and keratinocytes were concluded to be primarily the cause of released metal ions (Horie et al. 2012). However, Ivask et al. concluded that the toxicity of CuO, ZnO and Sb<sub>2</sub>O<sub>3</sub> nanoparticles to different mammalian cell cultures was driven by their dissolution, but the induction of ROS was found to be the key toxicity factor for Mn<sub>3</sub>O<sub>4</sub> and Co<sub>3</sub>O<sub>4</sub> NPs (Ivask et al. 2015). CuO and ZnO NPs were found to be the most toxic among 12 metal oxide nanoparticles also to algae and bacteria and the potency was attributed to the dissolved metal ions (Aruoja et al. 2015).

One key aspect of the antimicrobial effect of Ag NPs is the particle characteristics affecting the metal ion bioavailability and release of Ag ions and Ag NPs can be modified to be efficient vehicles of Ag ion delivery (Xiu et al. 2012). Bondarenko et al. also noted that the cell-particle contact is necessary for the enhanced Ag<sup>+</sup> delivery to bacterial cells (Bondarenko et al. 2013a).

### **1.3.1.2 Cellular oxidative stress caused by metal-based nanoparticles**

The generation of reactive oxygen species and resulting oxidative stress has been proposed as the major paradigm of nanoparticles toxicity both *in vitro* and *in vivo* with plenty of experimental data on the induction of ROS and oxidative injury by air-borne nanoparticles (Oberdorster et al. 2005b). However, toxicity to other organisms including environmental species and other toxicity routes have also been discovered and the generation of ROS is not always detected in nanoparticle toxicity studies, therefore the significance of ROS in NP toxicity is still unclear (von Moos and Slaveykova

2014). The mechanism for ROS generation is different for each NP and some studies have reported NPs toxicity without causing oxidative stress (Manke et al. 2013).

Oxidative stress is the imbalance between excess ROS and the depletion of cellular defence mechanisms (glutathione, antioxidant enzymes) and may lead to cytotoxicity. ROS such as singlet oxygen ( $O^*$ ), superoxide anion ( $O_2^{\bullet-}$ ), hydrogen peroxide ( $H_2O_2$ ) and hydroxyl radical ( $OH^*$ ) attack cellular macromolecules, leading to protein oxidation, lipid peroxidation and DNA damage (Wysocki and Tamas 2010).

The sources of ROS from NPs are based on different factors such as NPs shape, purity, crystal plane disruptions and structural defects, also the dissolution of catalytic metal ions from redox-active metal-based NPs, including Cu and Fe, and the triggering of Fenton-type reactions to yield hydroxyl radicals, other routes of ROS production include the interaction of NPs with the cell surface or intracellular processes such as mitochondrial respiration (von Moos and Slaveykova 2014). Redox-inactive metals may also induce oxidative stress through indirect mechanisms such as by inhibiting specific enzymes or by depleting pools of antioxidants (Wysocki and Tamas 2010). Photoactive NPs, mainly  $TiO_2$ , are triggered to produce ROS in the presence of light (von Moos and Slaveykova 2014) and  $TiO_2$  is known to induce strong antibacterial effects via the production of hydroxyl radicals and hydrogen peroxide and subsequent degradation of cell wall and cytoplasmic membrane (Foster et al. 2011). Different ROS species have been identified to be involved in the bactericidal effect of metallic nanoparticles of  $TiO_2$ , MgO and ZnO such as the hydroxyl radicals, superoxide anions and hydrogen peroxide (Djurisic et al. 2015, Lakshmi Prasanna and Vijayaraghavan 2015). Ag NPs and CuO NPs have been shown to induce the formation of ROS and cause broad spectrum antibacterial effects against *Escherichia coli*, *Pseudomonas aeruginosa* and *Staphylococcus aureus*, also lipid peroxidation, depletion of glutathione, DNA damages and eventual disintegration of the cell membrane were reported (Korshed et al. 2016, Ivask et al. 2010).

Studies with human lung epithelial cell line A549 have reported ROS formation and cytotoxicity by Ag and CuO NPs (Karlsson et al. 2008, Chairuangkitti et al. 2013), while differently coated 10-75nm Ag NPs did not produce intracellular cytosolic ROS in the human bronchial epithelial BEAS-2B cells (Gliga et al. 2014). Increased ROS production in Ag NPs-exposed yeast *Candida albicans* cells has been shown where the antifungal effect of Ag NPs was proposed to be related to mitochondrial dysfunction and apoptosis (Hwang et al. 2012), and in the fission yeast *Schizosaccharomyces pombe*, the toxicity of Ag NPs was attributed to intracellular uptake, release of  $Ag^+$  and generation of ROS (Lee et al. 2018).

### **1.3.1.3 Membrane damage caused by metal-based nanoparticles**

In unicellular organisms such as bacteria, yeasts and algae, the physical interactions between various metal-based nanoparticles and cell surface has been implicated in the toxic effects, and attachment of nanoparticles onto the cell surface, migration into the membranes, morphological changes and disruption of the structure and permeability of the cell membrane have been reported (Ivask et al. 2014b). The disturbance of bacterial cell membrane and increase of the membrane permeability by Ag NPs, ZnO NPs, MgO NPs and  $CeO_2$  NPs has been suggested to be induced by ROS and lipid peroxidation (Neal 2008).

The attraction between the nanoparticles and the bacterial cells can be explained by different types of physicochemical interactions like electrostatic forces between opposite-charged surfaces (negatively charged cell surface and positively charged nanoparticles), but may also include Van der Waals forces, hydrophobic interactions, as well as receptor-ligand interactions, for example via carboxyl, amide, phosphate or hydroxyl groups and carbohydrate moieties (Djurisic et al. 2015).

Surface charge-dependent antibacterial effects have been shown for Ag NPs with different surface-modifications, where BPEI-coated Ag NPs (zeta potential +40 mV) were significantly more toxic than negatively-charged Ag NPs and even Ag ions (El Badawy et al. 2011, Ivask et al. 2014a). A localized enhanced concentration of the toxic Ag<sup>+</sup> ions is created when the dissolution of Ag NPs takes place on the bacterial cell membrane, causing cell membrane damage and disintegration and eventually leading to Ag<sup>+</sup> ions and Ag NPs entering the bacterial cytosol (McQuillan et al. 2012). The disorganisation and perforation of *Escherichia coli* cell wall, damage to the cell membrane and leakage of intracellular content has been reported as the result of the accumulation of silver nanoparticles in the close vicinity of the cell (Pal et al. 2007, Gogoi et al. 2006, Morones et al. 2005).

Cell membrane damage by Ag NPs was shown by the adenylate kinase assay in human dermal keratinocyte HeCaT and cervical cancer HeLa cells (Mukherjee et al. 2012), and metallic Cu NPs but not CuO NPs were shown highly membrane-damaging in human lung epithelial A549 cells, although the membrane damage was explained by the metal release from Cu NPs at the cell membrane surface (Karlsson et al. 2013).

The antifungal activity of 3-nm and 1-nm Ag NPs on the yeast *C. albicans* has been reported to be caused by cell wall damage and membrane permeabilization and perforation as shown by electron microscopy (Kim et al. 2009, Lara et al. 2015).

#### **1.3.1.4 Internalization of nanoparticles by the cells and subsequent intracellular damage**

Higher eukaryotic cells of multicellular organisms (mammals) are known to internalize NPs, however, the uptake of NPs by unicellular eukaryotic cells, such as yeasts, and prokaryotes is not commonly reported and tends to be the result of membrane injury (Ivask et al. 2014b).

The cell membrane is the cell's barrier from the outside environment and is impermeable to large particles, while nanoparticles are proposed to be able to cross the cell membrane by passive diffusion or by the energy-dependent process of endocytosis (active uptake) (Kettler et al. 2014). The internalization efficiency, mechanism and intracellular routing of nanoparticles depends on the cell type and nanoparticle size, charge and other surface properties, as eukaryotic cells have different types of endocytosis, such as phagocytosis and pinocytosis, clathrin-mediated endocytosis (CME) and clathrin-independent endocytosis (Iversen et al. 2011). Cationic nanoparticles are more prone to attachment to the cell surface and therefore, more efficient endocytosis, than neutral or anionic nanoparticles (Zhu et al. 2013). The endocytosis of NPs is restricted by the size of the endocytic vesicles of different cell types, while only uncharged molecules with small size (a few nanometers) could penetrate the membrane by diffusion (Zhu et al. 2013). Several studies have shown that the size optimum for the endocytosis of nanoparticles by mammalian cells is

20-50 nm (Iversen et al. 2011). Assumably, the likely maximum nanoparticle size for internalization via clathrin-coated vesicles is 200 nm, however phagocytic mammalian cells internalize cells and bacteria with sizes 0.5-10  $\mu\text{m}$  (Kettler et al. 2014). Nanoparticles taken up by endocytosis in mammalian cells have been reported to localize in endosomes or lysosomes intracellularly (Iversen et al. 2011).

Following the uptake of metal-based NPs, the intracellular dissolution, especially in the acidic environment of the lysosome, and release of metal ions, called the Trojan-horse effect, is the main facilitator of toxicity (Limbach et al. 2007, Sabella et al. 2014). Furthermore, nanosilver uptake has been reported to trigger higher ROS production in mammalian *in vitro* cell lines, and the interaction of nanosilver with proteins and DNA and induction of genotoxicity also contribute to toxicity in both, human and bacterial cells (McShan et al. 2014). High uptake of CuO NPs and Ag NPs in human lung cell lines A549 and BEAS-2B resulted in cell death and DNA damage in CuO NPs-exposed, but not in Ag NPs-exposed cells (Cronholm et al. 2013).

In *S. cerevisiae* spheroplasts, the endocytosis of positively-charged gold nanoparticles (1.4nm) was demonstrated to be dependent on the END3 gene and occurred via vesicular endosomes and the vacuole (Prescianotto-Baschong and Riezman 1998).

#### **1.4 *Saccharomyces cerevisiae* as a unicellular eukaryotic model organism in toxicology**

The yeast *Saccharomyces cerevisiae* is a valuable unicellular eukaryotic model organism, because yeast cells exhibit the important features of the cells of higher organisms but are easily cultivated and maintained. Yeasts belong to the diverse eukaryotic Fungi kingdom and *S. cerevisiae* represents the unicellular budding yeast. As a eukaryotic model, the *S. cerevisiae* is cost-effective and genetically well-studied, with genome-wide methods available.

*S. cerevisiae* is a widely-used model organism for studying the fundamentals of eukaryotic cell biology. Availability of the genomic sequence and advanced genetic tools allows for high-throughput screening methods. Studies using *S. cerevisiae* provide valuable insights into cellular processes such as oxidative stress and ageing (Costa and Moradas-Ferreira 2001), response to metals (Bird 2015), endocytosis (Goode et al. 2015) and autophagy research, which was recognized by the 2016 Nobel Prize in Physiology or Medicine (Levine and Klionsky 2017). The use of yeast model in toxicological testing can be especially valuable in the light of the initiative to reduce animal testing (the 3Rs).

However, *S. cerevisiae* is also a relevant system for the study of antifungal compounds to target fungal infections and also serious plant and animal diseases caused by pathogenic fungi. *S. cerevisiae* is closely related to the pathogenic yeast *Candida albicans*, the major cause of yeast infections, particularly in immunocompromised persons (Hughes 2002). Because fungi are eukaryotic cells, the main obstacle in antifungal drug discovery is to find a selective target to avoid toxicity to patients (Lara et al. 2015). Most antifungal agents target either ergosterol, which is a unique component of the fungal cell membrane, or the fungal cell wall (Robbins et al. 2016).

The cell wall provides fungal cells with protection and osmotic integrity, defines the cell shape and morphology, acts as a permeability barrier and enables interactions with the environment and other fungal cells (Figure 3). The fungal cell wall is unique, although there are variations in the organization of the cell wall and the composition varies between species (Bowman and Free 2006). The *S. cerevisiae* cell wall is composed mainly of mannoproteins and  $\beta$ -glucans and a small amount of chitin, which are cross-linked to form a cell wall matrix (Orlean 2012).

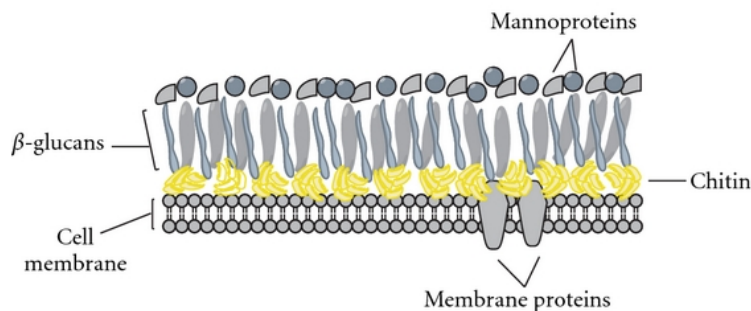


Figure 3. The structure of fungal cell wall (from (Vega and Kalkum 2012), is licensed under the Creative Commons Attribution License). The main components of fungal cell walls are mannoproteins, glucans and chitin.

Yeast cells have aerobic and anaerobic metabolic pathways to use various organic molecules (e. g. sugars) as the energy and carbon sources. Depending on the availability of sugars and oxygen, *S. cerevisiae* can grow either respiratively, respiro-fermentatively or fermentatively (Pronk et al. 1996, Kasemets et al. 2007). By using different carbon sources, such as glucose or glycerol, for example, either respirative or fermentative growth can be induced and therefore, the effects of NPs on mitochondria etc. can be studied.

Collections of *S. cerevisiae* single-gene deletion mutants, created by the *Saccharomyces* Genome Deletion Project consortium by systematically deleting nearly all of the open reading frames, are available. This is a powerful tool for studying gene function and the essential genes for yeast growth under various environmental conditions and stresses, and has been used previously to study the response to metals, for example. Many of the yeast genes have homologous genes in humans and therefore some mechanisms of metal toxicities could be extrapolated to mammalian systems (Jo et al. 2008). Currently, over 20 000 strains are available and can be obtained from EUROSCARF, for example (Institute of Microbiology, University of Frankfurt, Germany; <http://www.euroscarf.de>). Genome-wide collections of non-essential single-gene deletion mutants of *Escherichia coli* are also available and have been used for the toxicological profiling of nanoparticles (Ivask et al. 2012). In this study, specifically selected *Saccharomyces cerevisiae* single-gene deletion mutant strains were used for the first time for the toxicological screening of nanoparticles. The mutant strains were selected with deletions in genes of oxidative stress response, copper stress response, cell wall or membrane synthesis or maintenance and endocytosis.

#### **1.4.1 The response of *Saccharomyce cerevisiae* cells to oxidative stress**

During growth under aerobic conditions, yeast cells are continuously exposed to reactive oxygen species generated by the mitochondrial respiratory chain, and cellular damages are prevented by antioxidant defences (Costa and Moradas-Ferreira 2001). Glutathione (GSH), a non-enzymatic defence molecule is the most abundant redox scavenging molecule in cells, including yeasts, which acts with the redox-active sulphhydryl group reacting with oxidants to produce reduced glutathione (GSSG) (Jamieson 1998). Metallothioneins have an important role in intracellular sequestration of transition metal such as copper and iron, and minimizing the formation of OH<sup>•</sup> radicals (Moradas-Ferreira et al. 1996). Several enzymes are involved in removing oxygen radicals or repairing oxidative damage. Catalases, the catalase A and catalase T, are responsible for the breakdown of H<sub>2</sub>O<sub>2</sub> to O<sub>2</sub> and H<sub>2</sub>O in *S. cerevisiae* (Jamieson 1998). Two intracellular superoxide dismutases (SOD), the mitochondrially-located MnSod (encoded by the SOD2 gene) and the cytoplasmically-located Cu/ZnSod (encoded by the SOD1 gene), transform superoxide anion to H<sub>2</sub>O<sub>2</sub> and O<sub>2</sub> in *S. cerevisiae* (Moradas-Ferreira et al. 1996).

#### **1.4.2 The response of *Saccharomyces cerevisiae* cells to Ag and Cu ions**

The research of metal interactions with fungi has been driven mainly by the development of fungicidal preparations for agricultural and material preservation purposes, but also as model cell factories for eukaryotic biology and environmental perspectives (Gadd 1993). Many metals, including copper and silver, when in excess, can induce toxic effects in fungal cells, such as the blocking of functional groups of enzymes or transport systems, substitution of essential metal ions in biomolecules, denaturation of enzymes or disruption of membrane or organell integrity, and in addition, Ag and Cu can also produce free radicals (Gadd 1993).

For the regulation of metal levels in cells, the primary response of eukaryotes to metals is changes in gene expression to alter metal uptake, compartmentalization, storage and export (Bird 2015). *S. cerevisiae* has metal-regulated DNA-binding transcription factors known to respond to zinc (Zap1), copper (Mac1 plus Ace1, also known as Cup2) and iron (Aft1 plus Aft2 to iron) (Waldron et al. 2009). Mac1 activates transcription in response to low, and Ace1 (Cup2) to high copper concentration in *S. cerevisiae*. Ace1p regulates the transcription of metal-sequestering metallothionein CUP1, metallothionein-like protein CRS5, and cytosolic Cu/Zn superoxide dismutase SOD1 (Yasokawa et al. 2008). Mechanisms of fungal cells for survival in the presence of toxic metal concentrations include extracellular complexation, metal transformation, biosorption to cell walls, decreased transport, efflux, or intracellular compartmentation (Gadd 1993). Excess metals in yeast cells are compartmentalized to vacuoles, plasma-membrane exporters are known only for cadmium and arsenic (Wysocki and Tamas 2010).

The presence of copper in the growth medium induced the expression of *S. cerevisiae* copper metallothionein CUP1-1 and CUP1-2 more than 20-fold and some sulphur metabolism and oxidative stress response genes were also up-regulated (Yasokawa et al. 2008). Silver ions and silver NPs also caused the strong up-regulation of *S. cerevisiae* CUP1-1 and CUP1-2 genes, and in addition genes of ion transport and homeostasis or chemical stimuli, stress and transport processes were differently induced (Niazi et al. 2011).

### 1.4.3 Endocytosis in *Saccharomyces cerevisiae* cells

Endocytosis is the process of ingesting extracellular material into cells via engulfing by the cell membrane and packaging them into vesicles that are pinched off the membrane and enter the cytosol (Goode et al. 2015). It is the process for cells to collect nutrients, regulate plasma membrane-associated surface proteins, such as receptors, channels, and signaling proteins, and redistribute plasma membrane components. Clathrin-mediated endocytosis (CME) is used by all eukaryotic cells, including yeasts, and has been best characterized, while others, clathrin-independent endocytosis pathways have also been described (McMahon and Boucrot 2011).

The size of clathrin-coated vesicles varies between species, with an observed upper limit of about 200 nm in external diameter. Yeasts have small clathrin-coated vesicles of ~35-60 nm exterior diameters, indicating the internal vesicle diameter of ~15-25 nm (McMahon and Boucrot 2011). The main difference between the clathrin-mediated endocytosis in yeast and mammalian cells is the relative functional importance of clathrin and actin. Internalization at the CME sites in yeasts can proceed even in the absence of clathrin, whereas clathrin depletion in mammalian cells arrests CME (Goode et al. 2015).

After internalization, most molecules are transported to the vacuole for degradation. The transport occurs via membrane-bound compartments, the early and late endosomes (Prescianotto-Baschong and Riezman 1998). Over 50 different proteins are involved in the clathrin-mediated endocytosis process at the plasma membrane and many key aspects were first elucidated in yeast (Goode et al. 2015). The *S. cerevisiae* END3 gene encodes a protein directly required for the internalization step of endocytosis at the plasma membrane and not for subsequent transport to the vacuole (Munn et al. 1995). End3p is also necessary for the proper organization of actin cytoskeleton and correct distribution of chitin at the cell surface (Benedetti et al. 1994). *end3* mutant cells are defective for the internalization of both fluid phase and membrane-bound markers (Prescianotto-Baschong and Riezman 1998).

### 1.4.4 The toxicity of metal-based nanoparticles to yeast cells

There is already some research on the toxicity of different nanoparticles to yeast cells, for example there are over 100 publications available on the toxic effects of nanoparticles using the model yeast *S. cerevisiae* or the pathogenic *C. albicans* in the Scopus database ([www.scopus.com](http://www.scopus.com)). The toxicities of different metallic nanoparticles such as Ag, CuO, ZnO, NiO, MgO, TiO<sub>2</sub> as well as quantum dots and polystyrene NPs have been investigated.

3-nm Ag NPs showed the minimal inhibitory concentration (MIC) of 2 µg/mL against *C. albicans* and *S. cerevisiae* (Kim et al. 2009), while another study reported a MIC of 25-nm Ag NPs against *C. albicans* as low as 0.21 mg/L (Panacek et al. 2009). Previously, nano- and bulk-sized CuO have shown toxicity to *S. cerevisiae*, the 8-h EC<sub>50</sub> were 20.7 and 1297 mg CuO/L, respectively (Kasemets et al. 2009).

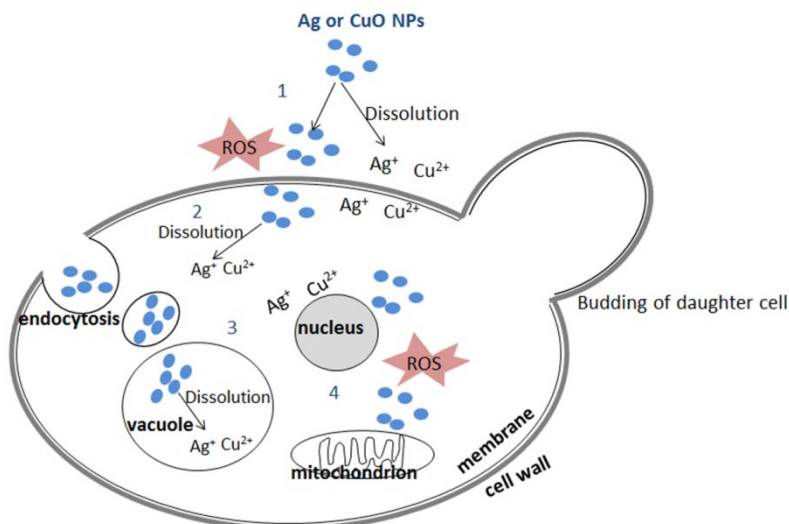


Figure 4. Possible interactions of the *Saccharomyces cerevisiae* cell with Ag or CuO NPs. 1) Adsorption of NPs or the dissolved metal ions on the surface of the yeast cell and interference with cell wall/membrane integrity by the induction of ROS, interaction of metal ions with membrane components or altering with the cell wall fluidity 2) internalization of NPs or metal ions by passive diffusion or active transport, endocytosis or via the damaged cell wall 3) intracellular compartmentalization or further dissolution of NPs in the vacuole or cytoplasm 4) intracellular interaction of NPs or metal ions with the mitochondrion or nucleic acids.

CuO and Ag NPs were found cytotoxic to *S. cerevisiae* cells and caused changes in the ultrastructure of *S. cerevisiae* cells, including the enlargement of the vacuoles, increased numbers of lipid droplets and disruption of intracellular components, as well as DNA damage in the Comet assay, whereas only CuO NPs showed oxidative potential in cell-free dichlorofluorescein assay (Bayat et al. 2014). Xiong et al. (Xiong et al. 2013) have studied the effect of silver NPs size, shape, capping agents and surface facets in the toxicity to *S. cerevisiae* cells. While the inhibition of yeast growth increased with decreasing NPs size, and silver nanoplates were more toxic compared to nanocubes and nanowires, the toxicity was proposed to be mainly defined by the crystal structures of silver nanoparticles. The authors concluded that the surface facets of silver NPs play the major role in toxicity, affecting the binding to capping agents and generation of ROS. A significant proportion of silver was found to enter the *S. cerevisiae* cells exposed to Ag nanocubes, but as no cubic Ag NPs were located in the cells, the authors believed that the uptake of Ag into cells occurred via the dissolved Ag ions (Xiong et al. 2013).

In a study of Ag NPs-exposed *C. albicans* cells, the MIC was reported to be 42 µg/mL, and the ultrastructural study revealed abundant accumulation of small-sized Ag NPs in the cell wall and cytoplasm, although this was hypothesized to be the result of Ag ions from extracellular Ag NPs penetrating the cell wall and intracellular formation of Ag NPs through reduction (Vazquez-Munoz et al. 2014). Small 2-nm silver NPs had MIC against *C. albicans* as low as 70 ng/mL and electron microscopy analysis

showed structural changes of silver NPs-exposed cells with Ag NPs adherence on the cell surface, aggregation of cells into clumps, alterations in the cell wall and membrane and increased number and enlargement of the vacuoles (Selvaraj et al. 2014).

Positively and negatively charged polystyrene latex nanoparticles (100 nm) were used to investigate the effect of nanoparticle's surface charge on cellular interaction, uptake and toxicity to *S. cerevisiae*. Results showed that the electrostatic interaction with positively charged polystyrene latex nanoparticles caused their adhesion to the cell surface and consequent cell death, whereas the uptake of the same positively charged polystyrene latex nanoparticles by the cells did not cause toxicity. The authors proposed that the clearance of nanoparticles from the cell surface by endocytosis was a defence mechanism to maintain the fluidity of the cell membrane (Nomura et al. 2013, Nomura et al. 2015). In a study of ZnO nanoparticles (20 nm) using *S. cerevisiae* wild-type and its gene-deletion mutant strains, TEM microscopy showed mechanical damage by the ZnO nanoparticles to the yeast cell walls, although no intracellular or cell-bound ZnO nanoparticles were found (Zhang et al. 2016). CdSe nanoparticles also showed toxicity to *S. cerevisiae* cells and the toxicity was attributed to End3-mediated endocytosis, ROS accumulation and an enhancement of vacuolar membrane permeabilization (Sun et al. 2014).

-----

In this PhD thesis, toxicity mechanisms of silver and copper oxide nanoparticles to *Saccharomyces cerevisiae* BY4741 wild-type and its single gene deletion mutants was studied to further understand the toxicity mechanisms. To our best knowledge, these were the first studies using *S. cerevisiae* single-gene deletion mutants for the study of nanoparticles toxicity mechanisms. Since we started this research, Bao et al., have used the *S. cerevisiae* deletion mutants for the study of the antimicrobial effects of CuO NPs (Bao et al. 2015) and also, the genome-wide collection of single-gene deletion mutants have been employed for high-throughput analysis of Ag NPs toxicity (Galvan Marquez et al. 2018). The possible toxicity mechanisms of Ag and CuO NPs to *S. cerevisiae* cells based on the literature are schematically represented in Figure 4.

## AIMS OF THE STUDY

The main aim of the study was to elucidate (i) the toxicity mechanism of CuO and Ag nanoparticles (NPs), to the yeast *Saccharomyces cerevisiae* and (ii) to develop a novel method for the testing of antimicrobial properties of nanoparticles.

The specific aims were:

- 1) Toxicity profiling of the CuO and Ag NPs using the single-gene deletion mutants of *Saccharomyces cerevisiae* BY4741,
- 2) Determine how the different physicochemical properties (intrinsic NPs properties such as chemical composition, size and surface coating/stabilizing agents) of the CuO and Ag NPs determine their toxic outcome,
- 3) Determine how environmental conditions (mainly test media) modulate the metal-based nanoparticles` physicochemical properties, bioavailability and toxicity,
- 4) To develop a novel method for the comparison of biocidal properties of nanoparticles to bacteria, yeast and algae in a test environment that minimizes the interference with the properties of metal-based nanoparticles (deionized water).

## 2. MATERIALS AND METHODS

### 2.1 The nanoparticles used in this study

The nanoparticles used in the studies (Publications I-IV) are listed in Table 1. A more detailed description and characterization are in the respective publications. For the NPs of Ag (Publications I-III) and CuO (Publications II, IV), soluble metal salts (AgNO<sub>3</sub> and CuSO<sub>4</sub>, respectively) were used in parallel to account for the effects of dissolved metal ions in the biological effects.

*Table 1. List of the nanoparticles used in this study*

<b>NPs (primary size)</b>	<b>Producer / synthesized by</b>	<b>Received as</b>	<b>Coating / stabilizer</b>	<b>Publication</b>
<b>Ag NPs</b>				
nAg (~86 nm)	Sigma-Aldrich	powder	none	I
nAg-PVP (~8 nm)	Synth. in the Lab of prof H. Tenhu*	powder	polyvinyl- pyrrolidone	I
nAg-col (~13 nm)	Laboratorios Argenol S. L.	powder	casein	I, II
nAg-PVP (~16 nm)	Partners in FP7 NanoValid	suspension in DI (40 g Ag/L)	polyvinyl- pyrrolidone	II
nAg-cit (10 nm)	MK Nano	suspension in DI (0.079 g Ag/L)	citrate	III
nAg-cit (20 nm)	MK Nano	suspension in DI (0.118 g Ag/L)	citrate	III
nAg-cit (40 nm)	MK Nano	suspension in DI (0.059 g Ag/L)	citrate	III
nAg-cit (60 nm)	MK Nano	suspension in DI (0.052 g Ag/L)	citrate	III
nAg-cit (80 nm)	MK Nano	suspension in DI (0.056 g Ag/L)	citrate	III
<b>CuO NPs**</b>				
nCuO (~30 nm)	Sigma-Aldrich	powder	none	II, IV
<b>Carbon NMs</b>				
MWCNTs (diameter ~10 nm; length >1000 nm)	Partners in FP7 NanoValid	powder	none	II

\*Laboratory of Polymer Chemistry, Department of Chemistry, University of Helsinki

\*\*In addition to CuO NPs, also bulk CuO particles (Sigma-Aldrich) were studied in Publication IV.

#### 2.1.1 Preparation of nanoparticle suspensions

The nanoparticles were received either as stock suspensions in deionized water or in powder form (see Table 1) in which case stock suspensions were prepared in deionized water with concentrations 0.5-5 g/L. Only vortexing was used in most cases to

distribute the nanoparticles equally in the suspension. The stock suspension of CuO NPs and bulk CuO (Publication IV) were ultrasonicated for 30 min in the ultrasonic bath (Branson 1510, USA) once after preparation. For the multi-wall carbon nanotubes (MWCNTs; Publication II), 0.01% Triton X-100 was used to homogenize the suspension of nanoparticles and in addition, ultrasonication probe was used, once for the preparation of the stock suspension as well as once, before the testing.

For the toxicity tests (Publications I-IV), determination of dissolved ion fraction (Publications I, III, IV), measurements of zeta potential and hydrodynamic diameter (Publications I-IV) and UV-vis spectroscopy (Publication I, III), the appropriate dilutions were prepared in deionized water and respective test medium.

### **2.1.2 The characterization of nanoparticles**

The primary sizes of the nanoparticles were provided by the producers or determined by other authors as referenced in the publications.

The hydrodynamic diameter ( $D_h$ ) and zeta potential measurements (Publications I-IV) were performed with the Zetasizer Nano ZS (Malvern Instruments, UK) at relevant concentrations in the respective medium (deionized water or growth medium) at 0-time point and the end-time point of the toxicity experiments.

UV-Vis absorption spectroscopy of the Ag NPs (Publications I, III) was performed with the Multiskan Spectrum spectrophotometer (Thermo Scientific, Finland) by measuring the absorption at 250-900 nm wavelength in a clear 1 mL cuvette or transparent 96-well microplates.

#### **2.1.2.1 The quantification of dissolved Cu and Ag**

For the measurement of the dissolved fraction of Cu and Ag NPs from the nanoparticles in the test media, the suspensions were incubated in conditions similar to the toxicity testing, after which the samples were ultracentrifuged at 390 000 g for 30-40 min to remove the non-soluble fraction and the Ag and Cu content in the supernatant was analyzed with atomic absorption spectroscopy. In the case of CuO particles (Publication IV), the solubility was determined also by the recombinant bioluminescent Cu-sensing bacteria *E. coli* MC1061 (pSLcueR/pDNPCopAlux).

### **2.2 The *Saccharomyces cerevisiae* BY4741 strains**

Throughout Publications I-IV, *Saccharomyces cerevisiae* BY4741 wild-type (MATa; his3 $\Delta$ 1; leu2 $\Delta$ 0; met15 $\Delta$ 0; ura3 $\Delta$ 0) was used. In Publications I and IV, the toxicity profiles of Ag and CuO nanoparticles to the wild-type and its single-gene deletion mutants were compared. All the yeast strains were purchased from EUROSCARF (European *Saccharomyces cerevisiae* Archive for Functional Analysis website, <http://web.uni-frankfurt.de/fb15/mikro/euroscarf/>) and are listed in Table 2.

Table 2. The *Saccharomyces cerevisiae* BY4741 gene-deletion strains used in this study and the cellular role of the deleted gene product (from *The Saccharomyces Genome Database*, <https://www.yeastgenome.org>)

Strain	Cellular role of gene product	Publication
wild-type		I, II, III, IV
BY4741		
<i>yap1Δ</i>	Basic leucine zipper (bZIP) transcription factor; required for oxidative stress tolerance; activated by H <sub>2</sub> O <sub>2</sub> through the multistep formation of disulfide bonds and transit from the cytoplasm to the nucleus; mediates resistance to cadmium	I, IV
<i>sod1Δ</i>	Cytosolic copper-zinc superoxide dismutase; detoxifies superoxide; phosphorylated by Dun1p, enters nucleus under oxidative stress to promote transcription of stress response genes	I, IV
<i>ccs1Δ</i>	Copper chaperone for superoxide dismutase Sod1p; involved in oxidative stress protection; required for regulation of yeast copper genes in response to DNA-damaging agents	IV
<i>sod2Δ</i>	Mitochondrial manganese superoxide dismutase; protects cells against oxygen toxicity and oxidative stress	I, IV
<i>cta1Δ</i>	Catalase A; breaks down hydrogen peroxide in the peroxisomal matrix formed by acyl-CoA oxidase (Pox1p) during fatty acid beta-oxidation	IV
<i>ctt1Δ</i>	Cytosolic catalase T; has a role in protection from oxidative damage by hydrogen peroxide	IV
<i>gsh1Δ</i>	Gamma glutamylcysteine synthetase; catalyzes the first step in glutathione (GSH) biosynthesis; expression induced by oxidants, cadmium, and mercury	IV
<i>glr1Δ</i>	Cytosolic and mitochondrial glutathione oxidoreductase; converts oxidized glutathione to reduced glutathione;	IV
<i>cup2Δ</i>	Copper-binding transcription factor; activates transcription of the metallothionein genes CUP1-1 and CUP1-2 in response to elevated copper concentrations	IV

<i>end3Δ</i>	EH domain-containing protein involved in endocytosis; actin cytoskeletal organization and cell wall morphogenesis	I
<i>gas1Δ</i>	Beta-1,3-glucanoyltransferase; required for cell wall assembly and also has a role in transcriptional silencing; localizes to cell surface via a glycosylphosphatidylinositol (GPI) anchor	I
<i>erg3Δ</i>	C-5 sterol desaturase; glycoprotein that catalyzes the introduction of a C-5(6) double bond into episterol, a precursor in ergosterol biosynthesis	I
<i>mnn10Δ</i>	Subunit of a Golgi mannosyltransferase complex; complex mediates elongation of the polysaccharide mannan backbone; membrane protein of the mannosyltransferase family	I
<i>kre6Δ</i>	Type II integral membrane protein; required for beta-1,6 glucan biosynthesis; putative beta-glucan synthase; localizes to ER, plasma membrane, sites of polarized growth and secretory vesicles	I
<i>knr4Δ</i>	Protein involved in the regulation of cell wall synthesis; proposed to be involved in coordinating cell cycle progression with cell wall integrity	I

## 2.3 Toxicity tests

### 2.3.1 *Saccharomyces cerevisiae* growth inhibition assay

The *Saccharomyces cerevisiae* growth inhibition assay in YPD was used in Publications I and IV with slight differences. More detailed descriptions of the methods are given in the respective publications.

Briefly, *S. cerevisiae* BY4741 cells from an overnight culture in YPD medium (1% yeast extract, 2% peptone and 2% glucose, pH 6.8) were diluted to the culture density of  $\sim 2.0 \times 10^6$  CFU/mL. 75  $\mu$ L of the cell culture was added to 75  $\mu$ L of the tested chemical suspension or solution in 96-well microplates (Falcon). Original YPD medium was used for Publication IV, but for the growth inhibition assay in Publication I, YPD medium was diluted (YPD<sub>mod</sub>) to contain 0.25% yeast extract, 0.5% peptone and 1% glucose (pH 6.8). The diluted medium was used to reduce the effects of medium components on the bioavailability of Ag compounds. The 96-well microplates were incubated at 30°C and in the end of the incubation (24 or 48 h), the culture density was measured as the optical density at 600 nm wavelength (OD<sub>600nm</sub>). Nanoparticles dilutions in cell-free YPD or YPD<sub>mod</sub> were used as turbidity controls and the NPs

absorbance ( $OD_{600nm}$ ) was subtracted from the respective value of the biotic sample. The half-inhibitory concentration values ( $IC_{50}$ ) were calculated as the concentration of chemical that inhibited the growth of the yeast cells by 50% compared to the control (not exposed).

### 2.3.2 *Saccharomyces cerevisiae* cell viability test

The *Saccharomyces cerevisiae* cell viability test was applied in the Publications I, III and IV with slight modifications and more detailed descriptions of the methods can be found in the respective publications. In this test, the yeast cells were exposed to the chemicals and nanoparticles on 96-well microplates in deionized water ( $18 M\Omega$ , pH 5.6  $\pm 0.1$ , Milli-Q, Millipore) and at the end of the exposure, the cell viability was assessed using various methods: the fluorescein-diacetate fluorescence detection (Publication I), the measurement of ATP concentration (Publication IV), or the traditional colony-count method (Publication III). The  $IC_{50}$  values were calculated as the concentration of chemical that was lethal to 50% of the yeast cells compared to the control.

### 2.3.3 The ‘Spot test’

The ‘Spot test’ was introduced in the Publication IV with the yeast cells and developed further in Publication II extending the method also to the bacterial and algae cells, and the methods as well as the organisms used are described in more detail in the Publication II. Essentially, it is performed similarly to the yeast cell viability test (see section 2.3.2.), where the cells were exposed to chemicals and nanoparticles in deionized water on 96-well microplates. After the exposure (up to 24 h), 2–5  $\mu L$  of exposed and not-exposed (control) culture are pipetted onto toxicant-free agar growth medium plates and the viability is assessed as the colony-forming ability of the cells (Figure 5). The minimal biocidal concentration (MBC) is determined as the lowest tested concentration of the toxicant that completely inhibits the growth of the organism.

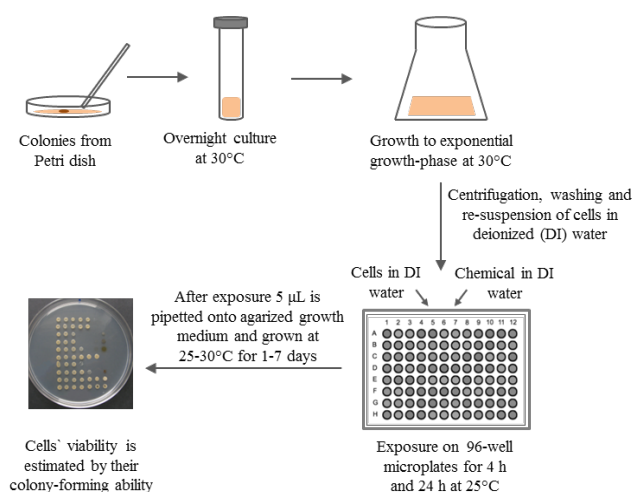


Figure 5. A schematic representation of the “Spot test” (Publication II).

### 3. RESULTS AND DISCUSSION

#### 3.1 Characterization of Ag and CuO NPs (Publications I and IV)

In this study, we investigated the nanoparticles of Ag and CuO, which are of interest due to their efficient antimicrobial properties. The characteristics of the Ag NPs and CuO nano- and bulk particles, which were studied in Publications I and IV are presented in Table 3.

*Table 3. The physicochemical characteristics of the studied CuO and Ag (nano)particles.*

NPs (coating)	nCuO	CuO bulk	nAg	nAg-col (casein)	nAg-PVP (polyvinylpyrrolidone)
Primary size, nm	30	Not available	86	13	8.0
<b>In DI</b>					
Hydrodynamic size, nm (0 h)	194	Not determined	104	43.3	100
Zeta potential, mV (0 h)	31.9	-13.1	-33.8	-35.3	-6.60
Dissolution, %* (24 h)	13	0.3	3.3	6.9	8.3
<b>In YPD**</b>					
Hydrodynamic size, nm (0 h)	5819	Not determined	251	43.7	84.6
Zeta potential, mV (0 h)	-15.6	-20.5	-27.2	-24.0	-5.00
Dissolution, %* (24/48 h***)	30	0.8	0.3	1.0	0.9

\*Dissolution of Ag NPs and CuO NPs, as quantified at near-IC<sub>50</sub> concentrations, \*\*Ag NPs were dispersed in ¼ YPD, \*\*\* CuO NPs dissolution was quantified at 24 h and Ag NPs dissolution at 48 h, representing the respective exposure times in the yeast growth inhibition tests.

The CuO nanoparticles immediately aggregated in deionized water and in the YPD medium, however, SEM imaging had previously shown that nano-sized particles were still present in the aqueous suspensions (Kahru et al. 2008). The zeta potential of bulk-CuO was similar in both test environments (-13...-20 mV), but the zeta potential of CuO NPs changed from +32 mV in DI water to -16 mV in YPD, which was probably due to the absorption of the growth medium components onto the surface of the CuO NPs.

Three different types of Ag NPs were studied. The uncoated Ag NPs were larger in primary size (~86 nm), but the casein-coated (nAg-col, collargol) and PVP-coated Ag NPs (nAg-PVP) were comparable in primary size (~10 nm). In DI water and YPD<sub>mod</sub>, the coated Ag NPs hydrodynamic diameters (D<sub>h</sub>) were ~40 nm (nAg-col) and 60-100 nm (nAg-PVP). Some of the increase in hydrodynamic size compared to the primary sizes can probably be attributed to the organic coatings, which are not visible by the transmission electron microscopy (TEM; used for the evaluation of NPs primary size). The uncoated Ag NPs (nAg) showed some agglomeration and precipitation in DI (average D<sub>h</sub> was 104 nm similarly to the coated Ag NPs, but the size distribution was wider than for the coated Ag NPs, and the polydispersity index higher; also UV-vis spectra indicated strong agglomeration and some precipitation was visible) and strong agglomeration with large aggregates in YPD<sub>mod</sub> (D<sub>h</sub> was 251 nm) and the agglomeration increased in time (48-h D<sub>h</sub> was 445 nm). Therefore, the coated Ag NPs were better dispersed in the test environment and thus, more bioavailable to the yeast cells.

The zeta potential of all the studied Ag NPs was negative in both test media, ranging from -5 mV to -35 mV.

Both, CuO and Ag NPs showed dissolution (release of ions) in the test environments (Table 3). The dissolution from the Ag NPs was greater in DI water compared to YPD<sub>mod</sub> medium, but on the contrary, the dissolution of CuO NPs was greater in YPD medium than in DI water.

### 3.2 Toxicity of CuO NPs to *Saccharomyces cerevisiae* BY4741 (Publication IV)

Cu compounds are known to have antibacterial properties and CuO NPs are developed for various purposes, including antiseptic applications. It is necessary to understand the mechanism of toxic action of CuO nanoparticles to avoid toxicity to humans but also for the efficient development of antibacterial and antifungal treatments.

This was one of the first studies on the toxicity of CuO NPs to the yeast *Saccharomyces cerevisiae*. The growth of *S. cerevisiae* BY4741 cells was measured, and their viability was assessed in the presence of CuO NPs with primary size ~30 nm. Comparatively, we assessed the effect of bulk CuO and the soluble salt CuSO<sub>4</sub>.

For the first time, a library of *S. cerevisiae* single-gene mutants was engaged to specifically address cellular processes which are thought to be of key importance in the cytotoxic effects of nanoparticles. To elucidate the role of oxidative stress and Cu<sup>2+</sup> ions in CuO NPs toxicity, 8 tentatively oxidative stress response-deficient *S. cerevisiae* deletion mutant strains (*yap1Δ*, *sod1Δ*, *sod2Δ*, *ccs1Δ*, *ctt1Δ*, *gsh1Δ*, *glr1Δ*, *cta1Δ*) and a copper stress response-deficient strain (*cup2Δ*) were used in the toxicity tests in comparison to the wild-type strain (Figure 6).

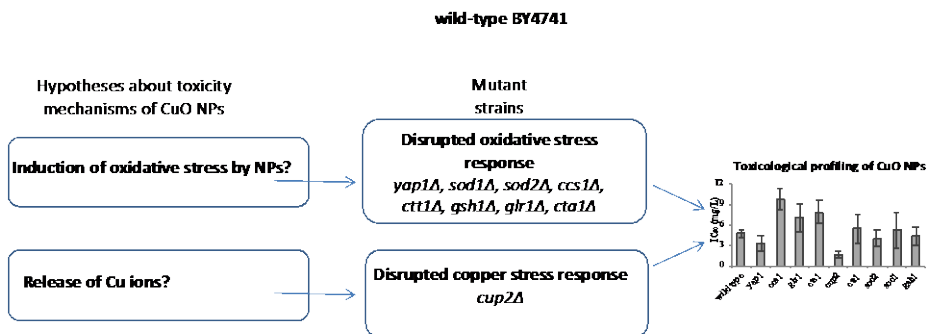


Figure 6. The selection of the *Saccharomyces cerevisiae* BY4741 single-gene deletion strains for the study of CuO NPs toxicity mechanisms was based on the hypotheses according to the literature.

### 3.2.1. Toxicity of CuO nano- and micro-sized (bulk) particles to *Saccharomyces cerevisiae* BY4741 wild-type cells

In both, the 24-h growth inhibition test in YPD medium and in the 24-h cell viability test in DI water at 30°C, the IC<sub>50</sub>-values show that CuO NPs were remarkably more toxic than the bulk CuO to *S. cerevisiae* BY4741 wild-type (wt) cells. The respective IC<sub>50</sub>-values for wt were 643 and >20000 mg/L in YPD and 4.8 and 155 mg/L in the DI water (Table 4).

The test format (medium) had an important influence on the toxicological outcome of copper compounds. The Cu ions as well as the CuO NPs and bulk CuO were remarkably more toxic (over 100 times) in the cell viability test in deionized water than the growth inhibition test in the YPD medium.

Table 4. Toxicity of bulk CuO and CuO nanoparticles, Cu ions (tested as CuSO<sub>4</sub>), menadione and hydrogen peroxide to *Saccharomyces cerevisiae* BY4741 in the 24-h growth inhibition test in YPD and in the 24-h cell viability test in deionized water (DI).

	24-h IC <sub>50</sub> in YPD (mg/L)	24-h IC <sub>50</sub> in DI (mg/L)
CuSO <sub>4</sub> (mg Cu/L)	516 ± 6.47	0.82 ± 0.32
CuO NPs	643 ± 52.0	4.80 ± 0.54
CuO bulk	>20 000	155 ± 38.7
Menadione	29.0 ± 4.05	37.1 ± 2.08
H <sub>2</sub> O <sub>2</sub>	85.2 ± 1.89	3.62 ± 0.42

### 3.2.2. Toxicity of CuO NPs to *Saccharomyces cerevisiae* BY4741 mutant strains: revealing the mechanisms of toxic action

The comparison of the toxicities of CuO nanoparticles, bulk particles and Cu ions to the wt and mutant strains showed that the *cup2Δ* mutant was the most sensitive strain in the cell viability test and the growth inhibition test (Figure 7). The Cup2p is a transcription factor regulating the expression of metallothioneins (Buchman et al. 1989) and the high sensitivity of the mutant strain to both, Cu ions and CuO nanoparticles suggests that the toxicity of CuO nanoparticles is caused by the dissolved Cu ion fraction.

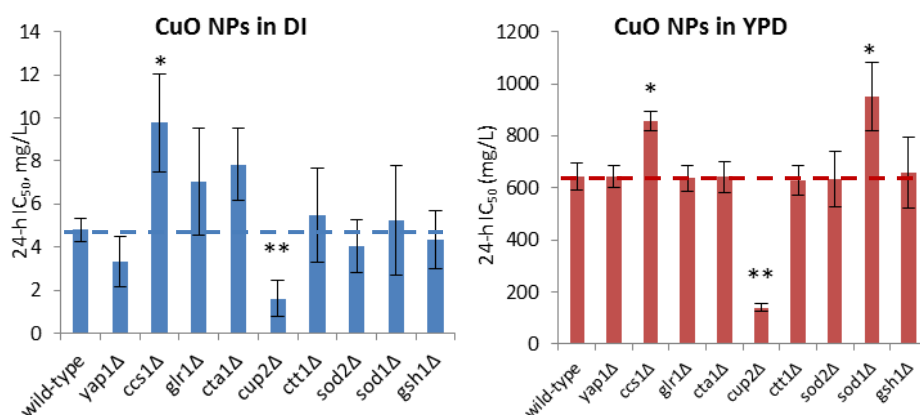


Figure 7. Toxicological profiling of *Saccharomyces cerevisiae* BY4741 wild-type (wt) and single-gene deletion mutants exposed to CuO NPs in deionized water (DI) or YPD medium. Note the different scales of Y-axis; single and double asterisks denote statistical difference from wt with 95% and 90% confidence, respectively; the dashed horizontal lines indicate the  $IC_{50}$  of the wt. Modified from Publication IV.

However, the menadione- (superoxide radical generator) and  $H_2O_2$ -sensitive strains (*yap1Δ*, *sod1Δ*, *sod2Δ*, and *ccs1Δ*) were not more sensitive to any of the tested Cu compounds. Although there is plenty of literature evidence of CuO nanoparticles and Cu ions triggering OS in both bacteria and mammalian cells, in this case our experimental data shows that the CuO nanoparticles and Cu ions did not cause toxicity to the cells via oxidative stress but by different mechanisms.

### 3.2.3. Analysis of dissolved copper in the toxicity tests

To elucidate the role of dissolved Cu fraction in the toxicity of CuO nanoparticles, we determined the concentration of solubilized Cu ions in the test conditions used for toxicity testing (in abiotic conditions, i.e., without cells) at the  $IC_{50}$  concentration of CuO NPs for the wild-type strain. In the viability test in deionized water the concentration of solubilized Cu-ions (~0.6 mg Cu/L) in CuO NPs suspension at the  $IC_{50wt}$  is comparable to the  $IC_{50wt}$  of  $CuSO_4$  (~0.8 mg Cu/L). Therefore, the toxicity of CuO NPs is mainly caused by the solubilized fraction of copper in the deionized water.

In YPD however, the concentration of solubilized Cu in CuO NPs suspensions at the IC<sub>50wt</sub> (~198 mg Cu/L) was much lower than the IC<sub>50</sub> of CuSO<sub>4</sub> (~516 mg Cu/L), which indicated that an additional fraction of copper (not detectable in abiotic conditions) causes the toxicity in YPD medium. Adsorption of the YPD medium proteins onto the surface of the CuO NPs possibly increased the particle-cell interactions and consequently solubility in the close vicinity of the cells or cellular uptake.

### 3.3 Toxicity of Ag NPs to *Saccharomyces cerevisiae* BY4741 (Publication I)

The toxicity and the underlying mechanisms of coated and uncoated Ag NPs to yeast *Saccharomyces cerevisiae* BY4741 was studied, using also a set of single-gene deletion mutants (Figure 8). In our previous work with CuO NPs, the OS response-deficient single-gene deletion mutants *yap1Δ*, *sod1Δ* and *sod2Δ* were the most sensitive to H<sub>2</sub>O<sub>2</sub> and menadione and therefore were selected for this study. Also, as the results with CuO NPs suggested that an adsorption of the NPs to the cell surface may have a role in the CuO NPs toxicity, we scanned the mutant strains with deletions in genes involved in cell wall/membrane integrity and maintenance for sensitivity toward sodium dodecyl sulfate (SDS) and the most sensitive strains (*gas1Δ*, *erg3Δ*, *end3Δ*, *mnn10Δ*, *kre6Δ*, *knr4Δ*) were included to the study of Ag nanoparticles` toxicity. Moreover, according to the literature data, Ag NPs and Ag ions may have the adverse effect on the cell wall and membrane integrity (Selvaraj et al. 2014). The *end3Δ* mutant strain represents a model to study the possible role of endocytosis in the Ag NPs toxicity, with a deletion in the END3 gene, which is required at the internalization step of endocytosis (Benedetti et al. 1994).

The toxicity was evaluated in two different test formats in different test media. The 48-h yeast growth inhibition test was conducted in a diluted YPD medium (YPD<sub>mod</sub>) to reduce the speciation of Ag compounds. The 24-h cell viability test was performed in deionized water.

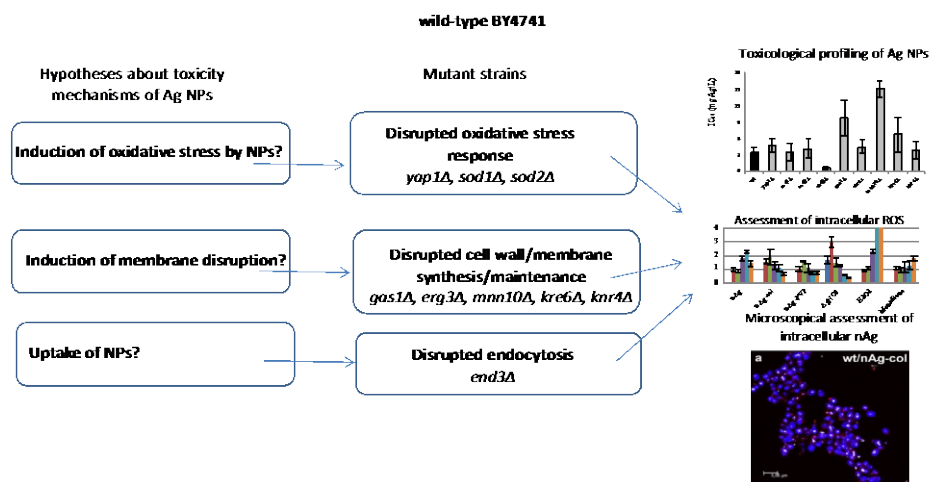


Figure 8. The selection of the *Saccharomyces cerevisiae* BY4741 single-gene deletion strains for the study of Ag NPs toxicity mechanisms was based on the hypotheses according to the literature and our previous study with CuO NPs.

### 3.3.1 Toxicity of coated and uncoated Ag NPs to *Saccharomyces cerevisiae* wild-type cells

The toxicity of the three different types of Ag NPs to *S. cerevisiae* BY4741 was compared to the toxicity of AgNO<sub>3</sub>, representing ionic silver control. The most toxic Ag compound in both test formats was AgNO<sub>3</sub>. Of the Ag NPs, both the coated Ag NPs were more toxic than the uncoated Ag NPs (Table 5).

All Ag compounds were 26-40 times more toxic to the wt strain in deionized water than in the YPD<sub>mod</sub>.

Table 5. Toxicity of Ag nanoparticles, AgNO<sub>3</sub>, sodium dodecyl sulfate (SDS) and hydrogen peroxide to *Saccharomyces cerevisiae* BY4741 wild-type cells in the 48-h growth inhibition test in YPD<sub>mod</sub> and in the 24-h cell viability test in deionized water (DI).

Chemicals	48-h IC <sub>50</sub> in YPD <sub>mod</sub> (mg/L)	24-h IC <sub>50</sub> in DI (mg/L)
AgNO <sub>3</sub> *	2.40 ± 0.30	0.09 ± 0.05
nAg*	576 ± 140	18.7 ± 3.41
nAg-col*	76.8 ± 22.8	2.71 ± 1.06
nAg-PVP*	148 ± 25.4	3.70 ± 0.79
SDS	1017 ± 162	1079 ± 137
H <sub>2</sub> O <sub>2</sub>	99.0 ± 7.73	11.8 ± 2.69

\*IC<sub>50</sub> values are given as mg Ag/L

### 3.3.2 Toxicity of coated and uncoated Ag NPs to *Saccharomyces cerevisiae* BY4741 single-gene deletion mutants

The IC<sub>50</sub> values of the mutant strains from both toxicity tests in DI water and YPD<sub>mod</sub> were compared to the respective IC<sub>50</sub> values for wild-type cells (Figure 9).

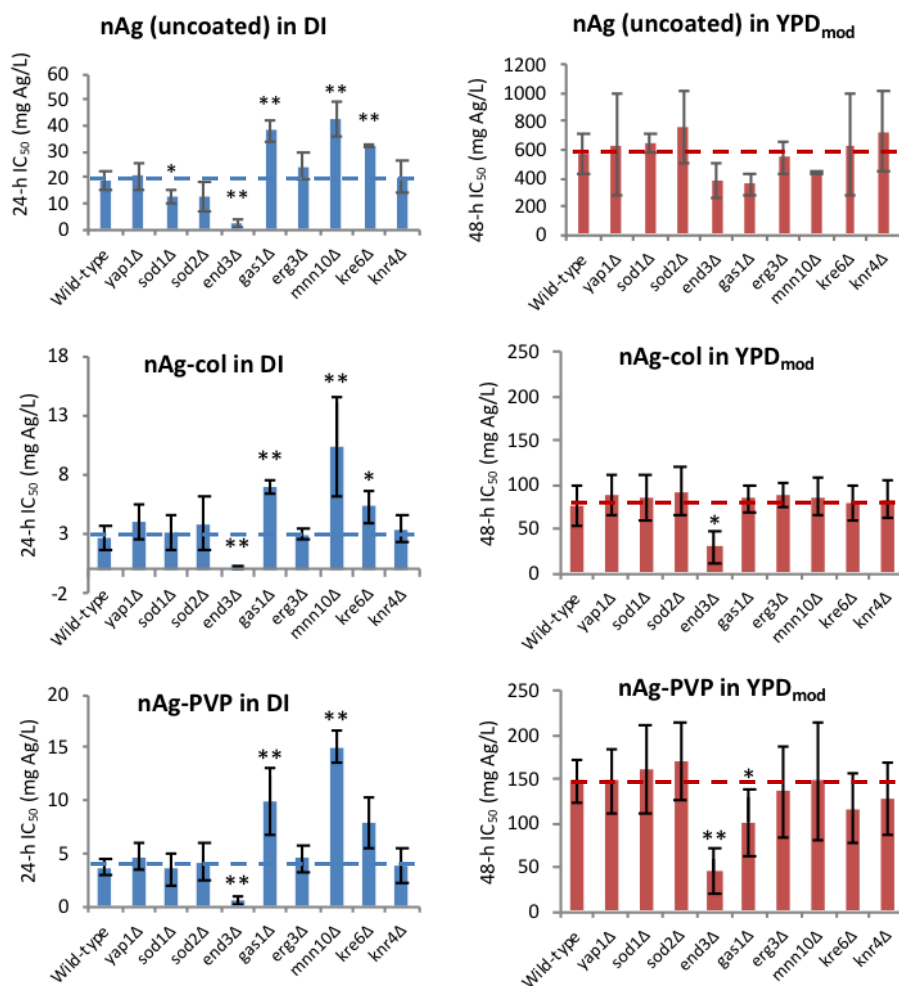


Figure 9. Toxicological profiling of *Saccharomyces cerevisiae* wild-type and single-gene deletion mutant strains exposed to  $\text{AgNO}_3$ , uncoated and coated Ag NPs in deionized water (DI) and  $\text{YPD}_{\text{mod}}$  medium. Note the different scale of Y-axis. Single and double asterisks denote statistical difference from wt with 95% and 90% confidence, respectively; the dashed horizontal lines indicate the  $\text{IC}_{50}$  of the wt. Modified from Publication I.

In the growth inhibition test in  $\text{YPD}_{\text{mod}}$  all the cell wall- or membrane-defective strains (*gas1Δ*, *erg3Δ*, *mnn10Δ*, *kre6Δ*, *knr4Δ*) were notably more sensitive than the wt strain to the membrane-solubilizing anionic detergent sodium dodecyl sulfate (SDS). Also, the *sod1Δ* and *end3Δ* strains were more sensitive than the wt to SDS. However, in the cell viability test in deionized water, only the *end3Δ*, *gas1Δ*, *erg3Δ* and *knr4Δ* showed increased sensitivity to SDS compared to the wt (Figure 3 in Publication I).

The OS response-defective strain *yap1Δ* was the most sensitive strain to the OS-inducing  $\text{H}_2\text{O}_2$  in the growth inhibition test and also the *sod2Δ* was more sensitive than the wt (Figure 3 in Publication I).

In general, the ROS-sensitive or the membrane stress-sensitive mutant strains did not show increased susceptibility compared to the wt to Ag-ions or the studied Ag NPs (Figure 9). These results suggest that the toxicity of Ag-ions and Ag NPs to the yeast *S. cerevisiae* BY4741 does not occur via the induction of oxidative stress or the permeabilization of the cell membrane.

The endocytosis-defective mutant *end3Δ* was statistically significantly the most sensitive mutant strain compared to wt to the coated Ag NPs (nAg-col and nAg-PVP), but also to H<sub>2</sub>O<sub>2</sub> and SDS. Contrarily to our hypothesis that the yeast cells with defective endocytosis would be more resistant to Ag NPs due to disrupted intracellular uptake of the particles, the *end3Δ* cells were instead more sensitive. The growth curve of the *end3Δ* strain in toxicant-free YPD<sub>mod</sub> showed no growth defect. Only very recently, a study was published, where the effect of Ag NPs was assessed on the whole genome-wide collection of *S. cerevisiae* strains (Galvan Marquez et al. 2018). The mutant strains most sensitive to Ag NPs had deletions in genes responsible for transcription and RNA processing, cellular respiration, and also in endocytosis and vesicular transport.

### 3.3.3 Assessment of intracellular ROS

To confirm the lack of the role of oxidative stress in the toxicity of Ag NPs to the yeast *S. cerevisiae* BY4741, we additionally used the 2',7'-dichlorodihydrofluorescein diacetate (H<sub>2</sub>DCF-DA) assay to measure the formation of intracellular ROS in the Ag NPs-exposed yeast cells (Figure 10). Some ROS was observed in cells exposed to 0.16 mg Ag/L AgNO<sub>3</sub>. Of the Ag NPs, the higher concentrations of uncoated nAg caused some increase in intracellular ROS only after 2-h exposure, but none was observed for the coated Ag NPs.

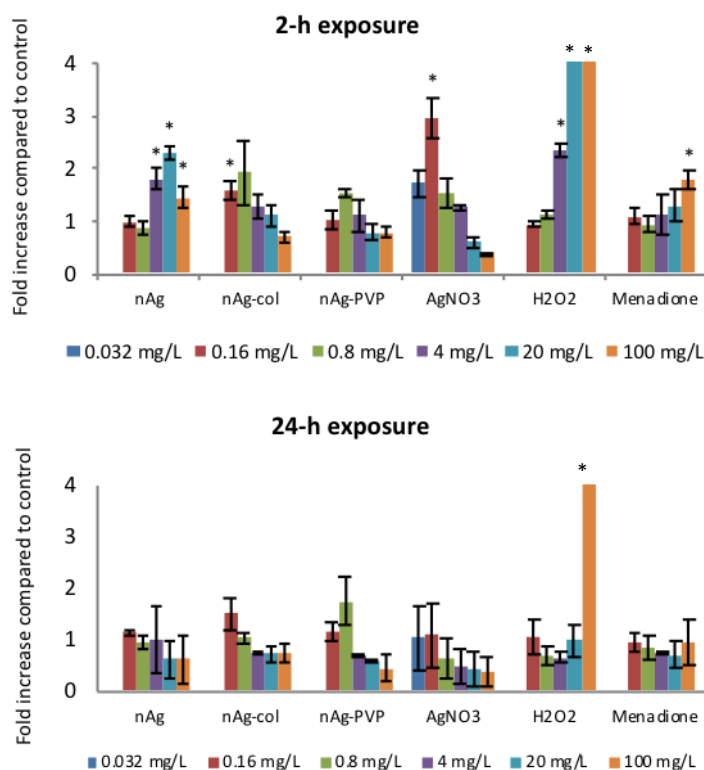


Figure 10. Intracellular ROS levels in *Saccharomyces cerevisiae* BY4741 wild-type cells after 2-h and 24-h exposure to Ag compounds and control chemicals in deionized water. Single and double asterisks denote statistical difference from wt with 95% and 90% confidence, respectively. Modified from Publication 1.

In conclusion, ~1.5-3-fold increase in the intracellular ROS was detected to the uncoated Ag NPs (nAg), casein-coated Ag NPs (nAg-col) and Ag ions (AgNO<sub>3</sub>) in yeast cells at the early stages of exposure (after 2 h), but no clear dose-dependent increase in intracellular ROS in Ag NPs-exposed cells occurred. After 24-h exposure the intracellular ROS in the Ag NPs exposed *S. cerevisiae* wt cells was not detectable. Therefore, the oxidative stress is probably not the main cause of Ag NPs toxicity in the yeast cells.

### 3.3.4 Assessment of the uptake of endocytosis marker Lucifer Yellow and Ag NPs into yeast cells using confocal laser scanning microscopy

To elucidate the role of cellular interactions or internalization in the toxicity of Ag NPs to yeast cells, confocal microscopy analysis of *S. cerevisiae* BY4741 wt and endocytosis-defective mutant strain *end3Δ* was performed. First, the absence of internalization of endocytosis marker Lucifer Yellow (LY) by *end3Δ* was confirmed (Figure 11). While LY was located inside all wild-type cells, *end3Δ* mutant cells did not exhibit intracellular LY fluorescence (some fluorescence not associated with cells can be seen). Therefore, we

confirmed the absence of endocytosis of the *end3Δ* mutant cells used in this study in our test conditions.

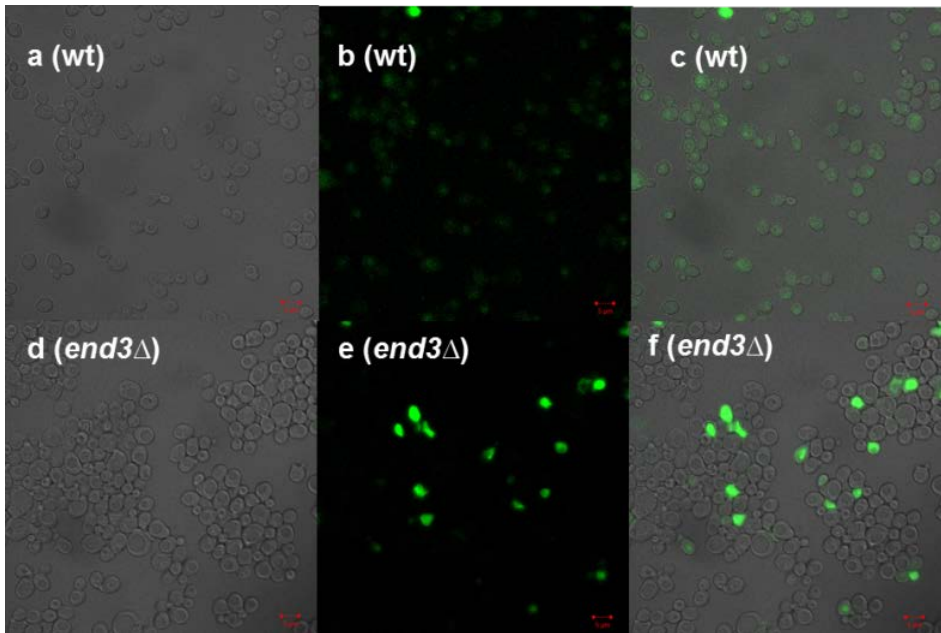


Figure 11. Confocal laser scanning microscopy images of *Saccharomyces cerevisiae* BY4741 wild-type (wt) (a-c) and *end3Δ* (d-f) strains after incubation with Lucifer Yellow for 2 h in YPD at 30°C. a, d – DIC images of cells; b, e - fluorescence of Lucifer Yellow; c, f – overlay of fluorescence and DIC images. Publication I, Supplementary material.

Finally, the uptake of nAg-col and nAg-PVP by wild-type and *end3Δ* mutant strain was assessed in YPD<sub>mod</sub> after 3-h exposure (Figure 12) by confocal microscopy. Cross-section analysis showed that nAg-col and nAg-PVP was detectable intracellularly in wild-type cells but not in *end3Δ* cells. In *end3Δ* cells the nAg-col was detectable near the surface of the cells (possible adsorption onto the cell surface). These results suggested that the coated Ag NPs were internalized by the End3p-mediated endocytosis in wt cells.

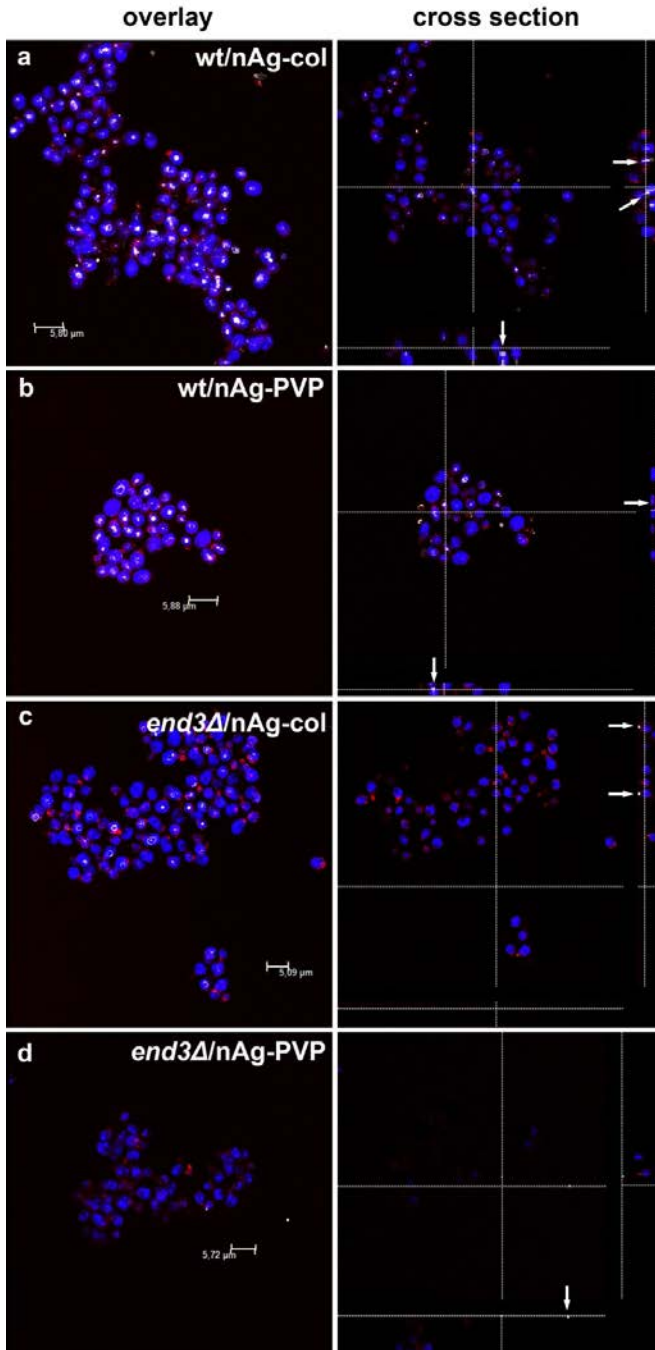


Figure 12. Uptake of coated Ag NPs nAg-col and nAg-PVP by wild-type (a and b) and end3 $\Delta$  mutant (c and d) incubated at sub-toxic concentration for 3 h in YPD<sub>mod</sub> at 30°C. Actin filaments were visualized with rhodamine-phalloidine staining (red), nuclei with DRAQ5™ (blue), and Ag NPs were visualized by laser reflection (white spots). White arrows on the cross-section pictures indicate to the Ag NPs. Publication I.

### 3.4 Size-dependent toxicity of Ag NPs to *Saccharomyces cerevisiae* BY4741 (Publication III)

To elucidate the effect of the Ag nanoparticles' size to their toxic effects, a homogenous set of citrate-coated Ag NPs (Ag-cit NPs) was used and the toxicity of 10-80 nm Ag-cit NPs to the yeast *Saccharomyces cerevisiae* BY4741 was assessed. The results showed that the toxicity increased with decreasing particle size (Figure 13, a). The 80-nm Ag-cit NPs caused the lowest toxicity, and the 10-nm Ag-cit NPs caused the highest toxicity, while the  $\text{AgNO}_3$  was still remarkably more toxic than even the 10-nm Ag-cit NPs.

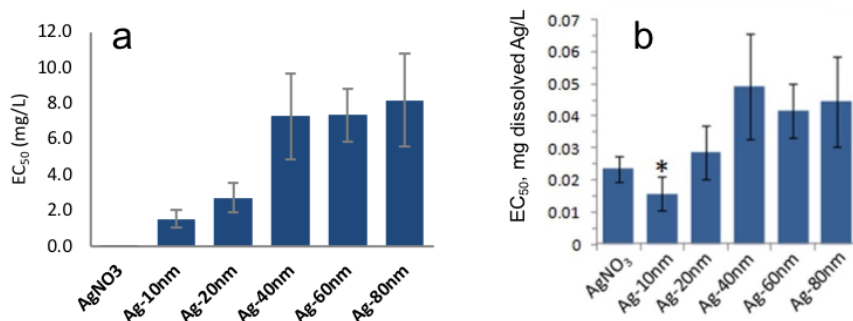


Figure 13. Effect of Ag ions and 10-80 nm citrate-stabilized Ag NPs on the viability of *Saccharomyces cerevisiae* BY4741 wild-type cells after 4-h exposure in deionized water (a) and dissolution-corrected  $\text{EC}_{50}$  values (b), asterisk denotes statistical difference from  $\text{EC}_{50}$  of  $\text{AgNO}_3$  with 95% confidence. Viability was determined by the colony-count method. Modified from Publication III.

The increase in toxicity of the smaller nanoparticles could be explained with higher dissolution compared to the larger nanoparticles. However, the 10-nm Ag-cit NPs proved to be more toxic than predictable from the soluble fraction of the NPs (Figure 13, b).

### 3.5 A novel method for the comparison of biocidal effects of metal-based nanoparticles to unicellular organisms bacteria, yeast and algae (Publication II)

Soluble metal compounds are subject to the influences of the test medium, such as complexing with organic molecules or salts. Therefore, for the comparison of the toxic potency of different metallic nanoparticles it is preferable to use the same test conditions (e.g., medium) for different organisms and also minimize the content of organic molecules (amino acids) and salts in the toxicity test environment, while retaining a suitable environment for the living organisms to maintain their viability. Nanoparticles are also known to interact with some components of cellular viability testing (e.g. lactate dehydrogenase or neutral red assay etc.) and interfere with the

assessment of optical density (Petersen et al. 2014), so the reliability of standard toxicity assays is a challenge for the evaluation of nanoparticles toxicity.

For this purpose, we developed a simple test strategy for evaluating the biocidal potency of different chemicals and nanomaterials to the colony-forming unicellular organisms, bacteria, yeast and alga (Publication II). The key aspect to this strategy is the exposure of the unicellular organisms to the toxic chemicals in deionized water, which is generally regarded as an unsuitable environment to living organisms due to the hypotonic conditions but has minimal effect on the bioavailability of metals.

As the test organisms, we chose seven different bacterial strains (both, Gram-negative and Gram-positive) to represent prokaryotic organisms, and two different eukaryotic microorganisms – yeast *Saccharomyces cerevisiae* BY4741 and the microalga *Pseudokirchneriella subcapitata*. Toxicity was determined as the minimum biocidal concentration (MBC), representing the lowest tested nominal concentration of the chemical which inhibited the formation of colonies on toxicant-free agar medium after the exposure. Assessment of the cells' colony-forming ability proved a reliable approach as the turbidity or the NPs samples does not interfere with the toxicity evaluation.

Because the biocidal effects of nanomaterials were the focus of developing this test, we tested two differently stabilized Ag NPs (nAg-PVP and nAg-Col), CuO NPs (nCuO) and TiO<sub>2</sub> NPs (Aeroxide® P25; nTiO<sub>2</sub>); and multi-wall carbon nanotubes (MWCNTs) were also included as a non-soluble nanomaterial. The biocidal effects of the Ag and CuO NPs were compared to the effects of the respective soluble metal salts AgNO<sub>3</sub> and CuSO<sub>4</sub>, and the commonly used biocidal positive controls 3,5-dichlorophenol, triclosan and H<sub>2</sub>O<sub>2</sub>.

### **3.5.1 Viability of cells in deionized water during toxicity test**

Deionized water is considered an unsuitable environment for living cells, but for the purposes of our toxicity testing, DI water was selected as the test “media” and before the application of the novel test, the viability of bacterial and yeast cells after incubation in deionized water for 24 h were evaluated. The colony-count method as well as live/dead staining with fluorescent viability dyes Fluorescein diacetate and Propidium iodide (Figures 14 and 15) revealed that there was no significant change in yeast and bacterial cell viability after incubation in deionized water for 24 h at 25°C.

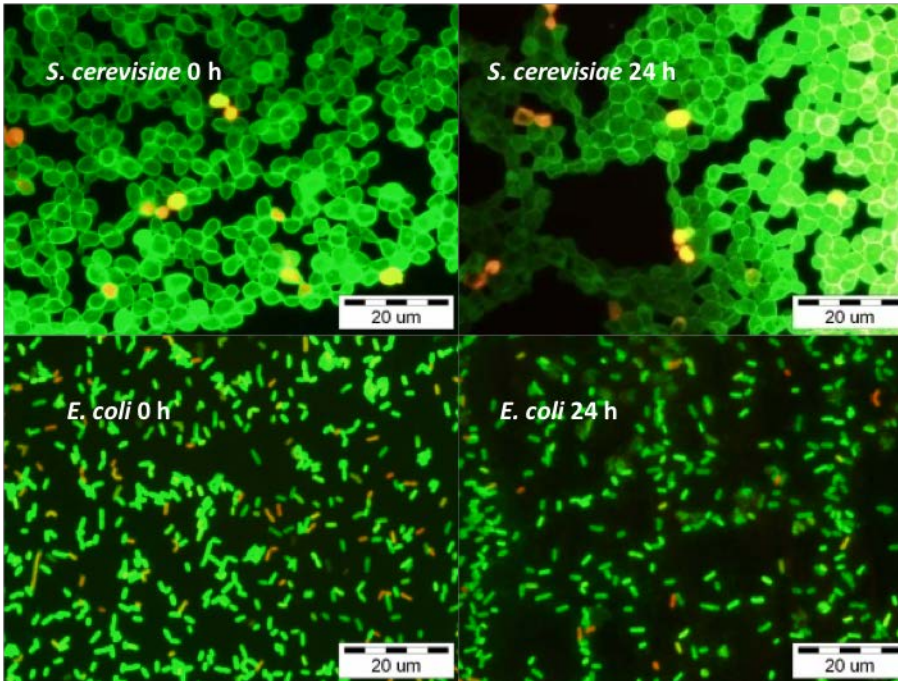


Figure 14. Representation of the viability of *Saccharomyces cerevisiae* BY4741 and *Escherichia coli* cells before and after the 24-h incubation in deionized water at 25°C. Modified from Publication II (Supplementary Material). The green-fluorescent cells represent viable cells (stained with Fluorescein diacetate) and the red-fluorescent cells represent dead cells (stained with Propidium iodide). The majority of the cell population is viable, both at the beginning (0 h) and end (24 h) of incubation in deionized water.

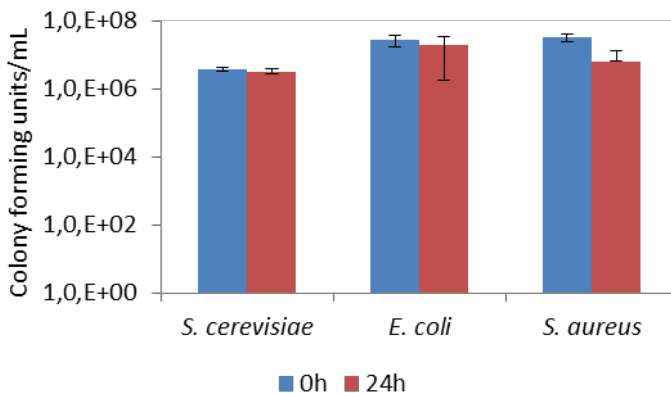


Figure 15. Number of cells (colony forming units/mL) in the control culture at the beginning (0 h) and end (24 h) of incubation in deionized water as determined by plating and counting the colonies of *Saccharomyces cerevisiae*, *Escherichia coli* (Gram-negative) and *Staphylococcus aureus* (Gram-positive). Modified from Publication II.

### 3.5.2 Biocidal potency of nanomaterials in deionized water and comparison with standard biocidal chemicals

In this test scenario, the nTiO<sub>2</sub> and MWCNTs in the highest tested concentrations (1000 mg/L and 250 mg/L, respectively) had almost no effect to the viability of the test organisms (Table 6). The only exceptions were *E. coli* and *Pseudomonas aeruginosa*, whose colony-forming ability was hindered after exposure to 1000 mg/L nTiO<sub>2</sub>. To specify, in this test, the exposure was conducted in the dark, i. e. without photo-activation, which is probably the main reason to the low toxicity of nTiO<sub>2</sub>.

The nanoparticles of Ag and CuO had the highest biocidal activity, whereas Ag NPs were generally more toxic than CuO NPs. The 24-h minimum biocidal concentration (MBC) for the two different Ag NPs ranged from 0.1-10 mg Ag/L among the bacteria and 1-10 mg Ag/L for *S. cerevisiae* and *P. subcapitata*. The nCuO 24-h MBC ranged from 1 to 100 mg CuO/L for the bacteria and from 10 to 1000 mg CuO/L for *S. cerevisiae* and *P. subcapitata*. In general, the eukaryotic organisms yeast and microalga were slightly less susceptible to the tested compounds than the bacteria, although not in all cases. Also, the Gram-positive bacteria were slightly less susceptible than the Gram-negative bacteria.

In order to highlight the impact of the test medium to the toxicity of metal-based nanomaterials, we performed the conventional broth microdilution test in comparison. After exposure to the test compounds in ½ Mueller-Hinton Broth (bacteria) or in ½ YPD (yeast) medium, the growth-ability was tested on the respective toxicant-free agar medium. The MBC for the organic compounds 3,5-DCP, triclosan and H<sub>2</sub>O<sub>2</sub> as well as for nTiO<sub>2</sub> and MWCNTs were generally similar after exposures in DI water or growth medium, with the difference up to 10 times. But for the Ag and Cu NPs and soluble salts the differences in the results of the two test environments were remarkable. The metal-based nanoparticles were 10-10 000 times more toxic in DI water compared to the growth medium.

Table 6. Minimum biocidal concentration (MBC) of the nanoparticles and control chemicals to the tested unicellular organisms after 24-h exposure in deionized water at 25°C and in ½ YPD (for yeast) and ½ cation-adjusted Mueller-Hinton Broth at 30°C. Modified from Publication II.

Chemicals, concentration unit	MBC								
	Yeast			Bacteria				Alga	
	<i>S. cerevisiae</i> BY4741	<i>E. coli</i> MG1655 (G-)	<i>S. aureus</i> RN4220 (G+)	<i>P. fluorescens</i> OS8 (G-)	<i>P. aeruginosa</i> DS10-129 (G-)	<i>Janthinobacterium</i> sp(G-)	<i>P. fluorescens</i> KC-1 (G-)	<i>M. testaceum</i> PCSB7 (G+)	<i>P. subcapitata</i>
MBC after 24-h exposure in DI									
3,5-DCP, mg/L	1000	100	100	100	100	100	100	100	100
Triclosan <sup>a</sup> , mg/L	1000	100	100	>1000	>1000	100	1000	100	1000
H <sub>2</sub> O <sub>2</sub> , mg/L	1000	100	1000	10	1000	100	100	1000	1000
AgNO <sub>3</sub> , mg Ag/L	1	0.1	1	1	0.1	0.1	0.1	1	10
nAg-PVP, mg Ag/L	1	0.1	1	1	1	0.1	1	1	10
nAg-Col, mg Ag/L	10	0.1	1	1	1	1	1	10	10
CuSO <sub>4</sub> , mg Cu/L	10	1	0.1	1	1	1	1	10	10
nCuO, mg/L	1000	10	1	1	1	10	10	100	10
nTiO <sub>2</sub> <sup>a</sup> , mg/L	>1000	1000	>1000	>1000	1000	>1000	>1000	>1000	>1000
MWCNTs <sup>a</sup> , mg/L	>250	>250	>250	>250	>250	>250	>250	>250	>250
MBC after 20- or 24-h exposure in growth medium									
3,5-DCP, mg/L	100	1000	1000						
Triclosan <sup>a</sup> , mg/L	1000	1000	1000						
H <sub>2</sub> O <sub>2</sub> , mg/L	1000	100	100						
AgNO <sub>3</sub> , mg Ag/L	10	100	100						
nAg-PVP, mg Ag/L	10	100	1000						
nAg-Col, mg Ag/L	1000	100	1000						
CuSO <sub>4</sub> , mg Cu/L	1000	1000	1000						
nCuO, mg/L	>1000	>1000	>1000						
nTiO <sub>2</sub> <sup>a</sup> , mg/L	>1000	>1000	>1000						
MWCNTs <sup>a</sup> , mg/L	>250	>250	>250						
									Not tested

## CONCLUSIONS

In this Thesis, the mechanisms of toxicity of Ag and CuO NPs to the yeast *Saccharomyces cerevisiae* BY4741 were studied. The novel aspect in this study was the use of *S. cerevisiae* BY4741 single-gene mutants to elucidate the role of dissolved ions, oxidative stress, cell wall/membrane damage and endocytosis in the toxicity of Ag and CuO NPs.

Our results showed, that

- Solubilisation of Ag and CuO NPs was driving the toxicity of Ag and CuO NPs to *S. cerevisiae*
- The toxic effect of 10, 20, 40, 60 and 80 nm Ag NPs to *S. cerevisiae* was size-dependent, however, dissolution explained the toxicity of 20-80 nm Ag NPs, but the 10 nm Ag NPs were more toxic than expected,
- Generation of ROS and oxidative stress was not the main mechanism of action of Ag and CuO NPs to *S. cerevisiae*,
- Ag NPs did not cause the permeabilization/disturbance of cell wall/membrane as observed for the surfactant SDS to cell wall/membrane components synthesis-defective single-gene deletion mutants,
- Ag NPs were taken up by *S. cerevisiae* cells via End3p-mediated endocytosis
- Contrarily to our initial hypothesis, mutant yeast cells lacking End3p-mediated endocytosis were more susceptible to toxic effects of Ag NPs than wild-type cells,
- Due to the speciation of Ag ions and Cu ions in most of the conventional toxicity testing media, the choice of test medium had a remarkable effect on the toxicity of Ag and CuO NPs. We showed that the use of deionized water as a non-complexing test medium enabled the comparison of the toxicities of different types of chemicals and nanoparticles (including metal-based NPs) to different bacteria, yeasts and algae.

In conclusion, the use of *S. cerevisiae* single-gene mutant collection is a valuable tool in the study of toxicity mechanisms of NPs. The uptake and endocytosis of NPs by the *S. cerevisiae* cells should be further studied, to elucidate the role of particle internalization in the toxic effects of NPs to the yeast cells.

## ACKNOWLEDGEMENTS

I am very grateful to my supervisors, Dr Kaja Kasemets and Dr Anne Kahru, who during my PhD studies have given me kind support and guidance, encouragement and advice and served as great examples of women in science.

I thank my co-supervisor Prof. Andres Õpik for helpfulness and attention during my studies.

I thank all the members of Laboratory of Environmental Toxicology (NICPB) for friendly environment, cooperation and words of wisdom.

I would also like to thank my family for their support and patience.

This study was carried out in the Laboratory of Environmental Toxicology of National Institute of Chemical Physics and Biophysics, Tallinn, Estonia (Head of the Lab Dr. Anne Kahru; supervisor Dr. K. Kasemets).

This study was financially supported by the Estonian Science Foundation Grants ETF9001, ETF7686, ETF8561, , ETF9347, the Institutional funding IUT 23-5 of the Estonian Ministry of Education and Research, Estonian target funding project SF0690063s08, European Regional Development Fund project TERIKVANT, EU FP7 Project NanoValid under Grant Agreement No. 263147, EU FP7 Project MODERN under Grant Agreement No. 309314, the United Kingdom Medical Research Council, Unit Programme No. U105960399, and the grant of Fondazione Cariplo to the project OverNanoTox (2013-0987).

This work has been partially supported by ASTRA “TUT Institutional Development Programme for 2016-2022” Graduate School of Functional Materials and Technologies (2014-2020.4.01.16-0032).

## ABSTRACT

### Toxicological Profiling of Silver and Copper Oxide Nanoparticles on *Saccharomyces cerevisiae* BY4741 Wild-Type and its Single-Gene Deletion Mutants

Silver and CuO NPs have shown great promise as antimicrobial agents and are being developed as antibacterial, antifungal and algacidal products. Ag and CuO NPs have high potency in the inhibition of microbes, while providing an alternative to common drugs that may have problems with toxicity to patients and the growing microbial resistance. It is important to understand the toxic effects and cellular interactions of the nanoparticles to ensure effective and safe NPs-based applications for consumer and medicinal use.

This research was carried out to elucidate the toxicity mechanism of Ag and CuO NPs to the yeast *Saccharomyces cerevisiae*. *S. cerevisiae* served as both, the model eukaryotic cell as well as fungal model. The main aim was to identify the link between the physical-chemical parameters of the Ag and CuO NPs and their toxic effects to *S. cerevisiae*. CuO NPs were studied in comparison with bulk CuO, and uncoated as well as differently coated (casein- and polyvinylpyrrolidone-coated) Ag NPs were studied. Two different toxicity test formats were used: the yeast growth inhibition assay in the rich growth medium YPD and the yeast cell viability test in deionized water (DI). We used the single-gene deletion mutants of *S. cerevisiae* BY4741 to test the most common hypotheses about the toxicity mechanisms of Ag and CuO NPs. Mutants with deletions in specific genes were selected to investigate the role of metal ions (*cup2Δ*), oxidative stress (*yap1Δ*, *sod1Δ*, *ccs1Δ*, *sod2Δ*, *cta1Δ*, *ctt1Δ*, *gsh1Δ*, *glr1Δ*), cell wall/membrane damage (*gas1Δ*, *erg3Δ*, *mnn10Δ*, *kre6Δ*, *knr4Δ*) and endocytosis (*end3Δ*) in the toxicity.

Our results showed that dissolution of Ag and CuO NPs played the crucial role in the NPs toxicity, including the size-dependent toxicity of Ag NPs. However, the toxicity of the smallest, 10-nm Ag NPs could not be explained only by the dissolved fraction of silver and the quantification of the dissolved fraction of Cu also indicated, that in the YPD medium, additional toxicity was caused by the particulate effects. The additional toxicity was explained by the possible adsorption of Ag or CuO NPs on the cells, which led to increased local ionic stress. Toxicity profiling of oxidative stress-sensitive mutant strains revealed that Ag and CuO NPs did not cause oxidative stress to *S. cerevisiae*. Also, cell wall/membrane permeabilization was not the main cause of toxicity of Ag NPs, as indicated by the mutant strains. However, endocytosis appeared to play a role in the toxicity of Ag NPs, as the endocytosis-defective mutant strain *end3Δ* was significantly more sensitive to the Ag NPs compared to the wild-type. Additional experiments displayed the internalization of casein- and PVP-coated Ag NPs by the wild-type *S. cerevisiae* cells but not the *end3Δ* mutant by confocal laser scanning microscopy.

In this work we also proposed a novel test strategy for testing the biocidal efficiency of NPs against bacteria, yeast and alga, by using deionized water as a non-modulating test environment for metal-based NPs. DI water was selected as the test medium to have a minimal effect on the properties of metal-based nanoparticles and we also showed by the colony-count method and by fluorescent viability staining that there was no decrease in the viability of bacterial and yeast cells during 24-h incubation.

## KOKKUVÕTE

### Hõbeda ja vaskoksiidi nanoosakeste toksilisuse iseloomustamine pärmi *Saccharomyces cerevisiae* BY4741 metsiktüvele ning geenikatkestusmutantidele

Hõbeda (Ag) ja vask-oksiidi (CuO) nanoosakesed (NO) on paljulubavad antimikroobsed ained ning neid kasutatakse bakterite, seente ning vetikate kasvu pidurdavate toodete väljatöötamises. Ag ja CuO nanoosakestel on tugev mikroobide-vastane efektiivsus ning nad võiksid olla alternatiiviks tavapärastele antimikroobsetele ühenditele, mille probleemiks on toksilisus patsientidele ning antibiootikumi-resistentsete mikroobide teke ja levik. Oluline on mõista NO võimalikke toksilisi mõjusid ja interaktsioone rakkudega, et luua nanoosakestel põhinevaid materjale, mida saaks kasutada nii tarbekaupades kui ka meditsiinilisteks rakendusteks.

Käesolev uurimistöö viidi läbi selleks, et välja selgitada Ag ning CuO nanoosakeste toksilisuse mehhanismid pärmile *Saccharomyces cerevisiae*. *S. cerevisiae* kasutati selles töös nii eukarüootse raku kui ka seeneraku mudelina. Peamiseks töö eesmärgiks oli hinnata, kuidas Ag ja CuO NO füüsikalised-keemilised parameetrid mõjutavad nende toksilisi efekte *S. cerevisiae* rakkudele. CuO NO võrreldi tavaliselt CuO osakestega ning uuriti nii ilma katteta kui ka kaetud (kaseiini- ning polüvinüülpirrolidooni-kattega) Ag NO. Kasutati kaht erinevat test-formaati: pärmi kasvu inhibitsiooni testi rikkas YPD kasvusöötmes ning pärmiraku elulevuse määramist deioniseeritud (DI) vee keskkonnas. Antud töös kasutati *S. cerevisiae* BY4741 geenikatkestus-mutante, et testida kirjanduses levinumaid hüpoteese Ag ja CuO nanoosakeste toksilisuse mehhanismide kohta. Valiti välja sellised mutantsed pärmitüved, millel oli katkestus spetsiifilistes geenides, mis muutsid need mutantsed tüved tundlikumaks metalli-ioonide (*cup2Δ*), oksüdatiivse stressi (*yap1Δ*, *sod1Δ*, *ccs1Δ*, *sod2Δ*, *cta1Δ*, *ctt1Δ*, *gsh1Δ*, *glr1Δ*) ja rakukesta/membraani kahjustuste suhtes (*gas1Δ*, *erg3Δ*, *mnn10Δ*, *kre6Δ*, *knr4Δ*). Lisaks testiti ka endotsütoosi-defektset *S. cerevisiae* BY4741 tüve (*end3Δ*), et välja selgitada endotsütoosi rolli uuritavate nanoosakeste raku sisenemisel ja toksilisuses.

Saadud tulemused näitasid, Ag ja CuO NO lahustuvus on antud nanoosakeste üks peamisi toksilisuse mehhanisme. Näitasime, et Ag NO suurusest (10, 20, 40, 60 ja 80 nm) sõltuv toksilisus oli eelkõige põhjustatud nende erinevast lahustuvusest testikeskkonnas - väiksemad osakesed olid toksilisemad ja samas ka lahustuvad. Siiski, 10-nm suuruste Ag nanoosakeste toksilisust *S. cerevisiae* rakkudele ei olnud võimalik ära seletada ainult Ag NO lahustuvusega testikeskkonnas. Lahustunud Cu fraktsiooni määramine viitas samuti sellele, et rikkas kasvusöötmes põhjustavad CuO nanoosakesed täiendavaid toksilisi efekte. Üheks hüpoteesiks oli, et antud täiendava toksilisuse põhjuseks võis olla Ag või CuO nanoosakeste adsorbeerumine rakupinnale või sisenemine raku, põhjustades täiendavat lokaalset ionset stressi. Oksüdatiivse stressi suhtes tundlike mutantide võrdlemine metsiktüvega näitas, et Ag ja CuO nanoosakeste toksilisuse põhjuseks *S. cerevisiae* rakkudele ei olnud oksüdatiivne stress. Katsed rakukesta või -membraani geenide katkestusmutantidega näitasid, et Ag nanoosakeste toksilisus ei olnud põhjustatud ka rakukesta permeabiliseerimisest. Selgus aga, et Ag nanoosakeste toksilisuses oli oluline roll endotsütoosil, kuna endotsütoos-negatiivne pärmitüvi *end3Δ* oli Ag nanoosakeste suhtes oluliselt tundlikum

võrreldes metsiktüüpi pärmirakkudega. Konfokaal-mikroskoopia katsete tulemusena näidati kaseiini- ning PVP-kattega Ag nanoosakeste sisenemist metsiktüüpi pärmirakkudesse, kuid mitte *end3Δ* tüve rakkudesse.

Lisaks töötati antud uurimistöös välja uudne meetod biotsiidsete nanoosakeste efektiivsuse määramiseks bakteri-, pärimi- ning vetikarakkudele, kasutades testkeskkonnaks deioniseeritud (DI) vett. DI vesi avaldab vähe mõju metallidel põhinevate nanoosakeste omadustele, ning samas näitasime ka kolooniate loendamise meetodil ning fluorestseeruvate elulevusräividega, et bakteri- ja pärmirakkude elulevus 24 h jooksul DI vees ei langenud.

## LITERATURE REFERENCES

- Ahonen, M., Kahru, A., Ivask, A., Kasemets, K., Kõljalg, S., Mantecca, P., Vinković Vrček, I., Keinänen-Toivola, M. M., and Crijns, F. 2017. "Proactive Approach for Safe Use of Antimicrobial Coatings in Healthcare Settings: Opinion of the COST Action Network AMiCI." *International Journal of Environmental Research and Public Health* no. 14 (4):366. doi: 10.3390/ijerph14040366.
- Alexander, J. W. 2009. "History of the medical use of silver." *Surg Infect (Larchmt)* no. 10 (3):289-92. doi: 10.1089/sur.2008.9941.
- Amde, M., Liu, J. F., Tan, Z. Q., and Bekana, D. 2017. "Transformation and bioavailability of metal oxide nanoparticles in aquatic and terrestrial environments. A review." *Environ Pollut* no. 230:250-267. doi: 10.1016/j.envpol.2017.06.064.
- Aruoja, V., Pokhrel, S., Sihtmae, M., Mortimer, M., Madler, L., and Kahru, A. 2015. "Toxicity of 12 metal-based nanoparticles to algae, bacteria and protozoa." *Environmental Science: Nano* no. 2 (6):630-644. doi: 10.1039/C5EN00057B.
- Bao, S., Lu, Q., Fang, T., Dai, H., and Zhang, C. 2015. "Assessment of the toxicity of CuO nanoparticles by using *Saccharomyces cerevisiae* mutants with multiple genes deleted." *Appl Environ Microbiol* no. 81 (23):8098-107. doi: 10.1128/aem.02035-15.
- Bayat, N., Rajapakse, K., Marinsek-Logar, R., Drobne, D., and Cristobal, S. 2014. "The effects of engineered nanoparticles on the cellular structure and growth of *Saccharomyces cerevisiae*." *Nanotoxicology* no. 8 (4):363-73. doi: 10.3109/17435390.2013.788748.
- Benedetti, H., Raths, S., Crausaz, F., and Riezman, H. 1994. "The END3 gene encodes a protein that is required for the internalization step of endocytosis and for actin cytoskeleton organization in yeast." *Mol Biol Cell* no. 5 (9):1023-37.
- Bird, A. J. 2015. "Cellular sensing and transport of metal ions: implications in micronutrient homeostasis." *J Nutr Biochem* no. 26 (11):1103-15. doi: 10.1016/j.jnutbio.2015.08.002.
- Blinova, I., Niskanen, J., Kajankari, P., Kanarbiik, L., Käkinen, A., Tenhu, H., Penttinen, O. P., and Kahru, A. 2013. "Toxicity of two types of silver nanoparticles to aquatic crustaceans *Daphnia magna* and *Thamnocephalus platyurus*." *Environ. Sci. Pollut. Res. Int.* no. 20 (5):3456-63. doi: 10.1007/s11356-012-1290-5.
- Bondarenko, O., Ivask, A., Käkinen, A., Kurvet, I., and Kahru, A. 2013a. "Particle-cell contact enhances antibacterial activity of silver nanoparticles." *PLoS One* no. 8 (5):e64060. doi: 10.1371/journal.pone.0064060.
- Bondarenko, O., Juganson, K., Ivask, A., Kasemets, K., Mortimer, M., and Kahru, A. 2013b. "Toxicity of Ag, CuO and ZnO nanoparticles to selected environmentally relevant test organisms and mammalian cells in vitro: a critical review." *Arch Toxicol* no. 87 (7):1181-1200. doi: 10.1007/s00204-013-1079-4.
- Bowman, S. M., and Free, S. J. 2006. "The structure and synthesis of the fungal cell wall." *Bioessays* no. 28 (8):799-808. doi: 10.1002/bies.20441.
- Buchman, C., Skroch, P., Welch, J., Fogel, S., and Karin, M. 1989. "The CUP2 gene product, regulator of yeast metallothionein expression, is a copper-activated DNA-binding protein." *Mol Cell Biol* no. 9 (9):4091-5.

- Cavassin, E. D., de Figueiredo, L. F., Otoch, J. P., Seckler, M. M., de Oliveira, R. A., Franco, F. F., Marangoni, V. S., Zucolotto, V., Levin, A. S., and Costa, S. F. 2015. "Comparison of methods to detect the in vitro activity of silver nanoparticles (AgNP) against multidrug resistant bacteria." *J Nanobiotechnology* no. 13:64. doi: 10.1186/s12951-015-0120-6.
- Chairuangkitti, P., Lawanprasert, S., Roytrakul, S., Aueviriyavit, S., Phummiratch, D., Kulthong, K., Chanvorachote, P., and Maniratanachote, R. 2013. "Silver nanoparticles induce toxicity in A549 cells via ROS-dependent and ROS-independent pathways." *Toxicol In Vitro* no. 27 (1):330-8. doi: 10.1016/j.tiv.2012.08.021.
- Chaloupka, K., Malam, Y., and Seifalian, A. M. 2010. "Nanosilver as a new generation of nanoparticle in biomedical applications." *Trends Biotechnol* no. 28 (11):580-8. doi: 10.1016/j.tibtech.2010.07.006.
- Coll, C., Notter, D., Gottschalk, F., Sun, T., Som, C., and Nowack, B. 2016. "Probabilistic environmental risk assessment of five nanomaterials (nano-TiO<sub>2</sub>, nano-Ag, nano-ZnO, CNT, and fullerenes)." *Nanotoxicology* no. 10 (4):436-44. doi: 10.3109/17435390.2015.1073812.
- Costa, V., and Moradas-Ferreira, P. 2001. "Oxidative stress and signal transduction in *Saccharomyces cerevisiae*: insights into ageing, apoptosis and diseases." *Mol Aspects Med* no. 22 (4-5):217-46.
- Cronholm, P., Karlsson, H. L., Hedberg, J., Lowe, T. A., Winnberg, L., Elihn, K., Wallinder, I. O., and Moller, L. 2013. "Intracellular uptake and toxicity of Ag and CuO nanoparticles: a comparison between nanoparticles and their corresponding metal ions." *Small* no. 9 (7):970-82. doi: 10.1002/smll.201201069.
- Djurisic, A. B., Leung, Y. H., Ng, A. M., Xu, X. Y., Lee, P. K., Degger, N., and Wu, R. S. 2015. "Toxicity of metal oxide nanoparticles: mechanisms, characterization, and avoiding experimental artefacts." *Small* no. 11 (1):26-44. doi: 10.1002/smll.201303947.
- Dunne, C. P., Keinanen-Toivola, M. M., Kahru, A., Teunissen, B., Olmez, H., Gouveia, I., Melo, L., Murzyn, K., Modic, M., Ahonen, M., Askew, P., Papadopoulos, T., Adlhart, C., and Crijns, F. R. L. 2017. "Anti-microbial coating innovations to prevent infectious diseases (AMiCI): Cost action ca15114." *Bioengineered* no. 8 (6):679-685. doi: 10.1080/21655979.2017.1323593.
- El Badawy, A. M., Silva, R. G., Morris, B., Scheckel, K. G., Suidan, M. T., and Tolaymat, T. M. 2011. "Surface charge-dependent toxicity of silver nanoparticles." *Environ Sci Technol* no. 45 (1):283-7. doi: 10.1021/es1034188.
- Fadeel, B., Fornara, A., Toprak, M. S., and Bhattacharya, K. 2015. "Keeping it real: The importance of material characterization in nanotoxicology." *Biochem Biophys Res Commun* no. 468 (3):498-503. doi: 10.1016/j.bbrc.2015.06.178.
- Foster, H. A., Ditta, I. B., Varghese, S., and Steele, A. 2011. "Photocatalytic disinfection using titanium dioxide: spectrum and mechanism of antimicrobial activity." *Appl Microbiol Biotechnol* no. 90 (6):1847-68. doi: 10.1007/s00253-011-3213-7.
- Gadd, G. M. 1993. "Interactions of fungi with toxic metals." *New Phytologist* no. 124:25-60.

- Galvan Marquez, I., Ghiyasvand, M., Massarsky, A., Babu, M., Samanfar, B., Omid, K., Moon, T. W., Smith, M. L., and Golshani, A. 2018. "Zinc oxide and silver nanoparticles toxicity in the baker's yeast, *Saccharomyces cerevisiae*." *PLoS One* no. 13 (3):e0193111. doi: 10.1371/journal.pone.0193111.
- Gliga, A. R., Skoglund, S., Wallinder, I. O., Fadeel, B., and Karlsson, H. L. 2014. "Size-dependent cytotoxicity of silver nanoparticles in human lung cells: the role of cellular uptake, agglomeration and Ag release." *Part Fibre Toxicol* no. 11:11. doi: 10.1186/1743-8977-11-11.
- Gogoi, S. K., Gopinath, P., Paul, A., Ramesh, A., Ghosh, S. S., and Chattopadhyay, A. 2006. "Green fluorescent protein-expressing *Escherichia coli* as a model system for investigating the antimicrobial activities of silver nanoparticles." *Langmuir* no. 22 (22):9322-8. doi: 10.1021/la060661v.
- Goode, B. L., Eskin, J. A., and Wendland, B. 2015. "Actin and endocytosis in budding yeast." *Genetics* no. 199 (2):315-58. doi: 10.1534/genetics.112.145540.
- Gottschalk, F., Sun, T., and Nowack, B. 2013. "Environmental concentrations of engineered nanomaterials: review of modeling and analytical studies." *Environ Pollut* no. 181:287-300. doi: 10.1016/j.envpol.2013.06.003.
- Hartig, S. M., Greene, R. R., DasGupta, J., Carlesso, G., Dikov, M. M., Prokop, A., and Davidson, J. M. 2007. "Multifunctional nanoparticulate polyelectrolyte complexes." *Pharm Res* no. 24 (12):2353-69. doi: 10.1007/s11095-007-9459-1.
- Hartung, T., and Sabbioni, E. 2011. "Alternative in vitro assays in nanomaterial toxicology." *Wiley Interdiscip Rev Nanomed Nanobiotechnol* no. 3 (6):545-73. doi: 10.1002/wnan.153.
- Heinlaan, M., Ivask, A., Blinova, I., Dubourguier, H.-C., and Kahru, A. 2008. "Toxicity of nanosized and bulk ZnO, CuO and TiO<sub>2</sub> to bacteria *Vibrio fischeri* and crustaceans *Daphnia magna* and *Thamnocephalus platyurus*." *Chemosphere* no. 71 (7):1308-16. doi: 10.1016/j.chemosphere.2007.11.047.
- Horie, M., Fujita, K., Kato, H., Endoh, S., Nishio, K., Komaba, L. K., Nakamura, A., Miyauchi, A., Kinugasa, S., Hagihara, Y., Niki, E., Yoshida, Y., and Iwahashi, H. 2012. "Association of the physical and chemical properties and the cytotoxicity of metal oxide nanoparticles: metal ion release, adsorption ability and specific surface area." *Metallomics* no. 4 (4):350-60. doi: 10.1039/c2mt20016c.
- Hosiner, D., Gerber, S., Lichtenberg-Frate, H., Glaser, W., Schuller, C., and Klipp, E. 2014. "Impact of acute metal stress in *Saccharomyces cerevisiae*." *PLoS One* no. 9 (1):e83330. doi: 10.1371/journal.pone.0083330.
- Hughes, T. R. 2002. "Yeast and drug discovery." *Funct Integr Genomics* no. 2 (4-5):199-211. doi: 10.1007/s10142-002-0059-1.
- Hwang, I. S., Lee, J., Hwang, J. H., Kim, K. J., and Lee, D. G. 2012. "Silver nanoparticles induce apoptotic cell death in *Candida albicans* through the increase of hydroxyl radicals." *Febs j* no. 279 (7):1327-38. doi: 10.1111/j.1742-4658.2012.08527.x.
- ISO. 2015. "Nano- technologies-Vocabulary-Part 1: Core Terms." *International Organization for Standardization* no. TS 80004-1:2015.

- Ivask, A., Bondarenko, O., Jepihhina, N., and Kahru, A. 2010. "Profiling of the reactive oxygen species-related ecotoxicity of CuO, ZnO, TiO<sub>2</sub>, silver and fullerene nanoparticles using a set of recombinant luminescent *Escherichia coli* strains: differentiating the impact of particles and solubilised metals." *Analytical and Bioanalytical Chemistry* no. 398 (2):701-716. doi: 10.1007/s00216-010-3962-7.
- Ivask, A., El Badawy, A., Kaweeteerawat, C., Boren, D., Fischer, H., Ji, Z., Chang, C. H., Liu, R., Tolaymat, T., Telesca, D., Zink, J. I., Cohen, Y., Holden, P. A., and Godwin, H. 2014a. "Toxicity Mechanisms in *Escherichia coli* Vary for Silver Nanoparticles and Differ from Ionic Silver." *ACS Nano* no. in press.
- Ivask, A., Juganson, K., Bondarenko, O., Mortimer, M., Aruoja, V., Kasemets, K., Blinova, I., Heinlaan, M., Slaveykova, V., and Kahru, A. 2014b. "Mechanisms of toxic action of Ag, ZnO and CuO nanoparticles to selected ecotoxicological test organisms and mammalian cells in vitro: a comparative review." *Nanotoxicology* no. 8 Suppl 1:57-71. doi: 10.3109/17435390.2013.855831.
- Ivask, A., Suarez, E., Patel, T., Boren, D., Ji, Z., Holden, P., Telesca, D., Damoiseaux, R., Bradley, K. A., and Godwin, H. 2012. "Genome-wide bacterial toxicity screening uncovers the mechanisms of toxicity of a cationic polystyrene nanomaterial." *Environ Sci Technol* no. 46 (4):2398-405. doi: 10.1021/es203087m.
- Ivask, A., Titma, T., Visnapuu, M., Vija, H., Kallinen, A., Sihtmae, M., Pokhrel, S., Madler, L., Heinlaan, M., Kisand, V., Shimmo, R., and Kahru, A. 2015. "Toxicity of 11 Metal Oxide Nanoparticles to Three Mammalian Cell Types In Vitro." *Curr Top Med Chem* no. 15 (18):1914-29.
- Iversen, T.-G., Skotland, T., and Sandvig, K. 2011. "Endocytosis and intracellular transport of nanoparticles: Present knowledge and need for future studies." *Nano Today* no. 6 (2):176-185. doi: <https://doi.org/10.1016/j.nantod.2011.02.003>.
- Jamieson, D. J. 1998. "Oxidative stress responses of the yeast *Saccharomyces cerevisiae*." *Yeast* no. 14 (16):1511-27. doi: 10.1002/(sici)1097-0061(199812)14:16<1511::aid-yea356>3.0.co;2-s.
- Jo, W. J., Loguinov, A., Chang, M., Wintz, H., Nislow, C., Arkin, A. P., Giaever, G., and Vulpe, C. D. 2008. "Identification of genes involved in the toxic response of *Saccharomyces cerevisiae* against iron and copper overload by parallel analysis of deletion mutants." *Toxicol Sci* no. 101 (1):140-51. doi: 10.1093/toxsci/kfm226.
- Jones, N., Ray, B., Ranjit, K. T., and Manna, A. C. 2008. "Antibacterial activity of ZnO nanoparticle suspensions on a broad spectrum of microorganisms." *FEMS Microbiol Lett* no. 279 (1):71-6. doi: 10.1111/j.1574-6968.2007.01012.x.
- Kahru, A., and Dubourguier, H.-C. 2010. "From ecotoxicology to nanoecotoxicology." *Toxicology* no. 269 (2-3):105-119. doi: DOI: 10.1016/j.tox.2009.08.016.
- Kahru, A., Dubourguier, H.-C., Blinova, I., Ivask, A., and Kasemets, K. 2008. "Biotests and biosensors for ecotoxicology of metal oxide nanoparticles: A minireview." *Sensors* no. 8:5153 - 5170.
- Kahru, A., and Ivask, A. 2013. "Mapping the Dawn of Nanoecotoxicological Research." *Acc Chem Res* no. 46 (3):823-833. doi: 10.1021/ar3000212.
- Karlsson, H. L., Cronholm, P., Gustafsson, J., and Moller, L. 2008. "Copper oxide nanoparticles are highly toxic: a comparison between metal oxide nanoparticles and carbon nanotubes." *Chem Res Toxicol* no. 21 (9):1726-32. doi: 10.1021/tx800064j.

- Karlsson, H. L., Cronholm, P., Hedberg, Y., Tornberg, M., De Battice, L., Svedhem, S., and Wallinder, I. O. 2013. "Cell membrane damage and protein interaction induced by copper containing nanoparticles--importance of the metal release process." *Toxicology* no. 313 (1):59-69. doi: 10.1016/j.tox.2013.07.012.
- Kasemets, K., Ivask, A., Dubourguier, H.-C., and Kahru, A. 2009. "Toxicity of nanoparticles of ZnO, CuO and TiO<sub>2</sub> to yeast *Saccharomyces cerevisiae*." *Toxicology in Vitro* no. 23 (6):1116-1122. doi: DOI: 10.1016/j.tiv.2009.05.015.
- Kasemets, K., Nisamedtinov, I., Laht, T. M., Abner, K., and Paalme, T. 2007. "Growth characteristics of *Saccharomyces cerevisiae* S288C in changing environmental conditions: auxo-accelerostat study." *Antonie Van Leeuwenhoek* no. 92 (1):109-28. doi: 10.1007/s10482-007-9141-y.
- Keller, A. A., Adeleye, A. S., Conway, J. R., Garner, K. L., Zhao, L., Cherr, G. N., Hong, J., Gardea-Torresdey, J. L., Godwin, H. A., Hanna, S., Ji, Z., Kaweeteerawat, C., Lin, S., Lenihan, H. S., Miller, R. J., Nel, A. E., Peralta-Videa, J. R., Walker, S. L., Taylor, A. A., Torres-Duarte, C., Zink, J. I., and Zuverza-Mena, N. 2017. "Comparative environmental fate and toxicity of copper nanomaterials." *NanoImpact* no. 7:28-40. doi: <https://doi.org/10.1016/j.impact.2017.05.003>.
- Keller, A. A., McFerran, S., Lazareva, A., and Suh, S. 2013. "Global life cycle releases of engineered nanomaterials." *Journal of Nanoparticle Research* no. 15 (6):1692. doi: 10.1007/s11051-013-1692-4.
- Kettler, K., Veltman, K., van de Meent, D., van Wezel, A., and Hendriks, A. J. 2014. "Cellular uptake of nanoparticles as determined by particle properties, experimental conditions, and cell type." *Environ Toxicol Chem* no. 33 (3):481-92. doi: 10.1002/etc.2470.
- Kim, K.-J., Sung, W., Suh, B., Moon, S.-K., Choi, J.-S., Kim, J., and Lee, D. . 2009. "Antifungal activity and mode of action of silver nano-particles on *Candida albicans*." *BioMetals* no. 22 (2):235-242. doi: 10.1007/s10534-008-9159-2.
- Korshed, P., Li, L., Liu, Z., and Wang, T. 2016. "The Molecular Mechanisms of the Antibacterial Effect of Picosecond Laser Generated Silver Nanoparticles and Their Toxicity to Human Cells." *PLoS One* no. 11 (8):e0160078. doi: 10.1371/journal.pone.0160078.
- Käkinen, A., Bondarenko, O., Ivask, A., and Kahru, A. 2011. "The Effect of Composition of Different Ecotoxicological Test Media on Free and Bioavailable Copper from CuSO<sub>4</sub> and CuO Nanoparticles: Comparative Evidence from a Cu-Selective Electrode and a Cu-Biosensor." *Sensors* no. 11:10502-10521.
- Lai, R. W. S., Yeung, K. W. Y., Yung, M. M. N., Djurisic, A. B., Giesy, J. P., and Leung, K. M. Y. 2018. "Regulation of engineered nanomaterials: current challenges, insights and future directions." *Environ Sci Pollut Res Int* no. 25 (4):3060-3077. doi: 10.1007/s11356-017-9489-0.
- Lakshmi Prasanna, V., and Vijayaraghavan, R. 2015. "Insight into the Mechanism of Antibacterial Activity of ZnO: Surface Defects Mediated Reactive Oxygen Species Even in the Dark." *Langmuir* no. 31 (33):9155-62. doi: 10.1021/acs.langmuir.5b02266.

- Lara, H. H., Romero-Urbina, D. G., Pierce, C., Lopez-Ribot, J. L., Arellano-Jimenez, M. J., and Jose-Yacamán, M. 2015. "Effect of silver nanoparticles on *Candida albicans* biofilms: an ultrastructural study." *J Nanobiotechnology* no. 13:91. doi: 10.1186/s12951-015-0147-8.
- Lee, A. R., Lee, S. J., Lee, M., Nam, M., Lee, S., Choi, J., Lee, H. J., Kim, D. U., and Hoe, K. L. 2018. "Editor's Highlight: A Genome-wide Screening of Target Genes Against Silver Nanoparticles in Fission Yeast." *Toxicol Sci* no. 161 (1):171-185. doi: 10.1093/toxsci/kfx208.
- Lee, C. R., Cho, I. H., Jeong, B. C., and Lee, S. H. 2013. "Strategies to minimize antibiotic resistance." *Int J Environ Res Public Health* no. 10 (9):4274-305. doi: 10.3390/ijerph10094274.
- Lemire, J. A., Harrison, J. J., and Turner, R. J. 2013. "Antimicrobial activity of metals: mechanisms, molecular targets and applications." *Nat Rev Microbiol* no. 11 (6):371-84. doi: 10.1038/nrmicro3028.
- Levard, C., Hotze, E. M., Lowry, G. V., and Brown, G. E., Jr. 2012. "Environmental transformations of silver nanoparticles: impact on stability and toxicity." *Environ Sci Technol* no. 46 (13):6900-14. doi: 10.1021/es2037405.
- Levine, B., and Klionsky, D. J. 2017. "Autophagy wins the 2016 Nobel Prize in Physiology or Medicine: Breakthroughs in baker's yeast fuel advances in biomedical research." *Proc Natl Acad Sci U S A* no. 114 (2):201-205. doi: 10.1073/pnas.1619876114.
- Limbach, L. K., Wick, P., Manser, P., Grass, R. N., Bruinink, A., and Stark, W. J. 2007. "Exposure of engineered nanoparticles to human lung epithelial cells: influence of chemical composition and catalytic activity on oxidative stress." *Environ Sci Technol* no. 41 (11):4158-63.
- Lok, C.-N., Ho, C.-M., Chen, R., He, Q.-Y., Yu, W.-Y., Sun, H., Tam, P., Chiu, J.-F., and Che, C.-M. 2007. "Silver nanoparticles: partial oxidation and antibacterial activities." *Journal of Biological Inorganic Chemistry* no. 12 (4):527-534. doi: 10.1007/s00775-007-0208-z.
- Love, S. A., Maurer-Jones, M. A., Thompson, J. W., Lin, Y. S., and Haynes, C. L. 2012. "Assessing nanoparticle toxicity." *Annu Rev Anal Chem (Palo Alto Calif)* no. 5:181-205. doi: 10.1146/annurev-anchem-062011-143134.
- Maillard, J. Y., and Hartemann, P. 2013. "Silver as an antimicrobial: facts and gaps in knowledge." *Crit Rev Microbiol* no. 39 (4):373-83. doi: 10.3109/1040841x.2012.713323.
- Manke, A., Wang, L., and Rojanasakul, Y. 2013. "Mechanisms of nanoparticle-induced oxidative stress and toxicity." *Biomed Res Int* no. 2013:942916. doi: 10.1155/2013/942916.
- Mantecca, P., Kasemets, K., Deokar, A., Perelshtein, I., Gedanken, A., Bahk, Y. K., Kianfar, B., and Wang, J. 2017. "Airborne Nanoparticle Release and Toxicological Risk from Metal-Oxide-Coated Textiles: Toward a Multiscale Safe-by-Design Approach." *Environ Sci Technol* no. 51 (16):9305-9317. doi: 10.1021/acs.est.7b02390.
- Martinez-Gutierrez, F., Olive, P. L., Banuelos, A., Orrantia, E., Nino, N., Sanchez, E. M., Ruiz, F., Bach, H., and Av-Gay, Y. 2010. "Synthesis, characterization, and evaluation of antimicrobial and cytotoxic effect of silver and titanium nanoparticles." *Nanomedicine* no. 6 (5):681-8. doi: 10.1016/j.nano.2010.02.001.

- Massarsky, A., Trudeau, V. L., and Moon, T. W. 2014. "Predicting the environmental impact of nanosilver." *Environ Toxicol Pharmacol* no. 38 (3):861-73. doi: 10.1016/j.etap.2014.10.006.
- McGillicuddy, E., Murray, I., Kavanagh, S., Morrison, L., Fogarty, A., Cormican, M., Dockery, P., Prendergast, M., Rowan, N., and Morris, D. 2017. "Silver nanoparticles in the environment: Sources, detection and ecotoxicology." *Sci Total Environ* no. 575:231-246. doi: 10.1016/j.scitotenv.2016.10.041.
- McMahon, H. T., and Boucrot, E. 2011. "Molecular mechanism and physiological functions of clathrin-mediated endocytosis." *Nat Rev Mol Cell Biol* no. 12 (8):517-33. doi: 10.1038/nrm3151.
- McQuillan, J. S., Infante, H. G., Stokes, E., and Shaw, A. M. 2012. "Silver nanoparticle enhanced silver ion stress response in Escherichia coli K12." *Nanotoxicology* no. 6:857-66. doi: 10.3109/17435390.2011.626532.
- McShan, D., Ray, P. C., and Yu, H. 2014. "Molecular toxicity mechanism of nanosilver." *J Food Drug Anal* no. 22 (1):116-127. doi: 10.1016/j.jfda.2014.01.010.
- Misra, S. K., Dybowska, A., Berhanu, D., Luoma, S. N., and Valsami-Jones, E. 2012. "The complexity of nanoparticle dissolution and its importance in nanotoxicological studies." *Sci Total Environ* no. 438:225-32. doi: 10.1016/j.scitotenv.2012.08.066.
- Moradas-Ferreira, P., Costa, V., Piper, P., and Mager, W. 1996. "The molecular defences against reactive oxygen species in yeast." *Mol Microbiol* no. 19 (4):651-8.
- Morones, J. R., Elechiguerra, J. L., Camacho, A., Holt, K., Kouri, J. B., Ramirez, J. T., and Yacaman, M. J. 2005. "The bactericidal effect of silver nanoparticles." *Nanotechnology* no. 16 (10):2346-53. doi: 10.1088/0957-4484/16/10/059.
- Mukherjee, S. G., O'Claonadh, N., Casey, A., and Chambers, G. 2012. "Comparative in vitro cytotoxicity study of silver nanoparticle on two mammalian cell lines." *Toxicol In Vitro* no. 26 (2):238-51. doi: 10.1016/j.tiv.2011.12.004.
- Munn, A. L., Stevenson, B. J., Geli, M. I., and Riezman, H. 1995. "end5, end6, and end7: mutations that cause actin delocalization and block the internalization step of endocytosis in Saccharomyces cerevisiae." *Mol Biol Cell* no. 6 (12):1721-42.
- Neal, A. L. 2008. "What can be inferred from bacterium-nanoparticle interactions about the potential consequences of environmental exposure to nanoparticles?" *Ecotoxicology* no. 17 (5):362-71. doi: 10.1007/s10646-008-0217-x.
- Nel, A. E., Madler, L., Velegol, D., Xia, T., Hoek, E. M. V., Somasundaran, P., Klaessig, F., Castranova, V., and Thompson, M. 2009. "Understanding biophysicochemical interactions at the nano-bio interface." *Nat Mater* no. 8 (7):543-557.
- Nel, A., Xia, T., Mädler, L., and Li, N. 2006. "Toxic Potential of Materials at the Nanolevel." *Science* no. 311 (5761):622-627. doi: 10.1126/science.1114397.
- Niazi, J. H., Sang, B. I., Kim, Y. S., and Gu, M. B. 2011. "Global gene response in Saccharomyces cerevisiae exposed to silver nanoparticles." *Appl Biochem Biotechnol* no. 164 (8):1278-91. doi: 10.1007/s12010-011-9212-4.
- Nomura, T., Kuriyama, Y., Tokumoto, H., and Konishi, Y. 2015. "Cytotoxicity of functionalized polystyrene latex nanoparticles toward lactic acid bacteria, and comparison with model microbes." *Journal of Nanoparticle Research* no. 17 (2):105. doi: 10.1007/s11051-015-2922-8.

- Nomura, T., Miyazaki, J., Miyamoto, A., Kuriyama, Y., Tokumoto, H., and Konishi, Y. 2013. "Exposure of the yeast *Saccharomyces cerevisiae* to functionalized polystyrene latex nanoparticles: influence of surface charge on toxicity." *Environ Sci Technol* no. 47 (7):3417-23. doi: 10.1021/es400053x.
- Oberdorster, G., Maynard, A., Donaldson, K., Castranova, V., Fitzpatrick, J., Ausman, K., Carter, J., Karn, B., Kreyling, W., Lai, D., Olin, S., Monteiro-Riviere, N., Warheit, D., and Yang, H. 2005a. "Principles for characterizing the potential human health effects from exposure to nanomaterials: elements of a screening strategy." *Part Fibre Toxicol* no. 2:8. doi: 10.1186/1743-8977-2-8.
- Oberdorster, G., Oberdorster, E., and Oberdorster, J. 2005b. "Nanotoxicology: an emerging discipline evolving from studies of ultrafine particles." *Environ Health Perspect* no. 113 (7):823-39.
- Orlean, P. 2012. "Architecture and biosynthesis of the *Saccharomyces cerevisiae* cell wall." *Genetics* no. 192 (3):775-818. doi: 10.1534/genetics.112.144485.
- Pal, S., Tak, Y. K., and Song, J. M. 2007. "Does the antibacterial activity of silver nanoparticles depend on the shape of the nanoparticle? A study of the Gram-negative bacterium *Escherichia coli*." *Appl Environ Microbiol* no. 73 (6):1712-20. doi: 10.1128/aem.02218-06.
- Panacek, A., Kolar, M., Vecerova, R., Pucek, R., Soukupova, J., Krystof, V., Hamal, P., Zboril, R., and Kvittek, L. 2009. "Antifungal activity of silver nanoparticles against *Candida* spp." *Biomaterials* no. 30 (31):6333-40. doi: 10.1016/j.biomaterials.2009.07.065.
- Petersen, E. J., Henry, T. B., Zhao, J., MacCuspie, R. I., Kirschling, T. L., Dobrovolskaia, M. A., Hackley, V., Xing, B., and White, J. C. 2014. "Identification and avoidance of potential artifacts and misinterpretations in nanomaterial ecotoxicity measurements." *Environ Sci Technol* no. 48 (8):4226-46. doi: 10.1021/es4052999.
- Piccinno, F., Gottschalk, F., Seeger, S., and Nowack, B. 2012. "Industrial production quantities and uses of ten engineered nanomaterials in Europe and the world." *J Nanopart Res* no. 14 (9):1-11. doi: 10.1007/s11051-012-1109-9.
- Pietrojusti, A., Campagnolo, L., and Fadeel, B. 2013. "Interactions of engineered nanoparticles with organs protected by internal biological barriers." *Small* no. 9 (9-10):1557-72. doi: 10.1002/smll.201201463.
- Prescianotto-Baschong, C., and Riezman, H. 1998. "Morphology of the yeast endocytic pathway." *Mol Biol Cell* no. 9 (1):173-89.
- Pronk, J. T., Yde Steensma, H., and Van Dijken, J. P. 1996. "Pyruvate metabolism in *Saccharomyces cerevisiae*." *Yeast* no. 12 (16):1607-33. doi: 10.1002/(SICI)1097-0061(199612)12:16<1607::AID-YEA70>3.0.CO;2-4.
- Robbins, N., Wright, G. D., and Cowen, L. E. 2016. "Antifungal Drugs: The Current Armamentarium and Development of New Agents." *Microbiol Spectr* no. 4 (5). doi: 10.1128/microbiolspec.FUNK-0002-2016.
- Sabella, S., Carney, R. P., Brunetti, V., Malvindi, M. A., Al-Juffali, N., Vecchio, G., Janes, S. M., Bakr, O. M., Cingolani, R., Stellacci, F., and Pompa, P. P. 2014. "A general mechanism for intracellular toxicity of metal-containing nanoparticles." *Nanoscale* no. 6 (12):7052-61. doi: 10.1039/c4nr01234h.

- Schrand, A. M., Rahman, M. F., Hussain, S. M., Schlager, J. J., Smith, D. A., and Syed, A. F. 2010. "Metal-based nanoparticles and their toxicity assessment." *Wiley Interdiscip Rev Nanomed Nanobiotechnol* no. 2 (5):544-68. doi: 10.1002/wnan.103.
- Seil, J. T., and Webster, T. J. 2012. "Antimicrobial applications of nanotechnology: methods and literature." *Int J Nanomedicine* no. 7:2767-81. doi: 10.2147/ijn.s24805.
- Selvaraj, M., Pandurangan, P., Ramasami, N., Rajendran, S. B., Sangilimuthu, S. N., and Perumal, P. 2014. "Highly potential antifungal activity of quantum-sized silver nanoparticles against *Candida albicans*." *Appl Biochem Biotechnol* no. 173 (1):55-66. doi: 10.1007/s12010-014-0782-9.
- Simon-Deckers, A., Loo, S., Mayne-L'hermite, M., Herlin-Boime, N., Menguy, N., Reynaud, C., Gouget, B., and Carriere, M. 2009. "Size-, composition- and shape-dependent toxicological impact of metal oxide nanoparticles and carbon nanotubes toward bacteria." *Environ Sci Technol* no. 43 (21):8423-9. doi: 10.1021/es9016975.
- Slavin, Y. N., Asnis, J., Hafeli, U. O., and Bach, H. 2017. "Metal nanoparticles: understanding the mechanisms behind antibacterial activity." *J Nanobiotechnology* no. 15 (1):65. doi: 10.1186/s12951-017-0308-z.
- Sun, M., Yu, Q., Liu, M., Chen, X., Liu, Z., Zhou, H., Yuan, Y., Liu, L., Li, M., and Zhang, C. 2014. "A novel toxicity mechanism of CdSe nanoparticles to *Saccharomyces cerevisiae*: enhancement of vacuolar membrane permeabilization (VMP)." *Chem Biol Interact* no. 220:208-13. doi: 10.1016/j.cbi.2014.07.002.
- Zhang, W., Bao, S., and Fang, T. 2016. "The neglected nano-specific toxicity of ZnO nanoparticles in the yeast *Saccharomyces cerevisiae*." *Sci Rep* no. 6:24839. doi: 10.1038/srep24839.
- Zhu, M., Nie, G., Meng, H., Xia, T., Nel, A., and Zhao, Y. 2013. "Physicochemical properties determine nanomaterial cellular uptake, transport, and fate." *Acc Chem Res* no. 46 (3):622-31. doi: 10.1021/ar300031y.
- Tolaymat, T., El Badawy, A., Genaidy, A., Abdelraheem, W., and Sequeira, R. 2017. "Analysis of metallic and metal oxide nanomaterial environmental emissions." *Journal of Cleaner Production* no. 143:401-412. doi: <https://doi.org/10.1016/j.jclepro.2016.12.094>.
- Usman, M. S., Zowalaty, M. E. E., Shamel, K., Zainuddin, N., Salama, M., and Ibrahim, N. A. 2013. "Synthesis, characterization, and antimicrobial properties of copper nanoparticles." *International Journal of Nanomedicine* no. 8:4467-4479. doi: 10.2147/IJN.S50837.
- Waldron, K. J., Rutherford, J. C., Ford, D., and Robinson, N. J. 2009. "Metalloproteins and metal sensing." *Nature* no. 460 (7257):823-30. doi: 10.1038/nature08300.
- Wang, L., Hu, C., and Shao, L. 2017. "The antimicrobial activity of nanoparticles: present situation and prospects for the future." *Int J Nanomedicine* no. 12:1227-1249. doi: 10.2147/ijn.s121956.
- Vazquez-Munoz, R., Avalos-Borja, M., and Castro-Longoria, E. 2014. "Ultrastructural analysis of *Candida albicans* when exposed to silver nanoparticles." *PLoS One* no. 9 (10):e108876. doi: 10.1371/journal.pone.0108876.

- Vega, K., and Kalkum, M. 2012. "Chitin, chitinase responses, and invasive fungal infections." *Int J Microbiol* no. 2012:920459. doi: 10.1155/2012/920459.
- von Moos, N., and Slaveykova, V. I. 2014. "Oxidative stress induced by inorganic nanoparticles in bacteria and aquatic microalgae--state of the art and knowledge gaps." *Nanotoxicology* no. 8 (6):605-30. doi: 10.3109/17435390.2013.809810.
- www.nanotechproject.org. Accessed 2018 March 13. *Project on emerging nanotechnologies* Accessed 2018 March 13].
- Wysocki, R., and Tamas, M. J. 2010. "How *Saccharomyces cerevisiae* copes with toxic metals and metalloids." *FEMS Microbiol Rev* no. 34 (6):925-51. doi: 10.1111/j.1574-6976.2010.00217.x.
- Xiong, Y., Brunson, M., Huh, J., Huang, A., Coster, A., Wendt, K., Fay, J., and Qin, D. 2013. "The role of surface chemistry on the toxicity of ag nanoparticles." *Small* no. 9 (15):2628-38. doi: 10.1002/smll.201202476.
- Xiu, Z. M., Zhang, Q. B., Puppala, H. L., Colvin, V. L., and Alvarez, P. J. 2012. "Negligible particle-specific antibacterial activity of silver nanoparticles." *Nano Lett* no. 12 (8):4271-5. doi: 10.1021/nl301934w.
- Yasokawa, D., Murata, S., Kitagawa, E., Iwahashi, Y., Nakagawa, R., Hashido, T., and Iwahashi, H. 2008. "Mechanisms of copper toxicity in *Saccharomyces cerevisiae* determined by microarray analysis." *Environ Toxicol* no. 23 (5):599-606. doi: 10.1002/tox.20406.



## APPENDIX

### PUBLICATION I

**Käosaar, S.**, Kahru, A., Mantecca, P., Kasemets, K. (2016). Profiling of the toxicity mechanisms of coated and uncoated silver nanoparticles to yeast *Saccharomyces cerevisiae* BY4741 using a set of its 9 single-gene deletion mutants defective in oxidative stress response, cell wall or membrane integrity and endocytosis. *Toxicology in Vitro*. 35, 149–162.





## Profiling of the toxicity mechanisms of coated and uncoated silver nanoparticles to yeast *Saccharomyces cerevisiae* BY4741 using a set of its 9 single-gene deletion mutants defective in oxidative stress response, cell wall or membrane integrity and endocytosis



Sandra Käosaar<sup>a,b</sup>, Anne Kahru<sup>a</sup>, Paride Mantecca<sup>c</sup>, Kaja Kasemets<sup>a,\*</sup>

<sup>a</sup> Laboratory of Environmental Toxicology, National Institute of Chemical Physics and Biophysics, Akadeemia tee 23, Tallinn 12618, Estonia

<sup>b</sup> Faculty of Chemical and Materials Technology, Tallinn University of Technology, Ehitajate tee 5, Tallinn 19086, Estonia

<sup>c</sup> Department of Earth and Environmental Sciences, Research Centre POLARIS, University of Milano–Bicocca, 1 Piazza della Scienza, Milano 20126, Italy

### article info

#### Article history:

Received 19 November 2015

Received in revised form 20 May 2016

Accepted 28 May 2016

Available online 31 May 2016

#### Keywords:

Silver nanoparticles

Dissolution

Speciation

Endocytosis

EUROSCARF strains

### abstract

The widespread use of nanosilver in various antibacterial, antifungal, and antiviral products warrants the studies of the toxicity pathways of nanosilver-enabled materials toward microbes and viruses. We profiled the toxicity mechanisms of uncoated, casein-coated, and polyvinylpyrrolidone-coated silver nanoparticles (AgNPs) using *Saccharomyces cerevisiae* wild-type (wt) and its 9 single-gene deletion mutants defective in oxidative stress (OS) defense, cell wall/membrane integrity, and endocytosis. The 48-h growth inhibition assay in organic-rich growth medium and 24-h cell viability assay in deionized (DI) water were applied whereas AgNO<sub>3</sub>, H<sub>2</sub>O<sub>2</sub>, and SDS served as positive controls. Both coated AgNPs (primary size 8–12 nm) were significantly more toxic than the uncoated (~85 nm) AgNPs. All studied AgNPs were ~30 times more toxic if exposed to yeast cells in DI water than in the rich growth medium: the IC<sub>50</sub> based on nominal concentration of AgNPs in the growth inhibition test ranged from 77 to 576 mg Ag/L and in the cell viability test from 2.7 to 18.7 mg Ag/L, respectively. Confocal microscopy showed that wt but not endocytosis mutant (end3Δ) internalized AgNPs. Comparison of toxicity patterns of wt and mutant strains defective in OS defense and membrane integrity revealed that the toxicity of the studied AgNPs to *S. cerevisiae* was not caused by the OS or cell wall/membrane permeabilization.

© 2016 Elsevier Ltd. All rights reserved.

## 1. Introduction

Nanotechnologies are contributing practically in every field of the current economy. Indeed, synthetic nanoparticles (NPs) with novel properties are included in a variety of products from electronics to water purification applications. Silver nanoparticles (AgNPs) are included in the biggest number of consumer products mainly due to their antibacterial, antifungal, and antiviral properties (Reidy et al., 2013). Silver compounds have been used for hundreds of years to treat wounds or to disinfect drinking water, in the form of silver sulfadiazine, silver nitrate, or colloidal silver (Nowack et al., 2011; Rai et al., 2009).

However, compared to the soluble forms of silver, the incorporation of silver NPs into antimicrobial products may yield more efficient products due to the unique properties of nano-sized materials and slow/controlled release of silver ions over a longer time-course (Atiyeh et al., 2007; Brandt et al., 2012). Although there is a number of articles

dedicated to the research on the biocidal action of silver, the mechanism of toxicity of Ag ions and AgNPs is still not fully elucidated (Marambio-Jones and Hoek, 2010; Rai et al., 2009; Reidy et al., 2013). Most often, interaction with cell membrane, subsequent membrane damage, interaction with DNA, disturbance of mitochondrial function, or the generation of reactive oxygen species (ROS) are reported (Bondarenko et al., 2013a; Feng et al., 2000; Ivask et al., 2014a; Jung et al., 2008; Kim et al., 2007). It is generally acknowledged that the release of Ag ions from AgNPs surface is a major determinant in their antimicrobial effect, but the role of specific AgNPs properties in toxicity is not clearly determined yet (Bondarenko et al., 2013a; Gliga et al., 2014; Ivask et al., 2014b; Reidy et al., 2013).

Physical–chemical properties of AgNPs such as size and surface charge are important determinants in their toxic effects. A clear size-dependent toxicity of citrate-coated AgNPs (10, 20, 40, 60, and 80 nm) toward bacteria *Escherichia coli*, yeast *Saccharomyces cerevisiae*, crustacean *Daphnia magna*, and mammalian fibroblasts in vitro has been shown, i.e., the smaller particles were more toxic than the bigger ones and the toxicity of 10 nm AgNPs was not caused only by the liberated ions (Ivask et al., 2014c). Also, the surface coating and charge of

\* Corresponding author.

E-mail addresses: [sandra.kaosaar@kbfi.ee](mailto:sandra.kaosaar@kbfi.ee) (S. Käosaar), [anne.kahru@kbfi.ee](mailto:anne.kahru@kbfi.ee) (A. Kahru), [paride.mantecca@unimib.it](mailto:paride.mantecca@unimib.it) (P. Mantecca), [kaja.kasemets@kbfi.ee](mailto:kaja.kasemets@kbfi.ee) (K. Kasemets).

AgNPs have been linked to the toxicity: positively charged AgNPs exerted higher antimicrobial effect than negatively charged NPs due to the interactions with negatively charged cell surface (El Badawy et al., 2011; Ivask et al., 2014b; Kasemets et al., 2014).

In the present study, we focused on the toxicity mechanism of differently coated and sized AgNPs to the yeast *S. cerevisiae*—a powerful model organism in eukaryotic biology especially since the sequencing of its complete genome in 1996 and creation of the single-gene deletion mutants' libraries (Botstein and Fink, 2011; Brachmann et al., 1998). The application of *S. cerevisiae* as an in vitro model ranges from the study of neurodegenerative diseases (Khurana and Lindquist, 2010) to toxicity mechanisms of heavy metals (Avery et al., 1996). AgNPs toxicity to different types of yeasts has been studied and various toxicity mechanisms shown. For example, the transcriptome profile study on AgNPs- and Ag ions-exposed *S. cerevisiae* showed that the most up-regulated genes were related to chemical stimuli, stress, and cellular transport, whereas the highest up-regulation was observed for CUP1-1 and CUP1-2 genes that code metallothioneins—proteins mediating resistance to copper and cadmium ions in *S. cerevisiae* (Niazi et al., 2011). The growth of the clinically important pathogenic yeast *Candida albicans* was inhibited by Ag ions and non-stabilized AgNPs (~25 nm) at a concentration of approximately 0.4 mg/L and PVP-stabilized AgNPs at 0.1–0.2 mg/L (Panacek et al., 2009) and by various sizes of PVP-stabilized silver NPs (5–60 nm) at a concentration of 0.4–1.6 mg/L (Monteiro et al., 2012). Kim et al. (2009) investigated the mode of action of silver NPs to *C. albicans* and reported a MIC (minimum inhibitory concentration) of 2 mg/L and proposed the disruption of membrane potential and destruction of membrane integrity as the mechanism of the toxic action of AgNPs.

In this study, we used a novel approach—profiling of the toxicity mechanisms of AgNPs in 9 *S. cerevisiae* single-gene deletion mutants. Comparatively, *S. cerevisiae* BY4741 wild-type (wt) and its single-gene deletion mutants defective in (i) oxidative stress (OS) response (*yap1Δ*, *sod1Δ*, and *sod2Δ*), (ii) cell wall/membrane components synthesis (*gas1Δ*, *erg3Δ*, *mnn10Δ*, *kre6Δ*, and *knr4Δ*), and (iii) endocytosis (*end3Δ*) were studied.

In our previous study on toxicity mechanisms of CuO NPs to *S. cerevisiae*, we showed that these OS-response-defective strains (*yap1Δ*, *sod1Δ*, and *sod2Δ*) were more susceptible to menadione (a superoxide radical inducer) and H<sub>2</sub>O<sub>2</sub> than wild-type yeast cells (Kasemets et al., 2013). In the current study, in addition to the above-described OS-response-defective strains, we used (i) the cell wall/membrane synthesis-defective strains having up to 5 times higher susceptibility to the membrane permeabilizing agent sodium dodecyl sulfate (SDS) compared to the wt, and (ii) the endocytosis-defective strain *end3Δ* as NPs can be internalized by eukaryotic cells (Oh and Park, 2014), including yeast cells via endocytic pathways, that may lead to additional toxic effects. Earlier, the internalization of 1.4 nm positively charged gold nanoparticles by *S. cerevisiae* spheroplasts (Prescianotto-Baschong and Riezman, 1998) and functionalized polystyrene latex and CdSe NPs by intact yeast cells via endocytosis (Nomura et al., 2013; Sun et al., 2014) has been reported.

Based on the previously published toxicity mechanisms of AgNPs toward different microbial cells, we hypothesized that

- (i) The oxidative stress- and cell wall/membrane components synthesis-defective mutants selected for this study will be more sensitive to the studied AgNPs than wt. This hypothesis is based on the previous knowledge showing that AgNPs may produce ROS and induce oxidative stress (Hwang et al., 2012; Marambio-Jones and Hoek, 2010; Reidy et al., 2013) and adsorb onto the cell wall inducing disturbances in the cell wall/membrane leading to the leakage of cellular content (Kim et al., 2009; Manshian et al., 2015; Marambio-Jones and Hoek, 2010);
- (ii) The endocytosis-defective mutant will be less sensitive than wt to the AgNPs, as AgNPs will not be internalized by cells and the additional intracellular solubilization and/or ROS production by internalized AgNPs will be excluded.

Three types of AgNPs were studied to reveal the role of coating in their toxic action: uncoated, protein (casein)-coated, and polyvinylpyrrolidone (PVP)-coated AgNPs. Also, different test media—deionized water and organic-rich growth medium—were used to assess the effects of organic ligands on the bioavailability and toxicity of Ag ions and AgNPs.

## 2. Materials and methods

### 2.1. Chemicals and nanoparticles

Uncoated AgNPs (nAg, primary size ~86 nm) were purchased from Sigma-Aldrich and casein-coated AgNPs (collargol, nAg-col; primary size ~13 nm) from Laboratorios Argel S. L. (batch N° 297). Polyvinylpyrrolidone-coated AgNPs (nAg-PVP, primary size ~8 nm) were synthesized in the Laboratory of Polymer Chemistry, University of Helsinki, by prof. H. Tenhu. The primary sizes and percentage of the coating of nAg-col and nAg-PVP have been measured from the TEM micro-graphs and by thermogravimetric analyses, respectively, as was characterized and described previously (Blinova et al., 2013).

All the concentrations of Ag compounds (AgNO<sub>3</sub> and AgNPs) in this work have been expressed on the basis of Ag mass (mg Ag/L) and not of total compound mass. The stock suspensions of nAg-col (1 g Ag/L) and nAg-PVP (2 g Ag/L) were prepared in deionized (DI) water (18 MΩ, pH 5.6 ± 0.1, Milli-Q, Millipore) and stored in the dark at ambient temperature. nAg-col and nAg-PVP formed stable suspension in DI water and therefore were not ultrasonicated. Non-coated AgNPs stock suspension (5 g/L) in DI water was unstable and was ultrasonicated once after preparation in the ultrasonic bath (Branson 1510, USA) for 30 min and stored up to 6 months in the dark at + 4 °C. Before testing, the AgNPs suspensions were vigorously vortexed and diluted in DI water.

H<sub>2</sub>O<sub>2</sub> (30%) was from Merck, sodium dodecyl sulfate (SDS) from Serva, menadione sodium bisulfite from Sigma-Aldrich and 0.1 M AgNO<sub>3</sub> from Fluka. The menadione (3 g/L) and AgNO<sub>3</sub> (5 g Ag/L) stocks were prepared in DI water and stored in the dark at + 4 °C or at room temperature, respectively.

### 2.2. Test media

Two different test media were used for AgNPs toxicity assessment and physical-chemical characterization: (i) DI water and (ii) modified yeast extract-peptone-dextrose medium (further referred to as YPD<sub>mod</sub>). YPD<sub>mod</sub> contained 0.25% yeast extract, 0.5% peptone and 1% glucose (pH 6.8). Compared to the original YPD medium the yeast extract and peptone content was reduced 4 times and glucose 2 times. Growth medium components, yeast extract and agar were purchased from Lab M (UK), peptone from BD (France), and glucose from Sigma-Aldrich.

### 2.3. Characterization of nanoparticles

#### 2.3.1. Hydrodynamic diameter and ζ-potential of AgNPs

Hydrodynamic diameter (D<sub>h</sub>) and ζ-potential of nAg, nAg-col, and nAg-PVP were studied in DI water and in YPD<sub>mod</sub> using Zetasizer Nano ZS (Malvern Instruments, UK). nAg-col and nAg-PVP were studied at the concentration of 50 mg Ag/L and nAg at the concentration of 250 mg/L in both test environments. The D<sub>h</sub> was measured in a clear 2 mL cuvette and the ζ-potential in 1 mL folded capillary cell (DTS1061, Malvern Instruments, UK) immediately after preparation (0 h) and after 24-h or 48-h incubation in DI water or YPD<sub>mod</sub>, respectively, at 30 °C without prior shaking mimicking the same conditions as in the toxicity tests.

#### 2.3.2. UV-vis absorption spectroscopy

UV-visible light (UV-vis) absorption spectra of nAg (200 mg/L), nAg-col, and nAg-PVP (both 20 mg Ag/L) dispersed in DI water and YPD<sub>mod</sub> were measured in a clear 1 mL cuvette at 250–900 nm (measurement

step 5 nm) using the Multiskan Spectrum spectrophotometer (Thermo Electron Corporation, Finland). The effect of the presence of yeast cells and yeast growth on the AgNPs suspension stability in YPD<sub>mod</sub> was assessed at cell density  $\sim 10^6$  CFU/mL in the cuvette. The measurements were made immediately after preparation (0 h) and after 24-h (DI water) or 48-h (YPD<sub>mod</sub>) incubation at 30 °C without prior shaking.

### 2.3.3. Quantification of dissolved silver

The dissolution of the AgNPs in DI water and YPD<sub>mod</sub> was quantified using atomic absorption spectroscopy (AAS). Dissolved Ag ions were quantified in DI water (nAg, nAg-col, and nAg-PVP at a concentration of 5 mg Ag/L) and in YPD<sub>mod</sub> medium (nAg at a concentration of 500 mg/L, nAg-col, and nAg-PVP at 100 mg Ag/L). In addition, Ag ions (5 mg Ag/L) recovery after incubation in DI water and YPD<sub>mod</sub> at 30 °C for 24 h or 48 h, respectively, was determined. The suspensions of AgNPs and Ag ions solution were incubated on 24-well microplates (Falcon) (1.6 mL per well) at 30 °C for 24 h (in DI water) or 48 h (in YPD<sub>mod</sub> medium). The AgNPs suspensions and Ag ions solution were ultracentrifuged at 390,000g for 40 min at 20 °C (Beckman L8-55 M Ultracentrifuge, USA) to remove the non-soluble fraction of AgNPs, and the supernatants were used for the further AAS analyses. AAS analysis of the supernatant was performed in a certified laboratory of the Institute of Chemistry of Tallinn University of Technology in Estonia according to the standard EVS-EN ISO/IEC 17025:2005 (AAS-graphite furnace).

### 2.4. *S. cerevisiae* strains and cultivation conditions

*S. cerevisiae* BY4741 wild-type (MATa; his3Δ 1; leu2Δ 0; met15Δ 0; ura3Δ 0) and its 9 isogenics single-gene deletion mutants were purchased from EUROSCARF (Institute of Microbiology, University of Frankfurt, Germany). The mutant strains used in this study are listed and characterized in Table S1. *S. cerevisiae* strains were stored at  $-80$  °C. To obtain the master plates, cells were plated and incubated on YPD agar medium (1% yeast extract, 2% peptone, 2% glucose, and 1.5% agar) at 30 °C for 72 h in a micro-aerobic environment (6% oxygen, 15% CO<sub>2</sub>, CampyGen, Oxoid) to avoid the selection toward the second site suppressors of oxygen-sensitive strains (e.g., sod1Δ). In the case of single-gene deletion mutants, YPD agar medium was supplemented with 300 mg/L of the selective antibiotic Geneticin (G418 sulfate, Sigma-Aldrich). The plates were stored up to 1 month at +4 °C.

The growth of the *S. cerevisiae* BY4741 wt and its single-gene deletion mutants in toxicant-free YPD<sub>mod</sub> medium was assessed on 96-well microplates at 30 °C during 48 h. For that, the overnight culture grown in YPD at 30 °C was diluted in YPD<sub>mod</sub> to a density of approximately  $10^6$  CFU/mL (OD<sub>600nm</sub> 0.05, Yenway 6300 Spectrophotometer, UK), and 150 μL was transferred into the microplate wells (each strain in 3 replicates). Yeast growth was estimated by the optical density at 600 nm using the microplate reader SpectraMax Paradigm (Molecular Devices, USA).

Membrane-impermeant fluorescent endocytosis marker Lucifer Yellow (Sigma-Aldrich) was used to confirm that the end3Δ strain used in the current study was defective in endocytosis (for method and microscopic images, see Supplementary material, Section 2). The method was adapted from Dulic et al. (1991) and Raths et al. (1993).

### 2.5. Toxicity testing

Three different AgNPs (nAg, nAg-col, and nAg-PVP) were tested in parallel with AgNO<sub>3</sub> as a control for Ag ions and H<sub>2</sub>O<sub>2</sub> and SDS as positive controls for oxidative stress and cell wall/membrane perturbation, respectively. Two different toxicity test formats were used: (1) 48-h growth inhibition assay in organic-rich growth medium (YPD<sub>mod</sub>) and (2) 24-h cell viability test in DI water. Toxicity tests were conducted in non-tissue culture treated 96-well flat bottom microplates (Falcon) at 30 °C in the dark, without shaking. The microplates were placed in plastic pouches (Oxoid) to minimize evaporation during the experiment.

After exposure to the toxicants for 48 h in YPD<sub>mod</sub> or 24 h in DI water, the colony-forming ability of the yeast cells on YPD agar medium was evaluated by the spot test (Suppi et al., 2015). Briefly, 5 μL of exposed and non-exposed culture (control culture) was pipetted onto toxicant-free YPD agar medium and the plates were incubated at 30 °C for 72 h. The colony-forming ability of the yeast strains was evaluated visually and agar plates with colonies were photographed.

#### 2.5.1. Growth inhibition test in YPD<sub>mod</sub> medium

In the growth inhibition assay, nAg was tested in the nominal concentration range of 62.5–2500 mg Ag/L, nAg-col in 15.625–500 mg Ag/L, nAg-PVP in 15.625–250 mg Ag/L, AgNO<sub>3</sub> in 0.75–12 mg Ag/L, H<sub>2</sub>O<sub>2</sub> in 10–320 mg/L, and SDS in 62.5–1600 mg/L in 2-fold dilution series. The selection of the concentration ranges of the studied compounds was based on the screening experiments. The growth inhibition test in the presence of test chemicals or without (control) was conducted in the YPD<sub>mod</sub> (Section 2.2). Diluted medium was used to reduce the effect of the organic ligands on the bioavailability of the silver compounds. A 48-h growth time was applied because in the YPD<sub>mod</sub>, the maximum growth rate of yeast cells was  $\sim 10$ –20% slower than in the original YPD medium and the cells reached to the late stationary phase by the 48th hour. The test was performed as described in (Kasemets et al., 2013). Cells in toxicant-free YPD<sub>mod</sub> were used as a control. Toxicant dilutions in cell-free YPD<sub>mod</sub> served as abiotic particle turbidity controls and the absorbance values (OD<sub>600nm</sub>) of the abiotic controls were subtracted from the respective values of the biotic samples. After a 48-h incubation at 30 °C in the dark without shaking, the OD<sub>600nm</sub> was measured by the Multiskan Spectrum microplate spectrophotometer (Thermo Electron Corporation, Finland). In the case of SDS, the microplate was shaken for  $\sim 30$  s before measurement. Toxicity was estimated as inhibition of growth of yeast culture upon exposure to the toxicants compared to the growth of toxicant-free controls.

#### 2.5.2. Cell viability test in deionized water

In the cell viability assay, nAg was tested in the nominal concentration range of 1.1–90 mg Ag/L, nAg-col in 0.032–20 mg Ag/L, nAg-PVP in 0.15–15 mg Ag/L, AgNO<sub>3</sub> in 0.007–0.60 mg Ag/L, H<sub>2</sub>O<sub>2</sub> in 0.56–60 mg/L, and SDS in 15–1200 mg/L in 3- to 5-fold dilution series. The selection of the concentration ranges was based on the screening experiments.

The concept of exposing yeast cells to the metal-based NPs in DI water to avoid possible changes in bioavailability caused by the growth medium's ligands (e.g., proteins, ions) has already been introduced and used previously (Kasemets et al., 2013; Suppi et al., 2015). Briefly, overnight culture of yeast cells was diluted in fresh YPD to OD<sub>600nm</sub> 0.2 (Yenway 6300 Spectrophotometer, UK) and further grown until mid-exponential growth phase ( $\sim 4.5$  h, until OD<sub>600nm</sub> 0.8–1.0) at 30 °C. Cells were collected by centrifugation at 3000 g for 10 min at 20 °C (Biofuge, Heraeus Instruments, UK) and washed twice with DI water. The cells were re-suspended in DI water to a density of approximately  $2 \times 10^7$  CFU/mL (OD<sub>600nm</sub> 1.2). 75 μL of cell suspension was added into the wells of the 96-well microplates containing 75 μL of the toxicants dilutions in DI water, and microplates were incubated for 24 h at 30 °C in the dark without shaking. Toxicant-free DI water was inoculated with cells as the viable cells control. Toxicant dilutions in cell-free DI water served as abiotic controls. After 24 h, the viability of the yeast cells was estimated by fluorescein diacetate (FDA) (Sigma-Aldrich). For that, 100 μL of cell suspension was transferred to black 96-well polypropylene microplate (Greiner Bio-One, Germany), 10 μL of FDA solution (1 mg/mL in acetone) was added, and the microplate was incubated for 20 min at 30 °C in the dark. Fluorescence was quantified using Fluoroskan Ascent FL microplate reader (Thermo Labsystems, Finland) at excitation and emission wavelengths of 485 nm and 527 nm, respectively.

### 2.5.3. Statistical analysis

IC<sub>50</sub> values were calculated using Excel Macro REGTOX (Vindimian, 2001). Each experiment was performed at least in three replicates and the given results represent the mean of three experiments  $\pm$  SD. A t-test was used to determine statistically significant differences between the wild-type and the mutant strains.

### 2.6. Assessment of intracellular reactive oxygen species

The potential of the studied AgNPs and Ag ions to induce the formation of intracellular ROS in *S. cerevisiae* BY4741 wt cells was assessed using 2',7'-dichlorodihydrofluorescein diacetate (H<sub>2</sub>DCF-DA, Molecular Probes). The cell-permeable non-fluorescent H<sub>2</sub>DCF-DA is de-esterified intracellularly and turns to highly fluorescent 2',7'-dichlorofluorescein upon oxidation. For ROS detection, yeast cells from exponentially growing culture were exposed to AgNPs, Ag ions, and positive controls H<sub>2</sub>O<sub>2</sub> and menadione in DI water at 30 °C for 2, 4, and 24 h in the dark on black 96-well polypropylene microplates. In this test, AgNPs, H<sub>2</sub>O<sub>2</sub>, and menadione were studied at the concentrations of 0.16–100 (mg Ag/L or mg/L respectively) and Ag ions at the concentration of 0.032–100 mg Ag/L in a 5-fold dilution series. The exposure concentrations were chosen according to the toxicity of these compounds in the cell viability test. The  $\sim 10^6$  CFU/mL yeast cell culture in DI water was prepared in the same manner as for the cell viability test (see Section 2.5.2), and 50  $\mu$ L was added to the wells of the microplates containing 50  $\mu$ L of the toxicants dilutions in DI water. The microplates were covered with a microplate sealing tape (Greiner Bio-One) and incubated for 2, 4, or 24 h at 30 °C in the dark without shaking. The H<sub>2</sub>DCF-DA stock solution was prepared in ethanol at 2.5 mg/mL and stored at  $-20$  °C. After incubation, 25  $\mu$ L of the H<sub>2</sub>DCF-DA working solution (250  $\mu$ g/mL in 25 mM Na-phosphate buffer, pH 7.2) was added to the samples in the wells of the microplate and was incubated for 1 h at room temperature. Fluorescence was recorded at excitation and emission wavelengths of 485 nm and 527 nm, respectively, using the Fluoroskan Ascent FL microplate reader (Thermo LabSystems, Finland). ROS levels in cells were calculated as fold-increase in fluorescence signal compared to the non-exposed cells. Results are given as mean of three experiments  $\pm$  SD.

### 2.7. Laser scanning confocal microscopy

Laser scanning confocal microscope in the laser reflection mode (Moschini et al., 2013) was used to study the internalization of the nAg-col and nAg-PVP by the wt and end3 $\Delta$  cells. Briefly, overnight culture of yeast cells was collected by centrifugation at 3000g for 10 min at 20 °C (Biofuge, Heraeus, UK) and washed twice and resuspended in YPD<sub>mod</sub> at the cell density of  $1.5 \times 10^7$  CFU/mL. Wild-type and end3 $\Delta$  cells were exposed to sub-toxic concentration of nAg-col and nAg-PVP (1 mg Ag/L) on the 12-well plates (Corning) in YPD<sub>mod</sub> for 3 h at 30 °C. After exposure, yeast cells were fixed by cold 4% paraformaldehyde overnight at 4 °C. After a washing step in phosphate-buffered saline (PBS, pH 7.4) and permeabilization in 0.5% Triton X–PBS solution (vol/vol) for 5 min at room temperature (RT), the cells were incubated in 100 nM rhodamine-phalloidine (Cytoskeleton Inc., actin probe) PBS solution for 30 min at RT in the dark and then in 6.6 nM DRAQ5™ (BioStatus Ltd., DNA probe) PBS solution for 10 min at 37 °C in the dark. Finally, the cells were suspended in 100  $\mu$ L DABCO (1,4-diazabicyclo[2.2.2]octane) mounting medium and 5  $\mu$ L of cell suspension was deposited onto the SuperFrost microscope slides (Menzel) and covered by the coverslips. A Leica TCS SP5 confocal microscope with reflected-light optics was used at a magnification of 40 $\times$  (1.25 NA Plan-Apochromat). Samples were illuminated with a 488 nm Argon/Krypton laser, using an intensity of the AOTF filter by 10% Images were processed with the Leica dedicated LAS AF software.

## 3. Results

### 3.1. Characterization of the silver nanoparticles

In this study, uncoated (nAg), protein-coated, and polyvinylpyrrolidone-coated AgNPs (nAg-col and nAg-PVP) were studied. The average hydrodynamic diameters ( $D_h$ ) of the coated AgNPs in DI water and YPD<sub>mod</sub> were  $\sim 40$  nm (nAg-col) and 60–100 nm (nAg-PVP) (Table 1). During the incubation for 24 h or 48 h, respectively, the coated AgNPs were well dispersed and showed relatively narrow one-peak size distribution in both test environments and were quite stable (no increase in the  $D_h$ , and the value of polydispersity index, pdi, was 0.2–0.4) (Table 1 and Fig. 1). Some agglomeration of nAg-PVP occurred in YPD<sub>mod</sub>, represented by a minor peak in size distribution at  $\sim 2$ –3  $\mu$ m (3–4% intensity) (Fig. 1). Compared to the primary sizes (measured from the TEM micrographs) of nAg-col ( $\sim 13$  nm) and nAg-PVP ( $\sim 8.4$  nm), the  $D_h$  in DI water and YPD<sub>mod</sub> was  $\sim 4$ –10 times larger, probably due to the organic coatings (casein and PVP, respectively, that is not possible to visualize by TEM) and some agglomeration.

Differently from coated AgNPs, the uncoated AgNPs agglomerated and visibly settled (Fig. 2). The uncoated AgNPs showed a slightly wider size distribution in DI water compared to the coated AgNPs, although the average  $D_h$  was still  $\sim 90$ –100 nm (Fig. 1). However, in YPD<sub>mod</sub>, the uncoated AgNPs formed a polydisperse suspension (pdi 0.5–0.6) with larger agglomerates, resulting in average  $D_h$  at 0 h and 48 h being 251 nm and 445 nm, respectively (Table 1). In general, uncoated AgNPs are unstable in aqueous suspension, and therefore different coating agents (e.g., organic polymers) are applied to modify the particles' properties such as agglomeration, stability, dissolution, and biological activity (Reidy et al., 2013). Coating of AgNPs with PVP provides stability due to steric repulsion of the large non-charged polymers (Huynh and Chen, 2011).

UV-vis absorption spectra of the AgNPs suspensions also showed stability of the coated AgNPs in DI water during 24 h, but with some agglomeration/sedimentation in YPD<sub>mod</sub> (48-h incubation). The majority of uncoated AgNPs settled within the first minutes both in DI water and in YPD<sub>mod</sub> and the characteristic UV-vis absorption peak for nAg at 400–500 nm was entirely missing already after the preparation (0 h) (Fig. 2).

Interestingly, we observed that the growth of yeast cells in the YPD<sub>mod</sub>, containing nAg-col and nAg-PVP at a sub-toxic concentration of 20 mg Ag/L, introduced changes in the color of the suspensions from yellow-brownish to black, accompanied by visible settling of the particles. Both these effects were not observed in the abiotic controls, i.e., in the absence of yeast cells (Fig. 2). UV-vis analysis also confirmed the lack of nanosized Ag particles in the yeast-AgNPs suspension after 48 h of yeast's growth (Fig. 2). As during the growth of yeast in YPD<sub>mod</sub> over 48 h, the pH of the culture gradually decreased from 6.8 to 4.7, we also tested the effect of pH on the stability of the nAg-col in yeast cell-free YPD<sub>mod</sub> (for methods and results see Supplementary material, Section 1). At the initial pH of 6.8, the average  $D_h$  of nAg-col was 48 nm and the  $\zeta$ -potential  $-26$  mV; as the pH decreased, the nAg-col particles' average  $D_h$  increased (over 4  $\mu$ m at pH 4.4) and  $\zeta$ -potential weakened ( $-15$  mV at pH 4.4) (Fig. S1), leading to visible settling of the particles. The coated AgNPs transformation and visible settling did not occur at higher (toxic) concentrations where the cell growth was inhibited and pH of the medium did not drop (data not shown). However, another possible explanation to the visible change in color and settling of the coated AgNPs in the presence of cell growth could be reacting of the particles with H<sub>2</sub>S produced by yeasts leading to covering of the particles with layer of Ag<sub>2</sub>S as H<sub>2</sub>S is known to cause precipitation of metals (Gadd, 1993).

The  $\zeta$ -potential of all the studied AgNPs was negative in both test media, ranging from  $-5$  mV to  $-35$  mV (Table 1). Interestingly, the  $\zeta$ -potential of uncoated nAg was comparable with nAg-col (approximately  $-30$  mV in DI water and in YPD<sub>mod</sub>), but differently from nAg-

Table 1

Characterization of silver nanoparticles (AgNPs). Average hydrodynamic diameter ( $D_h$ ) and  $\zeta$ -potential of AgNPs were measured in deionized (DI) water and in modified yeast extract-peptone-dextrose medium (YPD<sub>mod</sub>) after preparation (0 h) and after incubation for 24 h or 48 h, respectively, at 30 °C. The dissolution of AgNPs in DI water and YPD<sub>mod</sub> after 24-h or 48-h incubation, respectively, was measured at the same test conditions.

Characteristics	nAg-col	nAg-PVP	nAg
Coating	Protein (casein)	Polyvinylpyrrolidone	uncoated
Coating, % (mass fraction)	30 <sup>a</sup>	71 <sup>a</sup>	—
Primary size, nm	12.5 ± 4.0 <sup>a</sup>	8.40 ± 2.8 <sup>a</sup>	85.7 ± 29 <sup>b</sup>
$D_h$ in DI; 0 h	43.3 (0.2)	100 (0.3)	104 (0.4)
and 24 h, nm	42.8 (0.2)	95.8 (0.3)	92.6 (0.3)
$D_h$ in YPD <sub>mod</sub> ; 0 h	43.7 (0.2)	84.6 (0.4)	251 (0.5)
and 48 h, nm	37.8 (0.2)	61.0 (0.3)	445 (0.6)
$\zeta$ -potential in DI; 0 h	− 35.3	− 6.60	− 33.8
and 24 h, mV	− 31.6	− 7.60	− 32.5
$\zeta$ -potential in YPD <sub>mod</sub> ; 0 h	− 24.0	− 5.00	− 27.2
and 48 h, mV	− 21.4	− 8.40	− 27.3
24-h dissolution in DI, % <sup>c</sup>	6.9	8.3	3.3
48-h dissolution in YPD <sub>mod</sub> , % <sup>d</sup>	1.0	0.92	0.27

<sup>a</sup> Blinova et al., 2013; <sup>b</sup> Bondarenko et al., 2013b; in parentheses—polydispersity index;  $D_h$  and  $\zeta$ -potential were measured at the concentrations of 50 mg Ag/L (nAg-col and nAg-PVP) or 250 mg Ag/L (nAg); dissolution of AgNPs was measured by AAS in DI water at the concentration of 5 mg Ag/L and in <sup>d</sup>YPD<sub>mod</sub> at the concentrations of 100 mg Ag/L (nAg-col, nAg-PVP) or 500 mg Ag/L (nAg).

col, the suspension of nAg was unstable and the particles tended to settle (Table 1; Fig. 2) probably as the surface charge was not sufficient to provide charge-repulsion dependent stability. And contrarily, although the  $\zeta$ -potential of the PVP-coated AgNPs was − 7 mV in DI and − 8 mV in YPD<sub>mod</sub>, the suspension of nAg-PVP was quite stable in both test media, probably due to the steric hindrance of PVP coating. Indeed, organic-coated AgNPs are more stable in the different biological and environmental conditions mainly due to the electrostatic and steric stabilization (Sharma et al., 2014).

### 3.2. Dissolution of silver nanoparticles

It is generally acknowledged that in aqueous environment the release of silver ions from the oxidized surface of the NPs is the main factor contributing to AgNPs toxicity (Fabrega et al., 2011; Levard et al., 2012; Behra et al., 2013; Maurer et al., 2014).

The dissolution of AgNPs highly depends on the physical-chemical properties of the particles (size, surface coating, suspension stability etc.) as well as on the environmental conditions (the presence of organic compounds and oxygen, pH, temperature). Ag forms stable insoluble complexes with Cl<sup>−</sup> and HS<sup>−</sup> ions and has a high affinity toward sulfur, and the formation of respective complexes may reduce the bioavailability and toxicity of Ag ions (Gadd, 1993; Levard et al., 2012).

To assess the role of solubility in the toxicity of the studied AgNPs, we quantified the dissolved Ag fraction in DI water and YPD<sub>mod</sub> medium following the same test conditions that were applied in the toxicity tests (exposure concentrations and time, temperature, and test media) with one exception: the dissolution experiments were conducted in abiotic conditions, i.e., in the absence of the yeast cells. Data on the solubility of AgNPs in DI water and YPD<sub>mod</sub> are presented in Table 1. Recovery of Ag ions in DI water and YPD<sub>mod</sub> after 24-h incubation in cell-free DI water was ~100% and after 48-h incubation in YPD<sub>mod</sub> medium ~91%. The minor reduction in Ag ions recovery in YPD<sub>mod</sub> was probably caused by the formation of Ag ion complexes with the medium components (e.g., proteins) which probably settle during the ultracentrifugation (390,000g) of Ag ions solution in YPD<sub>mod</sub> medium.

In DI water, the 24-h dissolution of coated and uncoated AgNPs tested at 5 mg Ag/L was ~6.9–8.3% and ~3.3% respectively. However, in the YPD<sub>mod</sub> medium, the amount of dissolved/bioavailable Ag was lower than in DI water, namely, ~0.92–1.0% for coated AgNPs (tested at 100 mg Ag/L) and ~0.27% for uncoated AgNPs (tested at 500 mg/L). In this study, the coated AgNPs yielded more dissolved Ag ions at the end of incubation than the uncoated AgNPs, probably due to better dispersibility and smaller size of the particles in the test environments used.

### 3.3. Selection of the suite of single-gene deletion mutants of *S. cerevisiae* and growth of the strains in YPD<sub>mod</sub> medium

In this study, we used the *S. cerevisiae* BY4741 wild-type and its 9 isogenics single-gene deletion mutants (from the EUROSCARF) to assess the toxicity and mode of action of differently coated and uncoated AgNPs. The strains used are characterized in Table S1. To test the oxidative stress-inducing effect of the AgNPs, we chose menadiene- and H<sub>2</sub>O<sub>2</sub>-sensitive strains yap1Δ, sod1Δ, and sod2Δ (Kasemets et al., 2013), defective in the superoxide dismutase or yap1 transcription factor gene, respectively (Table S1). Since in the case of unicellular organisms the cell wall and membrane have an important protective role as barrier from harmful environmental influences and are one of the main targets of toxic action of Ag compounds (Marambio-Jones and Hoek, 2010), we screened the library of mutants with a deletion in cell wall/membrane components synthesis- or integrity-related genes (erg6Δ, erg2Δ, gas1Δ, sgl1Δ, mkk2Δ, erg3Δ, end3Δ, chs3Δ, ecm33Δ, mnn10Δ, fks1Δ, kre6Δ, knr4Δ, cwp2Δ, and ysr3Δ) for sensitivity toward sodium dodecyl sulfate (SDS). SDS is an anionic detergent shown to permeabilize the plasma membrane of bacteria and yeast (Woldringh and van Iterson, 1972; Kodedova et al., 2011). In the 24-h growth inhibition test in YPD containing 100 mg/L SDS, the mutants gas1Δ, erg3Δ, end3Δ, mnn10Δ, kre6Δ, and knr4Δ showed the highest sensitivity to SDS (inhibition of growth ~90% data not shown) and hence, were selected for further toxicity analysis of AgNPs. The gas1p, kre6p, and knr4p proteins (Hong et al., 1994; Ram et al., 1998) are required for cell wall beta-glycans biosynthesis, erg3p is involved in the synthesis of ergosterol (Arthington-Skaggs et al., 1996), an essential component in yeast cell membrane. Mnn10 protein is a subunit of a Golgi mannosyltransferase complex that mediates elongation of the polysaccharide mannan backbone in the yeast cell wall (Jungmann et al., 1999). End3 protein is involved in endocytosis (Benedetti et al., 1994) and it has been shown that the end3Δ mutant was unable to internalize positively charged 1.4 nm gold NPs (Prescianotto-Baschong and Riezman, 1998). In this study, the membrane-impermeant fluorescent endocytosis marker Lucifer Yellow (Dulic et al., 1991) was used to probe wt and end3Δ endocytosis ability/disability (for methods and results see Supplementary materials, Section 2). Confocal microscopy study showed that after 2 h exposure in YPD<sub>mod</sub> Lucifer Yellow was visible in all wt cells and there was no fluorescence present in the intact end3Δ cells, although the bright fluorescence was observed in the end3Δ lysed cells (Fig. S2).

Before the toxicity testing, the wt and the mutants were examined for their growth ability in YPD<sub>mod</sub>, which was the essential prerequisite for the use of the selected mutants in the growth inhibition assay. Fig. S3

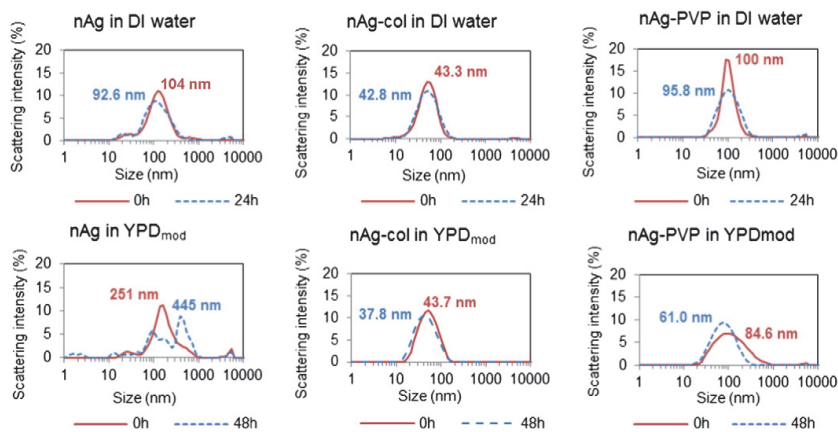


Fig. 1. Hydrodynamic size distribution of nAg (250 mg Ag/L), nAg-col, and nAg-PVP (both 50 mg Ag/L) suspensions in deionized (DI) water (upper panels) and in modified yeast extract-peptone–dextrose medium YPD<sub>mod</sub> (lower panels) measured after preparation (0 h, solid line) and after incubation for 24 or 48 h (dashed line) at 30 °C, respectively. The average hydrodynamic sizes of 0 h and 24 or 48 h, respectively, are indicated in each panel (see also Table 1).

shows that all the 9 single-gene deletion mutants were able to grow in YPD<sub>mod</sub> and the OS response-defective strains (*yap1Δ*, *sod1Δ*, and *sod2Δ*) had very similar specific growth rates to wt cells ( $\sim 0.4 \text{ h}^{-1}$ ); however, endocytosis- (*end3Δ*) and cell wall/membrane-defective strains (*gas1Δ*, *erg3Δ*, *mnn10Δ*, *kre6Δ*, and *knr4Δ*) grew 10–25% slower than wt (Table S2). After 48 h, all the studied yeast cultures were in the stationary growth phase (Fig. S3).

### 3.4. Toxicity of the silver nanoparticles to *S. cerevisiae* in the 48-h growth inhibition test

In the growth inhibition test, we used a modified YPD<sub>mod</sub> medium that is more diluted compared to the original YPD. The rationale of using more diluted medium was as follows: in full-strength YPD, the toxicity of studied AgNPs was very low (data not shown), probably due to the presence of high concentration of proteins and amino acids in full strength YPD that may considerably reduce the bioavailability of Ag ions (Behra et al., 2013).

Of the tested Ag compounds, the most toxic were Ag ions, followed by nAg-col, nAg-PVP, and uncoated AgNPs (nAg). The 48-h IC<sub>50</sub> values (mg Ag/L) to the wt were as follows: 2.4 for Ag ions, 76.8 for nAg-col, 148 for nAg-PVP, and 576 for the uncoated nAg (Fig. 3, Table S3). In general, Ag ions were  $\sim 30$ - to 60-fold more toxic than the coated AgNPs and  $\sim 240$ -fold more toxic than the uncoated AgNPs to wt strain.

Toxic effects of positive controls, SDS, and H<sub>2</sub>O<sub>2</sub> were also analyzed. Anionic detergent SDS was chosen as a toxicant acting on cell membranes. SDS has been used for a long time for membrane solubilization to investigate the substructure of the membranes (Auborn et al., 1971), and it has been shown that SDS can solubilize yeast plasma membrane resulting in the release of cellular proteins (Tukmachev et al., 1979).

In our experiments 48-h IC<sub>50</sub> of SDS for wt was 1017 mg/L. The mutant strains defective in cell wall/membrane components synthesis (Table S1), endocytosis (*end3Δ*) and OS-response (*sod1Δ*) were remarkably more sensitive to SDS than wt: the respective 48-h IC<sub>50</sub> values were 5–11 times lower compared to wt (Fig. 3, Table S3).

The other positive control chosen by us for oxidative stress was H<sub>2</sub>O<sub>2</sub> as there is a lot of information on the OS inducing effects of H<sub>2</sub>O<sub>2</sub> for microbial, yeast, and mammalian cells (Godon et al., 1998; Costa et al., 2002; Wijeratne et al., 2005; Suppi et al., 2015). The 48-h IC<sub>50</sub> of H<sub>2</sub>O<sub>2</sub> for wt in growth inhibition test was 99 mg/L, which was in accordance with our previous results (Kasemets et al., 2013). In addition to the

OS-sensitive mutants' *yap1Δ* and *sod2Δ*, also *end3Δ* and cell wall/membrane synthesis-defective strains *gas1Δ*, *erg3Δ*, and *mnn10Δ* were more sensitive to H<sub>2</sub>O<sub>2</sub> compared to wt (Fig. 3, Table S3). It has been shown that the oxidative degradation of membrane lipids may also cause membrane damage and leakage (Wijeratne et al., 2005).

When we compared the respective IC<sub>50</sub> values of AgNPs and Ag ions to wt, OS-response-defective (*yap1Δ*, *sod1Δ*, *sod2Δ*), and cell wall/membrane-defective (*gas1Δ*, *erg3Δ*, *mnn10Δ*, *kre6Δ*, *kre4Δ*) strains, there were no obvious differences (Fig. 3, Table S3). Therefore, unlike H<sub>2</sub>O<sub>2</sub> and SDS, respectively, the primary toxicity mechanism of Ag ions and studied AgNPs to growing *S. cerevisiae* was not oxidative stress or membrane permeabilization.

Surprisingly, the endocytosis-defective mutant *end3Δ* was  $\sim 1.5$ -times more sensitive than wt to Ag ions and uncoated AgNPs (nAg), and  $\sim 3$ -times more sensitive to the casein- and PVP-coated AgNPs (Fig. 3, Table S3). According to the IC<sub>50</sub> values (Fig. 3), the *end3Δ* mutant showed statistically significant difference from wt only to nAg-col and nAg-PVP. However, according to the colony-forming ability after exposure to Ag compounds (see Fig. S4), the *end3Δ* showed elevated sensitivity also to Ag ions and uncoated AgNPs.

### 3.5. Toxicity of the silver nanoparticles to *S. cerevisiae* in the 24-h cell viability assay

To determine the toxic potential of the Ag compounds without the complexing effects of YPD medium constituents, we used DI water as a test environment and measured cell viability as a toxicity endpoint. This is a novel and relatively unconventional approach recently introduced in Kasemets et al. (2013) and further developed in Suppi et al. (2015). Although in this test the yeast cells are incubated in hypotonic conditions (DI water) for 24 h, no loss in cell viability was observed (Kasemets et al., 2013; Suppi et al., 2015).

In the current study, the viability of the control (not exposed) and toxicant-exposed yeast cells was assessed by the fluorescein diacetate (FDA). FDA is taken up by the viable cells via passive diffusion and hydrolyzed by intracellular esterases to the fluorescent product accumulating in the cells (Breeuwer et al., 1995). The reliability of this method was evaluated in comparison with the viable plate counts methods with wt cells. Even though the viable plate count method was slightly more sensitive (IC<sub>50</sub> values for Ag compounds were  $\sim 2$ -fold lower), overall the results of the two methods were comparable (data not shown).

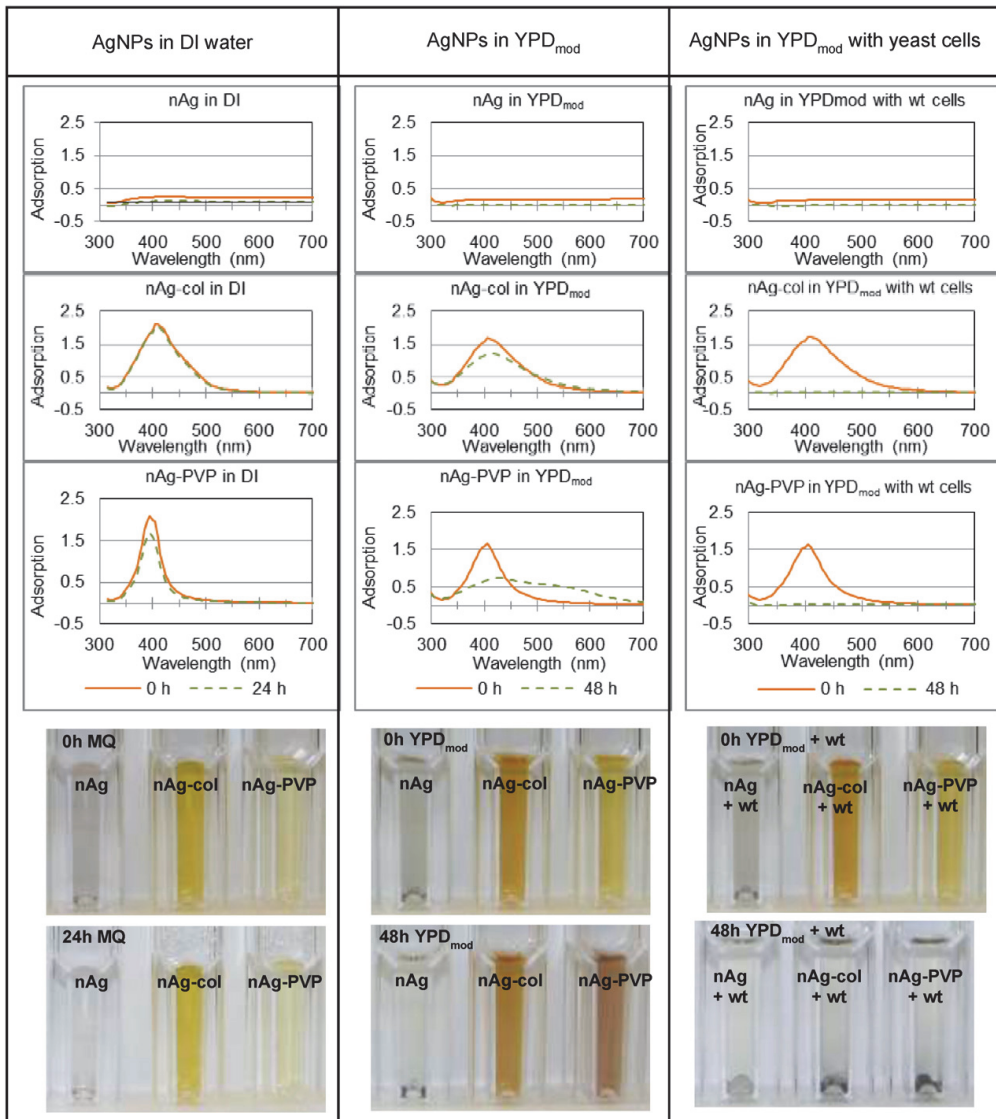


Fig. 2. UV-vis absorption spectra of nAg (200 mg Ag/L), nAg-col, and nAg-PVP (both 20 mg Ag/L) in deionized water (DI) and in modified yeast extract–peptone–dextrose medium YPD<sub>mod</sub> after 0 h (solid line) and 24 or 48 h of incubation (dashed line), respectively, with or without the presence of *S. cerevisiae* wt cells. Photographs below illustrate the stability of the AgNPs suspensions with and without the presence of yeast cells. All AgNPs concentrations used were sub-toxic to yeast.

The 24-h  $IC_{50}$  values of the cell viability test in DI water are presented in Fig. 4 and Table S4. Although the toxicity endpoints (inhibition of the growth and viability, respectively) in these two test formats are different, the big differences in toxicity values of silver compounds were due to the different composition of the respective test media. All the tested Ag compounds were 26–40-times more toxic to wt in DI water than in YPD<sub>mod</sub> (Figs. 3 and 4, Tables S3 and S4), indicating the impact of test medium on the bioavailability and toxicity of Ag compounds. The 24-h  $IC_{50}$  of Ag ions, nAg-col, nAg-PVP, and nAg to *S. cerevisiae* wt strain in DI water were 0.09, 2.71, 3.70, and 18.7 mg Ag/L, respectively. Similarly to the Ag compounds, also  $H_2O_2$  was more toxic to wt in DI water than in YPD<sub>mod</sub> (~8-times), probably due to the oxidation of

YPD medium constituents by  $H_2O_2$  and decrease of the effective concentration of  $H_2O_2$  in the test medium.

As expected, the toxicity of SDS did not remarkably depend on the test environment: the  $IC_{50}$  for wt were comparable in YPD<sub>mod</sub> and DI water (1079 and 1017 mg/L, respectively; Tables S3 and S4). In DI water, Ag ions were ~30- to 40-fold more toxic compared to the coated AgNPs (nAg-col and nAg-PVP) and ~200-fold more toxic compared to the uncoated AgNPs (nAg) to wt strain. These data are coherent with the 48-h growth inhibition assay data (see Section 3.4), demonstrating that most probably the observed toxic effect of AgNPs was mediated by the soluble fraction of Ag (bioavailable Ag).

As in the 48-h growth inhibition test, also in the 24-h viability assay in DI water, the *end3Δ* compared to the wt was ~2.5-times more sensitive to Ag ions and ~8-times to all the studied AgNPs, but statistically significant difference was only found in nAg-, nAg-col-, and nAg-PVP-exposed cells (Fig. 4).

Again, the cell wall/membrane-defective and the OS-sensitive strains showed no higher susceptibility compared to wt to any of the tested Ag compounds. Interestingly, in DI water, we observed that the *kre6Δ*, *gas1Δ* and especially *mnn10Δ* tolerated about ~2–5 times higher concentrations of Ag compounds and H<sub>2</sub>O<sub>2</sub> than wt cells. That effect was not evident for SDS (Fig. 4). These results were confirmed also by the spot test (Fig. S4).

### 3.6. Assessment of intracellular reactive oxygen species in silver compounds-exposed *S. cerevisiae* wild-type cells

One of the main paradigms in nanotoxicology is that NPs can cause toxicity to cells via the formation of reactive oxygen species (ROS). Our toxicity tests with H<sub>2</sub>O<sub>2</sub>- and menadione-sensitive strains *yap1Δ*,

*sod1Δ*, and *sod2Δ* in YPD<sub>mod</sub> and in DI water indicated that the induction of oxidative stress was not the mode of action of the studied AgNPs. For further proof, we used also the H<sub>2</sub>DCF-DA assay to evaluate the formation of intracellular ROS in silver compounds-exposed *S. cerevisiae* wt cells. The H<sub>2</sub>DCF-DA assay has been used to measure oxidative stress (OS) potential of various types of NPs (Ag, Al<sub>2</sub>O<sub>3</sub>, SWCNT, TiO<sub>2</sub>) in different cells, mostly in mammalian cell culture in vitro that are usually prone to cellular uptake of NPs (Gliga et al., 2014; Wang et al., 2014). H<sub>2</sub>O<sub>2</sub> and menadione were used as the positive controls for intracellular ROS formation, as both these chemicals have been shown to cause OS to yeast cells (Flattery-O'Brien et al., 1993; Moradas-Ferreira et al., 1996). The results are presented in Fig. 5.

After 24-h exposure to 20 mg/L H<sub>2</sub>O<sub>2</sub> (24-h IC<sub>50</sub> in DI water was 11.8 mg/L) and menadione (according to Kasemets et al. (2013), 24-h IC<sub>50</sub> in DI water was 37.1 mg/L), there was no increase in ROS levels in wt cells (Fig. 5, lower panel). Thus, it appeared that the measurement of intracellular ROS level after 24 h of exposure was not relevant as the reactive radicals were not detectable after the long incubation with cells. We therefore included also the 2-h and 4-h exposure times

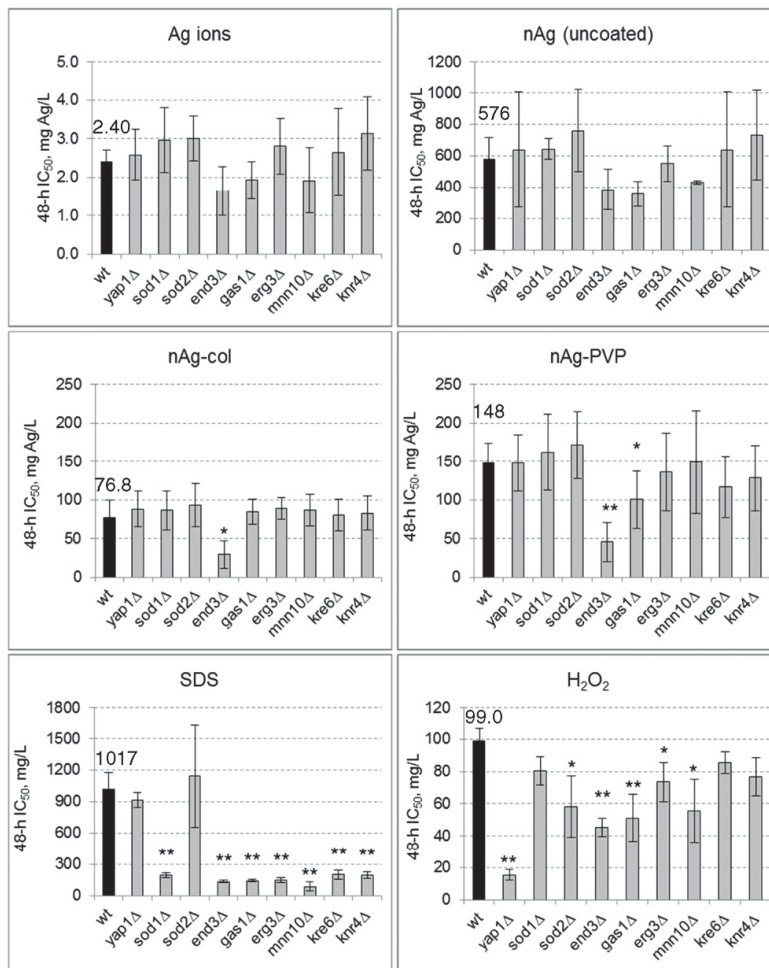


Fig. 3. Toxicity (48-h IC<sub>50</sub> values) of Ag ions, silver nanoparticles (mg Ag/L), positive controls SDS and H<sub>2</sub>O<sub>2</sub> (mg/L) in the growth inhibition test in YPD<sub>mod</sub> to *S. cerevisiae* BY4741 wild-type (wt) and its 9 mutant strains. Results are presented as the mean of at least 3 experiments ± SD. The mean IC<sub>50</sub> value for wt is indicated in each panel. \* and \*\* represent statistically significant difference from wt according to t-test ( $\alpha = 0.05$  and  $\alpha = 0.01$ , respectively). All concentrations are nominal. Data are plotted from Table S3.

to assess the more rapid ROS-formation potential of the chemicals. After 2- and 4-h exposure to  $H_2O_2$  there was an apparent dose-dependent increase in the amount of ROS in the wt cells (Fig. 5, two upper panels). Analogous dose-dependent increase in ROS was observed in the case of menadione but in a lower scale, probably as the  $H_2DCF$ -DA is not specific toward superoxide radicals. We observed a statistically significant elevated level of ROS in the cells exposed for 2 and 4 h to 0.16 mg/L of Ag ions (24-h  $IC_{50-90}$  in DI), but not in cells exposed to higher concentration of Ag ions (Fig. 5). Ag ions have been shown to generate intracellular ROS in bacterial cells (Park et al., 2009) and an unbalanced level of ROS in the yeast cells could result from (i) a decrease in intracellular antioxidants (ii) an increased production of reactive oxygen species, or both (Costa and Moradas-Ferreira, 2001). Highly toxic concentrations of Ag ions may also cause cells' functional impairments (e.g., effects on the respiratory enzymes, decrease in mitochondrial membrane potential, leakage of ROS from mitochondria, etc.) and consequently release of the secondary ROS (Ivask et al., 2014b).

Interestingly, we observed increased ROS levels in yeast cells exposed for 2 h to nAg (4, 20, and 100 mg Ag/L) and nAg-col (0.16 mg Ag/L), but after 4 h, the level of ROS were comparable to the unexposed cells (Fig. 5). Results of the toxicity tests performed on OS-sensitive mutants *yap1Δ*, *sod1Δ*, and *sod2Δ* showed that studied AgNPs toxicity to yeast *S. cerevisiae* was not ROS-mediated. Assuming, the ROS formed in the early exposure stages did not contribute so strongly to the overall toxicity of the nAg and nAg-col particles after 24-h exposure. In a study of AgNPs toxicity to the human bronchial epithelial BEAS-2B cells, Gliga et al. (2014) also found no intracellular ROS production by AgNPs but associated the AgNPs toxicity with the intracellular release of Ag ions.

### 3.7. Assessment of the uptake of nAg-col and nAg-PVP into the yeast cells by laser scanning confocal microscopy

To visualize AgNPs-yeast cells interactions laser scanning confocal microscopy in reflection mode was used. Wild-type and endocytosis-

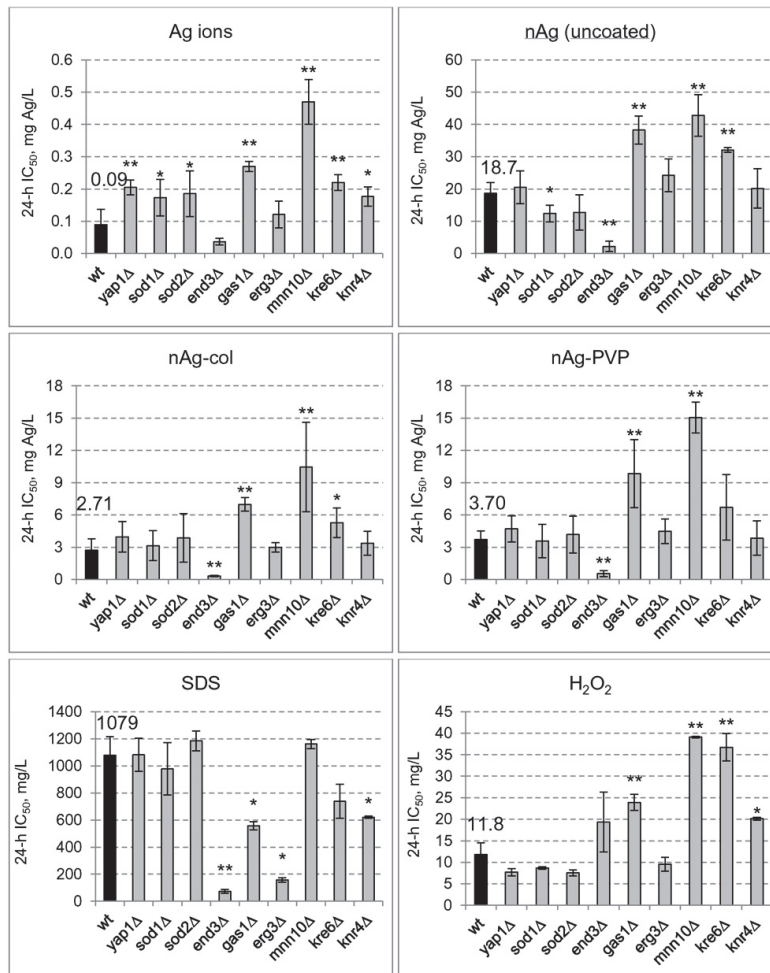


Fig. 4. Toxicity (24-h  $IC_{50}$  values) of Ag ions, coated and uncoated silver nanoparticles (mg Ag/L), positive controls SDS and  $H_2O_2$  (mg/L) in the cell viability test in deionized water to *S. cerevisiae* BY4741 wild-type (wt), and its 9 mutant strains as determined by the viability staining with fluorescein diacetate. Results are presented as the mean of 3 experiments  $\pm$  SD. The mean  $IC_{50}$  value (mg/L) for wt is indicated in each panel. \* and \*\* represent statistically significant difference from wt according to t-test ( $\alpha = 0.05$  and  $\alpha = 0.01$ , respectively). All concentrations are nominal. Data are plotted from Table S4.

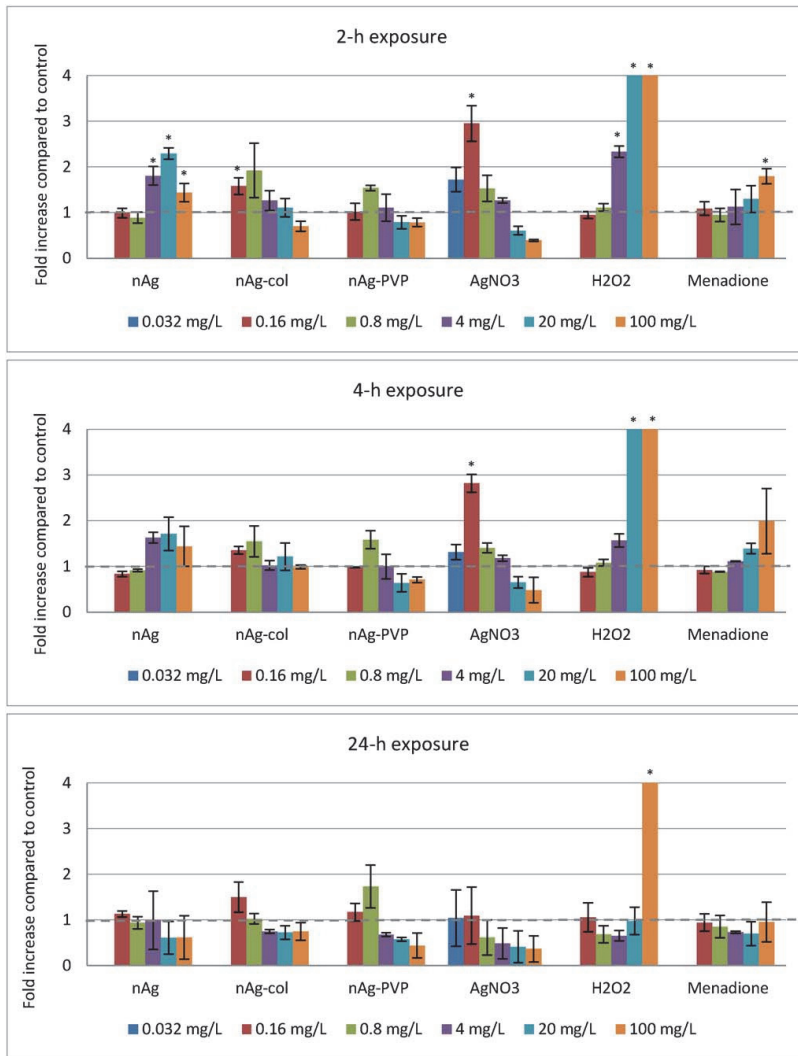


Fig. 5. Generation of reactive oxygen species (ROS) measured with fluorescent dye  $H_2DCF\text{-}DA$  in the *S. cerevisiae* BY4741 wild-type cells after 2-, 4-, and 24-h exposure to Ag ions (0.032–100 mg Ag/L), AgNPs (0.16–100 mg Ag/L),  $H_2O_2$ , and menadione (0.16–100 mg/L) in deionized water. The values are presented as fold-increase in fluorescence of exposed cells compared to unexposed cells; the mean of two experiments is given  $\pm$  SD. All exposure concentrations are nominal. The dashed horizontal line highlights the ROS level in the control cells (unexposed yeast cells).

defective mutant  $end3\Delta$  was studied after 3-h exposure to nAg-col and nAg-PVP particles in  $YPD_{mod}$ . To avoid the potential internalization of the AgNPs due to the disruption of the cell wall/membrane, the sub-toxic exposure concentration of AgNPs (1 mg Ag/L) was used. Results of the confocal microscopy visualization have been presented in the Figs. 6, S7, S8, S9, S10, and S11.

Confocal microscopy analyses showed that the studied nAg-col and nAg-PVP particles were internalized by the wt cells but not by  $end3\Delta$  cells (Fig. 6 a, b, c, d). Although the overlay picture of the nAg-col-exposed  $end3\Delta$  cells showed the presence of the silver nanoparticles in the sample (Fig. 6c, white spots), the detailed sectional analyses revealed that most of the AgNPs were in the first section of visualization where no yeast cells were visible (i.e., no DAPI-stained nuclei) (Fig. S10), and cross-sectional analyses showed that some nAg-col particles

detected in the next layers (Fig. S10) had adsorbed onto the  $end3\Delta$  cell surface (Fig. 6c, cross-section, see the white arrows).

Confocal microscopy visualization of the nAg-PVP-exposed  $end3\Delta$  also showed the presence of some silver nanoparticles in the sample, but cross-sectional analyses showed that these particles were not interacting with the cells (Fig. 6d).

Comparison of the morphology of the yeast cells did not reveal characteristic differences between non-treated (control) and AgNPs-treated wt and  $end3\Delta$  cells (Figs. 6a–d, S7), but we observed that the nuclei of nAg-PVP-exposed  $end3\Delta$  cells were fragmented (Fig. 6d), although the used exposure concentration was sub-toxic (1 mg Ag/L) (nAg-PVP 48-h  $IC_{50}$  for  $end3\Delta$  in  $YPD_{mod}$  was 45.5 mg Ag/L). Chromatin condensation and nuclei fragmentation is one of the signs of apoptosis in the yeast cells (Monteiro et al., 2012).

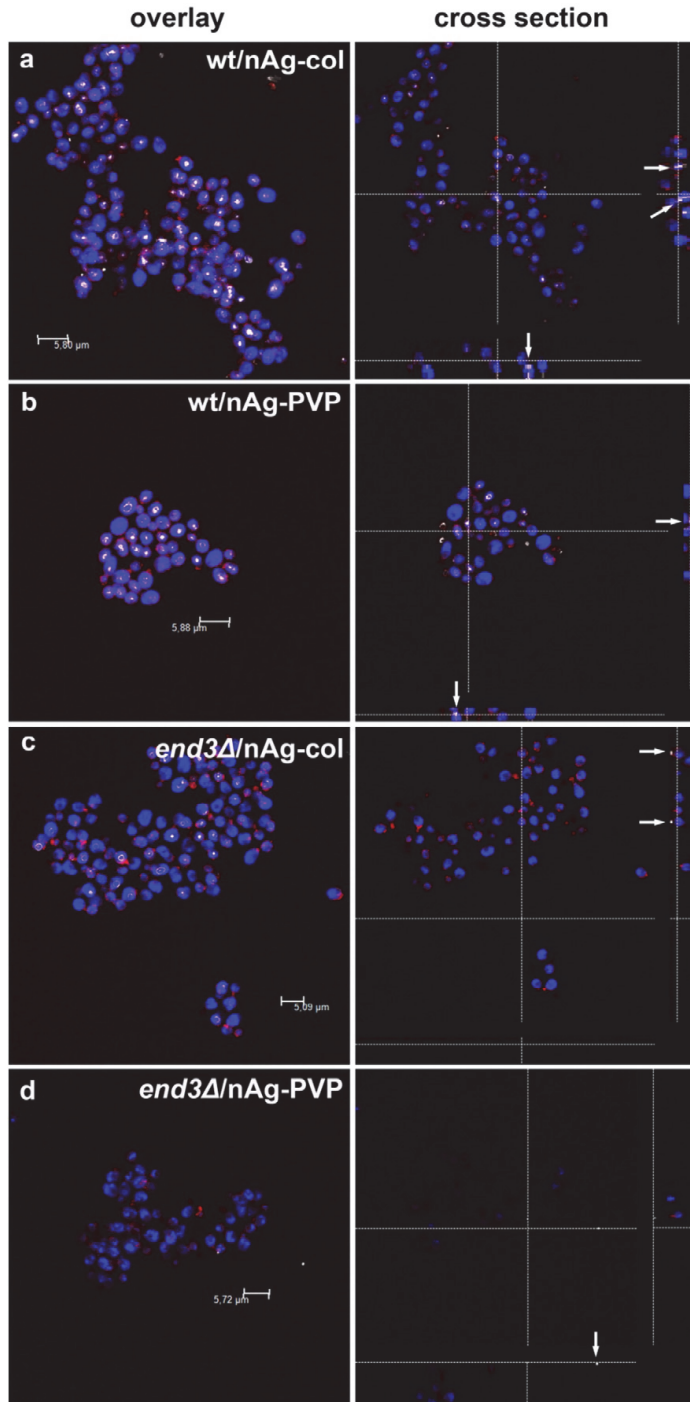


**Fig. 6.** Confocal microscopy analyses of *S. cerevisiae* BY4741 wild-type (a, b) and endocytosis-defective *end3Δ* cells (c, d) exposed to protein-coated (nAg-col) (a, c) and PVP-coated AgNPs (nAg-PVP) (b, d) (1 mg Ag/L) for 3 h in YPD<sub>mod</sub> at 30 °C. Actin filaments were visualized by rhodamine-phalloidine staining (red), nuclei by DRAQ5™ (blue pseudocolor), and AgNPs were visualized by laser reflection (white spots). White arrows on the cross-section's pictures indicate to the AgNPs. AgNPs exposure concentrations were sub-toxic (see also Figs. S7, S8, S9, S10, S11).

**Table 2**  
Nominal IC<sub>50</sub> (mg Ag/L) (data from Tables S3 and S4) and AgNPs dissolution-corrected IC<sub>50</sub> values (mg Ag ions/L) for *S. cerevisiae* BY4741 wild-type strain (see Table 1 for the AgNPs dissolution data).

AgNPs	24-h cell viability test in DI water		48-h growth inhibition test in YPD <sub>mod</sub>	
	Nominal 24-h IC <sub>50</sub>	Dissolution-corrected 24-h IC <sub>50</sub>	Nominal 48-h IC <sub>50</sub>	Dissolution-corrected 48-h IC <sub>50</sub>
IC <sub>50</sub> , mg Ag/L				
Ag ions <sup>a</sup>	0.09	0.09	2.40	2.19
nAg-col	2.71	0.18	76.8	0.79
nAg-PVP	3.70	0.30	148	1.36
nAg	18.7	0.39	576	1.53

<sup>a</sup> Ag ions IC<sub>50</sub> values have been corrected according to the Ag-ion recovery data in DI water or in YPD<sub>mod</sub> after 24 h or 48 h incubation, respectively, at 30 °C. Ag-ion recovery in DI water was 100% and in YPD<sub>mod</sub> ~92%. For the Ag-ion recovery assessment the same test conditions was used as in the AgNPs solubility test.

#### 4. Discussion

In this study, 3 different types of AgNPs were studied for their toxicological effects toward the yeast *S. cerevisiae* BY4741 wt and its 9 single-gene deletion mutants in YPD<sub>mod</sub> and DI water. All the studied Ag compounds were significantly more toxic if exposed to silver compounds in DI water compared to the exposure in YPD<sub>mod</sub> (Figs. 3 and 4, Tables S3 and S4). The higher toxicity in DI water was largely due to the higher solubility/bioavailability of silver in DI water compared to rich medium (Table 1). In addition, the different toxicity test formats may also influence the yeast cells stress response and susceptibility to the toxicants. Indeed, the nutrients-rich YPD<sub>mod</sub> medium supports the active metabolism of the cells (high glycolytic activity and ATP production rate) providing the cells with energetic resources to maintain the cells homeostasis (Kasemets et al., 2006). In DI water, the cells are in the starving conditions and also encounter the hypotonic conditions which may induce osmotic stress, at the same time the yeast cells have a rigid cell wall, which prevents the lysis of the protoplast (Zlotnik et al., 1984). Indeed, the yeast cells are able to remain viable in DI water at least up to 24 h (Kasemets et al., 2013; Suppi et al., 2015).

Toxicity order of Ag ions and studied AgNPs in the different test medium was as follows: full strength YPD  $\gg$  YPD<sub>mod</sub> (diluted)  $\gg$  DI water, indicating the important role of Ag ions in AgNPs toxicity toward yeast cells. According to the AgNPs solubility data in cell-free medium (Table 1) and taking into account the amount of dissolved Ag present at the AgNPs nominal IC<sub>50</sub> concentrations in DI water after 24-h incubation, the toxicity of studied AgNPs in DI water was seemingly solely driven by dissolved Ag-ions (Table 2).

In DI water, the dissolution-corrected IC<sub>50</sub> values (Table 2), however, were higher than the respective IC<sub>50</sub> value of Ag ions (0.09 mg Ag/L). That may be due to the use of the FDA assay for the viability evaluation as FDA assays is based on the determination of intracellular esterase's activity (metabolic activity) that may underestimate the toxicity in the stress conditions enhancing the metabolic activity as previously shown in monocarboxylic acids exposed yeast cells (Kasemets et al., 2006).

Similarly to cell viability test, also in the growth inhibition test in YPD<sub>mod</sub>, the toxicity of AgNPs was largely explainable by the dissolution (Table 2), although the toxicity of nAg-col to wt could not be explained only by the liberated Ag ions (Fig. S6). The dissolution of AgNPs in a protein-rich biological medium is a complex process. Although the release of Ag ions from the particles' surface takes place, simultaneously also the binding of dissolved Ag ions by medium ligands starts. In this study, for the AgNPs dissolution assessment, the NPs-suspensions were ultracentrifuged to remove the non-soluble fraction of the NPs, supernatants were acidified and the dissolved fraction of Ag was quantified by AAS, whereas the proportion of Ag in a complex-bound form in YPD<sub>mod</sub> medium (i.e., non-bioavailable) still remains unknown as using this method it is not possible to distinguish between the free and bound fraction of the Ag ions. Furthermore, the AgNPs dissolution was quantified in abiotic conditions. When the yeast cells grow in YPD<sub>mod</sub> medium, changes in the test environment occur such as

decrease in the pH of the medium due to the consumption of basic amino acids and excretion of acidic metabolic by-products (e.g., organic acids) (Coote and Kirsop, 1976), which can alter the physical-chemical properties of NPs such as surface charge, particle size, agglomeration (Fig. 2), dissolution of AgNPs, and bioavailable fraction of Ag.

In the growth inhibition test in YPD<sub>mod</sub> medium, none of the OS-sensitive strains (*yap1Δ*, *sod1Δ*, *sod2Δ*) was more sensitive than wt to the Ag ions and AgNPs indicating that the Ag ions and AgNPs toxicity to the growing *S. cerevisiae* cells did not occur via the H<sub>2</sub>O<sub>2</sub>- and menadione-like oxidative stress-inducing mechanism. SDS is an anionic detergent causing permeabilization of the lipid bilayer of cellular membranes and increase in permeability of the yeast cell wall (Heerklotz, 2008; Kodedova et al., 2011; Kragh-Hansen et al., 1998). According to Kodedova et al. (2011), 0.8 mM (230 mg/L) SDS caused membrane hyperpolarization due to the outflow of cations and 5 mM (1442 mg/L) SDS caused full permeabilization of the cell membrane and induced rapid lethality. The cell wall/membrane mutants used in the current study were more susceptible to SDS and H<sub>2</sub>O<sub>2</sub> than wt (Fig. 3), indicating the important role of cell wall beta-glucans, mannoproteins, and ergosterol in the cell wall/membrane stress conditions. As the SDS-sensitive cell wall/membrane mutants were not more susceptible than the wild-type to the studied Ag compounds, the toxicity mechanism of Ag ions and AgNPs were probably not the SDS-like permeabilization of cell wall/membrane.

Moreover, in viability test in DI water and not in YPD<sub>mod</sub> *kre6p*, *gas1p*, and *mnn10p* mutants were significantly less sensitive to the H<sub>2</sub>O<sub>2</sub>, AgNPs and especially to the Ag ions. It is not clear why the incubation of yeast cells in DI water and not in YPD<sub>mod</sub> might give an advantage to cell wall beta-glycans biosynthesis (*kre6Δ*, *gas1Δ*) and mannosyltransferase defective strain (*mnn10Δ*) in response to Ag compounds and H<sub>2</sub>O<sub>2</sub>. Ram et al. (1998) have proposed that the weakening of the cell wall due to the lower  $\beta$ -glucan content of the cell wall in *gas1Δ* and *knr4Δ* mutants was compensated by increased chitin and mannoproteins content in the cell wall. Hypothetically, increased chitin content leading to the thicker cell wall might have given the advantage to the *gas1Δ* and *knr4Δ* strains to cope better with and adapt to the Ag ions stress in DI water (hypotonic conditions) compared to the wt. Also the OS-sensitive mutants (*yap1Δ*, *sod1Δ*, *sod2Δ*) were statistically significantly more resistant to Ag ions, but not to the studied AgNPs, and positive controls H<sub>2</sub>O<sub>2</sub> and SDS. That gives additional proof that oxidative stress was probably not the cause of toxic effects of silver compounds to yeast.

Interestingly, only the endocytosis-defective *end3Δ* strain showed enhanced sensitivity compared to wt toward coated AgNPs and to a lesser extent to uncoated AgNPs and Ag ions. The *end3Δ* strain was also very sensitive to the membrane permeabilizing agent SDS and somewhat to H<sub>2</sub>O<sub>2</sub> (Figs. 3, 4, S4, S5). As endocytosis is an essential function for the viable yeast cells regulating plasma membrane composition and cell homeostasis (Goode et al., 2015), it might be also possible that mutation in *end3p* renders the cells more susceptible than wt to different stress conditions. It has been shown that most of the proteins involved in endocytosis (e.g., *end3p*, *end4p*, *end5p*, and *end7p*) have a

role in maintaining the organization of the cytoskeleton and are not required to retain yeast cells viability in favorable growth conditions, but are useful to maintain the cell viability under adverse conditions such as starving and high temperature stress (Munn, 2000). Thus, it can be assumed that in growth inhibition test in YPD<sub>mod</sub> the significantly higher sensitivity of the end3Δ strain to coated AgNPs, SDS, and H<sub>2</sub>O<sub>2</sub> compared to wt was not caused due to the end3Δ strain's inherent lower viability. Therefore, the higher toxicity of AgNPs, especially the coated AgNPs, to the end3Δ strain compared to wt cells was probably related to the inability of mutant cells to internalize AgNPs by endocytosis. So, contrarily to our initial hypothesis we observed that in the absence of endocytosis *S. cerevisiae* cells were more sensitive to AgNPs than wt. It has been shown that silver may damage the yeast cells due to reacting with sulfur-containing proteins (Saulou et al., 2010). Despax et al. (2011) also confirmed the affinity of silver entities to cellular proteinaceous compounds and showed by transmission electron microscopy (TEM) that in the case of AgNO<sub>3</sub> treatment, the large electron-dense nodules were located mostly at the yeast cell wall periphery and EDS analysis revealed the presence of the sulfur and nitrogen in these electron-dense nodules. In the cells defective in endocytosis the non-functional proteins are not recycled (Goode et al., 2015) and finally the cell wall/membrane functionality may decrease. Indeed in our study the end3Δ strain was ~2-times more sensitive than wt to the Ag-ions.

Moreover end3Δ cells were 3–8-times more sensitive than wt to the AgNPs, especially to nAg-col and nAg-PVP. Confocal laser scanning microscopy analyses of nAg-col- and nAg-PVP- exposed wt and end3Δ cells revealed that after 3-h incubations in YPD<sub>mod</sub> medium both the AgNPs were located inside of the wild-type cells (Figs. 6 a, b; S8, S9), but not in the endocytosis-defective strain end3Δ (Figs. 6 c, d; S10, S11). Moreover, we showed that nAg-col was absorbed onto the surface of the end3Δ cells (Fig. 6c, see white arrows). It could be assumed that if given AgNPs cannot be internalized, they may adhere and accumulate on the cell surface and (i) may disrupt the functioning of the cell wall and membrane or cause a decrease in the membrane fluidity as shown before for *S. cerevisiae* upon exposure to polystyrene latex NPs (Nomura et al., 2015; Nomura et al., 2013) or (ii) may lead to enhanced particle solubility and release of toxic Ag ions in the close vicinity of the cell surface as previously proposed by Bondarenko et al. (2013b) for bacterial cells. To sum up, we propose that the AgNPs caused more enhanced toxic effects to end3Δ strain primarily by attaching to the cells' surface that may lead to enhanced AgNPs solubilization in the close vicinity of the cell surface and adverse effects on the functionality of the cell wall/membrane. Despax et al. (2011) showed by TEM that differently from ionic silver, nanosilver accumulated mostly in the subcellular structures of the yeast cells. Thus, the uptake of the AgNPs via endocytosis probably leads to more controlled compartmentalization and detoxification of Ag within the cells.

## 5. Conclusions

Using confocal microscopy of wild-type and endocytosis-negative mutant end3Δ of *S. cerevisiae* exposed to sub-toxic concentrations of nAg-col and nAg-PVP we showed that *S. cerevisiae* was internalizing the AgNPs via endocytosis. Comparison of the toxicity patterns of a suite of 9 *S. cerevisiae* single-gene deletion mutant and wt cells to the studied AgNPs and Ag ions showed that (i) oxidative stress was not the mechanism of toxicity of AgNPs to *S. cerevisiae* and this conclusion was supported by the quantification of intracellular ROS using H<sub>2</sub>DCF-DA assay; (ii) AgNPs also did not cause SDS-like permeabilization and leakage of cell wall/membrane of yeast cells; (iii) the endocytosis-defective *S. cerevisiae* strain end3Δ proved more sensitive than wt to the tested Ag compounds (especially to the coated AgNPs), but also to SDS and H<sub>2</sub>O<sub>2</sub> showing the importance of the endocytosis in stress conditions; (iv) the higher toxicity of nAg-col to the end3Δ strain could be explained by adhesion of the particles to the mutants' cell surface, disturbing the membrane function. Further studies at subcellular level are needed to

better understand the role of bio-interactions in the AgNPs-induced toxicity on yeasts.

## Transparency document

The Transparency document associated with this article can be found, in online version.

## Acknowledgments

This work was supported by grants ETF9001 and Institutional funding IUT 23-5 of the Estonian Ministry of Education and Research and by the grant of Fondazione Cariplo to the project OverNanoTox (2013-0987). We thank Prof Heikki Tenhu (University of Helsinki, Finland) for providing the PVP-nAg. We thank Dr. Heiti Paves (Tallinn University of Technology, Estonia) and Dr. Umberto Fascio (University of Milano Bicocca) for their help with the confocal microscopy and MSC Imbi Kurvet (NICPB, Estonia) for technical assistance.

## Appendix A. Supplementary data

Supplementary data to this article can be found online at <http://dx.doi.org/10.1016/j.tiv.2016.05.018>.

## References

- Arthington-Skaggs, B.A., Crowell, D.N., Yang, H., Sturley, S.L., Bard, M., 1996. Positive and negative regulation of a sterol biosynthetic gene (ERG3) in the post-squalene portion of the yeast ergosterol pathway. *FEBS Lett.* 392, 161–165.
- Atiyeh, B.S., Costagliola, M., Hayek, S.N., Dibo, S.A., 2007. Effect of silver on burn wound infection control and healing: review of the literature. *Burns* 33, 139–148.
- Auborn, J.J., Eyring, E.M., Choules, G.L., 1971. Kinetics of sodium dodecyl sulfate solubilization of Mycoplasma laidlawii plasma membranes. *Proc. Natl. Acad. Sci. U. S. A.* 68, 1996–1998.
- Avery, S.V., Howlett, N.G., Radice, S., 1996. Copper toxicity towards *Saccharomyces cerevisiae*: dependence on plasma membrane fatty acid composition. *Appl. Environ. Microbiol.* 62, 3960–3966.
- Behra, R., Sigg, L., Clift, M.J.D., Herzog, F., Minghetti, M., Johnston, B., Petri-Fink, A., Rothen-Rutishauser, B., 2013. Bioavailability of silver nanoparticles and ions: from a chemical and biochemical perspective. *J. R. Soc. Interface* 10, 1–15.
- Benedetti, H., Rath, S., Crausaz, F., Riezman, H., 1994. The END3 gene encodes a protein that is required for the internalization step of endocytosis and for actin cytoskeleton organization in yeast. *Mol. Biol. Cell* 5, 1023–1037.
- Blinova, L., Niskanen, J., Kajankari, P., Kanarbiik, L., Käkkinen, A., Tenhu, H., Penttinen, O.P., Kahru, A., 2013. Toxicity of two types of silver nanoparticles to aquatic crustaceans *Daphnia magna* and *Thamnocephalus platyurus*. *Environ. Sci. Pollut. Res. Int.* 20, 3456–3463.
- Bondarenko, O., Ivask, A., Käkkinen, A., Kurvet, I., Kahru, A., 2013b. Particle-cell contact enhances antibacterial activity of silver nanoparticles. *PLoS One* 8, e64060.
- Bondarenko, O., Juganson, K., Ivask, A., Kasemets, K., Mortimer, M., Kahru, A., 2013a. Toxicity of Ag, CuO and ZnO nanoparticles to selected environmentally relevant test organisms and mammalian cells in vitro: a critical review. *Arch. Toxicol.* 87, 1181–1200.
- Botstein, D., Fink, G.R., 2011. Yeast: an experimental organism for 21st Century biology. *Genetics* 189, 695–704.
- Brachmann, C.B., Davies, A., Cost, G.J., Caputo, E., Li, J., Hieter, P., Boeke, J.D., 1998. Designer deletion strains derived from *Saccharomyces cerevisiae* S288C: a useful set of strains and plasmids for PCR-mediated gene disruption and other applications. *Yeast* 14, 115–132.
- Brandt, O., Mildner, M., Egger, A.E., Groessl, M., Rix, U., Posch, M., Keppler, B.K., Strupp, C., Mueller, B., Stingl, G., 2012. Nanoscale silver possesses broad-spectrum antimicrobial activities and exhibits fewer toxicological side effects than silver sulfadiazine. *Nanomedicine* 8, 478–488.
- Breeuwer, P., Drocourt, J.L., Bunschoten, N., Zwietering, M.H., Rombouts, F.M., Abee, T., 1995. Characterization of uptake and hydrolysis of fluorescein diacetate and carboxy-fluorescein diacetate by intracellular esterases in *Saccharomyces cerevisiae*, which result in accumulation of fluorescent product. *Appl. Environ. Microbiol.* 61, 1614–1619.
- Coote, N., Kirsop, B.H., 1976. Factors responsible for the decrease in pH during beer fermentations. *J. Inst. Brew.* 82, 149–153.
- Costa, V., Moradas-Ferreira, P., 2001. Oxidative stress and signal transduction in *Saccharomyces cerevisiae*: insights into ageing, apoptosis and diseases. *Mol. Asp. Med.* 22, 217–246.
- Costa, W.M.V., Amorim, M.A., Quintanilha, A., Moradas-Ferreira, P., 2002. Hydrogen peroxide-induced carbonylation of key metabolic enzymes in *Saccharomyces cerevisiae*: The involvement of the oxidative stress response regulators Yap1 and Skn7. *Free Radic. Biol. Med.* 33, 1507–1515.
- Despax, B., Saulou, C., Raynaud, P., Datas, L., Mercier-Bonin, M., 2011. Transmission electron microscopy for elucidating the impact of silver-based treatments (ionic silver

- versus nanosilver-containing coating) on the model yeast *Saccharomyces cerevisiae*. *Nanotechnology* 22, 175101 (13 pp).
- Dulic, V., Egerton, M., Elguindi, I., Rath, S., Singer, B., Riezman, H., 1991. Yeast endocytosis assays. *Methods Enzymol.* 194, 697–710.
- El Badawy, A.M., Silva, R.G., Morris, B., Scheckel, K.G., Suidan, M.T., Tolaymat, T.M., 2011. Surface charge-dependent toxicity of silver nanoparticles. *Environ. Sci. Technol.* 45, 283–287.
- Fabrega, J., Luoma, S.N., Tyler, C.R., Galloway, T.S., Lead, J.R., 2011. Silver nanoparticles: Behaviour and effects in the aquatic environment. *Environ. Int.* 37, 517–531.
- Feng, Q.L., Wu, J., Chen, G.Q., Cui, F.Z., Kim, T.N., Kim, J.O., 2000. A mechanistic study of the antibacterial effect of silver ions on *Escherichia coli* and *Staphylococcus aureus*. *J. Biomed. Mater. Res.* 52, 662–668.
- Flattery-O'Brien, J., Collinson, L.P., Dawes, I.W., 1993. *Saccharomyces cerevisiae* has an inducible response to menadione which differs from that to hydrogen peroxide. *J. Gen. Microbiol.* 139, 501–507.
- Gadd, G.M., 1993. Interactions of fungi with toxic metals. *New Phytol.* 124, 25–60.
- Gliga, A.R., Skoglund, S., Wallinder, I.O., Fadeel, B., Karlsson, H.L., 2014. Size-dependent cytotoxicity of silver nanoparticles in human lung cells: the role of cellular uptake, agglomeration and Ag release. *Part. Fibre Toxicol.* 11, 11.
- Godon, C., Lagniel, G., Lee, J., Buhler, J.M., Kieffer, S., Perrot, R., Boucherie, H., Toledano, M.B., Labarre, J., 1998. The H<sub>2</sub>O<sub>2</sub> stimulin in *Saccharomyces cerevisiae*. *J. Biol. Chem.* 273, 22480–22489.
- Goode, B.L., Eskin, J.A., Wendland, B., 2015. Actin and endocytosis in budding yeast. *Genetics* 199, 315–358.
- Heerklotz, H., 2008. Interactions of surfactants with lipid membranes. *Q. Rev. Biophys.* 41, 205–264.
- Hong, Z., Mann, P., Brown, N.H., Tran, L.E., Shaw, K.J., Hare, R.S., DiDomenico, B., 1994. Cloning and characterization of KNR4, a yeast gene involved in (1,3)-beta-D-glucan synthesis. *Mol. Cell Biol.* 14, 1017–1025.
- Huynh, K.A., Chen, K.L., 2011. Aggregation kinetics of citrate and polyvinylpyrrolidone coated silver nanoparticles in monovalent and divalent electrolyte solutions. *Environ. Sci. Technol.* 45, 5564–5571.
- Hwang, I.S., Lee, J., Hwang, J.H., Kim, K.J., Lee, D.G., 2012. Silver nanoparticles induce apoptotic cell death in *Candida albicans* through the increase of hydroxyl radicals. *FEBS J.* 279, 1327–1338.
- Ivask, A., ElBadawy, A., Kaweteerawat, C., Boren, D., Fischer, H., Ji, Z., Chang, C.H., Liu, R., Tolaymat, T., Telesa, D., Zink, J.J., Cohen, Y., Holden, P.A., Godwin, H., 2014c. Toxicity mechanisms in *Escherichia coli* vary for silver nanoparticles and differ from ionic silver. *ACS Nano* 8, 374–386.
- Ivask, A., Juganson, K., Bondarenko, O., Mortimer, M., Arooja, V., Kasemets, K., Blinova, I., Heinalaan, M., Slaveykova, V., Kahru, A., 2014a. Mechanisms of toxic action of Ag, ZnO and CuO nanoparticles to selected ecotoxicological test organisms and mammalian cells in vitro: a comparative review. *Nanotoxicology* 8 (Suppl. 1), 57–71.
- Ivask, A., Kurvet, I., Kasemets, K., Blinova, I., Arooja, V., Suppi, S., Vija, H., Kakinen, A., Titma, T., Heinalaan, M., Vissnapuu, M., Koller, D., Kisand, V., Kahru, A., 2014b. Size-dependent toxicity of silver nanoparticles to bacteria, yeast, algae, crustaceans and mammalian cells in vitro. *PLoS One* 9, e102108.
- Jung, W.K., Koo, H.C., Kim, K.W., Shin, S., Kim, S.H., Park, Y.H., 2008. Antibacterial activity and mechanism of action of the silver ion on *Staphylococcus aureus* and *Escherichia coli*. *Appl. Environ. Microbiol.* 02001–02007.
- Jungmann, J., Rayner, J.C., Munro, S., 1999. The *Saccharomyces cerevisiae* protein Mnn10p/Bed1p is a subunit of a Golgi mannosyltransferase complex. *J. Biol. Chem.* 274, 6579–6585.
- Kasemets, K., Kahru, J., Laht, T.-M., Paalme, 2006. Study of the toxic effect of short- and medium-chain monocarboxylic acids on the growth of *Saccharomyces cerevisiae* using the CO<sub>2</sub>-auxo-accelerostat fermentation system. *Int. J. Food Microbiol.* 111, 206–215.
- Kasemets, K., Suppi, S., Küniss-Beres, K., Kahru, A., 2013. Toxicity of CuO nanoparticles to yeast *Saccharomyces cerevisiae* BY4741 wild-type and its nine isogenic single-gene deletion mutants. *Chem. Res. Toxicol.* 26, 356–367.
- Kasemets, K., Suppi, S., Manteca, P., Kahru, A., 2014. Charge and size-dependent toxicity of silver nanoparticles to yeast cells. *Toxicol. Lett.* 229, S193–S194.
- Khurana, V., Lindquist, S., 2010. Modelling neurodegeneration in *Saccharomyces cerevisiae*: why cook with baker's yeast? *Nat. Rev. Neurosci.* 11, 436–449.
- Kim, J.S., Kuk, E., Yu, K.N., Kim, J.-H., Park, S.J., Lee, H.J., Kim, S.H., Park, Y.K., Park, Y.H., Hwang, C.-Y., Kim, Y.-K., Lee, Y.-S., Jeong, D.H., Cho, M.-H., 2007. Antimicrobial effects of silver nanoparticles. *Nanomedicine* 3, 95–101.
- Kim, K.-I., Sung, W., Suh, B., Moon, S.-K., Choi, J.-S., Kim, J., Lee, D., 2009. Antifungal activity and mode of action of silver nano-particles on *Candida albicans*. *Biomaterials* 22, 235–242.
- Kodedova, M., Sigler, K., Lemire, B.D., Gaskova, D., 2011. Fluorescence method for determining the mechanism and speed of action of surface-active drugs on yeast cells. *Biotechniques* 50, 58–63.
- Kragh-Hansen, U., le Maire, M., Møller, J.V., 1998. The mechanism of detergent solubilization of liposomes and protein-containing membranes. *Biophys. J.* 75, 2932–2946.
- Levard, C., Hotze, E.M., Lowry, G.V., Brown Jr., G.E., 2012. Environmental transformations of silver nanoparticles: impact on stability and toxicity. *Environ. Sci. Technol.* 46, 6900–6914.
- Manshian, B.B., Pfeiffer, C., Pelaz, B., Heimel, T., Gallego, M., Møller, M., Del Pino, P., Himelreich, U., Parak, W.J., Soenen, S.J., 2015. High-content imaging and gene expression approaches to unravel the effect of surface functionality on cellular interactions of silver nanoparticles. *ACS Nano* 9, 10431–10444.
- Marambio-Jones, C., Hoek, E.M.V., 2010. A review of the antibacterial effects of silver nanomaterials and potential implications for human health and the environment. *J. Nanopart. Res.* 12, 1531–1551.
- Maurer, E.I., Sharma, M., Schlager, J.J., Hussain, S.M., 2014. Systematic analysis of silver nanoparticle ionic dissolution by tangential flow filtration: toxicological implications. *Nanotoxicology* 8, 718–727.
- Monteiro, D.R., Silva, S., Negri, M., Gorup, L.F., de Camargo, E.R., Oliveira, R., Barbosa, D.B., Henriques, M., 2012. Silver nanoparticles: influence of stabilizing agent and diameter on antifungal activity against *Candida albicans* and *Candida glabrata* biofilms. *Letts. Appl. Microbiol.* 54, 383–391.
- Moradas-Ferreira, P., Costa, V., Piper, P., Mager, W., 1996. The molecular defences against reactive oxygen species in yeast. *Mol. Microbiol.* 19, 651–658.
- Moschini, E., Gualtieri, M., Colombo, M., Fascio, U., Camatini, M., Manteca, P., 2013. The modality of cell-particle interactions drives the toxicity of nanosized CuO and TiO<sub>2</sub> in human alveolar epithelial cells. *Toxicol. Lett.* 222, 102–116.
- Munn, A.L., 2000. The yeast endocytic membrane transport system. *Microsc. Res. Tech.* 51, 547–562.
- Niazji, J.H., Sang, B.J., Kim, Y.S., Gu, M.B., 2011. Global gene response in *Saccharomyces cerevisiae* exposed to silver nanoparticles. *Appl. Biochem. Biotechnol.* 164, 1278–1291.
- Nomura, T., Kuriyama, Y., Tokumoto, H., Konishi, Y., 2015. Cytotoxicity of functionalized polystyrene latex nanoparticles toward lactic acid bacteria, and comparison with model microbes. *J. Nanopart. Res.* 17, 1–10.
- Nomura, T., Miyazaki, J., Miyamoto, A., Kuriyama, Y., Tokumoto, H., Konishi, Y., 2013. Exposure of the yeast *Saccharomyces cerevisiae* to functionalized polystyrene latex nanoparticles: influence of surface charge on toxicity. *Environ. Sci. Technol.* 47, 3417–3423.
- Nowack, B., Krug, H.F., Height, M., 2011. 120 years of nanosilver history: implications for policy makers. *Environ. Sci. Technol.* 45, 1177–1183.
- Oh, N., Park, J.H., 2014. Endocytosis and exocytosis of nanoparticles in mammalian cells. *Int. J. Nanomedicine* 9 (Suppl. 1), 51–63.
- Panacek, A., Kolar, M., Vecerova, R., Prucek, R., Soukupova, J., Krystof, V., Hamal, P., Zboril, R., Kvitck, L., 2009. Antifungal activity of silver nanoparticles against *Candida* spp. *Biomaterials* 30, 6333–6340.
- Park, J.H., Kim, J.Y., Kim, J., Lee, J.H., Hahn, J.S., Gu, M.B., Yoon, J., 2009. Silver-ion-mediated reactive oxygen species generation affecting bactericidal activity. *Water Res.* 43, 1027–1032.
- Prescianotto-Baschong, C., Riezman, H., 1998. Morphology of the yeast endocytic pathway. *Mol. Biol. Cell* 9, 173–189.
- Rai, M., Yadav, A., Gade, A., 2009. Silver nanoparticles as a new generation of antimicrobials. *Biotechnol. Adv.* 27, 76–83.
- Ram, A.F., Kapteyn, J.C., Montijn, R.C., Caro, L.H., Douwes, J.E., Baginsky, W., Mazur, P., van den Ende, H., Klis, F.M., 1998. Loss of the plasma membrane-bound protein Gas1p in *Saccharomyces cerevisiae* results in the release of beta1,3-glucan into the medium and induces a compensation mechanism to ensure cell wall integrity. *J. Bacteriol.* 180, 1418–1424.
- Raths, S., Rohrer, J., Crausaz, F., Riezman, H., 1993. end3 and end4: two mutants defective in receptor-mediated and fluid-phase endocytosis in *Saccharomyces cerevisiae*. *J. Cell Biol.* 120, 55–65.
- Reidy, B., Haase, A., Luch, A., Dawson, K.A., Lynch, I., 2013. Mechanisms of Silver Nanoparticle Release, Transformation and Toxicity: A Critical Review of Current Knowledge and Recommendations for Future Studies and Applications. *Materials* 6, 2295–2350.
- Saulou, C., Jamme, F., Maranges, C., Fourquaux, I., Despax, B., Raynaud, P., Dumas, P., Mercier-Bonin, M., 2010. Synchrotron FTIR microspectroscopy of the yeast *Saccharomyces cerevisiae* after exposure to plasma-deposited nanosilver-containing coating. *Anal. Bioanal. Chem.* 396, 1441–1450.
- Sharma, K.V., Siskova, K.M., Zboril, R., Gardea-Torresdey, J.L., 2014. Organic-coated silver nanoparticles in biological and environmental conditions: Fate, stability and toxicity. *Adv. Colloid Interf. Sci.* 204, 15–34.
- Sun, M., Yu, Q., Liu, M., Chen, X., Liu, Z., Zhou, H., Yuan, Y., Liu, L., Li, M., Zhang, C., 2014. A novel toxicity mechanism of CdSe nanoparticles to *Saccharomyces cerevisiae*: enhancement of vacuolar membrane permeabilization (VMP). *Chem. Biol. Interact.* 220, 208–213.
- Suppi, S., Kasemets, K., Ivask, A., Kunnis-Beres, K., Sihtmae, M., Kurvet, I., Arooja, V., Kahru, A., 2015. A novel method for comparison of biocidal properties of nanomaterials to bacteria, yeasts and algae. *J. Hazard. Mater.* 286, 75–84.
- Tukmachev, V.A., Nedospasova, L.V., Zaslavskii, B., Rogozhin, S.V., 1979. Effect of sodium dodecyl sulfate on biological membranes. *Biofizika* 24, 55–60.
- Vindimian, E., 2001. REGTOX, Copyright (C) 2001. [http://www.normalesup.org/~vindimian/en\\_index.html](http://www.normalesup.org/~vindimian/en_index.html).
- Wang, L., Pal, A., Isaacs, J., Bello, D., Carrier, R., 2014. Nanomaterial induction of oxidative stress in lung epithelial cells and macrophages. *J. Nanopart. Res.* 16, 1–14.
- Wjeratne, S.S., Cuppett, S.L., Schlegel, V., 2005. Hydrogen peroxide induced oxidative stress damage and antioxidant enzyme response in Caco-2 human colon cells. *J. Agric. Food Chem.* 53, 8768–8774.
- Woldring, C.L., van Ieterson, W., 1972. Effects of treatment with sodium dodecyl sulfate on the ultrastructure of *Escherichia coli*. *J. Bacteriol.* 111, 801–813.
- Zlotnik, H., Fernandez, M.P., Bowers, B., Cabib, E., 1984. *Saccharomyces cerevisiae* mannoproteins form an extral cell wall layer that determines wall porosity. *J. Bacteriol.* 159, 1018–1026.

## SUPPLEMENTARY MATERIAL

**Profiling of the toxicity mechanisms of coated and uncoated silver nanoparticles to yeast *Saccharomyces cerevisiae* BY4741 using a set of its 9 single-gene deletion mutants defective in oxidative stress response, cell wall or membrane integrity and endocytosis.**

Käosaar, S.<sup>1,2</sup>, Kahru, A.<sup>1</sup>, Mantecca, P<sup>3</sup>, Kasemets, K.<sup>1</sup>

<sup>1</sup>*Laboratory of Environmental Toxicology, National Institute of Chemical Physics and Biophysics, Akadeemia tee 23, Tallinn 12618, Estonia*

<sup>2</sup>*Faculty of Chemical and Materials Technology, Tallinn University of Technology, Ehitajate tee 5, Tallinn 19086, Estonia*

<sup>3</sup>*Department of Earth and Environmental Sciences, Research Centre POLARIS, University of Milano-Bicocca, 1 Piazza della Scienza, Milano 20126, Italy*

\*Corresponding author E-mail address: [kaja.kasemets@kbfi.ee](mailto:kaja.kasemets@kbfi.ee)

*Authors e-mail addresses:*

*S. Käosaar: [sandra.kaosaar@kbfi.ee](mailto:sandra.kaosaar@kbfi.ee)*

*A. Kahru: [anne.kahru@kbfi.ee](mailto:anne.kahru@kbfi.ee)*

*P. Mantecca: [paride.mantecca@unimib.it](mailto:paride.mantecca@unimib.it)*

**Table S1**

*Saccharomyces cerevisiae* BY4741 (*MATa*; *his3Δ1*; *leu2Δ0*; *met15Δ0*; *ura3Δ0*) wild-type and its 9 isogenics single-gene deletion mutants used in this study; strains originate from the EUROSCARF collection (<http://web.uni-frankfurt.de/fb15/mikro/euroscarf/>)

Strains	EUROSCARF accession number	Deleted ORF <sup>a</sup>	Gene product/protein <sup>b</sup>
BY4741	Y00000	-	Wild-type (wt)
Oxidative stress (OS)-defective strains			
<i>yap1Δ</i>	Y00569	YML007w	Basic leucine-zipper transcription factor, required for oxidative stress tolerance
<i>sod1Δ</i>	Y06913	YJR104c	Cytosolic copper-zinc superoxide dismutase
<i>sod2Δ</i>	Y06605	YHR008c	Mitochondrial manganese superoxide dismutase
Endocytosis-defective strain			
<i>end3Δ</i>	Y02992	YNL084C	Eps15 homology (EH) domain-containing protein involved in endocytosis, actin cytoskeletal organization and cell wall morphogenesis
Cell wall/membrane-defective strains			
<i>gas1Δ</i>	Y00897	YMR307W	Beta-1,3-glucanosyltransferase
<i>erg3Δ</i>	Y02667	YLR056W	C-5 sterol desaturase, catalyzes the introduction of a C-5(6) double bond into episterol, a precursor in ergosterol biosynthesis
<i>mnn10Δ</i>	Y03604	YDR245W	Subunit of a Golgi mannosyltransferase complex
<i>kre6Δ</i>	Y05574	YPR159W	Type II integral membrane protein required for beta-1,6 glucan biosynthesis
<i>knr4Δ</i>	Y05882	YGR229C	Protein involved in the regulation of cell wall synthesis

<sup>a</sup>ORF - Open Reading Frame; <sup>b</sup>Description of the respective protein function based on the *Saccharomyces* Genome Database (SGD) (<http://www.yeastgenome.org/>).

### 1. Effect of pH of YPD<sub>mod</sub> medium on the stability of the protein-coated AgNPs (nAg-col)

Effect of pH on the stability of nAg-col particles (50 mg Ag/L) in cell-free YPD<sub>mod</sub> medium (0.25% yeast extract, 0.5% peptone and 1% glucose, pH 6.8) was studied by the gradual changing of the medium pH by titration from pH 6.8 to 2.0 (step 0.5) by 0.025 M and 0.25 M HNO<sub>3</sub> and 0.25 M NaOH. For the pH titration and for the hydrodynamic size and ζ-potential measurements, MPT-2 Multi Purpose Titrator or Zetasizer Nano ZS, respectively (Malvern, UK) were used.

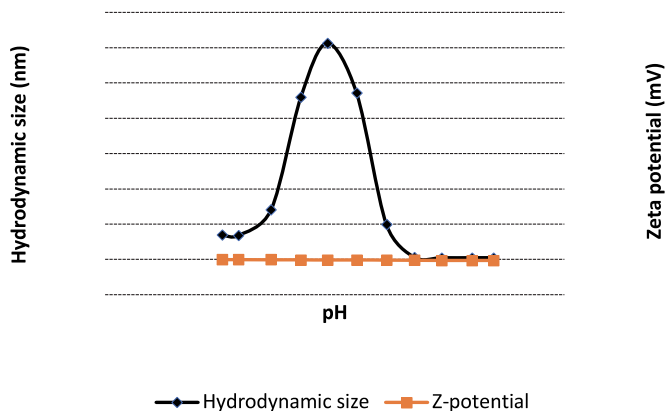


**Fig. S1.** The average hydrodynamic diameter ( $D_h$ ) and  $\zeta$ -potential of nAg-col in YPD<sub>mod</sub> (50 mg Ag/L) in the pH range of 6.8 to 2.0. At the start of the experiment at pH 6.8, the  $D_h$  of nAg-col was 48 nm and the  $\zeta$ -potential was -26 mV. As the pH decreased towards 4.7 (final pH of the yeast cells culture in YPD<sub>mod</sub> after 48-h growth), the nAg-col particles'  $D_h$  increased up to 3000-4000 nm and  $\zeta$ -potential approached -15 mV, leading to settling of the nanoparticles.

## 2. Study of the endocytosis ability/disability of *Saccharomyces cerevisiae* BY4741 wild-type (wt) and *end3Δ* cells by the membrane-impermeant fluorescent endocytosis marker Lucifer Yellow

Lucifer Yellow dilithium salt (Sigma-Aldrich) dissolved in DI water to a concentration of 40 mg/mL and stored at +4°C. For the experiment, the stock solution was diluted with deionized water to 8 mg/mL. Wt and *end3Δ* were inoculated from YPD agar plate colonies and grown overnight in YPD medium at 30°C. Both cultures were diluted to OD<sub>600nm</sub> 0.05 (~10<sup>6</sup> CFU/mL) (Yenway 6300 Spectrophotometer, UK) and grown for 16 h in YPD at 30°C. Cells were collected by centrifugation (3000 g, 7 min, Biofuge, Heraeus, UK) and re-suspended in fresh YPD. After 1 h of incubation at room temperature, cell density was adjusted to OD<sub>600nm</sub> 6 (~10<sup>8</sup> CFU/ml) with YPD. In the wells of 96-well microplate (Falcon), 75 μL of cell suspension was mixed with 75 μL of Lucifer Yellow dilution (final concentration 4 mg/mL). The microplate was incubated at 30°C without shaking in the dark for 2 h. After incubation the samples were centrifuged and washed with ice-cold 50 mM sodium-phosphate buffer, pH 7.0 three times (3000 g, 7 min, 4°C), re-suspended in 10 μL of the buffer and kept on ice. 3 μL of sample was mixed with 3 μL of low-melt agarose on a glass microscope slide and covered with a cover-slip. Images were acquired by the Zeiss LSM 510 DUO confocal laser scanning microscope using differential interference contrast (DIC) and Ar-laser 488 nm excitation and BP 505-550 nm emission filter.

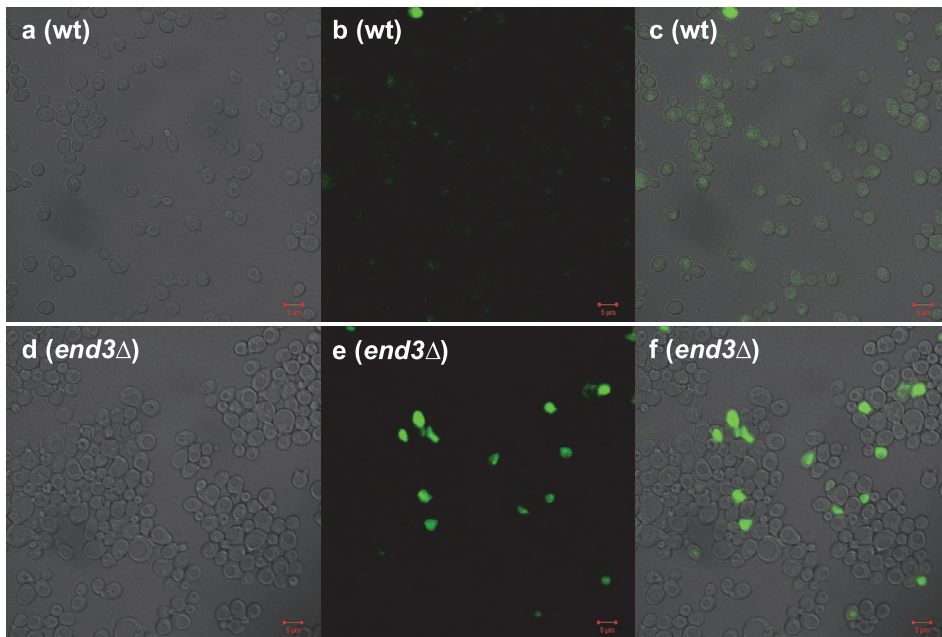


**Fig. S2.** Confocal laser scanning microscopy images of *Saccharomyces cerevisiae* BY4741 wild-type (wt) (a-c) and *end3Δ* (d-f) strains after incubation with Lucifer Yellow for 2 h in YPD at 30°C. a, d – DIC images of cells; b, e - fluorescence of Lucifer Yellow; c, f – overlay of fluorescence and DIC images.

### 3. Growth of *Saccharomyces cerevisiae* BY4741 wild-type and its 9 single-gene deletion mutants in modified yeast-extract-peptone-dextrose medium (YPD<sub>mod</sub>)

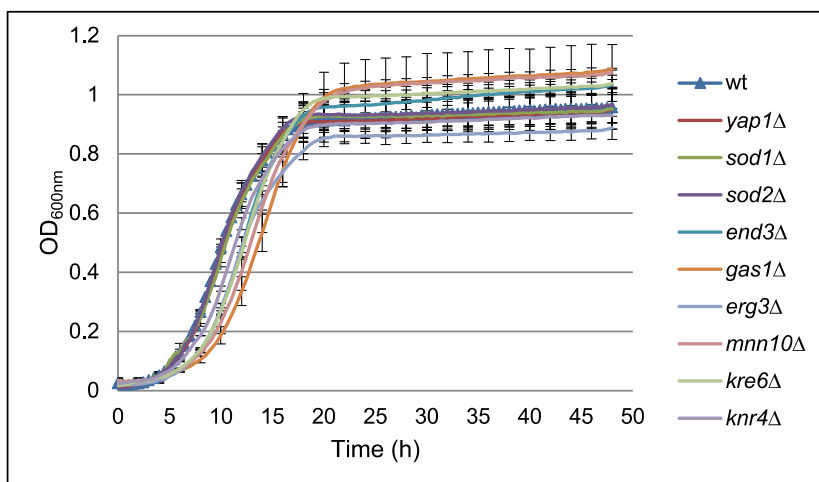


**Fig. S3.** Growth of *Saccharomyces cerevisiae* BY4741 wild-type (wt) and its 9 isogenics single-gene deletion mutants on 96-well microplate in YPD<sub>mod</sub> for 48 h at 30°C without shaking. Data are average of 2 independent experiments ± standard deviation. See also Table S2.

**Table S2**

The growth characteristics of *Saccharomyces cerevisiae* BY4741 wild-type and its 9 single-gene deletion mutants grown on 96-well microplates in YPD<sub>mod</sub> at 30°C, maximum specific growth rate ( $\mu_{\max}$ , h<sup>-1</sup>) was calculated from the respective growth curves (see Fig. S2).

Strains	$\mu_{\max}$ <sup>a</sup> , h <sup>-1</sup>	Doubling time (t <sub>d</sub> ) <sup>b</sup> , h
wild-type	0.42	1.66
<i>yap1Δ</i>	0.44	1.59
<i>sod1Δ</i>	0.38	1.84
<i>sod2Δ</i>	0.41	1.71
<i>end3Δ</i>	0.33	2.08
<i>gas1Δ</i>	0.30	2.30
<i>erg3Δ</i>	0.34	2.02
<i>mnn10Δ</i>	0.32	2.15
<i>kre6Δ</i>	0.33	2.09
<i>knr4Δ</i>	0.35	2.06

<sup>a</sup>Maximum specific growth rate ( $\mu_{\max}$ , h<sup>-1</sup>) was calculated from the slope of  $\ln OD$  versus time in the exponential growth phase, <sup>b</sup>doubling time (t<sub>d</sub>) was calculated from the equation of  $t_d = \ln 2 / \mu_{\max}$ .

#### 4. Toxicity (IC<sub>50</sub>) of Ag ions, AgNPs, SDS and H<sub>2</sub>O<sub>2</sub> to *Saccharomyces cerevisiae* BY4741 wild-type and its 9 isogenics single-gene deletion mutants in the 48-h growth inhibition test in YPD<sub>mod</sub> medium (Table S3) and in the 24-h cell viability test in deionized water (Table S4).

**Table S3**

48-h IC<sub>50</sub> of Ag ions, AgNPs (mg Ag/L), SDS and H<sub>2</sub>O<sub>2</sub> (mg/L) for *Saccharomyces cerevisiae* BY4741 wild-type and its isogenics single-gene deletion mutants in the growth inhibition test in YPD<sub>mod</sub> at 30°C. Cell growth was determined by the quantification of biomass by measuring optical density at 600 nm. The values are given as the mean of 2-3 experiments ± standard deviation. All the concentrations are nominal. See also Fig. 3.

Strains	AgNO <sub>3</sub>	nAg	nAg-col	nAg-PVP	SDS	H <sub>2</sub> O <sub>2</sub>
wild-type	2.40 ± 0.30	576 ± 140	76.8 ± 22.8	148 ± 25.4	1017 ± 162	99.0 ± 7.73
Oxidative stress response-defective strains						
<i>yap1Δ</i>	2.58 ± 0.65	638 ± 365	88.2 ± 22.7	148 ± 36.8	915 ± 72.8	15.4 ± 3.36
<i>sod1Δ</i>	2.97 ± 0.84	643 ± 65.0	86.3 ± 25.4	162 ± 49.4	194 ± 22.8	80.3 ± 8.70
<i>sod2Δ</i>	3.00 ± 0.58	760 ± 260	93.1 ± 27.6	171 ± 43.2	1145 ± 490	58.4 ± 19.1
Endocytosis-defective strain						
<i>end3Δ</i>	1.64 ± 0.64	385 ± 129	29.4 ± 17.9	45.5 ± 24.9	134 ± 11.5	45.2 ± 5.82
Cell wall/membrane-defective strains						
<i>gas1Δ</i>	1.92 ± 0.48	356 ± 80	84.7 ± 15.8	101 ± 37.1	144 ± 13.0	51.1 ± 14.7
<i>erg3Δ</i>	2.80 ± 0.72	550 ± 115	88.7 ± 14.2	136 ± 50.5	146 ± 23.7	73.4 ± 12.2
<i>mnn10Δ</i>	1.92 ± 0.85	431 ± 11.0	86.8 ± 20.5	149 ± 67.0	86.6 ± 43.4	55.7 ± 19.7
<i>kre6Δ</i>	2.65 ± 1.13	638 ± 365	80.1 ± 20.6	117 ± 39.7	201 ± 42.9	85.4 ± 6.64
<i>knr4Δ</i>	3.13 ± 0.95	730 ± 286	82.9 ± 21.6	128 ± 42.2	193 ± 31.2	76.9 ± 11.8

**Table S4**

24-h IC<sub>50</sub> of Ag ions, AgNPs (mg Ag/L), SDS and H<sub>2</sub>O<sub>2</sub> (mg/L) for *Saccharomyces cerevisiae* BY4741 wild-type and its isogenics single-gene deletion mutants in the cell viability test in deionised water at 30°C. Cell viability was determined by fluorescein diacetate. The IC<sub>50</sub> values are given as the mean of 3 experiments ± standard deviation. All the concentrations are nominal. See also Fig. 4.

Strains	AgNO <sub>3</sub>	nAg	nAg-col	nAg-PVP	SDS	H <sub>2</sub> O <sub>2</sub>
wild-type	0.09 ± 0.05	18.7 ± 3.41	2.71 ± 1.06	3.70 ± 0.79	1079 ± 137	11.8 ± 2.69
Oxidative stress response-defective strains						
<i>yap1Δ</i>	0.20 ± 0.02	20.5 ± 5.05	3.97 ± 1.41	4.70 ± 1.22	1083 ± 122	7.71 ± 0.86
<i>sod1Δ</i>	0.17 ± 0.06	12.4 ± 2.59	3.13 ± 1.40	3.57 ± 1.54	978 ± 193	8.69 ± 0.32
<i>sod2Δ</i>	0.19 ± 0.07	12.8 ± 5.45	3.86 ± 2.26	4.17 ± 1.72	1185 ± 73.4	7.54 ± 0.70
Endocytosis-defective strain						
<i>end3Δ</i>	0.04 ± 0.01	2.17 ± 1.61	0.31 ± 0.05	0.54 ± 0.29	72.2 ± 13.6	19.3 ± 6.96
Cell wall/membrane-defective strains						
<i>gas1Δ</i>	0.27 ± 0.02	38.3 ± 4.33	6.97 ± 0.62	9.84 ± 3.17	557 ± 30.3	23.9 ± 1.90
<i>erg3Δ</i>	0.12 ± 0.04	24.2 ± 5.09	2.98 ± 0.44	4.49 ± 1.15	157 ± 15.1	9.54 ± 1.61
<i>mnn10Δ</i>	0.47 ± 0.07	42.8 ± 6.47	10.4 ± 4.15	15.0 ± 5.52	1161 ± 35.2	39.1 ± 0.19
<i>kre6Δ</i>	0.22 ± 0.02	32.1 ± 0.76	5.28 ± 1.37	7.84 ± 2.47	738 ± 126	36.7 ± 3.20
<i>knr4Δ</i>	0.18 ± 0.03	20.2 ± 6.13	3.37 ± 1.12	3.85 ± 1.60	620 ± 8.10	20.1 ± 0.31

**5. Colony forming ability of *Saccharomyces cerevisiae* BY4741 wild-type and its single-gene deletion mutants on toxicant-free YPD agar medium: pipetted as a 5 μL spot after the exposure to the studied Ag compounds, SDS and H<sub>2</sub>O<sub>2</sub> in the 48-h growth inhibition test in YPD<sub>mod</sub> and in the 24-h cell viability test in deionized water. Inoculated agar plates were incubated for 3 days at 30°C before photographing.**

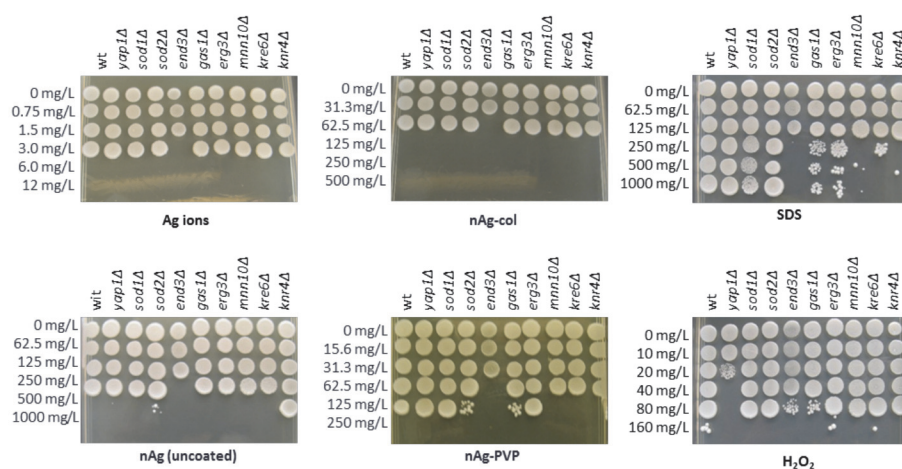


**Fig. S4.** Colony-forming ability of *Saccharomyces cerevisiae* BY4741 wild-type and its single-gene deletion mutants on toxicant-free YPD agar medium after 48-h exposure to Ag ions, AgNPs, SDS and H<sub>2</sub>O<sub>2</sub> in the growth inhibition test in YPD<sub>mod</sub>. The experiment was repeated 2-3 times.

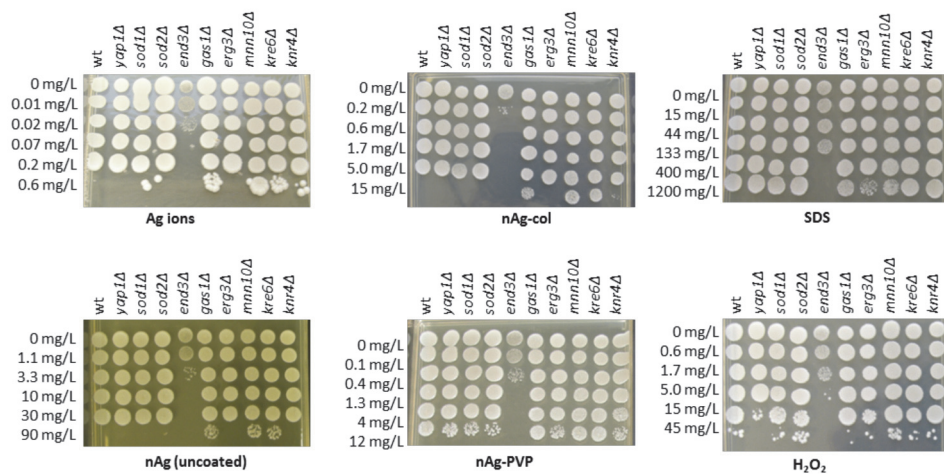


**Fig. S5.** Colony-forming ability of *Saccharomyces cerevisiae* BY4741 wild-type and its single-gene deletion mutants on toxicant-free YPD agar medium after 24-h exposure to Ag ions, AgNPs, SDS and H<sub>2</sub>O<sub>2</sub> in the cell viability test in deionized water. The experiment was repeated 3 times.

## 6. Dissolution/recovery corrected 48-h IC<sub>50</sub> values for *Saccharomyces cerevisiae* BY4741 wild-type strain in the growth inhibition test in YPD<sub>mod</sub>.

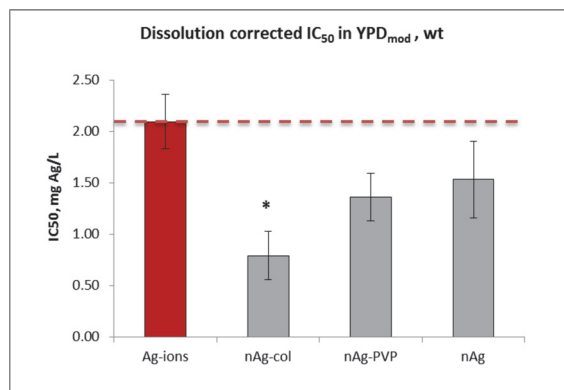


**Fig. S6.** Dissolution/recovery corrected 48-h IC<sub>50</sub> of AgNPs and Ag-ions (mg Ag/L) for *Saccharomyces cerevisiae* BY4741 wild-type strain in the growth inhibition test in YPD<sub>mod</sub>. \*represents statistically significant difference from the respective Ag ions-IC<sub>50</sub> according to the t-test ( $\alpha=0.05$ ) (see also **Table 1** and **Table 2**).

7. Laser scanning confocal microscopy analyses of *Saccharomyces cerevisiae* BY4741 wild-type (wt) and its isogenic endocytosis-defective strain *end3Δ*: non-treated (Fig. S7) and AgNPs exposed yeast cells (Fig. C8, S9, S10 and S11)

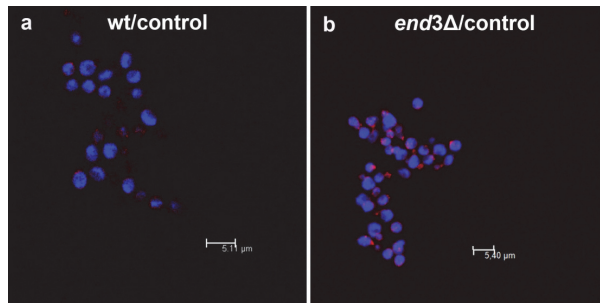


**Fig. S7.** Confocal microscopy images of non-treated *Saccharomyces cerevisiae* BY4741 (a) wild-type and (b) endocytosis-defective strain *end3Δ* after 3-h incubation in YPD<sub>mod</sub> medium at 30°C. Actin filaments were visualized by rhodamine-phalloidine staining (red) and nuclei by DRAQ5™ (blue pseudocolor).

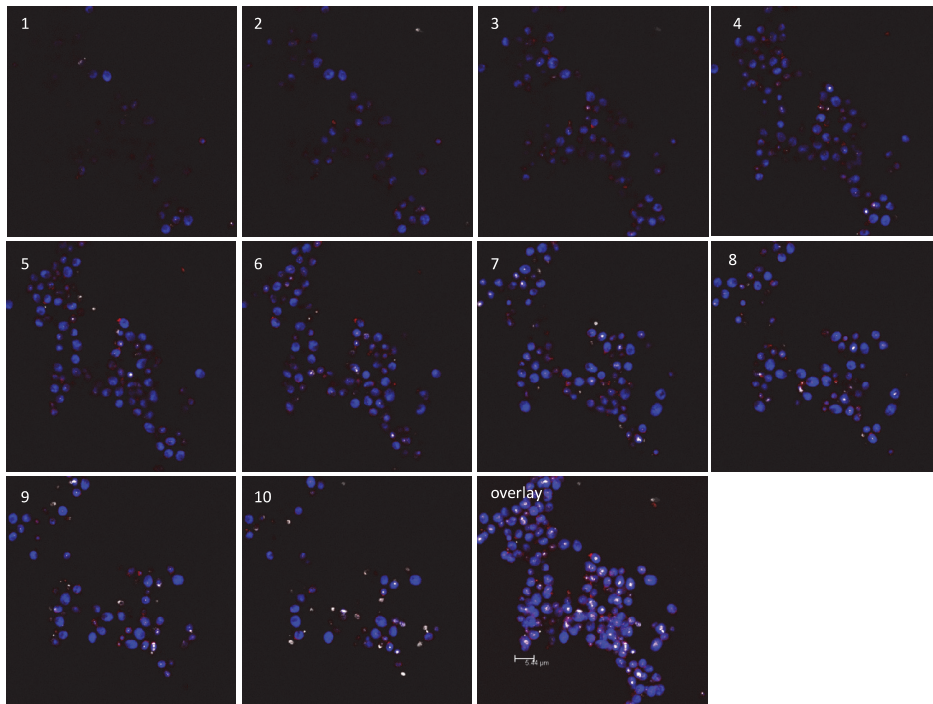


**Fig. S8.** Confocal microscopy images of *Saccharomyces cerevisiae* BY4741 wild-type cells exposed to nAg-Col (1 mg Ag/L) for 3 h in YPD<sub>mod</sub> at 30°C; serial sections and overlay of the sections. Actin filaments were visualized by rhodamine-phalloidine staining (red), nuclei by DRAQ5™ (blue pseudocolor) and AgNPs by laser reflection (white spots) (see also Fig. 6).

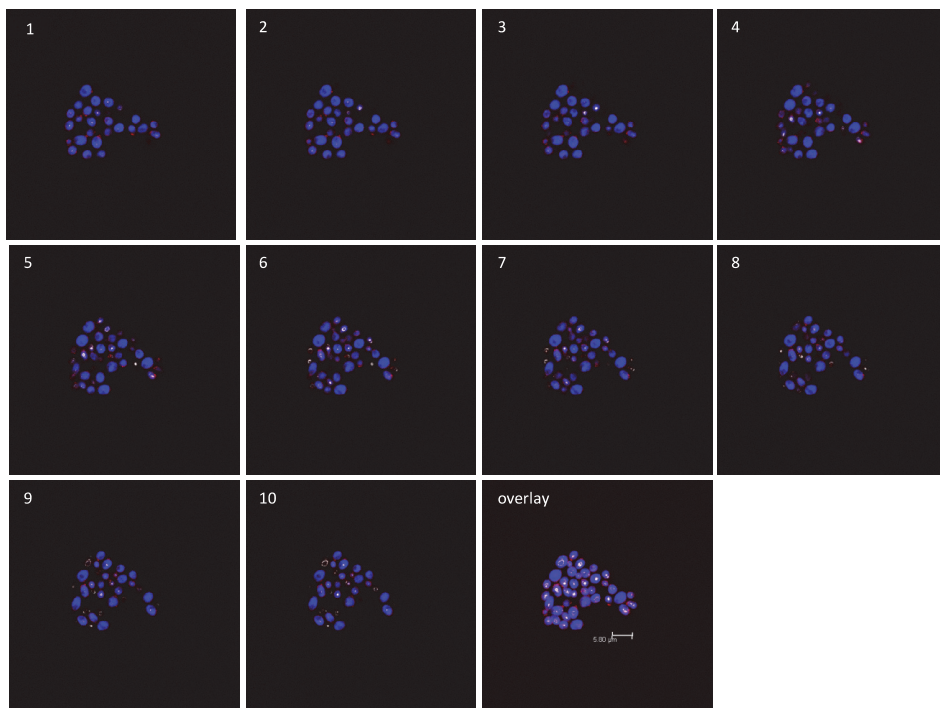


**Fig. S9.** Confocal microscopy images of *Saccharomyces cerevisiae* BY4741 wild-type cells exposed to nAg-PVP (1 mg Ag/L) for 3 h in YPD<sub>mod</sub> at 30°C; serial sections and overlay of the sections. Actin filaments were visualized by rhodamine-phalloidine staining (red), nuclei by DRAQ5™ (blue pseudocolor) and AgNPs by laser reflection (white spots) (see also Fig. 6).

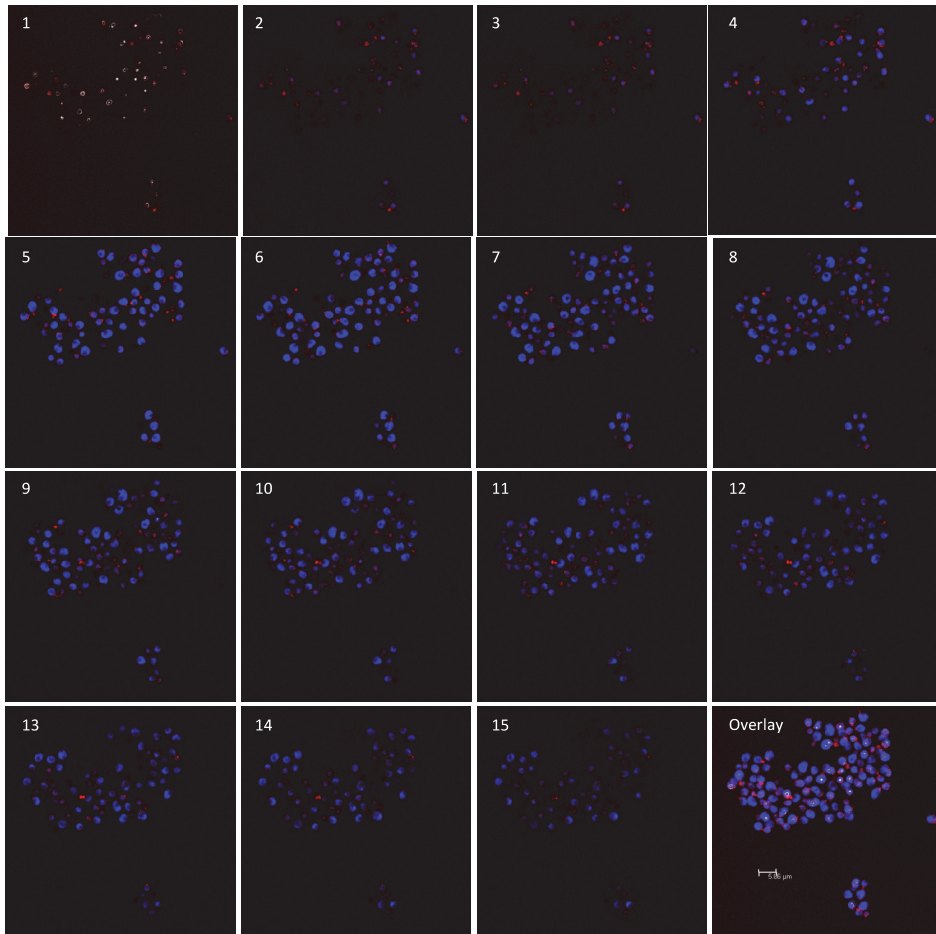


**Fig. S10.** Confocal microscopy images of *Saccharomyces cerevisiae* BY4741 endocytosis-defective *end3Δ* cells exposed to nAg-Col (1 mg Ag/L) for 3 h in YPD<sub>mod</sub> at 30°C; serial sections and overlay of the sections. Actin filaments were visualized by rhodamine-phalloidine staining (red), nuclei by DRAQ5<sup>TM</sup> (blue pseudocolor) and AgNPs by laser reflection (white spots) (see also Fig. 6).

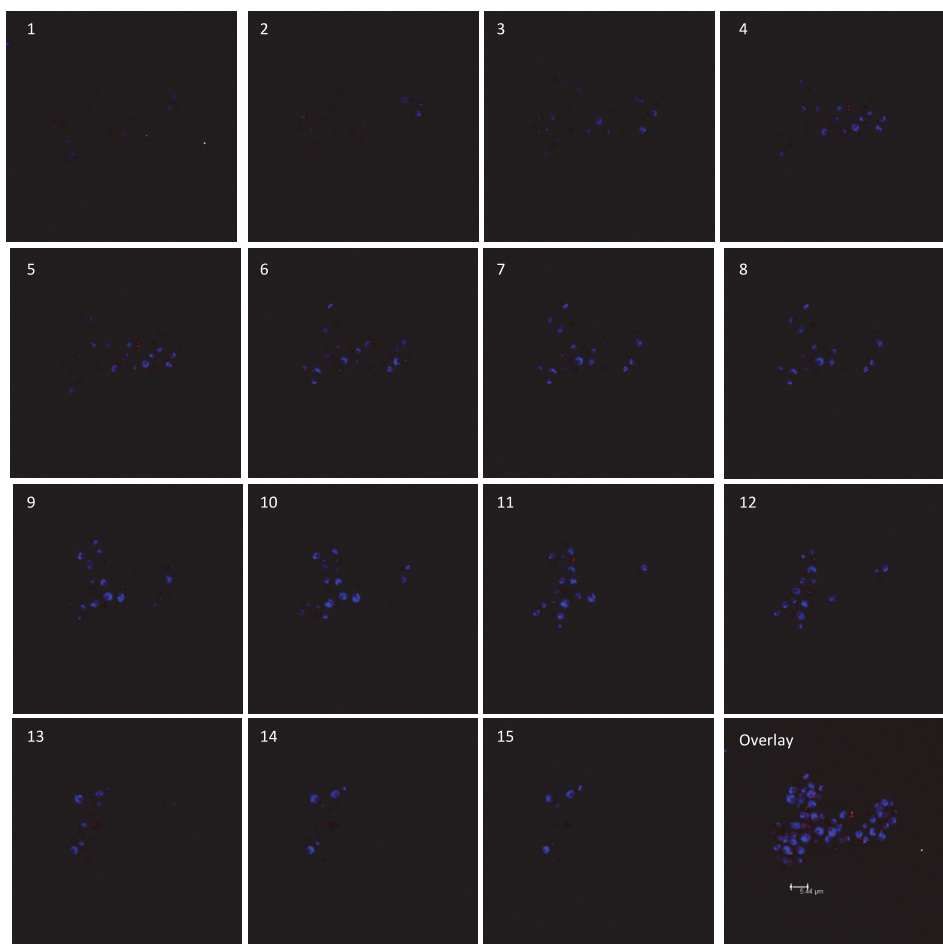


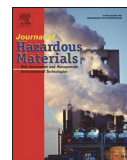
**Fig. S11.** Confocal microscopy images of *Saccharomyces cerevisiae* BY4741 endocytosis-defective *end3Δ* cells exposed to nAg-PVP (1 mg Ag/L) for 3 h in YPD<sub>mod</sub> at 30°C; serial sections and overlay of the sections. Actin filaments were visualized by rhodamine-phalloidine staining (red), nuclei by DRAQ5™ (blue pseudocolor) and AgNPs by laser reflection (white spots) (see also Fig. 6).



## **PUBLICATION II**

**Suppi, S.**, Kasemets, K., Ivask, A., Künnis-Beres, K., Sihtmäe, M., Kurvet, I., Aruoja, V., Kahru, A. (2015). A novel method for comparison of biocidal properties of nanomaterials to bacteria, yeasts and algae. *Journal of Hazardous Materials*. 286, 75–84.





## A novel method for comparison of biocidal properties of nanomaterials to bacteria, yeasts and algae

Sandra Suppi<sup>a,b</sup>, Kaja Kasemets<sup>a,\*</sup>, Angela Ivask<sup>a</sup>, Kai Künis-Beres<sup>a</sup>, Mariliis Sihtmäe<sup>a</sup>, Imbi Kurvet<sup>a</sup>, Villem Aruoja<sup>a</sup>, Anne Kahru<sup>a,\*</sup>

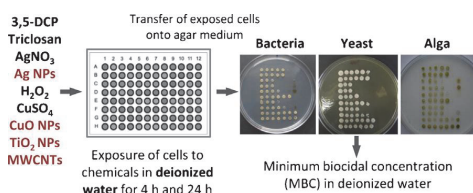
<sup>a</sup> Laboratory of Environmental Toxicology, National Institute of Chemical Physics and Biophysics, Akadeemia tee 23, Tallinn 12618, Estonia

<sup>b</sup> Faculty of Chemical and Materials Technology, Tallinn University of Technology, Ehitajate tee 5, Tallinn 19086, Estonia

### HIGHLIGHTS

- A novel method was introduced to evaluate biocidal efficiency of nanomaterials (NMs).
- Exposure to NMs is conducted in deionized water.
- Tested chemicals had similar toxicity pattern to the test organisms.
- Ag- and Cu-based NMs and their soluble salts proved the most toxic substances.

### GRAPHICAL ABSTRACT



### ARTICLE INFO

#### Article history:

Received 22 May 2014

Received in revised form 1 December 2014

Accepted 15 December 2014

Available online 23 December 2014

#### Keywords:

Nanoparticles

Toxicity

Heavy metals

Bioavailability

Minimum biocidal concentration

### ABSTRACT

Toxicity testing of nanomaterials (NMs) is experimentally challenging because NMs may interfere with test environment and assay components. In this work we propose a simple and reliable method – a ‘spot test’ to compare biocidal potency of NMs to unicellular microorganisms such as bacteria, yeasts and algae. The assay is straightforward: cells are incubated in deionized water suspensions of NMs for up to 24 h and then pipetted as a ‘spot’ on agarized medium. Altogether seven bacterial strains, yeast and a microalga were tested. CuO, TiO<sub>2</sub> and two different Ag NPs, multi-wall C-nanotubes (MWCNTs), AgNO<sub>3</sub>, CuSO<sub>4</sub>, 3,5-dichlorophenol, triclosan and H<sub>2</sub>O<sub>2</sub> were analyzed. The biocidal potency of tested substances ranged from 0.1 mg/L to >1000 mg/L; whereas, the least potent NMs toward all test species were TiO<sub>2</sub> NPs and MWCNTs and most potent Ag and CuO NPs. Based on the similar toxicity pattern of the tested chemicals on the nine unicellular organisms in deionized water we conclude that toxicity mechanism of biocidal chemicals seems to be similar, whatever the organism (bacteria, yeast, alga). Therefore, when the organisms are not ‘protected’ by their environment that usually includes various organic and inorganic supplements their tolerance to toxicants is chemical- rather than organism-dependent.

© 2014 Elsevier B.V. All rights reserved.

### 1. Introduction

At nanoscale materials behave differently compared to their micro-size counterparts, due to increased specific surface area and thus, higher reactivity [1]. However, the same physical-chemical properties which make nanomaterials (NMs) useful, can make them more harmful to biota [2]. Several NMs such as nanoscale Ag, CuO, ZnO and TiO<sub>2</sub>, zero-valent iron and chitosan-based nanocomposites are already widely used due to their biocidal properties [3,4]. Considering the increasing issue of bacterial resistance to

\* Corresponding authors. Tel.: +372 6398373; fax: +372 6398382.

E-mail addresses: [sandra.suppi@kbfi.ee](mailto:sandra.suppi@kbfi.ee) (S. Suppi), [kaja.kasemets@kbfi.ee](mailto:kaja.kasemets@kbfi.ee) (K. Kasemets), [angela.ivask@kbfi.ee](mailto:angela.ivask@kbfi.ee) (A. Ivask), [kai.kunnis@kbfi.ee](mailto:kai.kunnis@kbfi.ee) (K. Künis-Beres), [mariliis.sihmae@kbfi.ee](mailto:mariliis.sihmae@kbfi.ee) (M. Sihtmäe), [imbi.kurvet@kbfi.ee](mailto:imbi.kurvet@kbfi.ee) (I. Kurvet), [villem.aruoja@kbfi.ee](mailto:villem.aruoja@kbfi.ee) (V. Aruoja), [anne.kahru@kbfi.ee](mailto:anne.kahru@kbfi.ee) (A. Kahru).

antibiotics [5–7], nanoparticle-based antimicrobials are expected to provide alternatives to conventional antibiotics and biocidal chemicals. Due to their toxic properties [8] metal-containing NMs are good candidates for novel antimicrobial consumer and patient-care products [3]. Currently the most widely used biocidal nanomaterial is nanosilver: according to the Woodrow Wilson Database [9] there were more than 1600 nanotechnological consumer products on the market in October 2013, and 383 of them contained nanosilver.

It is important to note that according to the EU chemical safety policy REACH (Registration, Evaluation, Authorization and Restriction of Chemicals [10]) all chemicals, including NMs must be evaluated for their hazardous properties. Therefore reliable high-throughput and cost-efficient tests are needed for toxicological screening of NMs. There are several widely used microplate-format toxicity tests based on the viability of bacterial and eukaryotic cells using e.g., direct optical assessment of growth, viability dyes such as MTT, neutral red and resazurin, quantification of cellular ATP or lactate dehydrogenase activity [11,12]. In the case of NMs, however, the toxicity evaluation is experimentally challenging because (i) NMs may interfere with assay components [13,14] (ii) toxicity of NMs may depend on the test environment [15–17] and (iii) the turbidity of NMs suspensions may lead to false estimates in the case of optical endpoints [13,18–20]. As an example, Monteiro-Riviere et al. [21] showed reporter-dye adsorption in neutral red assay, abiotic reduction of MTT and fluorescence quenching in resazurin assay by carbon black and single-wall carbon nanotubes. Abiotic reduction of reporter-dye has also been shown for nano-TiO<sub>2</sub> in the MTT viability assay [22]. In addition, it is widely acknowledged that the 'rich' media used for conventional microbial growth inhibition assays are often unreliable for testing and comparing metal-based biocides because inorganic or organic components of the test media may bind dissolved metals [23].

The aim of the current study was to develop a simple and reliable method for the evaluation and comparison of biocidal potency of NMs to different types of unicellular target organisms such as bacteria, fungi and algae in the same test conditions. In this assay the test organisms are exposed to NMs in deionized (DI) water to minimize speciation-related effects on toxicity results. Throughout this paper, the novel test where the test organisms are exposed to toxicants in DI water and further sub-cultured to agarized growth media, is referred to as a 'spot test'. For the development and evaluation of the 'spot test' we chose nine unicellular species: prokaryotic test organisms were represented by 4 bacterial strains: *Escherichia coli* MG1655, *Staphylococcus aureus* RN4220, *Pseudomonas fluorescens* OS8, *P. aeruginosa* DS10–129 (further referred to as 'laboratory bacteria') and 3 bacterial strains newly isolated from the environment: *Janthinobacterium* sp., *P. fluorescens* KC-1, *Microbacterium testaceum* PCSB7 (further referred to as 'environmental bacteria'). Eukaryotic organisms were represented by yeast *Saccharomyces cerevisiae* BY4741 and microalga *Pseudokirchneriella subcapitata*. *E. coli*, *S. aureus*, and *P. aeruginosa* are all clinically important bacteria [24] and thus, target strains for antibiotic susceptibility testing. 'Environmental bacteria' isolated from soil, groundwater and drinking water system were included for comparison. Yeast *S. cerevisiae* was chosen as a representative of fungi – a group of microorganisms often targeted by biocidal antifungal compounds and unicellular alga *P. subcapitata* was added to address biocidal compounds developed to inhibit algal growth (algaecides).

Biocidal potency of five NMs – two different Ag, CuO and TiO<sub>2</sub> NPs as well as multi-wall carbon nanotubes (MWCNTs) – were studied and compared to AgNO<sub>3</sub>, CuSO<sub>4</sub>, 3,5-dichlorophenol, triclosan and H<sub>2</sub>O<sub>2</sub>. Ag and CuO NPs were chosen because of their wide biocidal use. Indeed, Ag NPs are used to inhibit growth of bacterial biofilms in medical catheters, prostheses, heart valves etc

and as algaecide in residential swimming pools [25]. CuO NPs have also been proposed as biocides to fight the undesirable growth of bacteria, fungi and algae [3,26]. As toxicity of CuO and Ag NPs to bacteria, yeast and algae is prevalently dissolution-driven [27] the soluble metal salts CuSO<sub>4</sub> and AgNO<sub>3</sub> with known antimicrobial action were used as ionic controls. 3,5-dichlorophenol is often used as a positive control in various toxicological tests [28], triclosan and H<sub>2</sub>O<sub>2</sub> are both widely used antiseptics [29].

'Spot test' combines three major novelties: (i) exposure in DI water minimizes the effects of test medium components on NMs bioavailability and toxicity and may reduce the agglomeration of NMs often accounted in test media [30], (ii) viability of the selected unicellular organisms was not affected by 24-h incubation in hypotonic conditions (DI water), and (iii) both prokaryotic (bacteria) and eukaryotic cells (yeast, alga) were used in the same test format applying the same toxicity endpoint – colony-forming ability of the exposed cells. In addition, a standard broth microdilution method in conventional 'rich' growth medium [31] was applied to determine the minimum biocidal concentration (MBC) values of all test chemicals to *E. coli*, *S. aureus* and *S. cerevisiae*, in order to compare the MBC values obtained in the 'spot test' in DI water as well as in the rich growth media.

## 2. Materials and methods

### 2.1. Chemicals and nanomaterials

3,5-dichlorophenol (3,5-DCP; analytical standard), 5-chloro-2-(2,4-dichlorophenoxy) phenol (Triclosan; ≥97.0%), AgNO<sub>3</sub> (ACS grade), nanosized CuO (nCuO; advertised particle size ~30 nm; 24-h solubility in DI water at concentration of 5 mg/L ~14% [32]) and nanosized TiO<sub>2</sub> (nTiO<sub>2</sub>) (Aeroxide® P25, advertised particle size ~21 nm; according to Ohtani et al. [33] P25 consists of 73–85% anatase, 14–17% rutile and 0–18% amorphous TiO<sub>2</sub>) were purchased from Sigma–Aldrich. H<sub>2</sub>O<sub>2</sub> was from Merck, CuSO<sub>4</sub> from Alfa Aesar and protein (casein)-coated colloidal Ag NPs (collargol; nAg-Col) with primary size ~12.5 nm from Laboratorios Argenol (Spain). Mass fraction of the organic coating of nAg-Col was 30% [34] and 4-h solubility in DI water at concentration of 10 mg/L was ~8% [35]. The aqueous suspensions of the studied nCuO and nAg-Col have been previously characterized by scanning and transmission electron microscopy [34,36]. Polyvinylpyrrolidone-stabilized Ag NPs (nAg-PVP; ~16 nm; aqueous dispersion, 4% w/w; PVP was used as a surfactant [37], 4-h solubility in DI water at concentration of 10 mg Ag/L was ~63%) and multi-wall carbon nanotubes (MWCNTs, no metal impurities as analysed using XPS method; Dr S. Misra (University of Birmingham, UK) personal communication) are NMs studied by FP7 project NanoValid ([www.nanovalid.eu/](http://www.nanovalid.eu/)) and originate from Colorobbia Group (Italy) and Nanocyl (Belgium), respectively. It has been shown that Ag NPs, coated by PVP which is strongly bound to the core of NPs are more stable in different test environments due to steric stabilization [38,39].

The stock solutions of 3,5-DCP (5 g/L), AgNO<sub>3</sub> (5 g Ag/L), nAg-Col (1 g Ag/L), nAg-PVP (5 g Ag/L) and CuSO<sub>4</sub> (5 g Cu/L), nCuO (5 g/L) and nTiO<sub>2</sub> (2 g/L) were prepared in DI water (pH 5.66 ± 0.1) (Milli-Q, Millipore). The stock solutions of nCuO and nTiO<sub>2</sub> were homogenized using ultrasonic probe (Branson Digital Sonifier®, USA) at 40 W for 4 min once after preparation. Before the 'spot test', the stocks were diluted in DI water. The stock solution of triclosan (100 g/L) was prepared in 70% ethanol. For the 'spot test', the stock solution of triclosan was diluted in DI water up to 2 g/L and then in 1.4% ethanol. Stock solution of MWCNTs (0.5 g/L) was prepared in 0.01% Triton X-100 (Fluka) and homogenized using the ultrasonic probe (see above) at 40 W for 4 min after preparation and for 30 s before dilution in 0.01% Triton X-100 for the 'spot test'. MWCNTs

could not be prepared at higher concentrations than 0.5 g/L as this was the maximal concentration that remained dispersed in 0.01% Triton X-100. Higher Triton X-100 concentrations proved toxic to the test organisms (data not shown). Stock solutions were stored at ambient temperature in the dark for 1–2 weeks. NMs stock suspensions were vortexed before testing.

## 2.2. Hydrodynamic diameter and $\zeta$ -potential measurements of nanomaterials

Average hydrodynamic diameter ( $d_h$ ) and zeta ( $\zeta$ ) potential of nAg-PVP, nAg-Col, nCuO and nTiO<sub>2</sub> in DI water, in half-strength ( $\frac{1}{2}$ ) cation-adjusted Mueller-Hinton Broth (pH 7.09  $\pm$  0.1) (CA-MHB) and in Yeast-Extract-Peptone-Dextrose (YPD) medium (pH 6.57  $\pm$  0.1) were measured using Zetasizer Nano ZS (Malvern Instruments, UK). For this, nAg-PVP, nAg-Col and nCuO were suspended in DI water, in  $\frac{1}{2}$  CA-MHB and in  $\frac{1}{2}$  YPD at a concentration of 50 mg/L and nTiO<sub>2</sub> at 100 mg/L. The  $d_h$  and  $\zeta$ -potential were measured in 1 mL DTS1061 folded capillary cell (Malvern Instruments, UK) immediately after preparation (0 h) and 24 h of incubation in DI water at ambient temperature or after 20 h or 24 h of incubation in  $\frac{1}{2}$  CA-MHB or in  $\frac{1}{2}$  YPD, respectively, at 30 °C in static conditions (no prior vortexing of the suspension) in the dark, to mimic the conditions during the toxicity testing.

## 2.3. 'Spot test' and broth microdilution susceptibility test

Test organisms and respective growth conditions are listed in Table S1. For culturing and handling of test organisms for the 'spot test' see Fig. 1 and Supplementary Material (SM). The 'spot test' was performed essentially as described in Kasemets et al. [32]. Briefly, 100  $\mu$ L of cell suspension in DI water was added to 100  $\mu$ L samples of nCuO, nTiO<sub>2</sub>, nAg-Col, nAg-PVP, AgNO<sub>3</sub>, CuSO<sub>4</sub>, H<sub>2</sub>O<sub>2</sub>, 3,5-DCP in DI water, triclosan in 1.4% ethanol and MWCNTs in 0.01% Triton X-100. All chemicals were tested in six nominal concentrations: 0.01, 0.1, 1.0, 10, 100 and 1000 mg/L except MWCNTs and nAg-Col where the highest tested concentrations were 250 mg/L and 500 mg Ag/L, respectively. Test organisms were exposed to chemicals in DI water on 96-well microplates (BD Falcon) at 25 °C for 4 or 24 h without shaking in the dark. Each experiment was repeated two or three

times. Viability of control cells was evaluated after 24-h incubation in DI water by plating and counting of colonies of bacterial and yeast cells on agarized growth medium and by staining with fluorescent viability dyes fluorescein diacetate (FDA) and propidium iodide (PI). In metabolically active cells FDA is non-specifically cleaved by intracellular esterases yielding a green fluorescent compound, fluorescein [40]. Contrarily, PI stains dead cells and cells with low membrane integrity yielding red fluorescence [41]. The above described viability dyes were not applicable for algae due to autofluorescence of algal cells. For staining and microscopy methods see SM.

After 4- and 24-h exposure, 5  $\mu$ L of the cell suspension was pipetted as a 'spot' onto respective toxicant-free agarized growth medium (Table S1) and the seeded agar plates were incubated for 24 h ('laboratory bacteria') or 72 h (yeast) at 30 °C or 48 h at 25 °C ('environmental bacteria'). Agar plates with algae were incubated at  $\sim$ 25 °C (in constant light) for 7 days. The ability of test organisms to grow on toxicant-free agarized growth medium, i.e., formation of a visible 'spot' (colonies) was used as a toxicity endpoint. Minimum biocidal concentration (MBC) of the tested NMs/chemicals was determined as the lowest tested nominal concentration of a chemical which completely inhibited the formation of visible colonies after sub-culturing on toxicant-free agar-media (Fig. 1). Broth microdilution test method is described in SM.

## 3. Results and discussion

In this study a 'spot test' was developed and evaluated for the analysis of biocidal potency of NMs. 'Spot test' allows direct comparison of biocidal potency of toxicants to bacteria, yeast and algae in the same conditions not masked and modulated by different test media and formats. As the test medium is DI water, the assay is especially valuable for the analysis of metallic compounds, which tend to form non-bioavailable complexes with ligands (e.g., proteins, salts etc.) in the conventional toxicological test media [16,23]. Although the 'spot test' format was introduced by us earlier to evaluate the CuO NPs toxicity to yeast [32], in the current study the test concept was expanded to include bacteria and algae – organisms that analogously to yeast form visible colonies on solid growth media. It is important to note that compared to rich culture

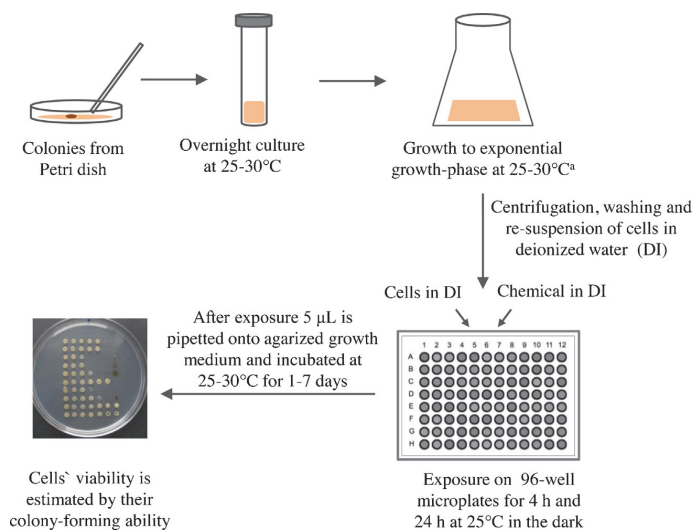


Fig. 1. Scheme of the 'spot test'. <sup>a</sup>Algal culture was started from the liquid maintenance culture and grown for  $\sim$ 4 days at 25 °C to exponential growth-phase.

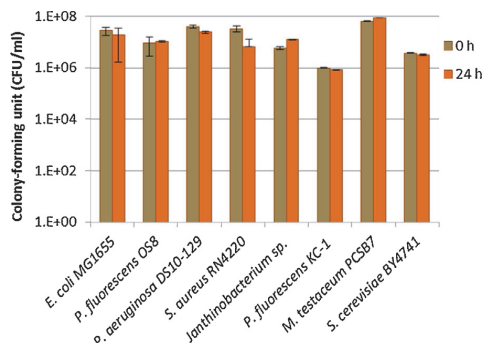


Fig. 2. Number of bacterial and yeast cells (CFU – colony-forming unit) before and after incubation in deionized water for 24 h at 25 °C.

media, DI water may be more similar to conditions in the natural environment as in the nature poor nutrient conditions often prevail and therefore starvation rather than active growth is the natural 'state' of bacteria [42]. On the other hand, DI water is hypotonic to living organisms and may itself affect their viability. Therefore, we first determined the viability of the bacterial and yeast cells in DI water. After 24 h of incubation in DI water no remarkable change in cell number was observed (Fig. 2 and Table S2). Also, fluorescence microscopy images before and after 24 h exposure in DI water did not show significant differences: most of the cells were stained by FDA and only a small fraction with PI (Fig. S1). Thus, the bacterial and yeast cells remained viable after 24-h incubation in DI water.

### 3.1. Characterization of nanomaterials

The following basic set of physical–chemical characteristics has been suggested to be analyzed for toxicological studies of NMs: chemical composition, primary size, shape, surface area and surface chemistry, hydrodynamic diameter and surface charge ( $\zeta$ -potential). In addition it is generally acknowledged that characterization of NMs in the actual biological test medium and context is essential since NM agglomeration, surface charge and solubilisation can change while in the test solution and these changes may have a significant impact on observed toxicological responses [43–45]. NMs are intrinsically unstable and tend to agglomerate due to their small size and high surface energy. To counterbalance the agglomeration, electrostatic and/or steric stabilization of NMs is used. For electrostatic stabilization a charge is added to NMs (for example, by the adsorption of citric acid) so that they can repel one another. For steric stabilization usually a thin layer of (organic) polymer (such as dextran, alginate, PEG, chitosan, PVP) is adsorbed onto the NPs surface to provide a steric barrier to prevent agglomeration [46–48]. It is important to note that the type of coating and especially the strength of interactions between coating and core material have a strong impact on environmental behavior and fate of NMs. For example, gold NPs that were stabilized by PVP ( $d_h$  6.6 nm,  $\zeta$ -potential  $-4.2$  mV) did not aggregate when tested in environmentally relevant conditions (pH, ionic strength). These NPs may remain as nanosize after discharge to the environment and are thus potentially more hazardous to aquatic organisms than NPs prone to agglomerate in the environment [49].

In the current study, the primary sizes of the tested NMs ranged from 12 to 30 nm. In DI water, the NMs agglomerated and the hydrodynamic sizes ranged from  $\sim 42$  to 268 nm (Table 1). The hydrodynamic size and  $\zeta$ -potential for MWCNTs could not be measured due to the high aspect ratio of these materials. Studied NMs in DI water tended to agglomerate but were quite monodisperse

(see the polydispersity indices in Table 1). During 24-h incubation in DI water hydrodynamic size of the NMs decreased somewhat (Table 1). The latter could be explained by the experimental setup: we did not mix the samples prior to the measurement and larger particles settled during the 24 h (Fig. S2).

Ag NPs that were stabilized either by protein (nAg-Col) or PVP (nAg-PVP) had hydrodynamic diameter in DI water of 41 nm and 114 nm, respectively, similar to the values in rich media (Table S3). Non-coated NPs, nCuO and nTiO<sub>2</sub> had bigger hydrodynamic diameters in DI water than coated Ag NPs, 145 nm and 251 nm, respectively, and remarkable increase in hydrodynamic diameter of CuO and TiO<sub>2</sub> NPs up to micrometer size was observed in rich growth media (Table S3). Differently from coated Ag NPs the uncoated nCuO and nTiO<sub>2</sub> settled visibly over time in media (Fig. S2). Interestingly, uncoated TiO<sub>2</sub> NPs were more stable (no visible settling for up to 4 h) in  $\frac{1}{2}$  CA-MHB, than in DI water and  $\frac{1}{2}$  YPD (Fig. S2). Thus, in the case of uncoated NPs the stability of suspension depended both on medium and particle type. However, despite the NMs agglomeration and settling the 'spot test' was reproducible (see the MBC values of replicate experiments in Table S4).

The  $\zeta$ -potential of nCuO and nTiO<sub>2</sub> in DI water was positive (at 24 h +36.3 mV and +22.5 mV, respectively) whereas, nAg-PVP and nAg-Col had negative  $\zeta$ -potentials,  $-7.00$  mV and  $-27.6$  mV, respectively (Table 1). In the rich media ( $\frac{1}{2}$  CA-MHB and  $\frac{1}{2}$  YPD) the  $\zeta$ -potential of all the tested NMs was uniformly negative ( $-2.28$  mV... $-20.6$  mV at 24 h) (Table S3). The latter can be explained by the formation of corona, i.e., binding of various cell culture medium constituents [50]. Indeed, both growth media contained particulate matter with hydrodynamic size of 282 nm and 268 nm (at 0 h), respectively, and the  $\zeta$ -potential of these particles was negative ( $-5.69$  and  $-11.2$  mV, respectively) (Table S3). As a rule, about  $\pm 30$  mV is the threshold  $\zeta$ -potential value for NPs that ensures dispersion stability by charge stabilization alone [49]. However, we observed remarkable sedimentation of nCuO in DI water despite the high  $\zeta$ -potential (+36.3 mV) (Fig. S2). On the other hand, quite stable dispersion of coated Ag NPs (nAg-Col and nAg-PVP) in DI water and growth media formed despite a  $\zeta$ -potential of less than  $-12$  mV, most likely due to the steric hindrance between the PVP or casein molecules coating these NPs.

### 3.2. Toxicity of the 'standard' biocidal chemicals in the 'spot test'

The results of the 'spot test' with 'standard' biocidal chemicals 3,5-DCP and triclosan showed quite low toxicity, MBC values were between 100–1000 mg/L (Table 2, Fig. 3). Response of all the species to 3,5-DCP was quite similar: the MBC for the yeast *S. cerevisiae* was 1000 mg/L and for the rest of the test species 100 mg/L. Toxicity of 3,5-DCP is expected to be similar to different cell types as 3,5-DCP is a polar narcotic compound that acts non-specifically on cellular membranes [51]. Triclosan (5-chloro-2-(2,4-dichlorophenoxy) phenol) which is the active ingredient in a multitude of health care products with germicidal and membrane-destabilizing properties [52,53] was even less toxic than 3,5-DCP in the current test conditions. 4-h and 24-h MBC of triclosan for *E. coli*, *S. aureus*, *J. anthinobacterium*, sp. and *M. testaceum* was 100 mg/L and 1000 or >1000 mg/L for other test species. The ability of *P. aeruginosa* to survive in the presence of triclosan concentrations in excess of 1000 mg/L has been attributed to the expression of multi-drug efflux pumps that excrete triclosan out of the cell [54]. Hydrogen peroxide (H<sub>2</sub>O<sub>2</sub>) was chosen due to its well-known efficacy in inhibiting various bacteria, bacterial spores, fungi and viruses [29]. In the current test conditions, 4-h MBC of H<sub>2</sub>O<sub>2</sub> was 1000 mg/L to the majority of test organisms except *P. fluorescens* OS8 (4-h MBC 100 mg/L). Prolongation of the exposure to 24 h increased the toxic effect of H<sub>2</sub>O<sub>2</sub> 10-times to bacteria *E. coli*, *Janthinobacterium* sp., *P. fluorescens* KC-1 (24-h BMC 100 mg/L) and *P. fluorescens* OS8 (24-h

**Table 1**

Primary size, average hydrodynamic size ( $d_h$ ) and  $\zeta$ -potential of the nanomaterials in deionized water after 0 h and 24 h incubation at 25 °C.  $d_h$  and  $\zeta$ -potential data are average of three measurements  $\pm$  standard deviation.

Nano-materials	Primary size (nm)	0 h		24 h	
		$d_h$ (nm)	$\zeta$ -potential (mV)	$d_h$ (nm)	$\zeta$ -potential (mV)
nAg-PVP	$\sim 16^a$	$121 \pm 0.4 (0.19)^b$	$-9.70 \pm 0.3$	$114 \pm 0.7 (0.25)^b$	$-7.00 \pm 0.4$
nAg-Col	$12.5 \pm 4.0^c$	$41.8 \pm 0.6 (0.23)^b$	$-20.0 \pm 0.3$	$41.1 \pm 0.3 (0.24)^b$	$-27.6 \pm 0.5$
nCuO	$\sim 30.0^d$	$172 \pm 0.7 (0.15)^b$	$+29.1 \pm 0.7$	$145 \pm 5.6 (0.13)^b$	$+36.3 \pm 0.6$
nTiO <sub>2</sub>	$\sim 21.0^d$	$268 \pm 49 (0.30)^b$	$+20.1 \pm 3.3$	$251 \pm 40 (0.20)^b$	$+22.5 \pm 6.6$
MWCNTs	$10.1 \pm 0.5$ (diameter), $>1000$ (length) <sup>e</sup>	nd	nd	nd	nd

<sup>a</sup> Laloy et al [37].

<sup>b</sup> In the brackets – polydispersity index.

<sup>c</sup> Blinova et al [34].

<sup>d</sup> According to the manufacturer.

<sup>e</sup> TEM data for MWCNTs were provided by Dr S. Misra (Natural History Museum, UK); nd – not determined.

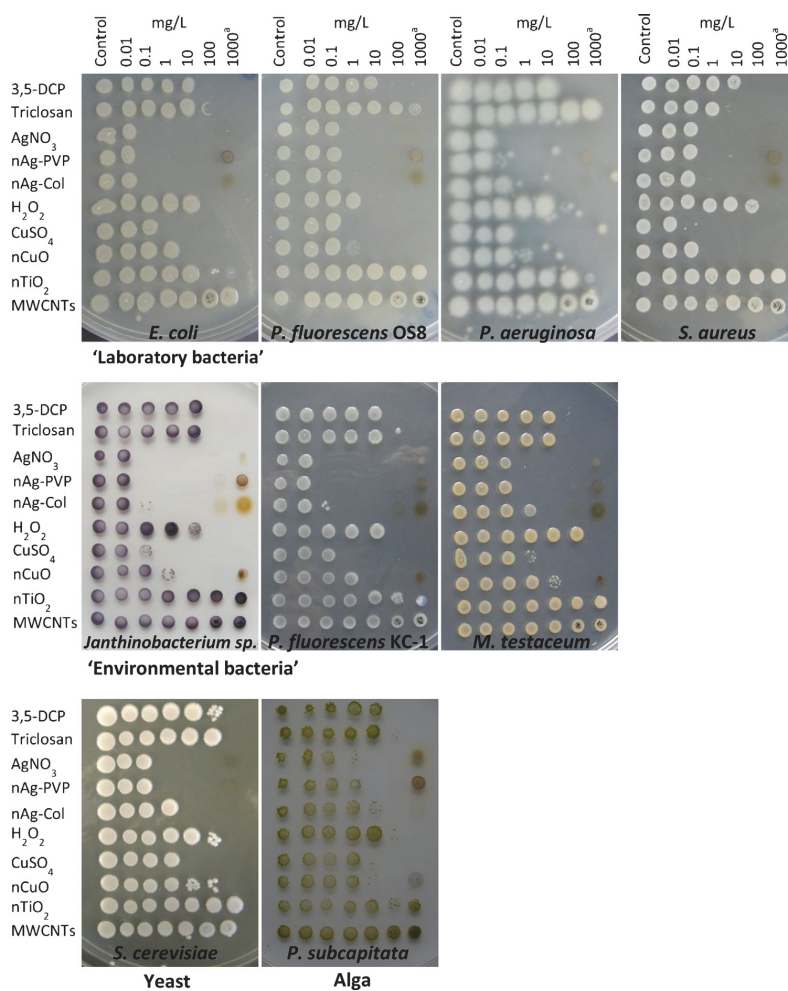


**Fig. 3.** Colony-forming ability of bacteria, yeast and alga after 24-h exposure to 3,5-DCP, triclosan, H<sub>2</sub>O<sub>2</sub> and Ag, CuO, TiO<sub>2</sub> nanoparticles, MWCNTs, Ag- and Cu-ions in deionized water at 25 °C. After exposure, cells (5  $\mu$ L) were transferred onto toxicant-free agarized growth medium. The concentrations of the chemicals are given as mg compound/L and mg metal/L for nAg-PVP, nAg-Col, AgNO<sub>3</sub> and CuSO<sub>4</sub>. \*The highest tested concentrations for nAg-Col and MWCNTs were 500 mg Ag/L and 250 mg/L, respectively. See also Table 2.

**Table 2**  
Minimum biocidal concentration (MBC) of the tested compounds to bacteria, yeast and alga after 4 h and 24 h exposure in deionized water at 25 °C. All chemicals were tested in nominal concentrations from 0.01 up to 1000 mg/L, except nAg-Col (up to 500 mg Ag/L) and MWCNTs (up to 250 mg/L). All experiments were done in two or three replicates. The data from the replicate experiments that yielded similar results are presented. See also Fig. 3.

Chemicals, concentration unit	MBC								
	Bacteria							Yeast	Alga
	<i>E. coli</i> MG1655 (G-)	<i>P. fluorescens</i> OS8 (G-)	<i>P. aeruginosa</i> DS10-129 (G-)	<i>S. aureus</i> RN4220 (G+)	<i>Janthinobacterium</i> sp (G-)	<i>P. fluorescens</i> KC-1 (G-)	<i>M. testaceum</i> PCSB7 (G+)	<i>S. cerevisiae</i> BY4741	<i>P. subcapitata</i>
4 h									
3,5-DCP, mg/L	100	100	100	100	100	100	100	1000	100
Triclosan <sup>a</sup> , mg/L	100	>1000	>1000	100	100	1000	100	1000	1000
H <sub>2</sub> O <sub>2</sub> , mg/L	1000	100	1000	1000	1000	1000	1000	1000	1000
AgNO <sub>3</sub> , mg Ag/L	0.1	1	0.1	1	0.1	1	1	1	10
nAg-PVP, mg Ag/L	0.1	1	0.1	1	0.1	1	1	1	100
nAg-Col, mg Ag/L	0.1	1	1	10	1	1	10	10	100
CuSO <sub>4</sub> , mg Cu/L	10	1	1	10	1	10	10	10	1000
nCuO, mg/L	10	10	10	100	10	100	100	1000	>1000
nTiO <sub>2</sub> <sup>a</sup> , mg/L	>1000	>1000	1000	>1000	>1000	>1000	>1000	>1000	>1000
MWCNTs <sup>a</sup> , mg/L	>250	>250	>250	>250	>250	>250	>250	>250	>250
24 h									
3,5-DCP, mg/L	100	100	100	100	100	100	100	1000	100
Triclosan <sup>a</sup> , mg/L	100	>1000	>1000	100	100	1000	100	1000	1000
H <sub>2</sub> O <sub>2</sub> , mg/L	100	10	1000	1000	100	100	1000	1000	1000
AgNO <sub>3</sub> , mg Ag/L	0.1	1	0.1	1	0.1	0.1	1	1	10
nAg-PVP, mg Ag/L	0.1	1	1	1	0.1	1	1	1	10
nAg-Col, mg Ag/L	0.1	1	1	1	1	1	10	10	10
CuSO <sub>4</sub> , mg Cu/L	1	1	1	0.1	1	1	10	10	10
nCuO, mg/L	10	1	1	1	10	10	100	1000	10
nTiO <sub>2</sub> <sup>a</sup> , mg/L	1000	>1000	1000	>1000	>1000	>1000	>1000	>1000	>1000
MWCNTs <sup>a</sup> , mg/L	>250	>250	>250	>250	>250	>250	>250	>250	>250

(G-) – Gram-negative bacteria; (G+) – Gram-positive bacteria; <sup>a</sup>experiments were done in two replicates

0.1 mg/L	10 mg/L	1000 mg/L
1 mg/L	100 mg/L	>250 or >1000 mg/L

MBC 10 mg/L). Differently from the H<sub>2</sub>O<sub>2</sub>, 3,5-DCP and triclosan did not exhibit time-dependent toxicity (4 h versus 24 h) to any of the tested organisms.

### 3.3. Toxicity of nanomaterials in the 'spot test'

The weakest biocidal effect in DI water was observed for nTiO<sub>2</sub> and MWCNTs: MBC >1000 and >250 mg/L, respectively (Table 2, Fig. 3). Our results are in agreement with literature data: toxicity of nTiO<sub>2</sub> has been shown to be low in comparison to other

nano-antimicrobials such as ZnO, CuO and Ag NPs [8], and nTiO<sub>2</sub> toxic properties are potentiated by photo-activation. In the current 'spot test' nTiO<sub>2</sub> like all other tested chemicals were assessed in the dark, i.e. without photo-activation. The reported concentrations of nTiO<sub>2</sub> required to affect bacterial viability usually vary between 100 and 1000 mg/L and are relatively inconsistent depending on the size and type of the particles and the intensity and wavelength of the light applied for photo-activation [8,55].

The most toxic NMs in the 'spot test' were Ag NPs. After 4 h of incubation, MBC of nAg-PVP and nAg-Col ranged from 0.1 to 10 mg

**Table 3**

Minimum biocidal concentrations (MBC) of the tested compounds to *E. coli*, *S. aureus* and *S. cerevisiae* in the broth microdilution test at 30 °C. For bacteria half-strength cation-adjusted Mueller-Hinton Broth and for yeast half-strength yeast-extract-peptone-dextrose was used as a test medium. All chemicals were tested in nominal concentrations from 0.01 up to 1000 mg/L, except nAg-Col (up to 500 mg Ag/L) and MWCNTs (up to 250 mg/L). All experiments were done in two replicates. See also Fig. 4.

Chemicals, concentration unit	MBC		
	Bacteria <sup>a</sup>		Yeast <sup>b</sup>
	<i>E. coli</i> MG1655 (G-)	<i>S. aureus</i> RN4220 (G+)	<i>S. cerevisiae</i> By4741
3,5-DCP, mg/L	1000	1000	100
Triclosan, mg/L	1000	1000	1000
H <sub>2</sub> O <sub>2</sub> , mg/L	100	100	1000
AgNO <sub>3</sub> , mg Ag/L	100	100	10
nAg-PVP, mg Ag/L	100	1000	10
nAg-Col, mg Ag/L	100	1000	1000
CuSO <sub>4</sub> , mg Cu/L	1000	1000	1000
nCuO, mg/L	>1000	>1000	>1000
nTiO <sub>2</sub> , mg/L	>1000	>1000	>1000
MWCNTs, mg/L	>250	>250	>250

<sup>a</sup>20-h MBC; <sup>b</sup>24-hMBC; (G-) – Gram-negative bacteria; (G+) – Gram-positive bacteria

10 mg/L	1000 mg/L
100 mg/L	250 or >1000 mg/L

Ag/L, except for alga (4-h MBC 100 mg/L) and were similar or 10-fold higher than the MBC for the soluble Ag-salt (AgNO<sub>3</sub>). In the case of Ag NPs, Gram-positive bacteria seemed to be slightly less susceptible than Gram-negative bacteria (Table 2).

CuO NPs in DI water were less biocidal than Ag NPs: 4-h MBC ranged from 10–100 mg/L, except for yeast (4-h MBC 1000 mg/L) and alga (>1000 mg/L). Toxicity of nCuO increased with increasing incubation time from 4 to 24 h. In general, the 4-h and 24-h MBC values for nCuO were 10-fold higher than the MBC values for soluble Cu-salt (CuSO<sub>4</sub>). Comparison of the biocidal potency of tested NMs showed that nanosilver compounds as well as nCuO proved very potent biocides when suspended in DI water, acting even at sub ppm level. In this respect, in the non-complexing environment these metallic NPs are as efficient as some known antibiotics e.g., gentamycin, kanamycin, trimethoprim [56]. Indeed, oligodynamic metals, such as silver and copper, have been used to fight bacteria and viruses [57] as well as algae [25] for more than 100 years. The ability of silver ions to bind sulfhydryl-groups may lead to the deterioration of the cellular membrane structures and inhibition of enzymes [14,57,58]. There are several mechanisms suggested for the antimicrobial action of copper including reactive-oxygen species-mediated adverse effects on membranes, proteins and DNA (for review and references therein, see [59]).

Despite differences in the sensitivities of the bacteria, yeast and alga to the tested compounds, the toxicity pattern in the case of all species was remarkably similar (Fig. 3). This 'toxicity fingerprint' (in our case visible as the letter 'E') illustrates similar toxic action of the tested NMs and chemicals to the different prokaryotic and eukaryotic cells.

#### 3.4. Comparison of the toxicity results of the 'spot test' and the conventional broth microdilution assay

To compare the MBC values obtained in the 'spot test' (DI water) and in organic-rich growth medium, the conventional broth microdilution test was performed. In the latter test, MBC values for *E. coli* and *S. aureus* were determined in ½ CA-MHB and for yeast *S. cerevisiae* in ½ YPD medium. Comparison of the 'spot test' (Table 2, Fig. 3) and standard broth microdilution assay (Table 3, Fig. 4) shows that in the case of organic compounds (3,5-DCP, triclosan, H<sub>2</sub>O<sub>2</sub>) the respective MBC values were similar, differing not more than 10 times (Table 4). The same was observed for nTiO<sub>2</sub> and MWCNTs (Tables 2 and 3). Interestingly, 3,5-DCP for *S. cerevisiae* and H<sub>2</sub>O<sub>2</sub> for *S. aureus* showed higher toxic potency in traditional broth microdilution test than in the 'spot test' indicating that these chemicals probably inhibit the active growth of these microbes that cannot occur in DI water.

However, the Ag-ions, nAg-PVP and nAg-Col were 100–1000 times more toxic to bacteria *E. coli* and *S. aureus* and 10–100-times to yeast *S. cerevisiae* in the 'spot test' compared to the broth microdilution assay (Tables 2–4). Similar tendency was observed for nCuO and Cu-ions as their toxicity in DI water was 100–10,000 times higher than in rich growth media (Table 2–4). When discussing and comparing the results of Ag and CuO NPs, it should be stressed that the toxicity of these NPs is driven mostly by the dissolved ions [27,32,35,60–62]. As shown earlier for ZnO NPs [63] and CuO NPs [16] organic ligands in test media may increase solubilisation of metallic NPs, however, at the same time reducing the bioavailability of dissolved ions. Thus, the conventional tests for determination

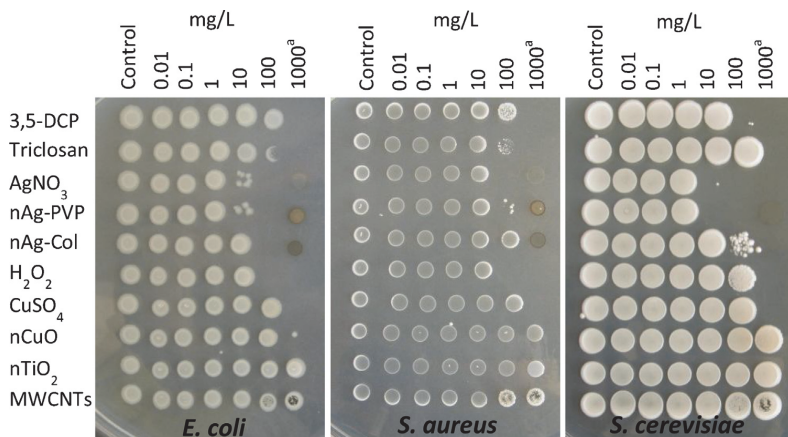


**Fig. 4.** Colony-forming ability of bacteria *Escherichia coli*, *Staphylococcus aureus* and yeast *Saccharomyces cerevisiae* after exposure to 3,5-DCP, triclosan,  $H_2O_2$  and Ag, CuO,  $TiO_2$  nanoparticles, MWCNTs, Ag- and Cu-ions in the broth microdilution test in half-strength cation-adjusted Mueller-Hinton Broth for 20 h (bacteria) or in half-strength yeast-extract-peptone-dextrose medium for 24 h (yeast) at 30 °C. After exposure, cells (5  $\mu$ L) were transferred onto toxicant-free agarized growth medium. The concentrations of the chemicals are given as mg compound/L and mg metal/L for nAg-PVP, nAg-Col,  $AgNO_3$  and  $CuSO_4$ . <sup>a</sup>The highest tested concentrations for nAg-Col and MWCNTs were 500 mg Ag/L and 250 mg/L, respectively. See also Table 3.

**Table 4**  
The ratio of minimum biocidal concentration (MBC) values obtained in the broth microdilution test in half-strength cation-adjusted Mueller-Hinton Broth (CA-MHB) (bacteria) or in half-strength yeast-extract-peptone-dextrose medium (YPD) (yeast) and respective MBC values in 'spot test' in deionized (DI) water. Ratios are calculated from Tables 2 and 3.

Chemicals	Ratio of MBC values ( $MBC_{1/2CA-MHB} / MBC_{DIwater}$ )		
	Bacteria		Yeast
	<i>E. coli</i> (G–)	<i>S. aureus</i> RN4220 (G+)	<i>S. cerevisiae</i> BY4741
3,5-DCP	10	10	0.1
Triclosan	10	10	1
$H_2O_2$	1	0.1	1
$AgNO_3$	1000	100	10
nAg-PVP	1000	1000	10
nAg-Col	1000	1000	100
$CuSO_4$	1000	10000	100
nCuO	>100	>1000	>1
n $TiO_2$	>1	>1	na <sup>d</sup>
MWCNTs	na <sup>b</sup>	na <sup>b</sup>	na <sup>b</sup>

(G–) – Gram-negative bacteria; (G+) – Gram-positive bacteria; na – not applicable as the MBC values in both test formats were <sup>a</sup>>1000 mg/L or <sup>b</sup>>250 mg/L (see also Tables 2 and 3).

of biocidal potency of chemicals (e.g., broth microdilution test) may mask the inherent antimicrobial potency of metal-based NPs, which is a function of solubilised bioavailable ions.

It has been shown that the solubility and toxicity of Ag and CuO NPs depends on several parameters such as particle size, coating, exposure time and temperature, and test medium [16,27,62,64]. Käkinen et al. [16] showed that copper speciation was the main reason behind the differences in apparent sensitivities of various aquatic organisms to Cu-ions and CuO NPs. The above mentioned study showed that although the  $EC_{50}$  values based on nominal concentrations of Cu-compounds for different test species (bacteria, yeasts, protozoa, algae and crustaceans) were different, the concentration of free copper was similar. It was concluded that different types of organisms have similar inherent sensitivity to copper [16]. Kasemets et al. [32] showed that despite higher solubility of CuO NPs in organics-rich growth medium (YPD) compared to DI water, the toxicity of CuO NPs to *S. cerevisiae* in DI water was ~130-times higher compared to YPD medium, demonstrating the decreased bioavailability of dissolved copper in the rich growth medium.

These findings underline the importance of a test environment that contains no or minimal amount of complexing ligands when testing and comparing toxicity of metal-containing compounds and NMs.

We have recently shown [65] that the toxicity and dissolution of citrate-stabilized Ag NPs in DI water clearly depended on the size of these NPs and the toxicity of 20–80 nm Ag NPs was induced by released Ag-ions. In the current study we observed a correlation between hydrodynamic size of NPs (nAg, nCuO and n $TiO_2$ ) and the respective toxic effect in DI-water but no correlation was observed between these parameters in rich test media or when the data for DI-water and rich media were pooled (data not shown). For example, the hydrodynamic size of nAg-PVP and nAg-Col in the both tests ('spot test' and broth microdilution assay) was comparable (42–120 nm; Table 1 and S3), but the respective toxic effects differed up to 1,000 times (Table 4). Also there was no clear correlation between the CuO NPs hydrodynamic size and toxicities. Indeed, in  $1/2$  CA-MHB nCuO was >100–1000-times less toxic than in DI water to bacteria (Table 4), while the difference in the hydrodynamic size was only ~5-times (145 versus 681 nm). Thus, although the

size/agglomeration plays a role in the adverse effects of metal-containing NMs, the toxic outcome is a complex interplay of various parameters of NMs (coatings, stabilizers, etc.) as well as of the test environment (low-complexing versus high-complexing).

#### 4. Conclusions and outlook

We have developed a simple and reliable method for the evaluation and comparison of biocidal potency of nanomaterials to different types of unicellular organisms that are usually targeted by biocidal compounds, i.e., bacteria, fungi and algae. Exposure to the toxicants in this assay is performed in deionized water that may be considered a promising test environment to evaluate the intrinsic toxic properties of chemicals and inherent sensitivity of microorganisms toward chemicals, especially metal-based NMs. The patterns of acute toxic effects of ten chemicals on nine unicellular organisms in DI water allows us to conclude that toxicity mechanism of biocidal chemicals (organic chemicals, metals) is similar, whatever the organism (bacteria, yeast, alga). Therefore, when the organisms are not 'protected' by their environment that usually includes various organic and inorganic supplements, their tolerance to toxicants is chemical-dependent rather than organism-dependent.

#### Supplementary material

List of the test species, their cultivation conditions, viability assessment of the test cells after 24-h incubation in DI water, culturing and handling of test organisms for 'spot test', both microdilution test, hydrodynamic size and  $\zeta$ -potential of studied NMs in 1/2 CA-MHB and 1/2 YPD medium, stability of NM suspension in three different test media and reproducibility of the 'spot test' are shown in the Supplementary material.

#### Acknowledgements

The authors thank three anonymous reviewers for their critical comments on the manuscript. This work was supported by grants ETF9001, ETF8561, Institutional funding IUT 23-5 of The Estonian Ministry of Education and Research, European Regional Development Fund project TERIKVANT, EU FP7 Project NanoValid under Grant Agreement No. 263147 and EU FP7 Project MODERN under Grant Agreement No. 309314. We thank Dr S. Misra from University of Birmingham, UK for providing the MWCNTs TEM data.

#### Appendix A. Supplementary data

Supplementary data associated with this article can be found, in the online version, at <http://dx.doi.org/10.1016/j.jhazmat.2014.12.027>.

#### References

- [1] A. Nel, T. Xia, L. Mädler, N. Li, Toxic potential of materials at the nanolevel, *Science* 311 (2006) 622–627.
- [2] A. Kahru, A. Ivask, Mapping the dawn of nanoeotoxicological research, *Acc. Chem. Res.* 46 (2013) 823–833.
- [3] S. Ivask, O. George, Metal-containing nano-antimicrobials: differentiating the impact of solubilized metals and particles, in: N. Cioffi (Ed.), *Nano-Antimicrobials – Progress and Prospects*, Springer, 2012, pp. 253–290.
- [4] F. Hossain, O.J. Perales-Perez, S. Hwang, F. Román, Antimicrobial nanomaterials as water disinfectant: applications, limitations and future perspectives, *Sci. Total Environ.* 466–467 (2014) 1047–1059.
- [5] A.L. Panlilio, D.H. Culver, R.P. Gaynes, S. Banerjee, T.S. Henderson, J.S. Tolson, W.J. Martone, Methicillin-resistant *Staphylococcus aureus* in U.S. hospitals, 1975–1991, *Infect. Control Hosp. Epidemiol.* 13 (1992) 582–586.
- [6] H. Goossens, M. Ferech, R. Vander Stichele, M. Elseviers, Outpatient antibiotic use in Europe and association with resistance: a cross-national database study, *Lancet* 365 (2005) 579–587.
- [7] A.D. Russell, Introduction of biocides into clinical practice and the impact on antibiotic-resistant bacteria, *J. Appl. Microbiol.* 92 (2002) 1215–1355.
- [8] A. Kahru, H.-C. Dubouquier, From ecotoxicology to nanoeotoxicology, *Toxicology* 269 (2010) 105–119.
- [9] Consumer products inventory Project on Emerging Nanotechnologies, a project of the Woodrow Wilson International Center for Scholars, <http://www.nanotechproject.org/cpi/in>, 2013.
- [10] EC, Regulation No. 1907/2006 of the European Parliament and of the Council of 18 December, 2006. Concerning the Registration, Evaluation, Authorisation and Restriction of Chemicals (REACH). In: Official Journal of the European Union, L396/1–849, European Commission, Brussels, Belgium, 2006.
- [11] E. Montoro, D. Lemus, M. Echemendia, A. Martin, F. Portaels, J.C. Palomino, Comparative evaluation of the nitrate reduction assay, the MTT test, and the resazurin microtitre assay for drug susceptibility testing of clinical isolates of *Mycobacterium tuberculosis*, *J. Antimicrob. Chemother.* 55 (2005) 500–505.
- [12] A.L. Niles, R.A. Moravec, T.L. Riss, Update on in vitro cytotoxicity assays for drug development, *Expert Opin. Drug Discovery* 3 (2008) 655–669.
- [13] A.L. Holder, R. Goth-Goldstein, D. Lucas, C.P. Koshland, Particle-induced artifacts in the MTT and LDH viability assays, *Chem. Res. Toxicol.* 25 (2012) 1885–1892.
- [14] A. Käkinen, F. Ding, P. Chen, M. Mortimer, A. Kahru, P.C. Ke, Interaction of firefly luciferase and silver nanoparticles and its impact on enzyme activity, *Nanotechnology* 24 (2013) 345101.
- [15] I. Blinova, A. Ivask, M. Heinlaan, M. Mortimer, A. Kahru, Ecotoxicity of nanoparticles of CuO and ZnO in natural water, *Environ. Pollut.* 158 (2010) 41–47.
- [16] A. Käkinen, O. Bondarenko, A. Ivask, A. Kahru, The effect of composition of different ecotoxicological test media on free and bioavailable copper from CuSO<sub>4</sub> and CuO nanoparticles: comparative evidence from a Cu-selective electrode and a Cu-biosensor, *Sensors* 11 (2011) 10502–10521.
- [17] I. Römer, A.J. Gavin, T.A. White, R.C. Merrifield, J.K. Chipman, M.R. Viant, J.R. Lead, The critical importance of defined media conditions in *Daphnia magna* nanotoxicity studies, *Toxicol. Lett.* 223 (2013) 103–108.
- [18] A. Besinis, T. De Peralta, R.D. Handy, The antibacterial effects of silver, titanium dioxide and silica dioxide nanoparticles compared to the dental disinfectant chlorhexidine on *Streptococcus mutans* using a suite of bioassays, *Nanotoxicology* 8 (2014) 1–16.
- [19] A. Dhawan, V. Sharma, Toxicity assessment of nanomaterials: methods and challenges, *Anal. Bioanal. Chem.* 398 (2010) 589–605.
- [20] K.J. Ong, T.J. MacCormack, R.J. Clark, J.D. Ede, V.A. Ortega, L.C. Felix, M.K. Dang, G. Ma, H. Fenniri, J.G. Veinot, G.G. Goss, Widespread nanoparticle-assay interference: implications for nanotoxicity testing, *PLoS One* 9 (2014) e90650.
- [21] N.A. Monteiro-Riviere, A.O. Inman, L.W. Zhang, Limitations and relative utility of screening assays to assess engineered nanoparticle toxicity in a human cell line, *Toxicol. Appl. Pharmacol.* 234 (2009) 222–235.
- [22] A.R. Lupu, T. Popescu, The noncellular reduction of MTT tetrazolium salt by TiO<sub>2</sub> nanoparticles and its implications for cytotoxicity assays, *Toxicol. In Vitro* 27 (2013) 1445–1450.
- [23] J.S. Angle, R.L. Chaney, Cadmium resistance screening in nitrilotriacetate-buffered minimal media, *Appl. Environ. Microbiol.* 55 (1989) 2101–2104.
- [24] L.R. Dartnell, T.A. Roberts, G. Moore, J.M. Ward, J.P. Muller, Fluorescence characterization of clinically-important bacteria, *PLoS One* 8 (2013) e75270.
- [25] B. Nowack, H.F. Krug, M. Height, 120 years of nanosilver history: implications for policy makers, *Environ. Sci. Technol.* 45 (2011) 1177–1183.
- [26] E. Almeida, T.C. Diamantino, O. de Sousa, Marine paints: the particular case of antifouling paints, *Prog. Org. Coat.* 59 (2007) 2–20.
- [27] O. Bondarenko, K. Juganson, A. Ivask, K. Kasemets, M. Mortimer, A. Kahru, Toxicity of Ag, CuO and ZnO nanoparticles to selected environmentally relevant test organisms and mammalian cells in vitro: a critical review, *Arch. Toxicol.* 87 (2013) 1181–1200.
- [28] M.T. Elnabarawy, R.R. Robideau, S.A. Beach, Comparison of three rapid toxicity test procedures: microtox, polytox, and activated sludge respiration inhibition, *Toxicity Assess.* 3 (1988) 361–370.
- [29] G. McDonnell, A.D. Russell, Antiseptics and disinfectants: activity, action, and resistance, *Clin. Microbiol. Rev.* 12 (1999) 147–179.
- [30] H. Johnston, G. Pojana, S. Zuin, N.R. Jacobsen, P. Moller, S. Loft, M. Semmler-Behnke, C. McGuiness, D. Balharry, A. Marcomini, H. Wallin, W. Kreyling, K. Donaldson, L. Tran, V. Stone, Engineered nanomaterial risk: lessons learnt from completed nanotoxicology studies: potential solutions to current and future challenges, *Crit. Rev. Toxicol.* 43 (2013) 1–20.
- [31] International Organization for Standards. Clinical laboratory testing and in vitro diagnostic test systems – Susceptibility testing of infectious agents and evaluation of performance of antimicrobial susceptibility test devices. 1. Reference method for testing the in vitro activity of antimicrobial agents against rapidly growing aerobic bacteria involved in infectious diseases. ISO 20,776–1. International Organization of Standards, Geneva, Switzerland, 15 November, 2006.
- [32] K. Kasemets, S. Suppi, K. Künnis-Beres, A. Kahru, Toxicity of CuO nanoparticles to yeast *Saccharomyces cerevisiae* BY4741 wild-type and its nine isogenic single-gene deletion mutants, *Chem. Res. Toxicol.* 26 (2013) 356–367.
- [33] B. Ohtani, O.O. Prieto-Mahoney, D. Li, R. Abe, What is degussa (evonik) P25? Crystalline composition analysis, reconstruction from isolated pure particles and photocatalytic activity test, *J. Photochem. Photobiol. A* 216 (2010) 179–182.

- [34] I. Blinova, J. Niskanen, P. Kajankari, L. Kanaribik, A. Käkinen, H. Tenhu, O.P. Penttinen, A. Kahru, Toxicity of two types of silver nanoparticles to aquatic crustaceans *Daphnia magna* and *Thamnocephalus platyurus*, *Environ. Sci. Pollut. Res. Int.* 20 (2013) 3456–3463.
- [35] O. Bondarenko, A. Ivask, A. Käkinen, I. Kurvet, A. Kahru, Particle-cell contact enhances antibacterial activity of silver nanoparticles, *PLoS One* 8 (2013) e64060.
- [36] A. Kahru, H.C. Dubourguier, I. Blinova, A. Ivask, K. Kasemets, Biotests and biosensors for ecotoxicology of metal oxide nanoparticles: a minireview, *Sensors* 8 (2008) 5153–5170.
- [37] J. Laloy, V. Minet, L. Alpan, F. Mullier, S. Beken, O. Toussaint, S. Lucas, J.-M. Dogne, Impact of silver nanoparticles on haemolysis, platelet function and coagulation, *Nanobiomedicine* 4 (2014), <http://dx.doi.org/10.5772/59346>.
- [38] M. Tejamaya, I. Romer, R.C. Merrifield, J.R. Lead, Stability of citrate, PVP, and PEG coated silver nanoparticles in ecotoxicology media, *Environ. Sci. Technol.* 46 (2012) 7011–7017.
- [39] V.K. Sharma, K.M. Siskova, R. Zboril, J.L. Gardea-Torresdey, Organic-coated silver nanoparticles in biological and environmental conditions: fate, stability and toxicity, *Adv. Colloid Interface Sci.* 204 (2014) 15–34.
- [40] P. Breeuwer, J.L. Drocourt, N. Bunschoten, M.H. Zwietering, F.M. Rombouts, T. Abee, Characterization of uptake and hydrolysis of fluorescein diacetate and carboxyfluorescein diacetate by intracellular esterases in *Saccharomyces cerevisiae*, which result in accumulation of fluorescent product, *Appl. Environ. Microbiol.* 61 (1995) 1614–1619.
- [41] D. Deere, J. Shen, G. Vesey, P. Bell, P. Bissinger, D. Veal, Flow cytometry and cell sorting for yeast viability assessment and cell selection, *Yeast* (Chichester, England) 14 (1998) 147–160.
- [42] J.E. Hobbie, E.A. Hobbie, Microbes in nature are limited by carbon and energy: the starving-survival lifestyle in soil and consequences for estimating microbial rates, *Front. Microbiol.* 4 (2013) 324.
- [43] K.W. Powers, S.C. Brown, V.B. Krishna, S.C. Wasdo, B.M. Moudgil, S.M. Roberts, Research strategies for safety evaluation of nanomaterials. Part VI. Characterization of nanoscale particles for toxicological evaluation, *Toxicol. Sci. Off. J. Soc. Toxicol.* 90 (2006) 296–303.
- [44] J. Jiang, G. Oberdörster, P. Biswas, Characterization of size, surface charge, and agglomeration state of nanoparticle dispersions for toxicological studies, *J. Nanopart. Res.* 11 (2009) 77–89.
- [45] S.N. Sorensen, A. Baun, Controlling silver nanoparticle exposure in algal toxicity testing – a matter of timing, *Nanotoxicology* (2014) 1–9.
- [46] R. Greenwood, K. Kendall, Selection of suitable dispersants for aqueous suspensions of zirconia and titania powders using acoustophoresis, *J. Eur. Ceram. Soc.* 19 (1999) 479–488.
- [47] S. Laurent, D. Forge, M. Port, A. Roch, C. Robic, L. Vander Elst, R.N. Muller, Magnetic iron oxide nanoparticles: synthesis, stabilization, vectorization, physicochemical characterizations, and biological applications, *Chem. Rev.* 108 (2008) 2064–2110.
- [48] S.H. Othman, R.S. Abdul, T.I.M. Ghazi, N. Abdullah, Dispersion and stabilization of photocatalytic TiO<sub>2</sub> nanoparticles in aqueous suspension for coatings applications, *J. Nanomater.* 2012 (2012) 10.
- [49] A. Hitchman, G.H. Sambrook Smith, Y. Ju-Nam, M. Sterling, J.R. Lead, The effect of environmentally relevant conditions on PVP stabilised gold nanoparticles, *Chemosphere* 90 (2013) 410–416.
- [50] M. Xu, J. Li, H. Iwai, Q. Mei, D. Fujita, H. Su, H. Chen, N. Hanagata, Formation of nano-bio-complex as nanomaterials dispersed in a biological solution for understanding nanobiological interactions, *Sci. Rep.* 2 (2012).
- [51] H.J.M. Verhaar, C.J. van Leeuwen, J.L.M. Hermens, Classifying environmental pollutants, *Chemosphere* 25 (1992) 471–491.
- [52] H.P. Schweizer, Triclosan: a widely used biocide and its link to antibiotics, *FEMS Microbiol. Lett.* 202 (2001) 1–7.
- [53] A.D. Russell, Whither triclosan? *J. Antimicrob. Chemother.* 53 (2004) 693–695.
- [54] R. Chuanchuen, R.R. Karkhoff-Schweizer, H.P. Schweizer, High-level triclosan resistance in *Pseudomonas aeruginosa* is solely a result of efflux, *Am. J. Infect. Control* 31 (2003) 124–127.
- [55] C. Wei, W.Y. Lin, Z. Zainal, N.E. Williams, K. Zhu, A.P. Kruzic, R.L. Smith, K. Rajeshwar, Bactericidal activity of TiO<sub>2</sub> photocatalyst in aqueous media: toward a solar-assisted water disinfection system, *Environ. Sci. Technol.* 28 (1994) 934–938.
- [56] J.M. Andrews, Determination of minimum inhibitory concentrations, *J. Antimicrob. Chemother.* 48 (Suppl. 1) (2001) 5–16.
- [57] R.B. Thurman, C.P. Gerba, The molecular mechanisms of copper and silver ion disinfection of bacteria and viruses, *Crit. Rev. Environ. Control* 18 (1988) 295–315.
- [58] A.L. Semeykina, V.P. Skulachev, Submicromolar Ag<sup>+</sup> increases passive Na<sup>+</sup> permeability and inhibits the respiration-supported formation of Na<sup>+</sup> gradient in *Bacillus* FTU vesicles, *FEBS Lett.* 269 (1990) 69–72.
- [59] J. O’Gorman, H. Humphreys, Application of copper to prevent and control infection. Where are we now? *J. Hosp. Infect.* 81 (2012) 217–223.
- [60] M. Heinlaan, A. Ivask, I. Blinova, H. Dubourguier, A. Kahru, Toxicity of nanosized and bulk ZnO, CuO and TiO<sub>2</sub> to bacteria *Vibrio fischeri* and crustaceans *Daphnia magna* and *Thamnocephalus platyurus*, *Chemosphere* 71 (2008) 1308–1316.
- [61] V. Aruoja, H.-C. Dubourguier, K. Kasemets, A. Kahru, Toxicity of nanoparticles of CuO, ZnO and TiO<sub>2</sub> to microalgae *Pseudokirchneriella subcapitata*, *Sci. Total Environ.* 407 (2009) 1461–1468.
- [62] A. Ivask, K. Juganson, O. Bondarenko, M. Mortimer, V. Aruoja, K. Kasemets, I. Blinova, M. Heinlaan, V. Slaveykova, A. Kahru, Mechanisms of toxic action of Ag, ZnO and CuO nanoparticles to selected ecotoxicological test organisms and mammalian cells in vitro: a comparative review, *Nanotoxicology* 1 (2014) 57–71.
- [63] M. Li, L. Zhu, D. Lin, Toxicity of ZnO nanoparticles to *Escherichia coli*: mechanism and the influence of medium components, *Environ. Sci. Technol.* 45 (2011) 1977–1983.
- [64] R. Behra, L. Sigg, M.J. Clift, F. Herzog, M. Minghetti, B. Johnston, A. Petri-Fink, B. Rothen-Rutishauser, Bioavailability of silver nanoparticles and ions: from a chemical and biochemical perspective, *J. R. Soc. Interface* 10 (2013) 20130396.
- [65] A. Ivask, I. Kurvet, K. Kasemets, I. Blinova, V. Aruoja, S. Suppi, H. Vija, A. Käkinen, T. Titma, M. Heinlaan, M. Visnapuu, D. Koller, V. Kisand, A. Kahru, Size-dependent toxicity of silver nanoparticles to bacteria, yeast, algae, crustaceans and mammalian cells in vitro, *PLoS One* 9 (2014) e102108.

## SUPPLEMENTARY MATERIAL

### A novel method for comparison of biocidal properties of nanomaterials to bacteria, yeasts and algae

Sandra Suppi<sup>1,2</sup>, Kaja Kasemets<sup>1\*</sup>, Angela Ivask<sup>1</sup>, Kai Künnis-Beres<sup>1</sup>, Imbi Kurvet<sup>1</sup>, Mariliis Sihtmäe<sup>1</sup>, Villem Aruoja<sup>1</sup>, Anne Kahru<sup>1\*</sup>

<sup>1</sup>Laboratory of Environmental Toxicology, National Institute of Chemical Physics and Biophysics, Akadeemia tee 23, Tallinn 12618, Estonia

<sup>2</sup>Faculty of Chemical and Materials Technology, Tallinn University of Technology, Ehitajate tee 5, Tallinn 19086, Estonia

\* corresponding authors

#### SUMMARY

##### 1. Materials and methods

**Table S1.** List of the test organisms used in this study and their cultivation conditions.

- 1.1. Viability assessment of bacterial and yeast cells by fluorescent viability dyes.
- 1.2. Culturing and handling of test organisms for the 'spot test'.
- 1.3. Broth microdilution susceptibility test

##### 2. Results

**Table S2.** Bacterial and yeast cell numbers (determined as colony forming units, CFU/mL) after incubation in deionized (DI) water for 0 h and 24 h at 25°C without shaking. CFU was determined by plating and counting the colonies on agarized growth medium.

**Table S3.** Primary size, average hydrodynamic size ( $d_h$ ) and  $\zeta$ -potential of the tested nanomaterials (NMs) in half-strength cation-adjusted Mueller-Hinton Broth (CA-MHB) and half-strength Yeast-Extract-Peptone-Dextrose medium (YPD) (growth medium for bacteria and yeast, respectively) after 0 h and 20 h or 24 h incubation at 30°C.  $d_h$  and  $\zeta$ -potential data are average of three measurements  $\pm$  standard deviation.

**Figure S1.** Viability of 'laboratory and 'environmental' bacterial and yeast cells in deionized (DI) water. Prior to staining, the cells were incubated in DI water for 0 or 24 h at 25°C. Two fluorescent viability dyes were used for staining: fluorescein diacetate (viable cells are green) and propidium iodide (non-viable cells are red). Name of the microorganism and in the case of bacteria, their Gram-staining (G+ or G-) is shown on images.

**Figure S2.** Visualisation of the stability of NM suspensions in three different test environment during 24 hours. Suspensions were incubated in (a) deionized (DI) water, (b) half-strength cation-adjusted Mueller-Hinton Broth (CA-MHB) and (c) half-strength Yeast-Extract-Peptone-Dextrose medium (YPD) at ambient temperature for 0, 4 and 24 h in static conditions. nAg-PVP, nAg-Col, nCuO were analyzed at concentration of 50 mg Ag/L and TiO<sub>2</sub> at 100 mg/L.

**Table S4.** Reproducibility of the 'spot test' in DI water. 24-h MBC minimum biocidal concentration (MBC) of 2–3 individual experiments are presented for 3,5-DCP, H<sub>2</sub>O<sub>2</sub>, AgNO<sub>3</sub>, CuSO<sub>4</sub>, nAg-Col and nCuO.

## 1. Materials and Methods

**Table S1.** List of the test organisms used in this study and their cultivation conditions.

Test species	Origin/information on the test strain	Growth medium <sup>a</sup>	Cultivation conditions
<b>'Laboratory bacteria'</b>  <i>Escherichia coli</i> MG1655  <i>Pseudomonas fluorescens</i> OS8  <i>Pseudomonas aeruginosa</i> DS10-129  <i>Staphylococcus aureus</i> RN4220	  <i>E. coli</i> genetic stock centre (Yale University) [1]  [2]  [3]	LB (g/L): tryptone 10 (LAB M), yeast extract 5 (LAB M); agarized medium contained 1.5% agar (LAB M) and 0.5% NaCl (Sigma Aldrich).	Grown in LB for 16–18 h <sup>b</sup> or 3–5 h <sup>c</sup> at 30°C on a rotary shaker at 200 rpm
<b>'Environmental bacteria'</b> <sup>d</sup>  <i>Janthinobacterium sp. TP-Snow-C76</i>  <i>Pseudomonas fluorescens</i> KC-1  <i>Microbacterium testaceum</i> PCSB7	Isolated from soil  Isolated from groundwater well  Isolated from drinking water system	R2A (Lab M) (g/L): proteose peptone 0.5, cas-amino acids 0.5, yeast extract 0.5, glucose 0.5, soluble starch 0.5, K <sub>2</sub> HPO <sub>4</sub> 0.3, MgSO <sub>4</sub> *7H <sub>2</sub> O 0.05, sodium pyruvate 0.3; agarized medium contained 1.5% agar (LAB M).	Grown in R2A for 16–18 h <sup>b</sup> or 4–5 h <sup>c</sup> at 25°C on a rotary shaker at 200 rpm
<b>Yeast:</b>  <i>Saccharomyces cerevisiae</i> BY4741	EUROSCARF (Institute of Microbiology, University of Frankfurt, Germany)	YPD (g/L): yeast extract 10 (Lab M), Bacto™ peptone 20 (Difco Laboratories), glucose 20 (Sigma Aldrich); agarized medium contained 2% agar (Lab M).	Grown in YPD for 16–18 h <sup>b</sup> or 4–4.5 h <sup>c</sup> at 30°C on a rotary shaker at 200 rpm
<b>Alga:</b>  <i>Pseudokirchneriella subcapitata</i>	Algaltoxkit F (MicroBioTests Inc., Nazareth, Belgium)	OECD 201 medium (mg/L): NH <sub>4</sub> Cl 15, MgCl <sub>2</sub> *6H <sub>2</sub> O 12, CaCl <sub>2</sub> *2H <sub>2</sub> O 18, MgSO <sub>4</sub> *7H <sub>2</sub> O 15, KH <sub>2</sub> PO <sub>4</sub> 1.6, NaHCO <sub>3</sub> 50, Na <sub>2</sub> EDTA*2H <sub>2</sub> O 0.1, FeCl <sub>3</sub> *6H <sub>2</sub> O 0.08, H <sub>3</sub> BO <sub>3</sub> 0.185, MnCl <sub>2</sub> *4H <sub>2</sub> O 0.415, ZnCl <sub>2</sub> 0.003, CoCl <sub>2</sub> *6H <sub>2</sub> O 0.0015, Na <sub>2</sub> MoO <sub>4</sub> *2H <sub>2</sub> O 0.007, CuCl <sub>2</sub> *2H <sub>2</sub> O 0.00001; agarized medium contained 1.5% agar (LAB M)	Grown in OECD 201 medium for 3-4 days <sup>c</sup> at ~25°C with constant illumination and once-daily shaking

<sup>a</sup>growth medium used to cultivate bacteria, yeast or alga to obtain viable cell suspension for the 'spot test'. Agarized growth medium were used to evaluate (i) cell viability by plating and counting colonies after 24-h incubation in DI water and (ii) colony-forming ability of toxicant-exposed cells after plating (spotting) on the toxicant-free solid growth medium; Incubation time of <sup>b</sup>overnight culture and <sup>c</sup>exponential culture; <sup>d</sup> 'Environmental bacteria' used in this study were newly isolated and identified in the Centre for Biology of Integrated Systems of Tallinn University of Technology, Estonia. Briefly,

the 16s ribosomal RNA gene regions V2-V3 of the three strains were sequenced using universal primers 5' - CTG CTG CCT YCC GTA - 3' and 5' - AGT TTG ATC CTG GCT CAG - 3'. Sequencing was performed on Applied Biosystems 3730xl DNA Analyzer using Applied Biosystems BigDye Terminator v3.1 Cycle Sequencing Kit according to the manufacturer's protocol. Resultant sequences were aligned with BLAST algorithm against NCBI database.

### **1.1. Culturing and handling of test organisms for the 'spot test'**

Exponentially growing bacterial, yeast and algal cells were used in the 'spot test'. For that, bacterial and yeast cells were first cultivated overnight in respective growth medium (Table S1), then diluted (for 'laboratory bacteria' 1:50; for 'environmental bacteria' 1:10; for yeast 1:40) in fresh growth medium (20 mL in 100 mL flask) and further cultivated at 30°C ('laboratory bacteria' and yeast) or 25°C ('environmental bacteria') with shaking at 200 rpm for 3–5 hours until mid-exponential growth phase (Fig. 1). The mid-exponential growth phase for bacteria and yeast was reached at OD600nm values ~0.6 and 0.8-1.0, respectively (measured by Jenway 6300 Spectrophotometer, UK). Algal culture was diluted with fresh growth medium to a density of ~10<sup>4</sup> cells/mL (cells were counted under microscope in the Neubauer haemocytometer) and cultivated for 3–4 days at ~25°C with constant illumination and once-daily shaking until mid-exponential growth phase.

The cells were harvested by centrifugation at 5000 g for 5–7 min (bacteria) or 3500 g for 10 min (yeast and alga) at 20°C (Sigma 3-16PK centrifuge, Germany) in 50 mL polypropylene centrifuge tubes (BD Falcon). After that the cells were suspended in DI water and centrifuged again. The cycle was repeated twice and finally, the cells were re-suspended in DI water to a density of ~10<sup>7</sup> CFU/mL for bacteria (OD600nm 0.1) and yeast (OD600nm 1.2) and 10<sup>6</sup> cells/mL for alga.

### **1.2. Viability assessment of bacterial and yeast cells by fluorescent viability dyes**

Prior to staining, cell suspension in DI water (2 mL per well) was incubated on 24-well microplates (non-Tissue Culture Treated, BD Falcon) at 25°C for 24 h. After incubation the cell suspension was centrifuged at 6500 rpm for 10 min (Thermo Scientific™ Heraeus) in 2 mL centrifuge tubes and cell pellet was re-suspended in 50 µL of DI water. 5 µL of fluorescein diacetate (FDA solution in acetone, 1 mg/mL) and 5 µL of propidium iodide (PI solution in DI, 1 mg/mL) were added to the cell suspension. The mixture was kept in dark for 5 min and then 5 µL of the dye-treated cell suspension was pipetted on a standard microscope slide and was dried at room temperature ~5-10 minutes, then a drop of immersion oil (Olympus, Japan) was placed on the sample for attaching and sample covered with a coverslip. FDA and PI fluorescence of the cell samples was observed using Olympus CX41 epifluorescence microscope fitted with a filter cassette (CX-DMB-2) containing an excitation filter BP475 (475 nm) and a barrier filter O515IF (515 nm). The microscope was fitted with an Olympus U-CMAD3 real time colour digital camera DP71 (Japan). The pictures were taken using CellB Software (Olympus Soft Imaging Solutions GmbH).

### **1.3. Broth microdilution susceptibility test**

The broth microdilution method was adapted from the reference method ISO 20776-1 [4] for antimicrobial susceptibility testing. The broth microdilution method was conducted with bacteria *E. coli* and *S. aureus* and yeast *S. cerevisiae*. For bacteria we used cation-adjusted

(CA) Mueller-Hinton Broth (MHB, Oxoid Microbiology Products) containing per 1 litre: dehydrated infusion from beef 300 g, casein hydrolysate 17.5 g, starch 1.5 g, Ca<sup>2+</sup> 25 mg and Mg<sup>2+</sup> 12.5 mg. Yeast-Extract-Peptone-Dextrose (YPD) medium (Table S1) was used for yeast. The bacterial and yeast cells were first cultivated overnight in CA-MHB or YPD medium, respectively, at 30°C with shaking at 200 rpm, and then diluted with fresh medium to a culture density of ~10<sup>6</sup> CFU/mL. Since the stock concentrations of tested chemicals in DI water were not the same, then in order to achieve exactly the same-fold dilution of the test medium for all the toxicants, we conducted the broth microdilution test in half-strength CA-MHB or half-strength YPD. Briefly, 50 µL of serial dilutions of toxicant suspensions in DI water (prepared exactly as for the 'spot test', see Materials and methods) were pipetted onto 96-well microplates (BD Falcon), then 50 µL of bacterial or yeast suspension in CA-MHB or YPD, respectively was added. Wells containing 50 µL of toxicant-free DI water and 50 µL of bacterial or yeast culture in CA-MHB or YPD medium were included for each strain tested and served as non-treated controls. The inoculated 96-well microplates were incubated at 30°C for 20 h (bacteria) or for 24 h (yeast) without shaking in the dark. Each concentration of the tested chemicals and control culture was studied in triplicate. After 20 h or 24 h incubation, 5 µL of sample from each well was pipetted onto the toxicant-free Mueller-Hinton (Oxoid Microbiology Products) or YPD agar plates. The inoculated agar plates were incubated for 24 h (bacteria) or 72 h (yeast) at 30°C. The concentration that yielded no visible growth/colonies of the exposed organism after sub-culturing on toxicant-free agar-medium was defined as minimum biocidal concentration.

## 2. Results

**Table S2.** Bacterial and yeast cell numbers (measured as colony forming units, CFU/mL) after incubation in deionized (DI) water for 0 h and 24 h at 25°C without shaking. CFU was determined by plating and counting the colonies on nutrient agar (see Table S1).

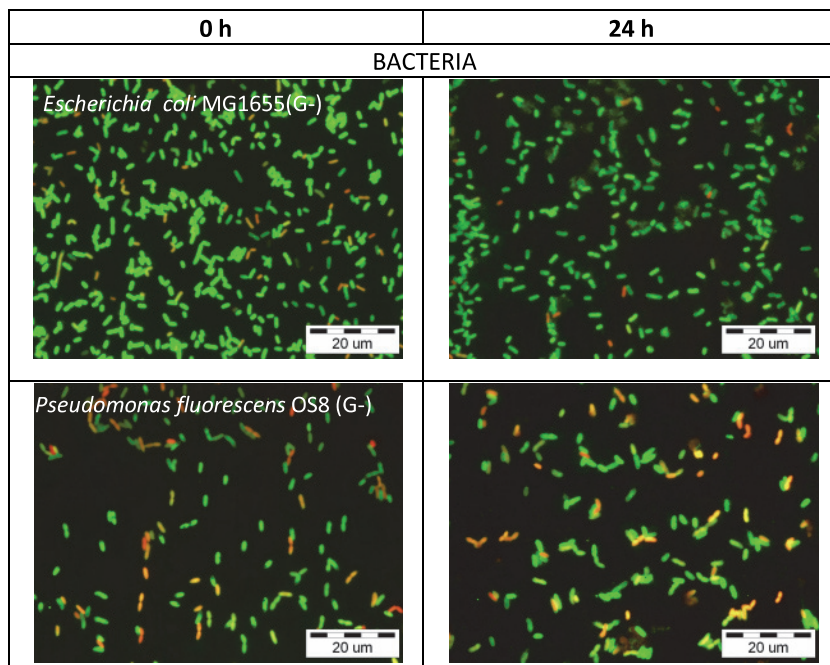
Microorganisms	Test species	Incubation time	
		0 h	24 h
Bacteria	<i>Escherichia coli</i> MG1655	2.8*10 <sup>7</sup>	1.9*10 <sup>7</sup>
	<i>Pseudomonas fluorescens</i> OS8	9.1*10 <sup>6</sup>	1.1*10 <sup>7</sup>
	<i>Pseudomonas aeruginosa</i> DS10-129	3.9*10 <sup>7</sup>	2.5*10 <sup>7</sup>
	<i>Staphylococcus aureus</i> RN4220	3.3*10 <sup>7</sup>	6.4*10 <sup>6</sup>
	<i>Janthinobacterium sp. TP-Snow-C76</i>	5.7*10 <sup>6</sup>	1.25*10 <sup>7</sup>
	<i>Pseudomonas fluorescens</i> KC-1	1.0*10 <sup>6</sup>	8.5*10 <sup>5</sup>
	<i>Microbacterium testaceum</i> PCSB7	6.5*10 <sup>7</sup>	8.8*10 <sup>7</sup>
Yeast	<i>Saccharomyces cerevisiae</i> BY4741	3.8*10 <sup>6</sup>	3.2*10 <sup>6</sup>

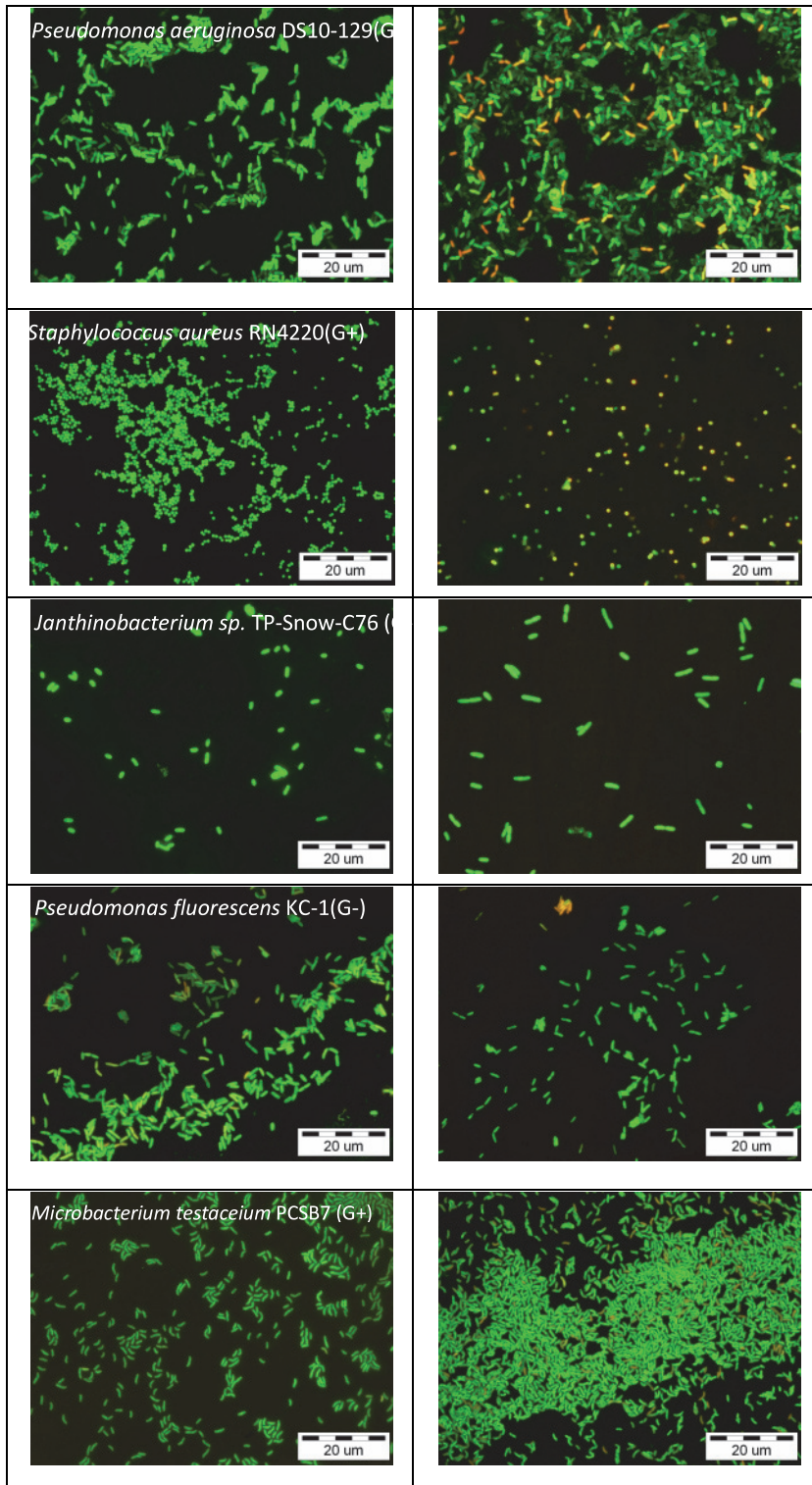
**Table S3.** Primary size, average hydrodynamic size ( $d_h$ ) and  $\zeta$ -potential of the tested nanomaterials (NMs) in half-strength cation-adjusted Mueller-Hinton Broth (CA-MHB) and half-strength Yeast-Extract-Peptone-Dextrose medium (YPD) (growth medium for bacteria and yeast, respectively) after 0 h and 20 h or 24 h incubation at 30°C.  $d_h$  and  $\zeta$ -potential data are average of three measurements  $\pm$  standard deviation.

NMs/ test media	Primary size (nm)	0 h		20 or 24 h	
		$d_h$ (nm)	$\zeta$ -potential (mV)	$d_h$ (nm)	$\zeta$ -potential (mV)
In ½ CA-MHB (0 h and 20 h)					
nAg-PVP	~16 <sup>a</sup>	107 $\pm$ 0.9	-2.23 $\pm$ 0.2	82.5 $\pm$ 0.7	-12.3 $\pm$ 0.1

		(0.19) <sup>b</sup>		(0.23) <sup>b</sup>	
nAg-Col	12.5 ± 4 <sup>c</sup>	44.2 ± 0.4 (0.34) <sup>b</sup>	-3.94 ± 0.8	60.6 ± 2.8 (0.44) <sup>b</sup>	-3.28 ± 0.7
nCuO	~30.0 <sup>d</sup>	201 ± 1.0 (0.19) <sup>b</sup>	-18.5 ± 0.3	681 ± 152 (0.71) <sup>b</sup>	-9.01 ± 0.1
nTiO <sub>2</sub>	~21.0 <sup>d</sup>	390 ± 5.9 (0.24) <sup>b</sup>	-14.5 ± 0.7	450 ± 7.0 (0.26) <sup>b</sup>	-18.1 ± 0.6
½ CA-MHB	—	282 ± 67 (0.95)	-5.69 ± 1.1	188 ± 4.0 (0.92)	-4.47 ± 0.6
In ½ YPD (0 h and 24 h)					
nAg-PVP	~16 <sup>a</sup>	119 ± 2.8 (0.20) <sup>b</sup>	-3.29 ± 0.2	112 ± 0.2 (0.19) <sup>b</sup>	-8.41 ± 1.7
nAg-Col	12.5 ± 4 <sup>c</sup>	46.4 ± 0.3 (0.26) <sup>b</sup>	-14.8 ± 0.3	56.8 ± 0.3 (0.23) <sup>b</sup>	-15.4 ± 1.1
nCuO	~30.0 <sup>d</sup>	1012 ± 41 (0.23) <sup>b</sup>	-20.6 ± 0.6	1475 ± 186 (0.43) <sup>b</sup>	-20.6 ± 0.8
nTiO <sub>2</sub>	~21.0 <sup>d</sup>	1023 ± 120 (0.21) <sup>b</sup>	-17.0 ± 0.6	1045 ± 70 (0.24) <sup>b</sup>	-17.1 ± 0.4
½ YPD	—	268 ± 41 (0.70)	-11.2 ± 0.1	259 ± 54 (0.81)	-14.6 ± 2.1

<sup>a</sup>Laloy *et al* [5]; <sup>b</sup>in the brackets - polydispersity index; <sup>c</sup>Blinova *et al* [6]; <sup>d</sup>according to the manufacturer





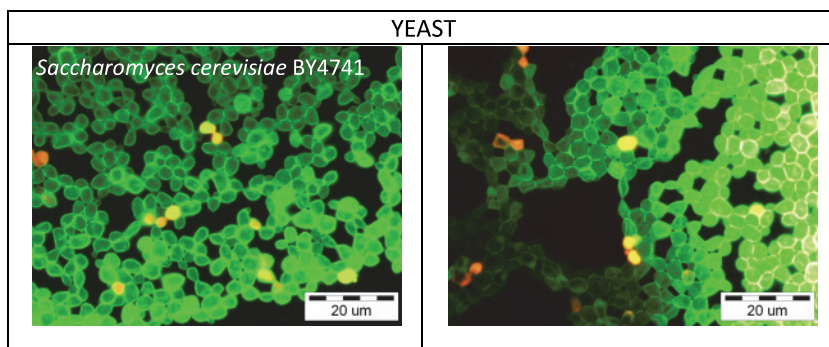


**Figure S1.** Viability of ‘laboratory and ‘environmental’ bacterial and yeast cells in deionized (DI) water. Prior to staining, the cells were incubated in DI water for 0 or 24 h at 25°C. Two fluorescent viability dyes were used for staining: fluorescein diacetate (viable cells are green) and propidium iodide (non-viable cells are red). Name of the microorganism and in the case of bacteria, their Gram-staining (G+ or G-) is shown on images.

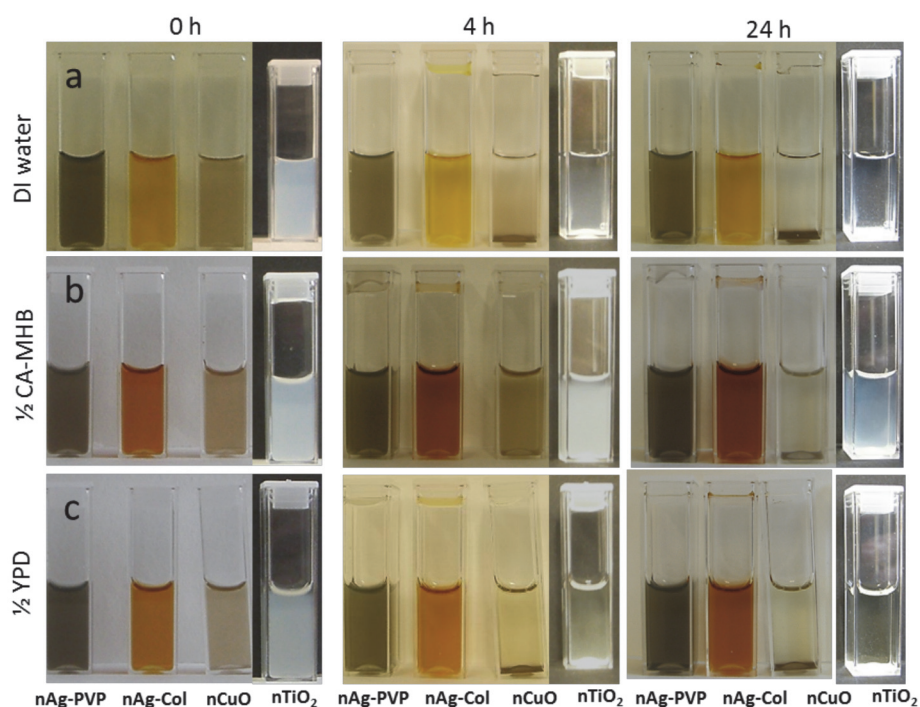


**Figure S2.** Visualisation of the stability of NM suspensions in three different test environments during 24 hours. Suspensions were incubated in **(a)** deionized (DI) water, **(b)** half-strength cation-adjusted Mueller-Hinton Broth (CA-MHB) and **(c)** half-strength Yeast-Extract-Peptone-Dextrose medium (YPD) at ambient temperature for 0, 4 and 24 h under static conditions. nAg-PVP, nAg-Col, nCuO were analyzed at concentration of 50 mg Ag/L and TiO<sub>2</sub> at 100 mg/L.

**Table S4.** Reproducibility of the 'spot test' in deionized water. 24-h MBC minimum biocidal concentration (MBC) of 2–3 individual experiments are presented for 3,5-DCP, H<sub>2</sub>O<sub>2</sub>, AgNO<sub>3</sub>, CuSO<sub>4</sub>, nAg-Col and nCuO.

Chemicals, concentration unit	MBC									
	Experiment, No	Bacteria						Yeast	Alga	
		<i>E. coli</i> MG1655 (G-)	<i>P. fluorescens</i> OS8 (G-)	<i>P. aeruginosa</i> DS10-129 (G-)	<i>S. aureus</i> RN4220 (G+)	<i>Janthinobacterium</i> sp (G-)	<i>P. fluorescens</i> KC-1 (G-)	<i>M. testaceum</i> PCSB7 (G+)	<i>S. cerevisiae</i> BY4741	<i>P. subcapitata</i>
3,5-DCP, mg/L	1	100	100 <sup>a</sup>	100	100	100	100	nd	1000	100
	2	100	100 <sup>a</sup>	100	100	100	100	100	1000	100
	3	100	1000	100	100	100	100	100	1000	100
H <sub>2</sub> O <sub>2</sub> , mg/L	1	100	10 <sup>a</sup>	100	1000	1	100	nd	1000	100
	2	100	10 <sup>a</sup>	1000 <sup>a</sup>	1000	100 <sup>a</sup>	100	1000	1000	1000 <sup>a</sup>
	3	100	100	1000 <sup>a</sup>	1000	100 <sup>a</sup>	100	1000	1000	1000 <sup>a</sup>
AgNO <sub>3</sub> , mg Ag/L	1	0.1	0.1 <sup>a</sup>	1	1	0.1	1	nd	1	10
	2	0.1	1	0.1 <sup>a</sup>	1	0.1	1	1	1	10
	3	0.1	0.1 <sup>a</sup>	0.1 <sup>a</sup>	1	0.1	1	1	1	10
nAg-Col, mg Ag/L	1	0.1	1	1	1	0.1	1	nd	10 <sup>a</sup>	10 <sup>a</sup>
	2	0.1	1	1	1	1 <sup>a</sup>	1	10	100	100
	3	0.1	1	1	1	1 <sup>a</sup>	1	10	10 <sup>a</sup>	10 <sup>a</sup>
CuSO <sub>4</sub> , mg Cu/L	1	1 <sup>a</sup>	1	1 <sup>a</sup>	1	1	1	nd	10	10
	2	10	1	1 <sup>a</sup>	0.1 <sup>a</sup>	1	1	10	10	10
	3	1 <sup>a</sup>	1	10	0.1 <sup>a</sup>	1	1	10	10	10
nCuO, mg/L	1	10	10	1 <sup>a</sup>	1	1	1 <sup>a</sup>	nd	>1000	10
	2	10	10	10	1	10 <sup>a</sup>	10	10	1000 <sup>a</sup>	10
	3	10	10	1 <sup>a</sup>	1	10 <sup>a</sup>	1 <sup>a</sup>	10	1000 <sup>a</sup>	10

(G-) – Gram-negative bacteria; (G+) – Gram-positive bacteria; nd- not determined. <sup>a</sup>If the MBC replicate values were different, the value of two similar replicates was presented in Table 2.

0.1 mg/L	10 mg/L	1000 mg/L
1 mg/L	100 mg/L	>1000 mg/L

## References

[1] I. Sarand, H. Haario, K.S. Jorgensen, M. Romantschuk, Effect of inoculation of a TOL plasmid containing mycorrhizosphere bacterium on development of Scots pine seedlings, their mycorrhizosphere and the microbial flora in m-toluate-amended soil, FEMS Microbiol. Ecol. 31 (2000) 127–141.

- [2] K.S.M. Rahman, T.J. Rahman, P. Lakshmanaperumalsamy, R. Marchant, I.M. Banat, The potential of bacterial isolates for emulsification with a range of hydrocarbons, *Acta Biotechnol.* 23 (2003) 335–345.
- [3] B.N. Kreiswirth, S. Lofdahl, M.J. Betley, M. O'Reilly, P.M. Schlievert, M.S. Bergdoll, R.P. Novick, The toxic shock syndrome exotoxin structural gene is not detectably transmitted by a prophage, *Nature* 305 (1983) 709–712.
- [4] International Organization for Standards. Clinical laboratory testing and in vitro diagnostic test systems - Susceptibility testing of infectious agents and evaluation of performance of antimicrobial susceptibility test devices. 1. Reference method for testing the in vitro activity of antimicrobial agents against rapidly growing aerobic bacteria involved in infectious diseases. ISO 20776-1. International Organization of Standards, Geneva, Switzerland, 15 November 2006.
- [5] J. Laloy, V. Minet, L. Alpan, F. Mullier, S. Beken, O. Toussaint, S. Lucas, J.-M. Dogne, Impact of Silver Nanoparticles on Haemolysis, Platelet Function and Coagulation, *Nanobiomedicine*, 4; doi: 10.5772/59346 (2014).
- [6] I. Blinova, J. Niskanen, P. Kajankari, L. Kanarbik, A. Käkinen, H. Tenhu, O.P. Penttinen, A. Kahru, Toxicity of two types of silver nanoparticles to aquatic crustaceans *Daphnia magna* and *Thamnocephalus platyurus*, *Environ. Sci. Pollut. Res. Int.*, 20 (2013) 3456-3463.



## PUBLICATION III

Ivask, A., Kurvet, I., Kasemets, K., Blinova, I., Aruoja, V., **Suppi, S.**, Vija, H., Käkinen, A., Titma, T., Heinlaan, M., Visnapuu, M., Koller, D., Kisand, V., Kahru, A. (2014). Size-dependent toxicity of silver nanoparticles to bacteria, yeast, algae, crustaceans and mammalian cells in vitro. *PLoS One*. 9, e102108.

This work is licensed under a Creative Commons Attribution 4.0 International License.





# Size-Dependent Toxicity of Silver Nanoparticles to Bacteria, Yeast, Algae, Crustaceans and Mammalian Cells *In Vitro*

Angela Ivask<sup>1\*</sup>, Imbi Kurvet<sup>1</sup>, Kaja Kasemets<sup>1</sup>, Irina Blinova<sup>1</sup>, Villem Aruoja<sup>1</sup>, Sandra Suppi<sup>1</sup>, Heiki Vija<sup>1</sup>, Aleksandr Käkinen<sup>1</sup>, Tiina Titma<sup>1</sup>, Margit Heinlaan<sup>1</sup>, Meeri Visnapuu<sup>1,2</sup>, Dagmar Koller<sup>3</sup>, Vambola Kisand<sup>2</sup>, Anne Kahru<sup>1\*</sup>

**1** Laboratory of Environmental Toxicology, National Institute of Chemical Physics and Biophysics, Tallinn, Estonia, **2** Institute of Physics, Faculty of Science and Technology, University of Tartu, Tartu, Estonia, **3** Biomineral Research Group, Medical Research Council Human Nutrition Research, Cambridge, United Kingdom

## Abstract

The concept of nanotechnologies is based on size-dependent properties of particles in the 1–100 nm range. However, the relation between the particle size and biological effects is still unclear. The aim of the current paper was to generate and analyse a homogenous set of experimental toxicity data on Ag nanoparticles (Ag NPs) of similar coating (citrate) but of 5 different primary sizes (10, 20, 40, 60 and 80 nm) to different types of organisms/cells commonly used in toxicity assays: bacterial, yeast and algal cells, crustaceans and mammalian cells *in vitro*. When possible, the assays were conducted in ultrapure water to minimise the effect of medium components on silver speciation. The toxic effects of NPs to different organisms varied about two orders of magnitude, being the lowest (~0.1 mg Ag/L) for crustaceans and algae and the highest (~26 mg Ag/L) for mammalian cells. To quantify the role of Ag ions in the toxicity of Ag NPs, we normalized the EC<sub>50</sub> values to Ag ions that dissolved from the NPs. The analysis showed that the toxicity of 20–80 nm Ag NPs could fully be explained by released Ag ions whereas 10 nm Ag NPs proved more toxic than predicted. Using *E. coli* Ag-biosensor, we demonstrated that 10 nm Ag NPs were more bioavailable to *E. coli* than silver salt (AgNO<sub>3</sub>). Thus, one may infer that 10 nm Ag NPs had more efficient cell-particle contact resulting in higher intracellular bioavailability of silver than in case of bigger NPs. Although the latter conclusion is initially based on one test organism, it may lead to an explanation for “size-dependent” biological effects of silver NPs. This study, for the first time, investigated the size-dependent toxic effects of a well-characterized library of Ag NPs to several microbial species, protozoans, algae, crustaceans and mammalian cells *in vitro*.

**Citation:** Ivask A, Kurvet I, Kasemets K, Blinova I, Aruoja V, et al. (2014) Size-Dependent Toxicity of Silver Nanoparticles to Bacteria, Yeast, Algae, Crustaceans and Mammalian Cells *In Vitro*. PLoS ONE 9(7): e102108. doi:10.1371/journal.pone.0102108

**Editor:** Antonietta Quigg, Texas A&M University, United States of America

**Received:** April 4, 2014; **Accepted:** June 15, 2014; **Published:** July 21, 2014

**Copyright:** © 2014 Ivask et al. This is an open-access article distributed under the terms of the Creative Commons Attribution License, which permits unrestricted use, distribution, and reproduction in any medium, provided the original author and source are credited.

**Data Availability:** The authors confirm that all data underlying the findings are fully available without restriction. All relevant data are within the paper and its Supporting Information files.

**Funding:** This study was supported by Estonian Targeted Funding projects SF0690063s08 (authors from NICPB), IUT23-5 (authors from NICPB), Estonian Science Foundation projects ETF9001 (KK, SS), ETF9347 (MH, IB, AK), ETF8561 (AI, AK, Anne K), by the European Regional Development Fund project TERIKVANT (AI, IB, Anne K), EU FP7 grant NanoValid under Grant Agreement No. 263147 (AI, MH, Anne K), EU FP7 Project MODERN under Grant Agreement No. 309314 (VA, Anne K) and by the United Kingdom Medical Research Council, Unit Programme no. U105960399 (DK). The funders had no role in study design, data collection and analysis, decision to publish, or preparation of the manuscript.

**Competing Interests:** The authors have declared that no competing interests exist.

\* Email: angela.ivask@kbfi.ee (AI); anne.kahru@kbfi.ee (AK)

## Introduction

The novel properties of man-made nanoparticles (NPs), i.e., particles having at least one dimension between 1–100 nm, are attributed to their small size, increased specific surface area and concomitant surface display of their constituent atoms. These properties in turn translate into higher surface reactivity and display of new electronic, optical, quantum mechanical and magnetic properties of nanosize particles. The physico-chemical properties that are responsible for technological breakthroughs could also lead to increased bioavailability and toxicity of engineered NPs compared to corresponding microsize compounds [1]. Although some types of the nanomaterials are already produced in industrial amounts, the data on their toxicological implications are just emerging [2].

As the main concept of nanotechnologies lies in specific “nano” effects of small sized particulates, it is reasonable to assume that size-dependent biological effects, e.g. toxicity, within the nano-scale range (i.e. between 1–100 nm) could also be proven by appropriate experiments. According to Thomson Reuters ISI WoS, since 1990 the number of papers on toxic effects of NPs has rapidly increased and currently about 3500 papers are published on that theme annually. The papers focusing specifically on size-dependent toxic effects started to emerge about 15 years later and are still relatively rare (Figure S1). In total, the search (see SI) term “size-dependent toxic\* AND nano\*” yielded altogether about 200 papers. Currently, most of the studies that report higher toxicity of NPs compared to their microsize counterparts have been conducted by comparing nano-and microsize particles, mostly metal oxides and/or silver. As an example, the remarkable

difference between toxicity of nano- and microsize CuO has been demonstrated in case of bacteria, algae, crustaceans, ciliates, fish, yeasts and nematodes: CuO NPs were shown to be 16-fold more toxic to algae and 48-fold more toxic to crustaceans than microsize CuO [3]. On the other hand, ZnO NPs and microsize ZnO were of comparable toxicity for the above described organism groups [3] which may be due to significant release of Zn ions from ZnO particles (for review, see [4]).

In addition to the comparisons between micro- and nanosize compounds, there are already some (mostly recent) studies where the toxicity of small “libraries” of NPs (mostly metal oxides or silver) of different sizes has been evaluated (Table 1, Figure S2). It is interesting to note, that although the majority of the results prove the hypothesis of toxicity increase with decreased particle size there are also experimental data showing that smaller NPs either were less toxic or, of no size-dependent toxicity (Table 1). One reason for these contradictory data could be that the NPs used for the toxicity tests are not usually monodisperse so theoretically, causing toxic effects of different magnitude. Due to the scarcity of experimental data on size-specific toxic effects (Figure S1) and contradictory experimental results obtained so far (Table 1), it is not surprising that there is no clear understanding of the effects of particle size on toxicity and no consensus exists on nano-threshold in (eco)toxicity [5]. Consequently, nanoparticle (NP) size has not been included as an important parameter in toxicity prediction models (QSAR or QNAR models) [6] and if NP size is bigger than 15–20 nm, it is not considered to be an important variable in determining their biological effects [7] [8]. This suggests that 15 nm could be considered as the maximum size for the “NP” of biological impact. Indeed, the nanotoxicity threshold at about 10 nm was also experimentally demonstrated by De Jong et al. [9], who showed that among gold NPs with primary particle sizes of 10, 50, 100 and 250 nm, only 10 nm particles were distributed in almost all organ systems, such as blood, liver, spleen, kidney, testis, thymus, heart, lung and brain after intravenous administration. Yet, given the scarcity of data, it is vital that more high quality experimental data will be available to improve the understanding on size-related biological effects of NPs.

The aim of the current paper was to generate and analyze a homogenous set of experimental toxicity data on silver NPs (Ag NPs) with similar coating (citrate) but of five different sizes ranging from 10 to 80 nm. Silver NPs were chosen for several reasons: (i) they are currently the NPs of the widest application area (e.g., as antimicrobials in medical equipment coatings, cosmetic products, textiles, sprays [10]; with the estimated global annual production of 22 tons [11]; (ii) among three biocidal NPs (CuO, ZnO and Ag), so far Ag NPs were shown to be the most toxic especially to crustaceans and algae (Table S1) – important representatives of the aquatic food webs [4]; (iii) there is a lack of comparable good quality toxicity data on Ag NPs (see the variability in currently available toxicity data in Table 1 and in Figure S3). In this paper, we present toxicity values of 10, 20, 40, 60 and 80 nm Ag NPs for bacteria *Escherichia coli* and *Pseudomonas fluorescens*, yeast *Saccharomyces cerevisiae*, algae *Pseudokirchneriella subcapitata*, crustacean *Daphnia magna* and murine fibroblast cell line Balb/3T3. We suggest that experiments conducted in the same laboratory using a well characterized library of monodisperse Ag NPs provide meaningful information on mechanisms of toxic action relating to different primary size of NPs and may be used as an input for quantitative toxicity modelling.

## Materials and Methods

### Chemicals

All the purchased chemicals were at least of analytical grade. Media components: yeast extract, tryptone, agar were from Lab M (Lancashire, UK) and peptone was from BD. Phosphate buffered saline (PBS), Dulbecco's Modified Eagle's Medium (DMEM) with high glucose content (4.5 g/L), Newborn calf serum (NBCS) and the mixture of penicillin and streptomycin (10 000 U/mL or 10 000 µg/mL, respectively) were purchased from Life Technologies. Neutral red (NR) was from Applichem. AgNO<sub>3</sub> was purchased as 0.1 M solution from Fluka, 2,7- dichlorodihydrofluorescein diacetate from Invitrogen. Ultrapure water (UP water, pH 5.6±0.1) from MilliQ equipment (18 MΩ) was used throughout the study.

### Characteristics of the studied Ag nanoparticles

The characterisation and testing procedure is schematically depicted in Figure S4. Monodisperse Ag NP suspensions were purchased from MK Nano (Mississauga, Canada). According to the manufacturer, the NPs were stabilized with 2 mg/L of citrate and were supplied at 50–100 mg/L of Ag, in primary sizes of 10, 20, 40, 60 and 80 nm. Ag content in NP suspensions was determined by digestion in 1% HNO<sub>3</sub> using Elan DRC Plus ICP-MS (Perkin Elmer). The morphology and the size of the particles were evaluated using transmission electron microscope (TEM) FEI-Philips Tecnai 10 operating at 80 kV and scanning electron microscope (SEM) FEI Helios NanoLab 600 (equipped with energy-dispersive X-ray spectroscopy (EDX) function) with accelerating voltage of 10 kV. Drops of aqueous Ag NP suspensions were placed onto Formvar/Carbon Coated copper-grids and silicon wafers for TEM and SEM/EDX analysis, respectively. The samples were allowed to dry at ambient conditions *prior* to imaging. EDX mapping was conducted using primary electron beam with acceleration voltage of 10 kV to detect Ag L $\alpha$  X-ray fluorescence (2.98 keV). Particles on the obtained images were measured using ImageJ software [12]; average primary particle diameter was calculated from 20–30 particles.

Hydrodynamic diameter and surface charge ( $\zeta$ -potential) of the Ag NPs (5–8 mg/L) in UP water and in test media used for bioassays were measured using Malvern Zetasizer (Nano-ZS, Malvern Instruments, UK). The pH of the purchased NP suspensions was determined by Thermo Orion 9863BN Micro pH Electrode (Thermo Scientific). UV-Vis absorption spectra of the Ag NPs were analysed on transparent 96-well polystyrene microplates (Greiner Bio-One) using plate spectrophotometer Multiskan (Thermo Scientific) at 300–800 nm wavelengths. Sedimentation of particles was determined by measuring 1 mL of NP suspensions in 1 cm polystyrene cuvettes over time (every 30 seconds from 0 till 60 minutes) using the Multiskan spectrophotometer at 420 nm.

To analyze the dissolution of Ag NPs in UP water, OECD 202 artificial freshwater (AFW) or algal growth medium (OECD 201), 1 mg Ag/L suspensions of Ag NPs or 0.01 mg Ag/L solution of AgNO<sub>3</sub> (ionic control) in these media were incubated for 4, 24, 48 or 72 hours, respectively (the incubation time was selected according to the respective toxicity test protocol, see below). To analyze Ag NPs dissolution in mammalian cell culture medium, 10 mg Ag/L suspensions of Ag NPs or 1 mg Ag/L suspension of AgNO<sub>3</sub> in cell culture medium were incubated for 24 hours. No test organisms/cells were used in dissolution experiments. Concentrations of Ag NPs or AgNO<sub>3</sub> for the dissolution experiments were chosen according to the approximate EC<sub>50</sub> values for

**Table 1.** Summary of currently available nanoparticle size-related toxicity data for selected (eco)toxicological test organisms.

Nanoparticles (size)	Toxicity endpoint and the test organisms	Results	Additional (mechanistic) information provided	Reference
<b>PAPERS SHOWING HIGHER TOXICITY OF SMALLER PARTICLES</b>				
<b>BACTERIA</b>				
Gallic-acid stabilised Ag NPs (7 nm and 29 nm)	Antibacterial properties; <i>Escherichia coli</i> and <i>Staphylococcus aureus</i>	MIC of 7 nm NPs was 6.25 mg/L ( <i>E. coli</i> ) and 7.5 mg/L ( <i>S. aureus</i> ); 29 nm particles were less potent; MIC = 13 mg/L ( <i>E. coli</i> ) and 17 mg/L ( <i>S. aureus</i> ).	n.a.	[42]
PVP-Ag NPs (mean sizes 5, 15 and 55 nm)	Antibacterial properties; five anaerobic oral pathogenic bacteria and aerobic bacteria <i>Escherichia coli</i>	For anaerobic bacteria, 5 nm particles were most effective (MIC 25 mg/L). Also for <i>E. coli</i> : 5 nm the most effective (MIC 6 mg/L)	The higher toxicity in aerobic conditions compared to anaerobiosis may be due to higher release of Ag <sup>+</sup> from Ag NPs.	[43]
Ag NPs (20, 50, 110 nm)	Viability, bacteria <i>Escherichia coli</i>	Viability of <i>E. coli</i> depended on particle size (dose-dependent response)	Dissolution of Ag ions from the surface of the particles causing toxicity.	[44]
<b>BACTERIA AND CRUSTACEANS</b>				
Ag NPs (Branched PEI-coated 10 ± 4.6 nm; citrate-coated 56 ± 14 nm; PVP-coated 72 ± 24 nm)	3 h inhibition of β-galactosidase, <i>Escherichia coli</i> ; Acute toxicity (48 h immobilisation), <i>Daphnia magna</i>	Particle size, surface charge, and concentration dependent toxicity for both the test organisms was shown (AgNO <sub>3</sub> > BPEI-Ag NP > Citrate-Ag NP > PVP-Ag NP). The 48 h LC <sub>50</sub> values for <i>D. magna</i> were 0.41 μg/L (BPEI-Ag NPs), 2.88 (citrate Ag NPs), and 4.79 μg/L (PVP Ag NPs), the enzyme inhibition endpoint ( <i>E. coli</i> assay) showed EC <sub>50</sub> values of 305, 791 and 2040 μg/L, respectively.	Bacteria <i>E. coli</i> : negligible contribution of dissolved Ag ion to the observed toxicity of Ag NPs.	[45]
<b>CRUSTACEANS</b>				
ZnO NPs (30 nm and 80–100 nm) and ZnO microsized particles (>200 nm)	Feeding inhibition, 48 h immobilisation and reproduction of <i>Daphnia magna</i>	The 48-h LC <sub>50</sub> for immobilization ranged between 0.76 mg Zn L <sup>-1</sup> for the ionic zinc and 1.32 mg Zn L <sup>-1</sup> for ZnO NPs of 80 nm to 100 nm.	Toxicity was explained by solubilised ions (endpoints: immobilisation, reproduction)	[46]
<b>MAMMALIAN CELLS</b>				
Ag NPs (10, 40 and 75 nm citrate coated, 10, 50 PVP coated)	Cytotoxicity (lactate dehydrogenase release and Alamar blue staining)	Only 10 nm Ag NPs, regardless of coating, were toxic to human lung cells BEAS-2B.	Toxicity of 10 nm particles was due to particle uptake and subsequent intracellular release of Ag <sup>+</sup> ions	[28]
Ag NPs (20 and 110 nm PVP coated, 20 and 1000 nm citrate coated)	Cytotoxicity (MTS assay) and cellular uptake	Smaller NPs were more toxic and were taken up by BEAS-2B cells more efficiently than larger particles	Higher toxicity of smaller particles was due to higher specific surface area and consequently, dissolution	[47]
<b>PAPERS SHOWING LOWER TOXICITY OF SMALLER PARTICLES</b>				
<b>BACTERIA</b>				
Dextrose-encapsulated Au NPs (25, 60, and 120 nm ± 5 nm)	Antibacterial properties (effect on the growth, morphology and ultrastructural properties) to Gram-negative ( <i>E. coli</i> ) and Gram-positive bacteria ( <i>Staphylococcus epidermidis</i> )	Both 120-nm and 60-nm gold NPs inhibited the proliferation of <i>E. coli</i> in a concentration-dependent manner with MIC of 16 · 10 <sup>10</sup> and 16 · 10 <sup>11</sup> NPs/mL, respectively. The 25-nm NPs did not significantly affect the proliferation of <i>E. coli</i> even at concentration as high as 128 · 10 <sup>11</sup> NPs/mL.	Bactericidal activity was mediated via disruption of the bacterial cell membrane which led to the leakage of cytoplasmic content.	[48]
<b>PAPERS SHOWING NO EVIDENT SIZE-DEPENDENT TOXICITY</b>				
<b>BACTERIA</b>				
SiO <sub>2</sub> NPs (15, 50 and 500 nm)	Antibacterial properties, <i>Bacillus subtilis</i> , <i>B. megaterium</i> , <i>E. coli</i> K12, <i>Listeria innocua</i> and <i>Pseudomonas fluorescens</i> .	No correlation between the size of SiO <sub>2</sub> particles and effect on bacterial viability.		[49]

Table 1. Cont.

Nanoparticles (size)	Toxicity endpoint and the test organisms	Results	Additional (mechanistic) information provided	Reference
CeO <sub>2</sub> NPs (<25 nm (N25), <50 nm (N50), N10, N60); microsize CeO <sub>2</sub> (<5000 nm) (N50)	<b>CYANOBACTERIA AND ALGAE</b> Inhibition of the self-luminescence, cyanobacterial recombinant strain <i>Anabaena</i> CP94337. Inhibition of the growth, green alga <i>Pseudokirchneriella subcapitata</i>	<i>Anabaena</i> : 24 h EC <sub>50</sub> from 0.27 to 6.3 mg/L; <i>P. subcapitata</i> : 72 h EC <sub>50</sub> 2.4–29.6 mg/L. Algae: N50 was most toxic (EC <sub>50</sub> <1 mg/L; growth measured by OD). Order of the toxicity was N50 > N25 > N60 > N10 > B5000. Also, for <i>Anabaena</i> N50 was the most toxic NP (EC <sub>50</sub> <1 mg/L). Both organisms: no obvious relationship between primary size and toxic effect.	Uptake of NPs was not observed. Direct contact between NPs and cells was a prerequisite for toxic effect.	[50]
Ag NPs (20, 50, 110 nm)	<b>FISH</b> Mortality, abnormal motility, zebrafish <i>Danio rerio</i>	NP-size-dependent response did not manifest in zebrafish when observing mortality for all Ag NP treatments	20 nm Ag NPs elicited the highest incidence of(44) abnormal motility and induced slower development.	

n.a. – not available.  
doi:10.1371/journal.pone.0102108.t001

different test organisms in the respective media. After incubation, dissolved Ag species were separated from particulate matter by ultracentrifugation at 390 000 g for 30 min (Beckman-Coulter ultracentrifuge L8-55 M) and dissolved Ag was determined from supernatants using GF-AAS in a certified laboratory of Tallinn University of Technology, Estonia, applying the standard EVS-EN ISO/IEC 17025:2005. According to the calculations, under these conditions all Ag NPs and Ag-protein complexes with the molecular mass above 5 kDa should settle [13]. To prove that the majority of NPs had been removed by 30-min centrifugation at 390 000 g, the supernatants were also analysed using single particle (SP)-ICP-MS *via* an Elan DRC Plus (Perkin Elmer). By parallel analysis of the supernatant of the centrifuged NP suspensions and NP suspensions, very dilute original NP suspensions (5, 10, 50 and 100 pg/mL) and comparing the data with appropriate standards for Ag NPs (BBI, Cardiff, UK), it was possible to calculate the concentration of NPs in the centrifuged extracts. The data were evaluated, using the algorithm essentially by Peters et al. [14]. Clearly, the centrifugation had removed 99.4–99.9% of NPs and only 0.6, 0.15 and 0.02% of particles was present in supernatants of Ag 10, 20 and 80 nm NPs, respectively.

### Toxicity tests

**4 h acute toxicity assay using bacteria and yeast.** The inhibitory effects of aqueous (prepared in UP water) suspensions of Ag NPs to bacteria *Escherichia coli* K12 (BW30270 from *E. coli* genetic stock Center, Yale University), *Pseudomonas fluorescens* OSB [15] or *Saccharomyces cerevisiae* BY4741 from EURO-SCARF collection (Institute of Microbiology, University of Frankfurt, Germany) was analysed. As a toxicity endpoint, the colony-forming ability of silver-exposed bacteria/yeast cells on agarized growth medium was used.

To start the microbial culture for the toxicity test, one colony was transferred from the agar plates to liquid growth medium and incubated overnight (30°C, 200 rpm). For growing the bacteria, NaCl-free LB medium (5 g/L yeast extract and 10 g/L tryptone; pH 7) and for yeast YPD medium (10 g/L of yeast extract, 20 g/L of peptone, 20 g/L of glucose; pH 6.6±0.1) was used. After overnight incubation, bacterial and yeast cultures were diluted 1:50 into fresh medium and cultivated till the logarithmic growth phase. Then the cells were washed twice with UP water by centrifugation at 3500 g for 10 min and resuspended in UP water. The density of the microbial cell suspension in UP water was adjusted to 2–3·10<sup>7</sup> cells/mL and used for the toxicity assays. For that, 100 µL of Ag NPs or AgNO<sub>3</sub> dilution in UP water was first pipetted into microplate wells and then 100 µL of microbial suspension in UP water was added. The test plates with cells and chemicals were incubated at room temperature for 4 hours. Thereafter step-wise decimal dilutions from 10<sup>1</sup> till 10<sup>7</sup> from the exposed microbial cultures were prepared and 10–15 µL of such prepared solution was pipetted onto LB (bacterial assays) or YPD agar plate (yeast assay). To prepare agar plates, 1.5% agar was added to the bacterial and yeast growth media described above. The inoculated agar plates were incubated for 24–30 hours (bacterial assays) or for 48 hours (yeast assay) at 30°C and the grown colonies were counted. Colony forming units (CFU) per mL were calculated and EC<sub>50</sub> values for Ag NPs and AgNO<sub>3</sub> were calculated using GraphPad Prism program (GraphPad Software, Inc., USA) or Excel Macro Regtox [10]. To ensure that the exposure of bacterial/yeast cells in UP water for 4 hours had no influence on the viability of the cells we also determined the CFU values of non-exposed controls at the beginning and at the end of the 4-hour incubation period in UP water. No significant reduction of microbial cell numbers (CFU) was observed except

for *E. coli* where the CFU/mL slightly decreased (from  $3.2 \cdot 10^7$  to  $2.6 \cdot 10^7$  i.e., by 18% upon 4-hour exposure).

**24 h cytotoxicity assay with mammalian fibroblasts.** The inhibitory effect of Ag NPs and AgNO<sub>3</sub> to murine fibroblasts Balb/3T3 (ATCC CCL-163) was analyzed using a Neutral Red (NR) assay. The cells were first grown in DMEM medium supplemented with 10% Newborn Calf Serum (NBCS), 100 U/mL penicillin and 100 µg/mL streptomycin mixture at 37°C and 5% CO<sub>2</sub> till approximately 70% confluency. Then the cells were replated to transparent 96-well plates (5000 cells and 100 µL of cell culture medium per well) and further grown for 24 h at 37°C and 5% CO<sub>2</sub>. Next, the culture medium was removed and 100 µL of Ag NPs or AgNO<sub>3</sub> diluted in fresh culture medium was added to the cells and the plates were incubated for 24 h at 37°C and 5% CO<sub>2</sub>. The plate was emptied again, the cells were washed with PBS and 100 µL of neutral red (NR) 5 mg/L solution in cell culture medium was added to all the wells. The plate was incubated for 3 h at 37°C and 5% CO<sub>2</sub> and NR reagent was removed. The plate was washed with PBS and 100 µL of NR dilution reagent (50% ethanol, 1% glacial acetic acid) was added to the wells. This was followed by shaking the plate for 30 min at room temperature and measuring the absorbance at 540 nm using the plate reader Multiskan (Thermo Scientific). Abiotic values (NPs without fibroblasts) were always subtracted from the results obtained with Balb/3T3 cells. EC<sub>50</sub> was calculated using GraphPad Software. Sodium dodecyl sulphate (SDS) was included every time in the assay as a positive control.

**72 h growth inhibition assay with algae *Pseudokirchneriella subcapitata*.** In general the OECD 201 algal growth inhibition test protocol was followed. The algal test medium

(OECD 201; 15 mg NH<sub>4</sub>Cl, 12 mg MgCl<sub>2</sub>·6H<sub>2</sub>O, 18 mg CaCl<sub>2</sub>·2H<sub>2</sub>O, 15 mg MgSO<sub>4</sub>·7H<sub>2</sub>O, 1.6 mg KH<sub>2</sub>PO<sub>4</sub>, 0.08 mg FeCl<sub>3</sub>·6H<sub>2</sub>O, 0.1 mg Na<sub>2</sub>EDTA·2H<sub>2</sub>O, 0.185 mg H<sub>3</sub>BO<sub>3</sub>, 0.415 mg MnCl<sub>2</sub>·4H<sub>2</sub>O, 0.003 mg ZnCl<sub>2</sub>, 0.0015 mg CoCl<sub>2</sub>·6H<sub>2</sub>O, 0.00001 mg CuCl<sub>2</sub>·2H<sub>2</sub>O, 0.007 mg Na<sub>2</sub>MoO<sub>4</sub>·2H<sub>2</sub>O and 50 mg NaHCO<sub>3</sub> per L; pH 8) was used. The *Pseudokirchneriella subcapitata* stock culture for the inoculation originated from the commercial test system Algal Toxkit F (MicroBioTests Inc., Nazareth, Belgium). 5 mL of algal test medium or Ag NP or AgNO<sub>3</sub> dilutions in the algal test medium were inoculated with exponentially growing algal cells. The number of algae in the inoculum was counted under the microscope in the Neubauer haemocytometer and adjusted to yield 10 000 cells/mL in the sample after inoculation. For the assay, the algae were incubated in 20-mL glass vials on a transparent shaking table and constantly illuminated from below with Philips TL-D 38 W aquarelle fluorescent tubes at  $24 \pm 1^\circ\text{C}$  for 72 h. Only the bottoms of the vials received light with illuminance of  $15 \text{ klx} \pm 2 \text{ klx}$ . During the 72 h the concentration of algal cells in the control culture increased at least 16 times and the pH did not change more than by 0.5 units. The algal biomass measurements were performed at least daily. The biomass was measured by chlorophyll fluorescence as described by Arooja et al. [16]. Briefly, 50 µL of culture samples were transferred to 96-well plate, 200 µL of ethanol was added to each well and the plate was shaken for 3 h in the dark. Thereafter the fluorescence was measured with microplate fluorometer (excitation 440 nm, emission 670 nm; Fluoroskan Ascent, Thermo Labsystems, Finland). All the assays were run twice and each sample was analysed in duplicate with eight controls distributed evenly across the transpar-

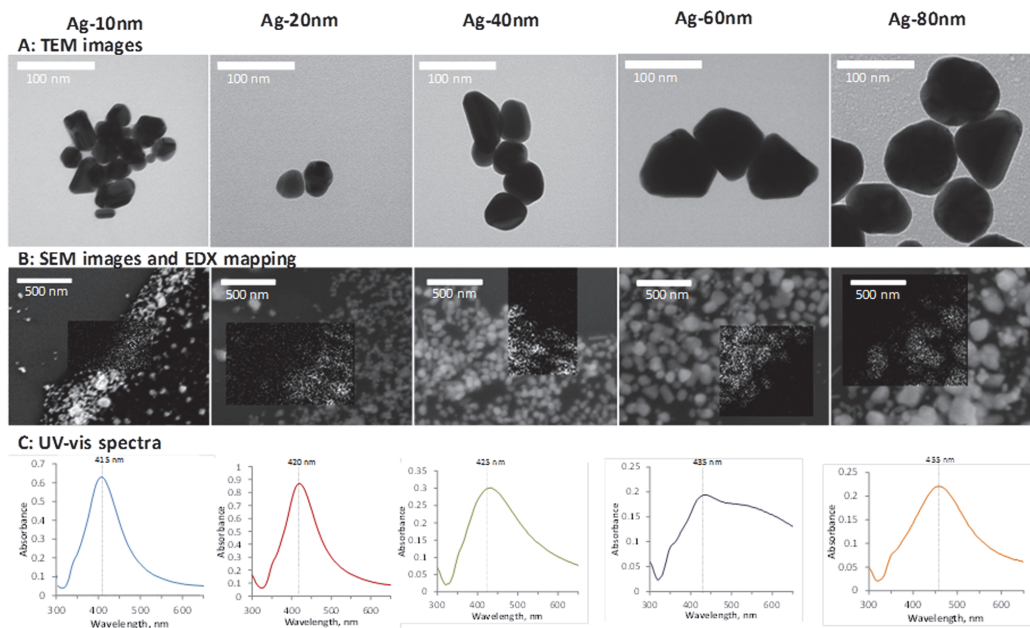


**Figure 1. Electron microscopy images and UV-Vis absorption spectra of the studied citrate-stabilised Ag nanoparticles.** A: TEM photos of the particles; B: SEM photos with EDX mapping; C: UV-Vis absorption spectra (Ag-10 nm 8 mg/L, Ag-20 nm 11 mg/L, Ag-40 nm, Ag-60 nm and Ag-80 nm 5 mg/L in ultrapure (UP) water. Maximum absorption is indicated with a vertical dotted line; wide absorption spectrum indicates polydispersity of the sample. doi:10.1371/journal.pone.0102108.g001

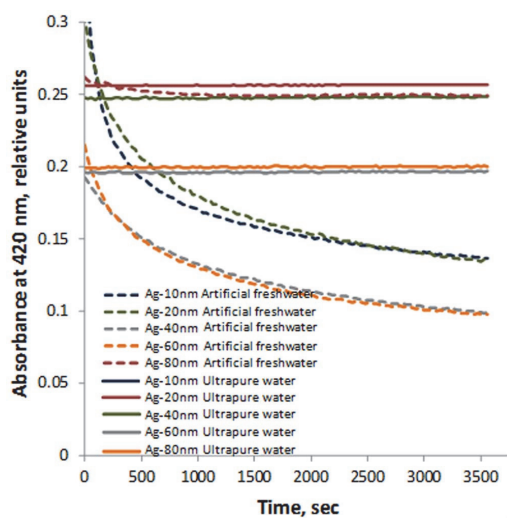


**Figure 2. Sedimentation of Ag NPs in ultrapure water and in artificial freshwater during 60 min.** Concentrations of Ag NPs were: Ag-10 nm 8 mg/L, Ag-20 nm 11 mg/L, Ag-40 nm, Ag-60 nm and Ag-80 nm 5 mg/L. Decreased absorption of light (420 nm) by Ag particles in artificial freshwater (test medium for *D. magna*) (dotted line) is due to settling over time. In ultrapure water (solid line) no decrease in absorption was observed.  
doi:10.1371/journal.pone.0102108.g002

ent table. EC<sub>50</sub> values were calculated using Excel Macro Regtox [10].

**48 h acute toxicity assay with crustacean *Daphnia magna* (immobilization test).** The acute toxicity assay with crustacean *Daphnia magna* was performed according to OECD 202 guideline. Deviating from the standard test procedure, *D. magna* neonates used in the test were not originating from the laboratory culture but were hatched from the dormant “eggs” (ephippia) purchased from MicroBioTests Inc. (Nazareth, Belgium) prior to testing. OECD 202 artificial freshwater (AFW) containing 294 mg CaCl<sub>2</sub>·2H<sub>2</sub>O, 123.25 mg MgSO<sub>4</sub>·7H<sub>2</sub>O, 64.75 mg NaHCO<sub>3</sub>, 5.75 mg KCl per L, pH = 7.8 ± 0.2 was used as the control medium as well as the diluent for Ag NPs and AgNO<sub>3</sub>. Five *D. magna* neonates (less than 24 h old) were added to 10 ml of test sample and each concentration was analysed in four replicates, i.e. in total, 20 neonates per concentration were used. Test vessels with the exposed neonates were incubated in the dark at 20°C for 48 hours. The immobilization of the crustaceans was recorded after 24 and 48 h. The daphnids not able to swim within 15 seconds after gentle agitation of the test medium were considered immobilized (dead). EC<sub>50</sub> values were calculated using GraphPad Prism program. Each NP/chemical was analyzed in at least two independent experiments.

**Analysis of the bioavailable fraction of the studied silver preparations to recombinant *Escherichia coli* Ag-sensor.** Bioavailability of Ag was analyzed by sensor bacteria *Escherichia coli* MC1061(pSLcucR/pDNPcopAlux), which is a Cu- and Ag-induced recombinant bioluminescent bacterium [17]. Bioluminescent response of this bacterium is mediated via Ag and Cu binding CueR protein which in the presence of intracellular silver or copper ions activates bioluminescence encoding genes and thus leads to an increase in light output. This increase in

**Table 2. Physico-chemical characteristics of the studied citrate-stabilised Ag nanoparticles.**

Ag NPs	pH <sup>a</sup>	Primary size, nm	N° of particles/mL <sup>d</sup>	Hydrodynamic size, nm (pdi)			ζ-potential, mV				
				UP water <sup>e</sup>	AFW <sup>f</sup>	Algal growth medium <sup>g</sup>	UP water <sup>e</sup>	AFW <sup>f</sup>	Cell culture medium <sup>g</sup>		
Ag-10 nm	7.7	11.6 ± 5.2	13	2.3 · 10 <sup>11</sup>	6.00 (0.48)	n.a.*	9.70 (0.49)	68.6 (0.29)	-25	-20	-9.59
Ag-20 nm	8.1	17.8 ± 8	17	2.3 · 10 <sup>10</sup>	11.0 (0.43)	n.a.*	14.00 (0.43)	76.0 (0.31)	-25	-15	-10.0
Ag-40 nm	7.2	47.7 ± 8	n.a.	n.a.	16.0 (0.28)	n.a.*	17.20 (0.28)	107 (0.26)	-24	-19	-4.84
Ag-60 nm	7.2	56.5 ± 9.6	n.a.	n.a.	58.0 (0.25)	n.a.*	110 (0.22)	162 (0.14)	-15	-18	-8.29
Ag-80 nm	7.1	94.8 ± 54	74	6 · 10 <sup>7</sup>	68.0 (0.30)	n.a.*	89.0 (0.25)	153 (0.23)	-16	-15	-9.20

<sup>a</sup>measured from Ag NPs stock suspension.  
<sup>b</sup>measured from SEM images, 20–30 particles (see also Figure 1).  
<sup>c</sup>according to single particle (SP)ICP-MS.  
<sup>d</sup>measured using SP-ICP-MS.  
<sup>e</sup>UP water – ultrapure water.  
<sup>f</sup>AFW – OECD 202 artificial freshwater used as test medium for crustaceans *Daphnia magna*.  
<sup>g</sup>DMEM (cell culture medium) with 10% NBSC.  
 pdi – polydispersity index.  
 n.a. not available.  
 \* the samples were too polydispersed.  
 doi:10.1371/journal.pone.0102108.t002

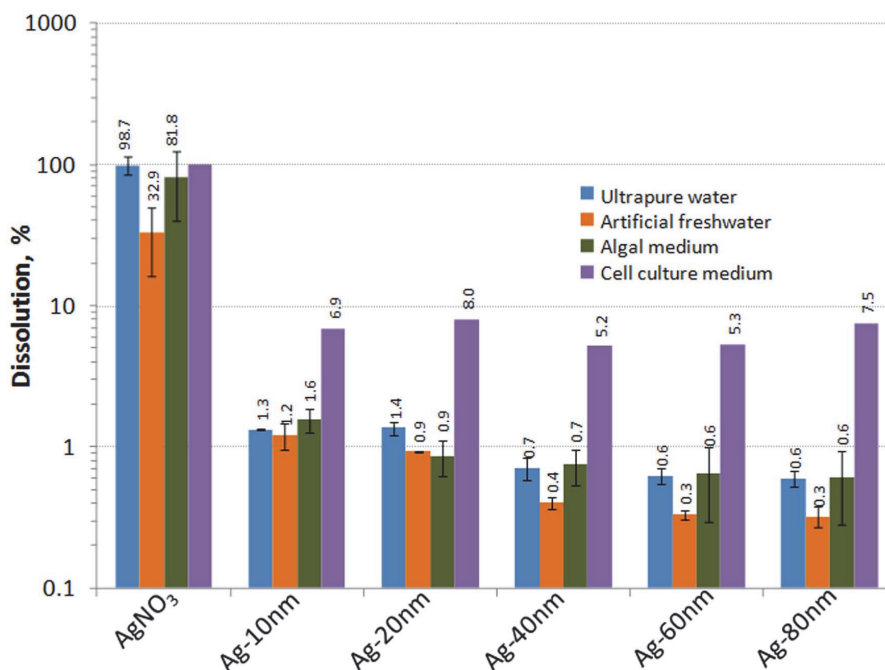


**Figure 3. Dissolution (%) of Ag NPs in different test media.** Ultrapure water was used as a solvent to mimic the dissolution in the bacterial and yeast assays, OECD 202 artificial freshwater was used for *Daphnia magna* assay, algal test medium for *Pseudokirchneriella subcapitata* and cell culture medium for Balb/3T3 murine fibroblast assay. Dissolved ionic Ag was measured after incubation of 1 mg/L Ag NPs or 0.01 mg/L AgNO<sub>3</sub> for 4 hours (ultrapure water), 24 hours (cell culture medium), 48 hours (artificial freshwater) or 72 hours (algal medium), depending on the length of the toxicity assay. The results shown were measured from Ag NPs suspensions and AgNO<sub>3</sub> solution after ultracentrifugation. These results were confirmed by single particle (SP)-ICP-MS according to which 1.4% of 10 nm Ag NPs, 1% of 20 nm Ag NPs and 0.5% of 10 nm Ag NPs had been dissolved in ultrapure water.

doi:10.1371/journal.pone.0102108.g003

bioluminescence is concentration dependent and allows to calculate the amount of intracellular silver or copper ions [17]. Prior to analysis, sensor bacteria were cultivated overnight in NaCl-free LB medium (see above) with 10 µg/mL of tetracycline and 100 µg/mL of ampicillin. This was followed by 1:50 dilution using new medium and sensor bacteria were further cultivated till logarithmic growth phase and then washed twice with UP water using centrifugation at 3500 g. The final number of sensor bacterial cells in the test was 10<sup>7</sup>/mL. For the bioavailability assay, 100 µL of Ag NPs or AgNO<sub>3</sub> dilution in UP water was pipetted into the wells of a white 96-well microplate and then 100 µL of sensor bacteria suspension was added automatically by Luminometer Orion II (Berthold Detection Systems). Bioluminescence of the sensor bacteria was continuously registered during the first 10 sec of incubation and then once after 20 min and 4 hours of incubation. Bioluminescence induction of the bacteria was calculated as follows:

$$\text{Induction(fold)} = \text{RLU}_{\text{SAMPLE}} / \text{RLU}_{\text{BACKGROUND}}$$

where RLU<sub>SAMPLE</sub> is the bioluminescence of Ag-biosensor cells in the test sample (Ag-preparations in UP water) at the specified timepoint and RLU<sub>BACKGROUND</sub> is the bacterial bioluminescence in UP water at the same time point. 2-fold induction was

considered significant and was used in intracellular bioavailability calculations. Intracellular Ag was determined by using the log-log linear regression equations derived from the linear region of the dose-response curves of Ag-biosensor to AgNO<sub>3</sub> and Ag NPs, whereas AgNO<sub>3</sub> was considered 100% bioavailable and used as a standard. Each experiment was performed on two different days.

**Analysis of the formation of abiotic reactive oxygen species (ROS) by the studied Ag formulations.** To determine abiotic ROS, a procedure published by Priester et al. [18] was essentially followed. Briefly, 2,7-dichlorofluorescein diacetate (H<sub>2</sub>DCFDA) was dissolved in ethanol at 5 mM. 0.5 mL of 2,7-H<sub>2</sub>DCFDA was mixed with 10 mL of NaOH (final concentration 0.01 N) and incubated for 30 minutes in the dark. Then 40 mL of 25 mM sodium phosphate buffer (pH 7.2) was added and the mixture was further kept on ice. The final concentration of 2,7-H<sub>2</sub>DCFDA in the mixture was 0.05 mM. 80 µL of AgNO<sub>3</sub> or Ag NPs suspension in UP water was pipetted into 96-well black microplate and 150 µL of the dye mixture was added. The fluorescence (excitation/emission = 485/528 ± 20 nm) was measured immediately and after 1 hour using Fluoroskan plate reader (Thermo Scientific). Increase in dye fluorescence was calculated using the following formula:

**Table 3.** Nominal, dissolution- and bioavailability-corrected EC<sub>50</sub> values (mg Ag/L) of different sized Ag NPs and ionic AgNO<sub>3</sub> for various test organisms.

	Nominal EC <sub>50</sub>	EC <sub>50</sub> corrected to Ag dissolution <sup>a</sup>	EC <sub>50</sub> corrected to Ag bioavailability <sup>b</sup>
<b>Bacteria</b> (4 h; UP water; colony forming ability on agarised LB medium)			
<i>Escherichia coli</i>			
AgNO <sub>3</sub>	0.01±0.004	0.010±0.004	0.010±0.004
Ag-10 nm	0.27±0.2	0.004±0.0026	0.012±0.00011
Ag-20 nm	0.51±0.24	0.006±0.003	0.016±0.00009
Ag-40 nm	1.51±1.12	0.012±0.0091	0.016±0.0001
Ag-60 nm	2.56±1.6	0.017±0.011	0.020±0.00009
Ag-80 nm	2.96±1.83	0.019±0.012	0.020±0.00008
Average (for AgNPs):	1.56	0.011	0.016
<i>Pseudomonas fluorescens</i>			
AgNO <sub>3</sub>	0.02±0.007	0.02±0.007	0.02±0.007
Ag-10 nm	0.55±0.22	0.007±0.003	0.024±0.0009
Ag-20 nm	0.99±0.4	0.013±0.005	0.030±0.002
Ag-40 nm	2.12±1.11	0.015±0.008	0.022±0.005
Ag-60 nm	3.81±1.22	0.023±0.008	0.030±0.006
Ag-80 nm	5.25±1.82	0.031±0.01	0.035±0.009
Average (for AgNPs):	2.54	0.018	0.028
<b>Yeast</b> <i>Saccharomyces cerevisiae</i> (4 h; UP water; colony forming ability on agarised YPD medium)			
AgNO <sub>3</sub>	0.023±0.004	0.023±0.004	not calculated <sup>c</sup>
Ag-10 nm	1.53±0.51	0.016±0.0053	not calculated <sup>c</sup>
Ag-20 nm	2.72±0.8	0.029±0.0084	not calculated <sup>c</sup>
Ag-40 nm	7.28±2.42	0.049±0.163	not calculated <sup>c</sup>
Ag-60 nm	7.33±1.5	0.042±0.0085	not calculated <sup>c</sup>
Ag-80 nm	8.17±2.59	0.044±0.014	not calculated <sup>c</sup>
Average (for AgNPs):	5.4	0.036	not calculated <sup>c</sup>
<b>Algae</b> <i>Pseudokirchneriella subcapitata</i> (72 h; algal growth medium; growth inhibition)			
AgNO <sub>3</sub>	0.007±0.002	0.007±0.0023	not calculated <sup>c</sup>
Ag-10 nm	0.18±0.06	0.002±0.0009	not calculated <sup>c</sup>
Ag-20 nm	0.52±0.36	0.005±0.0037	not calculated <sup>c</sup>
Ag-40 nm	0.82±0.25	0.007±0.0022	not calculated <sup>c</sup>
Ag-60 nm	0.94±0.49	0.009±0.0044	not calculated <sup>c</sup>
Ag-80 nm	1.14±0.32	0.010±0.0027	not calculated <sup>c</sup>
Average (for AgNPs):	0.72	0.0067	not calculated <sup>c</sup>
<b>Crustacean</b> <i>Daphnia magna</i> (48 h; artificial freshwater; immobilisation of neonates)			
AgNO <sub>3</sub>	0.002±0.001	0.00039±0.00012	not calculated <sup>c</sup>
Ag-10 nm	0.010±0.014	0.00014±0.00006	not calculated <sup>c</sup>
Ag-20 nm	0.034±0.01	0.00031±0.00009	not calculated <sup>c</sup>
Ag-40 nm	0.141	0.00060	not calculated <sup>c</sup>
Ag-60 nm	0.168±0.0073	0.00053±0.00013	not calculated <sup>c</sup>
Ag-80 nm	0.218	0.00062	not calculated <sup>c</sup>
Average (for AgNPs):	0.11	0.0004	not calculated <sup>c</sup>
<b>Mammalian cells:</b> murine fibroblast line BALB/3T3 (24 h; DMEM with 10% NBCS; viability)			
AgNO <sub>3</sub>	1.7±0.57	1.70±0.58	not calculated <sup>c</sup>
Ag-10 nm	16.9±1.9	1.18±0.14	not calculated <sup>c</sup>
Ag-20 nm	22.0±1.3	1.76±0.11	not calculated <sup>c</sup>

**Table 3.** Cont.

	Nominal EC <sub>50</sub>	EC <sub>50</sub> corrected to Ag dissolution <sup>a</sup>	EC <sub>50</sub> corrected to Ag bioavailability <sup>b</sup>
Ag-40 nm	28.7 ± 1.6	1.48 ± 0.09	not calculated <sup>c</sup>
Ag-60 nm	30.9 ± 2.1	1.65 ± 0.12	not calculated <sup>c</sup>
Ag-80 nm	34.9 ± 2.3	2.62 ± 0.17	not calculated <sup>c</sup>
Average (for AgNPs):	26.7	1.73	not calculated <sup>c</sup>

<sup>a</sup>Dissolved ionic Ag was determined from the supernatant of ultracentrifuged nanoparticles suspension. See Table S2.

<sup>b</sup>Bioavailable Ag was analyzed using recombinant bioluminescent Ag-sensor bacteria *E. coli* MC1061(pSLcueR/pDNPcopAlux). See also Materials and Methods and Figure 6.

<sup>c</sup>not calculated as the bioavailability measurement was relevant only for bacterial cells.

UP water – ultrapure water.

doi:10.1371/journal.pone.0102108.t003

Fluorescence(%) =

$$100 \times (RFU_{S,t=1h} - RFU_{S,t=0} / RFU_{B,t=1h} - RFU_{B,t=0})$$

where RFU<sub>S</sub> is fluorescence after exposure to the Ag sample and RFU<sub>B</sub> is fluorescence in UP water (background fluorescence) at time point zero (t = 0) or after 1 hour (t = 1 h). Hydrogen peroxide was used as the positive control for ROS; in every assay, induction of 2,7-H<sub>2</sub>DCFDA fluorescence by 0.1–1.5% H<sub>2</sub>O<sub>2</sub> was evident.

## Results and Discussion

### Characteristics of Ag nanoparticles

Citrate-coated Ag NPs of different primary sizes (Figure 1, Table 2), purchased from MK Nano were used throughout the tests. The particles' stock suspensions provided by the producer were well dispersed. In UP water and in algal test medium the hydrodynamic size of the particles was close to their primary size and no sedimentation was observed (Figure 2, Table 2). In AFW (test medium for *D. magna*) the particle hydrodynamic diameter was enlarged so that the measurements were not possible (Table 2) and the particles settled in time (Figure 2). This was probably due to the presence of high levels of divalent cations that have been shown to increase Ag NP aggregation [19]. The particles surface charge (ζ-potential) in all the three test media was negative, varying from −15 mV till −29 mV (Table 2).

### Toxicological profiles of Ag nanoparticles

a. **Dissolution of Ag NPs in different test media.** It has been suggested that the toxicity of particulate silver (as well as of ZnO and CuO) is largely due to the dissolved fraction [20] [21]. To study the contribution of the soluble fraction (Ag ions) to the toxicity of Ag NPs, we quantified the amount of Ag ions after incubation of Ag NPs in the test media used in the current study. The incubation time after which the particles were separated from dissolved ions by ultracentrifugation (Figure S4) was specific to the respective toxicity test. In general, the dissolution of ionic Ag from NPs was relatively low, usually less than 1% of the total Ag. In UP water, AFW and algal test medium the release of Ag ions depended clearly on the primary size of the Ag NPs (Figure 3, Table S2). For example, in UP water 1.3% of Ag was released as ions from 10 nm Ag NPs and only 0.6% of Ag was dissolved from 80 nm Ag NPs. Roughly similar results were obtained in algal test medium. Higher dissolution of smaller Ag NPs is coherent with the previous studies by [22] [23] and could be explained by their higher specific surface area.

In OECD 202 AFW that was used as test medium in crustacean immobilization assay the dissolution of Ag NPs was slightly lower compared to UP water and algal test medium yet followed the similar trend: smaller particles dissolved more (Figure 3). Lower dissolution of Ag NPs in AFW (Figure 3) could be explained by formation of insoluble Ag complexes as shown also by Miao et al. [24]. For example, in AFW, only 33% of the added AgNO<sub>3</sub> was present as ionic form showing that most likely 80% of Ag ions settled during ultracentrifugation in the form of insoluble Ag.

Dissolution of Ag NPs in mammalian cell culture medium (DMEM with 10% serum) was remarkably different from what was observed in crustacean and algal test media. The fraction of dissolved Ag in cell culture medium was relatively high (5–7%; Figure 3) and no clear size-dependent dissolution was observed. The observed high dissolution of Ag NPs may be due to high organics content in this medium. As reported earlier for ZnO NPs [25] and CuO NPs [26] organic media components may promote metallic NPs' solubility.

### b. Toxicity of Ag NPs to different test organisms/cells.

The EC<sub>50</sub> values obtained in this work for Ag NPs as well as for Ag ions (Table 3) indicate that the most sensitive organism to silver NPs was crustacean *D. magna*, followed by algae *P. subcapitata*, bacteria *E. coli* and *P. fluorescens*, yeast *S. cerevisiae*, and finally, mammalian fibroblasts *in vitro* (Table 3, Figure S5). This order of sensitivity is in agreement with the literature data presented in Figure S3. The nominal Ag NPs-based EC<sub>50</sub> data from the current study varied almost 3 orders of magnitude, ranging from 0.1 (*D. magna*) to 26 mg/L (fibroblasts) being again in agreement with previously reported literature data (Figure S3). These differences in EC<sub>50</sub> values are likely due to differences in the used test media [27] as well inherent properties of the test organisms/cells (Table 3). Indeed, Blinova et al [27] showed that natural water (dissolved organic carbon content 5–35 mg C/L) mitigated the toxicity of the studied silver compounds to crustaceans *D. magna* and *T. platyurus* up to 8-fold compared to artificial freshwater. Different inherent sensitivity of organisms towards silver is evident by comparing the EC<sub>50</sub> values of bacteria, yeast, algae and crustaceans. Although these assays were performed in mineral media or in UP water, toxicity of silver to these organisms was different (Table 3). Sensitivity pattern of the organisms towards silver agrees with that in Table S1, reported in Bondarenko et al [4].

c. **Particle-size dependent toxicity of Ag NPs towards different test organisms/cells.** When the toxic effect of Ag NPs towards each test organism/cell was analysed for each

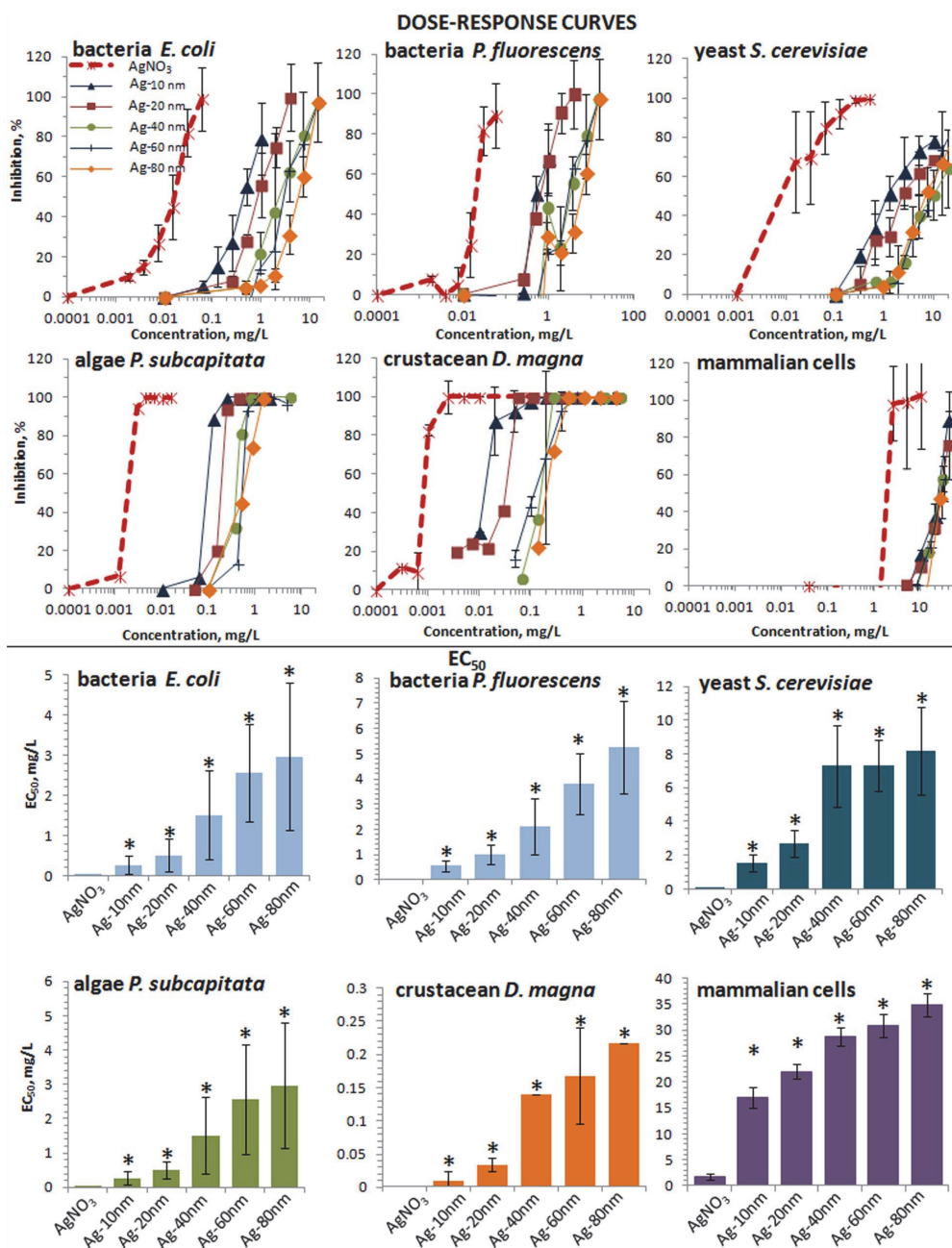


**Figure 4. Dose-response curves and the respective EC<sub>50</sub> values of Ag formulations to test organisms and cells.** Upper panel (A–D): dose-response curves; lower panel (E–H): EC<sub>50</sub> values. X-axis shows nominal Ag concentrations. \* - significantly (p < 0.05) different from EC<sub>50</sub> value of AgNO<sub>3</sub>.  
doi:10.1371/journal.pone.0102108.g004

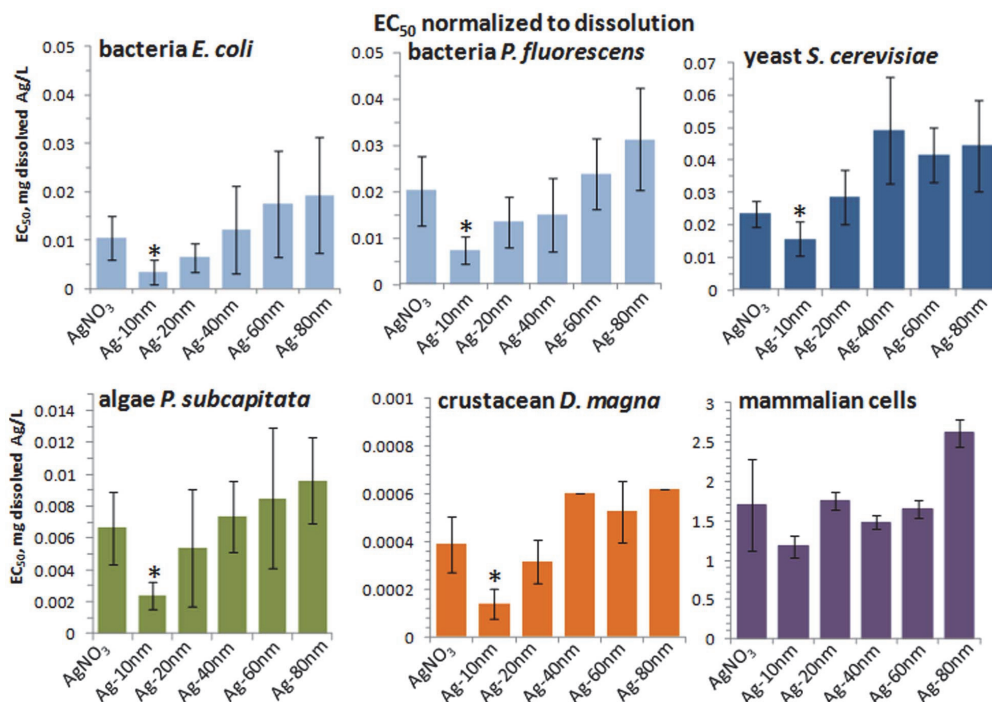


**Figure 5. Dissolution-corrected EC<sub>50</sub> values of 10–80 nm Ag NPs and AgNO<sub>3</sub>.** EC<sub>50</sub> values presented in Figure 4 (lower panel) were normalized for dissolved Ag (for dissolution, see Figure 3). \* - significantly (p<0.05) different from EC<sub>50</sub> of AgNO<sub>3</sub>. doi:10.1371/journal.pone.0102108.g005

size separately, more subtle effects became evident. Nominal concentrations-based dose-response curves for Ag NPs with various primary sizes and AgNO<sub>3</sub> for bacteria, yeast,

crustaceans and algae are shown in Figure 4 upper panel and the respective EC<sub>50</sub> values in the lower panel. For all the test organisms/cells, AgNO<sub>3</sub> was the most toxic compound

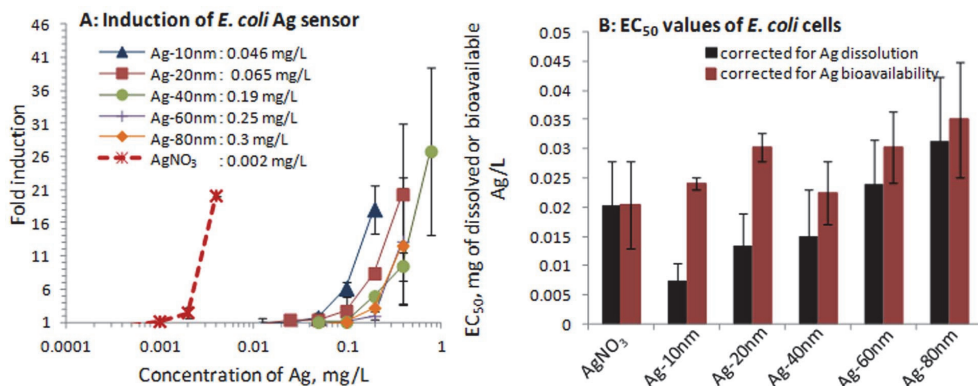


**Figure 6. Response of *E. coli* sensor to subtoxic concentrations of Ag formulations and bioavailability-corrected EC<sub>50</sub> values.** (A) Induction of bioluminescence in Ag-inducible *E. coli* bioreporter strain by AgNO<sub>3</sub> and 10–80 nm Ag NPs. Concentration of different Ag formulations at 2-fold induction is shown; (B) 4-h EC<sub>50</sub> of AgNO<sub>3</sub> and Ag NPs, corrected for dissolved Ag (see Figure 3) or bioavailable Ag, calculated from bioluminescence induction of Ag bioreporter strain (see panel A). doi:10.1371/journal.pone.0102108.g006

and, as a rule, the toxicity of Ag NPs decreased with increasing primary particle size. Similarities in the slopes of the dose-response curves for the test species for AgNO<sub>3</sub> and Ag NPs varying in size (Figure 4, upper panel) also indicate that the tested Ag compounds may have a common mechanism of action, i.e. acting *via* solubilized silver.

As expected, toxicity of Ag NPs increased with decreasing particle size. The difference in toxicity of 80 nm Ag NPs and 10 nm Ag NPs was the biggest for *D. magna* (about 20 fold) and the smallest for mammalian fibroblasts (1.7-fold) (Figure S6). To quantify the role of Ag ions in the toxicity of Ag NPs, we normalized the Ag NP EC<sub>50</sub> values for all the test organisms/cells to dissolved Ag ions (Figure 5). The dissolution-corrected EC<sub>50</sub> d. aes of Ag 20, 40, 60 and 80 nm NPs were similar to those of AgNO<sub>3</sub>, indicating that in case of these particles, toxicity was induced by released Ag ions. However, the toxicity of 10 nm Ag NPs was higher than predicted by soluble Ag-ions and this effect was statistically significant (Figure 5). It seems that 10 nm Ag NPs have additional not-dissolution driven toxic properties compared to 20–80 nm Ag NPs. Interestingly, similar observation, dissolution independent toxicity of ≤10 nm Ag NPs was recently published by Gliga et al. [28]. Consequently, it appears that the real size threshold for novel biological effects of particles is closer to <20 nm and not 100 nm as suggested in the current ‘nano’ legislation [29]. In order to determine the factors inducing these additional size-dependent toxic effects, we hypothesized that due to their small size, the 10 nm Ag NPs may induce ROS and/or induce increased bioavailability of silver.

**d. Evaluation of the size-dependent reactive oxygen species (ROS)-production potential of Ag NPs.** In order to study the factors behind the surplus toxic effects of 10 nm Ag NPs, we first tested whether enhanced production of extracellular ROS could contribute to their ‘excess’ toxicity. Moreover, induction of ROS is, in addition to ion release theory, one of the best acknowledged mechanisms of toxic action of Ag NPs [30]. Although AgNO<sub>3</sub> at concentrations > 1 mg/L, 10 nm Ag NPs at concentrations >10 mg/L and 20 nm Ag NPs at concentrations >50 mg/L increased the fluorescence of ROS indicator dye 2,7-H<sub>2</sub>DCFDA, these concentrations were much higher than the EC<sub>50</sub> values of AgNO<sub>3</sub> or the respective Ag NPs (Table 3, Figure 4). At the EC<sub>50</sub> concentrations for most of our test organisms no ROS-induced increase in 2,7-H<sub>2</sub>DCFDA fluorescence was detected (Table S3). Thus, ROS were most probably not involved in Ag NPs toxicity and did not explain the excess toxicity of 10 nm Ag NPs. Slight induction of the ROS-indicator dye was registered at the EC<sub>50</sub> concentrations of AgNO<sub>3</sub> (1.7 mg Ag/L) and 10 nm Ag NPs (16.9 mg Ag/L) to mammalian fibroblasts (Table S3) indicating that ROS may be involved in silver toxicity for these cells.

**e. Analysis of the effect of particle size in particle-cell direct contact for bioavailability of silver.** Since abiotic ROS did not explain the enhanced toxicity of 10 nm Ag NPs (see above) and our previous studies [31] have shown that the main driver for Ag NP toxicity is the contact between the organism/cell and NPs, we next analyzed direct cellular bioavailability of the Ag NPs. According to our previous studies, bioavailability of metals from NPs [31] and other solid matrices (soils, sediments; [32] [33] [34] [35]) is not always equal to metal dissolution. Specifically, in close contact with the particulate matter, cells may release and import higher

concentrations of metals than are dissolved in abiotic conditions. Thus, we analyzed Ag bioavailability from Ag NPs and AgNO<sub>3</sub> (an ionic control) using *E. coli* biosensor cells that exhibit induced bioluminescence in response to subtoxic concentrations of Ag ions that enter the cells [17]. Similarly to the tendency in Ag NPs’ toxicity (Figure 4) and dissolution (Figure 3), the bioluminescent response of sensor bacteria increased with decreasing Ag NP’s size. The latter indicates that more Ag ions entered bacterial cells in case of the same mass of smaller Ag NPs compared to larger ones (Figure 6A). When the 4h EC<sub>50</sub> values of differently sized Ag NPs for *E. coli* (Figure 4; upper panel) were normalized to bioavailable Ag, measured by *E. coli* Ag-sensor bacteria, no 10 nm NP threshold effect was observed any more (Figure 6B). Thus, the toxic effects of all the Ag NPs, including 10 nm ones, could be completely explained by intracellular bioavailable Ag. Although our data showed that the toxic effects of Ag NPs to bacteria were due to intracellular bioavailable silver, we do not have analogous experimental proof to claim that this was also the case for other test organisms. In addition, even if the toxicity was due to bioavailable Ag ions, we do not have enough information on mechanisms by which these Ag ions became bioavailable. As shown in this study and also in our previous studies [31], the direct contact between metallic NPs and cells is essential for increased bioavailability of metals. However, it is still unclear whether the NPs enter the cells and then become bioavailable or dissolve extracellularly in close vicinity of cell surface before entering the cells and becoming bioavailable to the living cells. In the scientific literature both, uptake of NPs by microbial cells [36] [37] [24] as well as increased dissolution of NPs in the vicinity of microbial cells have been suggested [38] [39] [40]. In case of three marine phytoplankton species exposure to polystyrene NPs increased the production of exopolymers [41] which indicates that NPs may significantly interfere with cellular physiology. However as the interaction of NPs with living cells and *vice versa* is a dynamic process, determination of the exact sequence of cellular events triggered by NP exposure remains to be elucidated.

## Conclusions

In conclusion, the toxicity of Ag NPs was strictly dependent on NPs dissolution but the bulk dissolution explained the toxicity of 20–80 nm Ag NPs but not of 10 nm Ag NPs. This discrepancy was clarified by using *E. coli* Ag-biosensor that showed equal intracellular bioavailability of nanosilver, whatever the particle size. Therefore, 10 nm and smaller particles seem to interact with cells and become more bioavailable either by dissolving in the close vicinity of the outer cell surface or inside the cells. These results indicate that in order to obtain more efficient Ag NPs antimicrobials, one has to stream towards <10 nm particles. More research is needed to find out the exact mechanism driving the enhanced bioavailability and toxicity of ≤10 nm Ag particles. Whether Ag ion bioavailability is driving the toxicity of ≤10 nm Ag NPs also to other test organisms than bacteria remains also to be elucidated.

## Supporting Information

**Figure S1 Number of papers registered in Thomson Reuters ISI Web of Science on search terms “toxic\* AND nano\*” and “size-dependent toxic\* AND nano\*” in different years.** Search was performed on December 8, 2013.

(TIF)

**Figure S2 Number of published papers on toxicity of nanosilver to different organisms.** Search was performed in Thomson Reuters ISI Web of Science (all years). Search term “effect of size and silver and nano\*” that yielded altogether 3363 papers was refined by additional search terms referring to organisms/organism groups which are indicated on x-axis. Most information was available for bacteria (270 papers in total) and most of the bacteria-related papers concerned *Escherichia coli* (246 papers) – a model bacterium widely used in hygienic and/or medical studies in design of novel antimicrobials. Search was performed on December 8, 2013.

(TIF)

**Figure S3 Variability of currently published toxicity data on nanosilver.** Toxicity of Ag NPs varies remarkably; analysis of the literature data (from [4]) showed that the data varied even within the same organism group: remarkable differences were 500-fold in the case of bacteria, 4240-fold in the case of algae and 275-fold in the case of mammalian cells *in vitro*. It was suggested that this high variability in nanosilver toxicity was due to differences in NPs as well as in testing conditions.

(TIF)

**Figure S4 Schematic representation of experiments conducted in this study.**

(TIF)

**Figure S5 Organismal differences in sensitivity to Ag NPs and AgNO<sub>3</sub>.** Average values for all the five studied sizes of Ag NPs 10, 20, 40, 60 and 80 nm are presented (see also Table 3). Nominal concentrations-based EC<sub>50</sub> values are shown. Note the logarithmic Y-scale.

(TIF)

**Figure S6 Organismal differences in sensitivity to differently sized Ag NPs.** (A) Nominal EC<sub>50</sub> values for

different test organisms. Note the logarithmic Y-scale; (B) Ratio between EC<sub>50</sub> of Ag-80 nm and EC<sub>50</sub> of Ag-10 nm.

(TIF)

**Table S1 Toxicity of Ag NPs and Ag ions to bacteria, yeast, algae, crustaceans, fish and mammalian cells *in vitro*.** The values are selected and summarized from [4]. Altogether 119 L(E)C<sub>50</sub> or MIC values were found for Ag NPs and 72 L(E)C<sub>50</sub> or MIC values were found for Ag ions. Crustaceans (daphnids), algae and fish—the aquatic test organisms proposed for the classification and labelling of chemicals by EU REACH regulation—proved the most sensitive groups of organisms in respect to the toxic action of Ag NPs.

(DOCX)

**Table S2 Dissolution of Ag NPs (%) in test media used for different toxicity assays.**

(DOCX)

**Table S3 Abiotic production of reactive oxygen species (ROS) by Ag NPs of different sizes and AgNO<sub>3</sub>.** The potential for abiotic ROS was measured at EC<sub>50</sub> concentrations (Table 3) of the different Ag formulations.

(DOCX)

## Acknowledgments

We thank Mr. Rando Saar from Estonian Nanotechnology Competence Centre for his practical help with SEM/EDX. The authors thank Dr. Marika Mannerström and Mirja Hyppönen from Finnish Centre for Alternative Methods for their help and advice in cell culture experiments.

## Author Contributions

Conceived and designed the experiments: AI A. Kahru. Performed the experiments: IK KK IB VA SS HV A. Käkkinen MH MV DK TT. Analyzed the data: AI IK KK IB VA SS HV A. Käkkinen MH MV DK VK A. Kahru. Contributed reagents/materials/analysis tools: AI KK DK VK A. Kahru. Contributed to the writing of the manuscript: AI A. Kahru.

## References

- Nel A, Xia T, Mädler L, Li N (2006) Toxic Potential of Materials at the Nanolevel. *Science* 311: 622–627.
- Kahru A, Ivask A (2012) Mapping the Dawn of Nanocotoxicological Research. *Acc Chem Res* 46: 823–833.
- Kahru A, Dubourgier H-C (2010) From ecotoxicology to nanocotoxicology. *Toxicology* 269: 105–119.
- Bondarenko O, Juganson K, Ivask A, Kasemets K, Mortimer M, et al. (2013) Toxicity of Ag, CuO and ZnO nanoparticles to selected environmentally relevant test organisms and mammalian cells *in vitro*: a critical review. *Arch Toxicol* 87: 1181–1200.
- Bai Y, Wu F, White JC, Xing B (2014) 100 Nanometers: A Potentially Inappropriate Threshold for Environmental and Ecological Effects of Nanoparticles. *Environ Sci Technol* 48: 3098–3099.
- Ivask A, Juganson K, Bondarenko O, Mortimer M, Aruoja V, et al. (in press) Mechanisms of toxic action of Ag, ZnO and CuO nanoparticles to selected ecotoxicological test organisms and mammalian cells *in vitro*: A comparative review. *Nanotoxicology*.
- Burello E, Worth AP (2011) QSAR modeling of nanomaterials. *WIREs Nanomed Nanobiotechnol* 3: 298–306.
- Puzyn T, Rasulev B, Gajewicz A, Hu X, Dasari TP, et al. (2011) Using nano-QSAR to predict the cytotoxicity of metal oxide nanoparticles. *Nat Nano* 6: 175–178.
- De Jong WH, Hagens WI, Krystek P, Burger MC, Sips AJAM, et al. (2008) Particle size-dependent organ distribution of gold nanoparticles after intravenous administration. *Biomaterials* 29: 1912–1919.
- Project on emerging nanotechnologies website. Available: [www.nanotechproject.org](http://www.nanotechproject.org). Accessed 2014 June 23.
- Piccinno F, Gottschalk F, Seeger S, Nowack B (2012) Industrial production quantities and uses of ten engineered nanomaterials in Europe and the world. *J Nanopart Res* 14: 1–11.
- Image J website. Available: <http://imagej.nih.gov/>. Accessed 2014 June 23.
- Tsao TM, Wang MK, Huang PM (2009) Automated Ultrafiltration Device for Efficient Collection of Environmental Nanoparticles from Aqueous Suspensions. *Soil Sci Soc Am J* 73: 1808–1816.
- Peters RB, Rivera Z, Bommel G, Marvin HP, et al. (2014) Development and validation of single particle ICP-MS for sizing and quantitative determination of nano-silver in chicken meat. *Anal Bioanal Chem*. 1–11.
- Sarand I, Haario H, Jorgenson K, Romantshuk M (2000) Effect of inoculation of a TOL plasmid containing mycorrhizosphere bacterium on development of Scots pine seedlings, their mycorrhizosphere and the microbial flora in m-toluuate-amended soil. *FEMS Microbiol Ecol* 31: 127–141.
- Aruoja V, Kurvet I, Dubourgier H-C, Kahru A (2004) Toxicity testing of heavy-metal-polluted soils with algae *Selenastrum capricornutum*: A soil suspension assay. *Environ Toxicol* 19: 396–402.
- Ivask A, Rolova T, Kahru A (2009) A suite of recombinant luminescent bacterial strains for the quantification of bioavailable heavy metals and toxicity testing. *BMC Biotechnol* 9: 41.
- Priester JH, Stoimenov PK, Mielke RE, Webb SM, Ehrhardt C, et al. (2009) Effects of Soluble Cadmium Salts Versus CdSe Quantum Dots on the Growth of Planktonic *Pseudomonas aeruginosa*. *Environ Sci Technol* 43: 2589–2594.
- Jin X, Li M, Wang J, Marambio-Jones C, Peng F (2010) High-Throughput Screening of Silver Nanoparticle Stability and Bacterial Inactivation in Aquatic Media: Influence of Specific Ions. *Environ Sci Technol* 44: 7321–7328.
- Ivask A, George S, Bondarenko O, Kahru A (2012) Metal-containing nanomicrobials: differentiating the impact of solubilized metals and particles. In: Cioffi N, editor. *Nano-antimicrobials - Progress and Prospects*: Springer. pp. 253–290.
- Xiu Z-M, Zhang Q-B, Puppala HL, Colvin VL, Alvarez PJJ (2012) Negligible Particle-Specific Antibacterial Activity of Silver Nanoparticles. *Nano Lett* 12: 4271–4275.
- Ma R, Levard C, Marinakos SM, Cheng Y, Liu J, et al. (2012) Size-Controlled Dissolution of Organic-Coated Silver Nanoparticles. *Environ Sci Technol* 46: 752–759.

23. Ivask A, ElBadawy A, Kaweeterawat C, Boren D, Fischer H, et al. (2014) Toxicity Mechanisms in *Escherichia coli* Vary for Silver Nanoparticles and Differ from Ionic Silver. *ACS Nano* 8: 374–386.
24. Miao A-J, Luo Z, Chen C-S, Chin W-C, Santschi PH, et al. (2010) Intracellular Uptake: A Possible Mechanism for Silver Engineered Nanoparticle Toxicity to a Freshwater Alga *Ochromonas danica*. *PLOS One* 5:e15196.
25. Li M, Zhu L, Lin D (2011) Toxicity of ZnO Nanoparticles to *Escherichia coli*: Mechanism and the Influence of Medium Components. *Environ Sci Technol* 45: 1977–1983.
26. Käkinen A, Bondarenko O, Ivask A, Kahru A (2011) The Effect of Composition of Different Ecotoxicological Test Media on Free and Bioavailable Copper from CuSO<sub>4</sub> and CuO Nanoparticles: Comparative Evidence from a Cu-Selective Electrode and a Cu-Biosensor. *Sensors* 11: 10502–10521.
27. Blinova I, Niskanen J, Kajankari P, Kanarbik L, Käkinen A, et al. (2013) Toxicity of two types of silver nanoparticles to aquatic crustaceans *Daphnia magna* and *Thamnocephalus platyurus*. *Environ Sci Poll Res* 20: 3456–3463.
28. Gliga A, Skoglund S, Odnevall Wallinder I, Fadel B, et al. (2014) Size-dependent cytotoxicity of silver nanoparticles in human lung cells: the role of cellular uptake, agglomeration and Ag release. *Part Fibre Toxicol* 11: 11.
29. Commission (2011) Commission recommendation of 18 October 2011 on the definition of nanomaterial. Official Journal of the European Union. L275/38.
30. Manke A, Wang L, Rojasasakul Y (2013) Mechanisms of Nanoparticle-Induced Oxidative Stress and Toxicity. *BioMed Res Int* 2013: 15.
31. Bondarenko O, Ivask A, Käkinen A, Kurvet I, Kahru A (2013) Particle-Cell Contact Enhances Antibacterial Activity of Silver Nanoparticles. *PLoS ONE* 8: e64060.
32. Ivask A, Virta M, Kahru A (2002) Construction and use of specific luminescent recombinant bacterial sensors for the assessment of bioavailable fraction of cadmium, zinc, mercury and chromium in the soil. *Soil Biol Biochem* 34: 1439–1447.
33. Ivask A, Francois M, Kahru A, Dubourgier H, Virta M, et al. (2004) Recombinant luminescent bacterial sensors for the measurement of bioavailability of cadmium and lead in soils polluted by metal smelters. *Chemosphere* 55: 147–156.
34. Ivask A, Green T, Polyak B, Mor A, Kahru A, et al. (2007) Fibre-optic bacterial biosensors and their application for the analysis of bioavailable Hg and As in soils and sediments from Aznalcollar mining area in Spain. *Biosens Bioelectron* 22: 1396–1402.
35. Peltola P, Ivask A, Åström M, Virta M (2005) Lead and Cu in contaminated urban soils: Extraction with chemical reagents and bioluminescent bacteria and yeast. *Sci Tot Environ*, 350: 194–203.
36. Lok C-N, Ho C-M, Chen R, He Q-Y, Yu W-Y, et al. (2007) Silver nanoparticles: partial oxidation and antibacterial activities. *J Biol Inorg Chem* 12: 527–534.
37. Applerot G, Lipovsky A, Dror R, Perkas N, Nitzan Y, et al. (2009) Enhanced Antibacterial Activity of Nanocrystalline ZnO Due to Increased ROS-Mediated Cell Injury. *Adv Funct Mat*, 19: 842–852.
38. Choi O, Hu Z (2008) Size Dependent and Reactive Oxygen Species Related Nanosilver Toxicity to Nitrifying Bacteria. *Environ Sci Technol* 42: 4583–4588.
39. Morones JR, Elechiguerra JL, Camacho A, Holt KB (2005) The bactericidal effect of silver nanoparticles. *Nanotechnology* 16: 2346–53.
40. Sondi I, Salopek-Sondi B (2004) Silver nanoparticles as antimicrobial agent: a case study on *E. coli* as a model for Gram-negative bacteria. *J Colloid Interface Sci* 275: 177–182.
41. Chen C-S, Anaya JM, Zhang S, Spurgin J, Chuang C-Y, et al. (2011) Effects of Engineered Nanoparticles on the Assembly of Exopolymeric Substances from Phytoplankton. *PLoS ONE* 6: e21865.
42. Martínez-Castañón G, Niño-Martínez N, Martínez-Gutiérrez F, Martínez-Mendoza J, et al. (2008) Synthesis and antibacterial activity of silver nanoparticles with different sizes. *J Nanopart Res* 10: 1343–1348.
43. Lu Z, Rong K, Li J, Yang H, Chen R (2013) Size-dependent antibacterial activities of silver nanoparticles against oral anaerobic pathogenic bacteria. *J Mat Sci: Mat Med* 24: 1465–1471.
44. Bowman CR, Bailey FC, Elrod-Erickson M, Neigh AM, Otter RR (2012) Effects of silver nanoparticles on zebrafish (*Danio rerio*) and *Escherichia coli* (ATCC 25922): A comparison of toxicity based on total surface area versus mass concentration of particles in a model eukaryotic and prokaryotic system. *Environ Toxicol Chem* 31: 1793–1800.
45. Silva T, Pokhrel LR, Dubey B, Tolaymat TM, et al. (2014) Particle size, surface charge and concentration dependent ecotoxicity of three organo-coated silver nanoparticles: Comparison between general linear model-predicted and observed toxicity. *Sci Tot Environ* 468–469: 968–976.
46. Lopes S, Ribeiro F, Wojnarowicz J, Łojkowski W, Jurkschat K, et al. (2014) Zinc oxide nanoparticles toxicity to *Daphnia magna*: size-dependent effects and dissolution. *Environ Toxicol Chem* 33: 190–198.
47. Wang X, Ji Z, Chang CH, Zhang H, Wang M, et al. (2014) Use of Coated Silver Nanoparticles to Understand the Relationship of Particle Dissolution and Bioavailability to Cell and Lung Toxicological Potential. *Small* 10: 385–398.
48. Badwaik V, Vangala L, Pender D, Willis C, Aguilar Z, et al. (2012) Size-dependent antimicrobial properties of sugar-encapsulated gold nanoparticles synthesized by a green method. *Nanoscale Res Lett* 7: 1–11.
49. Wehling J, Volkman E, Grieb T, Rosenauer A, Maas M, et al. (2013) A critical study: Assessment of the effect of silica particles from 15 to 500 nm on bacterial viability. *Environ Poll* 176: 292–299.
50. Rodea-Palomares I, Boltes K, Fernández-Piñas F, Leganés F, García-Calvo E, et al. (2011) Physicochemical Characterization and Ecotoxicological Assessment of CeO<sub>2</sub> Nanoparticles Using Two Aquatic Microorganisms. *Toxicol Sci* 119: 135–145.

## PUBLICATION IV

Kasemets, K., **Suppi, S.**, Künnis-Beres, K., Kahru, A., (2013). Toxicity of CuO nanoparticles to yeast *Saccharomyces cerevisiae* BY4741 wild-type and its nine isogenic single-gene deletion mutants. *Chemical Research in Toxicology*. 26, 356–367.

Reprinted with permission from Kasemets, K., **Suppi, S.**, Künnis-Beres, K., Kahru, A., (2013). Toxicity of CuO nanoparticles to yeast *Saccharomyces cerevisiae* BY4741 wild-type and its nine isogenic single-gene deletion mutants. *Chemical Research in Toxicology*. 26, 356–367. Copyright 2013 American Chemical Society.



# Toxicity of CuO Nanoparticles to Yeast *Saccharomyces cerevisiae* BY4741 Wild-Type and Its Nine Isogenic Single-Gene Deletion Mutants

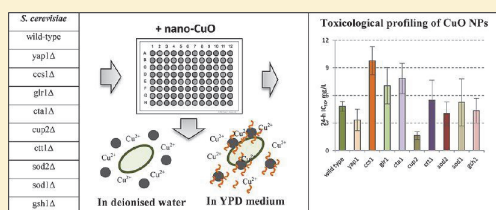
Kaja Kasemets,<sup>\*,†</sup> Sandra Suppi,<sup>†,‡</sup> Kai Künnis-Beres,<sup>†</sup> and Anne Kahru<sup>†</sup>

<sup>†</sup>National Institute of Chemical Physics and Biophysics, Laboratory of Environmental Toxicology, Akadeemia tee 23, Tallinn 12618, Estonia

<sup>‡</sup>Department of Chemical and Materials Technology, Tallinn University of Technology, Ehitajate tee 5, Tallinn 19086, Estonia

Supporting Information

**ABSTRACT:** A suite of eight tentatively oxidative stress response-deficient *Saccharomyces cerevisiae* BY4741 single-gene mutants (*sod1Δ*, *sod2Δ*, *yap1Δ*, *cta1Δ*, *ctt1Δ*, *gsh1Δ*, *glr1Δ*, and *ccs1Δ*) and one copper-vulnerable mutant (*cup2Δ*) was used to elucidate whether the toxicity of CuO nanoparticles to *S. cerevisiae* is mediated by oxidative stress (OS). Specifically, sensitivity profiles of mutants' phenotypes and wild-type (wt) upon exposure to nano-CuO were compared. As controls, CuSO<sub>4</sub> (solubility), bulk-CuO (size), H<sub>2</sub>O<sub>2</sub>, and menadione (OS) were used. Growth inhibition of wt and mutant strains was studied in rich YPD medium and cell viability in deionized water (DI).



To wt strain nano-CuO was 32-fold more toxic than bulk-CuO: 24-h IC<sub>50</sub> 4.8 and 155 mg/L in DI and 643 and >20000 mg/L in YPD, respectively. In toxicant-free YPD medium, all mutants had practically similar growth patterns as wt. However, the mutant strains *sod1Δ*, *sod2Δ*, *ccs1Δ*, and *yap1Δ* showed up to 12-fold elevated sensitivity toward OS standard chemicals menadione and H<sub>2</sub>O<sub>2</sub> but not to nano-CuO, indicating that CuO nanoparticles exerted toxicity to yeast cells via different mechanisms. The most vulnerable strain to all studied Cu compounds was the copper stress response-deficient strain *cup2Δ* (~16-fold difference with wt), indicating that the toxic effect of CuO (nano)particles proceeds via dissolved Cu-ions. The dissolved copper solely explained the toxicity of nano-CuO in DI but not in YPD. Assumingly, in YPD nano-CuO acquired a coating of peptides/proteins and sorbed onto the yeast's outer surface, resulting in their increased solubility in the close vicinity of yeast cells and increased uptake of Cu-ions that was not registered by the assays used for the analysis of dissolved Cu-ions in the test medium. Lastly, as yeast retained its viability in DI even by 24th hour of incubation, the profiling of the acute basal toxicity of chemicals toward yeasts may be conducted in DI.

## INTRODUCTION

Despite the intensive use of engineered nanoparticles (NPs) in various consumer and industrial products, data on their potential hazards are still rare and mechanisms of action only partially understood.<sup>1</sup> As the toxicity of NPs varies, depending on e.g., composition, coating, and weathering as well as on environmental factors, cost-efficient screening methods are needed for the toxicological analysis of synthetic NPs. The yeast *Saccharomyces cerevisiae* is a promising unicellular eukaryotic organism for the toxicological evaluation of NPs as its cellular structure and functional organization have many similarities to those of higher-level organisms. Because of this, *S. cerevisiae* is a widely used model organism in eukaryotic cell biology to study the oxidative stress and aging as well as regulation of cancer cells metabolism.<sup>2</sup> In addition, yeasts have short generation time and can easily be cultivated in the laboratory. A remarkable development of the mechanistic studies in cell biology has occurred due to the *Saccharomyces* Genome Deletion Project that created a unique collection of

yeast single-gene deletion mutants<sup>3</sup> in which each open reading frame (ORF) was systematically replaced with a *kanMX4* disruption-deletion cassette.<sup>4</sup> The availability of systematic genome-wide mutant collections of *S. cerevisiae* (e.g., EURO-SCARF<sup>5</sup>) is a powerful tool for the toxicological profiling of chemicals, e.g., in a high-throughput manner.<sup>6,7</sup>

Compared to many other metal oxide NPs (e.g., TiO<sub>2</sub>, ZnO and SiO<sub>2</sub>), the potential hazardous effects of CuO nanoparticles are poorly studied,<sup>8</sup> which needs reconsideration since CuO NPs are increasingly used and toxic to aquatic organisms.<sup>1,9</sup> Indeed, copper compounds have been historically used as biocides and with the advent of nanotechnologies, copper has been increasingly used in the form of NPs and applied in, e.g., antimicrobial textiles, hospital equipment, wood preservation and antifouling paints.<sup>10</sup> However, the mechanism of toxicity of nano-CuO is still only partially understood.<sup>11</sup>

Received: November 20, 2012

Published: January 22, 2013

The adverse effects of nano-CuO toward a wide range of bacteria, mostly at concentrations between 10–100 mg/L, has been reported.<sup>12,13</sup> However, using recombinant bioluminescent sensor bacteria *Escherichia coli* responding to subtoxic concentrations of oxidative stress- and DNA damage-inducing chemicals, it was shown that the formation of superoxide anions, hydrogen peroxide, and single-stranded DNA was induced by the CuO NPs already at very low subtoxic levels: 0.1 mg Cu/L.<sup>11</sup> To aquatic crustaceans *Thamnocephalus platyurus* and *Daphnia magna* and algae *Pseudokirchneriella subcapitata*, CuO nanoparticles were remarkably toxic: IC<sub>50</sub> was 3.2, 0.18, and <1 mg/L, respectively.<sup>14,15</sup> Solubility of nano-CuO has been shown as a key factor in its aquatic toxicity<sup>16</sup> as well as in terrestrial isopods (*Porcellio scaber*) where the solubility of Cu NPs in the gut was the key factor in copper accumulation in the tissue.<sup>17</sup> Differently, the dissolution of nano-CuO did not fully explain the toxic effect of CuO NPs toward protozoa *Tetrahymena thermophila*,<sup>18</sup> crustaceans *D. magna*,<sup>19</sup> and duckweed *Landoltia punctata*.<sup>20</sup> As a general hypothesis for explaining the toxicity of NPs, their propensity to generate reactive oxygen species (ROS) has been suggested.<sup>21</sup> Indeed, in the protozoan *T. thermophila* nano-CuO induced the generation of ROS and changes in membrane fatty-acid composition.<sup>18</sup> Several *in vitro* studies using human lung epithelial cells (A549) have reported that nano-CuO triggered ROS production and induced oxidative stress, mitochondrial depolarization, and DNA damage but that the released copper fraction into the cell medium was not fully explaining the observed phenomena.<sup>22–24</sup> In our previous study,<sup>25</sup> we also showed that the growth inhibitory effect of nano-CuO to *S. cerevisiae* S288C was not solely explained by the dissolved fraction of copper, and we hypothesized that particle-related toxicity (e.g., oxidative stress) was involved in the observed toxic effect of nano-CuO.

The current study is a continuation of our previous one<sup>25</sup> and was initiated to elucidate the mechanisms of action of nano-CuO using a phenotypic profiling approach. For that, a different *Saccharomyces cerevisiae* BY4741 wild-type and its isogenic single-gene mutants derived from EUROSCARF<sup>5</sup> collection were used. On the basis of literature data on the regulation of oxidative stress response in yeast, the following tentatively OS-response deficient strains *sod1Δ*, *sod2Δ*, *yap1Δ*, *cta1Δ*, *ctl1Δ*, *gsh1Δ*, *glr1Δ*, and *ccs1Δ* were chosen for the study. Because of the compensatory mechanisms in the cells, the deficiency in a single gene may not necessarily result in the expected (sensitive) phenotype.<sup>26,27</sup> Therefore, several OS-response deficient single-gene deletion mutants were selected for the toxicological profiling of nano-CuO. In addition, a strain deficient in the transcription factor-regulated response to copper stress (*cup2Δ*) was selected. Bulk-CuO (size control), CuSO<sub>4</sub> (solubility control), and OS-inducing positive controls such as H<sub>2</sub>O<sub>2</sub> and menadione (superoxide radical generator) were analyzed in parallel. Recombinant Cu-sensing bacteria and atomic absorption spectroscopy (AAS) were used to quantify the dissolved fraction of copper. To our knowledge, this is the first study where EUROSCARF *S. cerevisiae* single-gene deletion mutants have been used for toxicological profiling of synthetic nanoparticles. The test format refined and reported herein could be promising for the mechanism based phenotypic profiling of NPs also in high-throughput manner. Although the profiling was performed on yeast *S. cerevisiae*, the results obtained are also indicative of other eukaryotic organisms/cells

that a priori are not internalizing NPs, such as other types of yeasts and unicellular algae.

## MATERIALS AND METHODS

**Test Chemicals.** Nanosized CuO (advertised particle size ~30 nm) and menadione sodium bisulphite were purchased from Sigma-Aldrich, bulk-CuO and CuSO<sub>4</sub> from Alfa Aesar, and H<sub>2</sub>O<sub>2</sub> (30%) from Merck. All of the tested chemicals were of analytical grade. The nano-CuO and bulk-CuO stock solutions (40 and 80 g/L, respectively) were prepared in sterile deionized water (DI) (pH 5.6 ± 0.1) (Milli-Q Millipore), ultrasonicated in the ultrasonic bath (Branson 1510, USA) for 30 min, and stored in the dark at ambient temperature. The stock solutions of CuSO<sub>4</sub> (159.6 g/L) and menadione sodium bisulphite (49.72 g/L) were prepared in DI and stored in the dark at ambient temperature or at +4 °C, respectively. For the tests, stock solutions of chemicals and 30% H<sub>2</sub>O<sub>2</sub> were further diluted in DI or in YPD medium (pH 6.6 ± 0.1) containing 1% yeast extract (Lab M), 2% Bacto Peptone (Difco Laboratories), and 2% glucose (Sigma-Aldrich). Before testing, stock solutions of nano-CuO and bulk-CuO were vigorously vortexed.

**Characterization of CuO (Nano)Particles.** The hydrodynamic diameter of nano-CuO and the Z-potential of nano-CuO and bulk-CuO in DI and YPD were measured using Zetasizer Nano ZS (Malvern Instruments, UK). For this, nano-CuO was incubated on 24-well microplates (1 mL per well) in DI and YPD at concentrations of 5.0 and 640 mg/L, respectively, and bulk-CuO at concentrations of 200 and 20000 mg/L, respectively, at 30 °C for 24 h without shaking, following the same experimental setup as in the toxicity assays (see below).

**Yeast Strains and Cultivation Conditions.** *S. cerevisiae* BY4741 wild-type (*MATa*; *his3Δ1*; *leu2Δ0*; *met15Δ0*; *ura3Δ0*) and its nine isogenic single-gene deletion mutants were purchased from EUROSCARF (Institute of Microbiology, University of Frankfurt, Germany). The *S. cerevisiae* mutants used in this study are characterized in Table S1 in Supporting Information.

Frozen permanent copies of *S. cerevisiae* strains were stored at –80 °C. Master plates of the strains were incubated on YPD-agar (ventilated Petri dishes; Greiner Bio-One) at 30 °C for 72 h in a microaerophilic environment (6% oxygen, 15% CO<sub>2</sub>; CampyGen, Oxoid) to avoid the selection toward the second site suppressors of oxygen-sensitive strains (e.g., *sod1Δ*) and further maintained at 4 °C. In the case of the single-gene deletion mutants (constructed by the *kanMX4* disruption-deletion cassette), the solid YPD medium also contained a selective antibiotic for eukaryotic cells, Geneticin 300 mg/L (G418 sulfate; Sigma-Aldrich), that is an analogue of kanamycin. To prepare the preculture for the toxicity testing, 2–3 colonies from the respective master-plates were transferred to 3 mL of YPD and incubated overnight at 30 °C without shaking. To compare the growth curves (growth pattern) of *S. cerevisiae* BY4741 wild-type and respective single-gene deletion mutants, the yeast strains were cultivated on 96-well microplates in YPD medium at 30 °C for 24 h in the absence of tested chemicals following the same experimental setup as in the growth inhibition test (see below). On the basis of the culture density (optical density, OD<sub>600 nm</sub>), the maximum specific growth rate ( $\mu_{max}$ , h<sup>-1</sup>) and generation time ( $t_d$ , h) were calculated (see Supporting Information for the details).

**Toxicity Testing.** For the toxicity studies, wild-type and single-gene deletion mutants were incubated/cultivated with or without varying concentrations of tested chemicals on 96-well microplates in deionized water (cell viability test) or in YPD medium (growth inhibition test) at 30 °C for 24 h without shaking. For both test formats, non-tissue culture treated 96-well flat bottom microplates (Falcon) were used. To minimize the evaporation during the experiments, the edges of microplates were sealed with ParafilmM. The following nominal concentrations of chemicals (mg/L) were chosen for the testing according to the results of prescreenings: (i) for the viability assay in DI, nano-CuO (0.48–160), bulk-CuO (4.8–1600), CuSO<sub>4</sub> (0.06–6.0 mg Cu/L), menadione (1.0–300), and H<sub>2</sub>O<sub>2</sub> (0.05–15); (ii) for the growth inhibition test in YPD, nano-CuO

**Table 1. Characteristics of Nano-CuO and Bulk-CuO, YPD Medium (Contains Protein Particles/Colloids) and Yeast Cells (*Saccharomyces cerevisiae* BY4741 Wild-Type) Measured by the Malvern Zetasizer Nano ZS**

test medium	characteristics	contact time (h)	nano-CuO	bulk-CuO	
deionized water (DI) <sup>c</sup> (pH 5.6 ± 0.1)	particle size in powder <sup>a</sup> (nm)		30.0	not available	
	specific surface area (SSA) of the powder <sup>b</sup> (m <sup>2</sup> /g)		25.5 ± 0.80	0.64 ± 0.02	
	hydrodynamic size (nm)	0	194 ± 16.9	not determined	
		24	162 ± 3.72	not determined	
	Z-potential (mV)	0	31.9 ± 7.31	-13.1 ± 0.69	
		24	22.8 ± 2.73	-22.1 ± 4.73	
YPD medium (a growth medium) <sup>d</sup> (pH 6.6 ± 0.1)	hydrodynamic size (nm)	0	5819 ± 476	not determined	
		24	2561 ± 249	not determined	
	Z-potential (mV)	0	-15.6 ± 1.13	-20.5 ± 1.19	
		24	-14.7 ± 0.10	-19.4 ± 1.59	
	YPD Medium (Without Added Nano-CuO and Bulk-Cuo Particles)				
	hydrodynamic size (nm)	0	260 ± 78.1		
	24	90.1 ± 38.8			
	Z-potential (mV)	0	-13.2 ± 1.10		
		24	-11.6 ± 4.73		
deionized water (DI) <sup>e</sup> (pH 5.6 ± 0.1)	Yeast Cells ( <i>S. cerevisiae</i> BY4741 Wild-Type)				
	hydrodynamic size (nm)	0	not determined		
		24	not determined		
	Z-potential (mV)	0	-37.0 ± 2.90		
		24	-33.1 ± 1.25		
YPD medium <sup>f</sup> (pH 6.6 ± 0.1)	hydrodynamic size (nm)	0	not determined		
		24	not determined		
	Z-potential (mV)	0	-2.58 ± 0.42		
		24	-1.94 ± 0.42		

<sup>a</sup>According to the manufacturer. <sup>b</sup>Measured by Brunauer–Emmet–Teller (BET) analysis. <sup>c</sup>Nano-CuO and bulk-CuO were analyzed at concentrations of 5.0 and 200 mg/L, respectively. <sup>d</sup>Nano-CuO and bulk-CuO were analyzed at concentrations of 640 and 20000 mg/L, respectively. <sup>e</sup>Used as a medium for the viability test. <sup>f</sup>Used as a medium for the growth inhibition test.

(200–3200), bulk-CuO (2500–20000), CuSO<sub>4</sub> (100–800 mg Cu/L), menadione (5.0–80), and H<sub>2</sub>O<sub>2</sub> (20–320).

**Cell Viability Assay.** Cell viability was assessed by measuring the ATP concentration of the yeast cells after 24-h exposure to the tested chemicals compared to the nonexposed control. Tests were performed in deionized water (DI), and the test was initiated from the exponentially growing yeast culture. For this, an overnight culture of yeast cells grown in YPD medium at 30 °C was diluted to OD<sub>600 nm</sub> 0.2 (Yenway 6300 Spectrophotometer, UK) and further cultivated in YPD at 30 °C to midlog phase (OD<sub>600 nm</sub> 0.8–1.0). Then, the yeast cells were harvested by centrifugation at 3500g for 10 min at 20 °C (Sigma 3-16PK, Germany) and washed twice with DI. The cell pellet was resuspended and diluted with DI to OD<sub>600 nm</sub> 1.2 (corresponding to ~2.4 × 10<sup>7</sup> CFU/mL (CFU = cell forming units) determined by the plating and incubating at 30 °C for 72 h and counting the colonies on YPD-agar plates). Then, 75 μL of yeast suspension and 75 μL of tested chemical suspension/solution in DI (each concentration in duplicate) were pipetted into the 96-well microplates. DI without test chemicals was inoculated with test strains in parallel and served as a control culture (not treated, biotic control). After 24 h, ATP was extracted from the yeast cells and quantified using the luciferin–luciferase method as described in Kasemets et al.<sup>28</sup> The effect of prolonged incubation (24 h) on yeast cell viability in DI compared to that in YPD medium was assessed in prescreening experiments by the fluorescent viability dye Acridine Orange (see Supporting Information for the details on the methods).

**Growth Inhibition Assay.** Difference in the increase of yeast biomass upon exposure to the respective chemicals for 24 h compared to the nonexposed control was used as a toxicity end point for the growth inhibition assay. Yeast biomass was evaluated by the optical density (OD<sub>600 nm</sub>) of the yeast suspensions. Tests were performed in YPD, and the test was initiated from the overnight culture (16–18 h, OD<sub>600 nm</sub> 10–11), harvested by centrifugation at 3500g for 10 min (Sigma 3–16PK, Germany) at 20 °C, and washed twice with YPD.

The cell pellet was resuspended and diluted with YPD to OD<sub>600 nm</sub> 0.1, and 75 μL of yeast culture and 75 μL of tested chemical suspension/solution in YPD (each concentration in duplicate) were pipetted into the 96-well microplates (Falcon). YPD without test chemicals was inoculated with test strains in parallel and served as a control culture (not treated, biotic control). The initial culture OD<sub>600 nm</sub> in the growth inhibition test was 0.05 (1.0 × 10<sup>6</sup> CFU/mL). After 24 h, the culture density (OD<sub>600 nm</sub>) was recorded by a Multiskan Spectrum microplate spectrophotometer (Thermo Electron Corporation, Finland). To take into account the turbidity of nano-CuO and bulk-CuO suspensions and color of CuSO<sub>4</sub> solution, the abiotic controls without yeast cells were included throughout, and these OD-values were subtracted from the respective culture OD-values.

Toxicity values (24-h IC<sub>50</sub>, mg/L), i.e., concentration of chemical which inhibited the growth of yeast cells or reduced cell viability by 50% compared to the control and their confidence intervals (95%), were computed using Log-normal model in the Excel macro REGTOX.<sup>29</sup> Throughout the study, the outcome of gene deficiency on cell viability or growth of single-gene mutants compared to wt upon exposure to the studied chemicals was evaluated by the comparison of the respective IC<sub>50</sub> values. One-way analysis of variance (ANOVA) was used to determine statistical significance of the differences between toxicity values.

**Spot Assay.** In both toxicity tests, yeast cells were studied for their ability to grow on YPD-agar plates after 24-h exposure to the tested chemicals. For this, 2 μL of yeast cell culture (treated or not treated) was pipetted onto the YPD-agar plates and incubated for 72 h at 30 °C. The growth (formation of colonies) of yeast cells was visually evaluated.

**Quantification of Dissolved Fraction of Copper.** Dissolved fraction of copper in DI and in YPD was quantified using two methods: atomic absorption spectroscopy (AAS) and recombinant Cu-sensing bacteria. For the analyses, the suspensions of nano-CuO and bulk-CuO, prepared in DI or YPD, respectively, were incubated

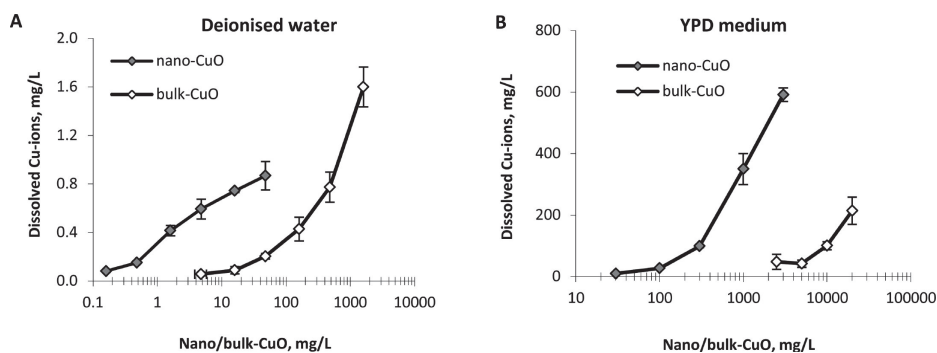


**Figure 1.** Dissolution of nano-CuO and bulk-CuO (A) in deionized water and (B) in YPD medium after 24-h exposure at 30 °C as measured by Cu-biosensor *Escherichia coli* MC1061 (pSLcueR/pDNPcopAlux). Data are the mean of 2 independent experiments  $\pm$  ranges of values.

on 24-well microplates (1 mL per well) (Falcon) at 30 °C for 24 h. To remove the nonsolubilized particles, the nano-CuO and bulk-CuO DI- and YPD-suspensions were filtered through a sterile Minisart 0.1  $\mu$ m filter (Sartorius) or ultracentrifuged at 364326g for 30 min (Beckman L8–55 M ultracentrifuge). The absence of particles in the filtrates or centrifuged supernatants of CuO-suspensions was confirmed by the Malvern Zetasizer Nano ZS as residual particles may influence the quantification of the dissolved fraction of copper in the AAS-analysis.<sup>19</sup> For the analysis of the dissolved copper, recombinant bioluminescent Cu-sensor bacteria *E. coli* MC1061 (pSLcueR/pDNPcopAlux)<sup>30</sup> and constitutively luminescent control strain *E. coli* MC1061 (pDNLux)<sup>31</sup> were used. Briefly, 100  $\mu$ L of filtrate/supernatant of nano-CuO and bulk-CuO suspension and 100  $\mu$ L of sensor/control bacteria in the special analysis medium (0.9% NaCl, 0.1% cas-amino acids and 0.1% glucose) or in YPD were mixed on white 96-well microplates (ThermoLabsystems, Finland) and incubated at 30 °C for 2 h in the dark. Luminescence was recorded with Fluoroskan Ascent luminometer (ThermoLabsystems, Finland). The amount of solubilized Cu-ions was quantified using the CuSO<sub>4</sub> calibration curve in DI or YPD, respectively. AAS-analysis of ultracentrifuged nano-CuO and bulk-CuO supernatants was performed according to standard procedures (AAS-graphite furnace; EVS-EN ISO/IEC 17025:2005) in a certified laboratory of the Institute of Chemistry of Tallinn University of Technology, Estonia.

## RESULTS

**Characterization of Nano-CuO and Bulk-CuO.** The CuO suspensions in DI and YPD medium were characterized for the hydrodynamic size and Z-potential using Malvern Zetasizer Nano ZS. The characterization was made at respective IC<sub>50</sub> concentrations of nano-CuO and bulk-CuO for the wt strain. The average hydrodynamic size of the nano-CuO at 5.0 mg/L in DI and 640 mg/L in YPD at 0 h (after the preparation of nano-CuO suspensions) was 194  $\pm$  16.9 and 5819  $\pm$  476 nm, respectively (Table 1). Thus, CuO NPs immediately aggregated in DI and especially in YPD medium. At 24 h, however, the size of nano-CuO particles/aggregates did not increase and in YPD even decreased. However, previously performed scanning electron microscopy characterization of the aqueous suspensions of studied nano-CuO<sup>16</sup> showed that despite the aggregation, the nanoscale particles were still present in the nano-CuO suspension. The Z-potential of CuO nanoparticles in DI at 0 and 24 h was 31.9  $\pm$  7.31 and 22.8  $\pm$  2.73 mV, respectively, and in YPD –15.6  $\pm$  1.13 and –14.7  $\pm$  0.10 mV, respectively. YPD medium (without CuO particles) also contained particles/proteins with average hydrodynamic size of 260  $\pm$  78.1 and 90.1  $\pm$  38.8 at 0 and 24 h, respectively,

and the Z-potential of these particles was –13.2  $\pm$  1.10 and –11.6  $\pm$  4.73, respectively (Table 1).

**Analysis of the Solubilization of Copper Ions from Nano-CuO and Bulk-CuO.** To elucidate the role of Cu-ions in the toxicity of nano-CuO as well as bulk-CuO, the solubilized fraction of copper was quantified in DI and YPD using in parallel Cu-biosensor and AAS-analysis. As the biosensor-based quantification of solubilization of metal-based nano- and microparticles is a novel bioanalysis tool,<sup>11,14,15,25</sup> AAS-analysis was used as the control/reference method. Before the analysis, suspensions of nano-CuO and bulk-CuO were filtered through the 0.1  $\mu$ m pore size filter or ultracentrifuged (364326g, 30 min). This ultracentrifugation speed and duration should settle the nanoparticles exceeding the size of 10 nm.<sup>32</sup> Analysis of the samples with Malvern Zetasizer Nano ZS showed the presence of particles in the filtrated/ultracentrifuged nano- or bulk-CuO YPD-suspensions (mean count rate >100) at low level (attenuator value was 11.0) but not in the suspensions made in deionized water (mean count rate <100). However, the same particle count rate was obtained with ultracentrifuged or filtrated YPD (i.e., nano-CuO and bulk-CuO were not added), showing the presence of particles, e.g., protein fraction (average hydrodynamic size of 3.22 and 6.21 nm, respectively), originating from the YPD medium.

The AAS-analysis and Cu-sensing bacteria yielded comparable results (Figure S1 in Supporting Information) as the chemical analysis was performed once and Cu-sensor analysis twice (independent experiments); the Cu-sensor data on the dissolution of nano-CuO and bulk-CuO in DI and YPD are presented in Figure 1. The quantification of the dissolved fraction of copper showed that the solubility of nano-CuO and bulk-CuO depended on the test environment and that nano-CuO was more soluble than bulk-CuO in both test media (Figures 1 and S1 in Supporting Information). The nano-CuO and bulk-CuO were 15–16-times more soluble in YPD than in DI (Figure 1) despite the fact that nano-CuO was more prone to aggregate in YPD than in DI and that the pH of DI was more acidic than that of YPD (Table 1). To elucidate that the organic ligand-bound copper in YPD was not removed by ultracentrifugation or filtration, YPD was supplemented with CuSO<sub>4</sub> (510 mg Cu/L), incubated at 30 °C for 24 h, and then ultracentrifuged/filtrated or not treated and analyzed by the AAS. The copper concentration in not-treated and ultracentrifuged or filtrated solutions was practically similar (495–

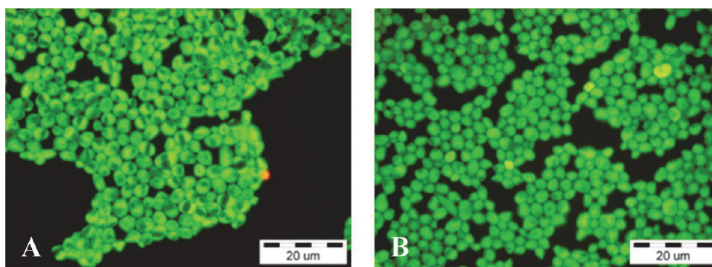


**Figure 2.** *Saccharomyces cerevisiae* BY4741 wild-type cells in control culture stained by Acridine Orange and visualized by fluorescence microscope; photos were taken after 24-h exposure of yeast cells on 96-well microplates at 30 °C (A) in deionized water and (B) in YPD medium.

513 mg Cu/L) indicating that the methods used for the removal of CuO particles prior to the quantification of solubilized Cu-ions did not influence the analysis results.

**Growth of *Saccharomyces cerevisiae* BY4741 Wild-Type and Its Single-Gene Mutants in YPD Medium.** First, the growth of *S. cerevisiae* BY4741 wild-type and mutated strains in YPD medium was studied to determine the growth pattern (duration of the lag-phase and maximum specific growth rate) of tested strains in the absence of toxicants. In general, the culture of wild-type and respective single-gene deletion mutants had similar lag-phase duration (~3 h after inoculation); the exponential growth phase was between 4 and 8 h, and by the 24th hour, the stationary phase was reached. A slightly longer lag-phase was observed in the case of the *ccs1Δ* mutant (Figure S2 in Supporting Information). The wild-type and mutated strains had comparable maximum specific growth rates ( $\mu_{max}$ ). The maximum specific growth rate of wild-type cells was  $0.47 \pm 0.03 \text{ h}^{-1}$ , only *ccs1Δ* and *sod1Δ* strains had 6–7% lower  $\mu_{max}$  ( $0.44 \pm 0.01 \text{ h}^{-1}$ ) than wt (Table S2 in Supporting Information). Thus, *S. cerevisiae* wt and its single-gene deletion mutants selected for this study had similar lag-phase duration and maximum specific growth rate in nonstress conditions.

**Viability of Biotic Controls in Cell Viability and Growth Inhibition Assays.** It is important to note that the use of deionized water as a test medium for the toxicity assay is quite unusual because in general, the test medium should be isotonic for the given test organisms. To evaluate the viability of *S. cerevisiae* BY4741 wt cells in deionized water (DI) compared to that in YPD (an optimal medium for yeast growth), the yeast cells were stained after 24-h incubation in DI or YPD by the fluorescent dye Acridine Orange (AO). AO is a DNA-intercalating dye that is taken up by both viable and dead cells and produces bright-green fluorescence when bound to double-stranded nucleic acids (predominant in viable cells) and red fluorescence when single-stranded nucleic acid prevails (predominant in stressed cells). The AO-stained control yeast cells had bright-green fluorescence (Figure 2) showing that after 24-h incubation both the cells in YPD medium as well as those in DI were viable.

**Toxicity of Nano-CuO and Bulk-CuO to *Saccharomyces cerevisiae* BY4741 Wild-Type and Its Single-Gene Mutants.** Two different test environments, deionized water for the cell viability studies and rich YPD medium for the growth inhibition analysis were used in parallel. In both cases, the cells were incubated with toxicants at 30 °C for 24 h. Toxicities, i.e.,  $IC_{50}$ -values for nano-CuO and bulk-CuO to all studied yeast strains, are presented in Figure 3 and the respective numerical

values in Table 2. The comparison of the  $IC_{50}$ -values of copper oxides to wild-type and mutated strains shows that in both toxicity assays nano-CuO was remarkably more toxic than bulk-CuO (Figure 3A–D; Table 2). For example,  $IC_{50}$ -values for nano-CuO and bulk-CuO in viability assays for *S. cerevisiae* BY4741 wt were  $4.80 \pm 0.54$  and  $155 \pm 38.7 \text{ mg/L}$ , respectively, and in the growth inhibition assay  $643 \pm 52$  and  $>20000 \text{ mg/L}$  (Figure 3A–D; Table 2). The bulk-CuO did not inhibit the growth of wt as well as single-gene deletion mutants even at 20000 mg/L except in the case of *cup2Δ* ( $IC_{50}$  13000  $\pm$  3000 mg/L) (Figure 3D; Table 2). Nano-CuO and bulk-CuO were remarkably more toxic to yeast cells when studied in distilled water compared to that in YPD medium (Figure 3A–D; Table 2). Compared to the wt, the most sensitive mutated strain in both test conditions toward nano-CuO was *cup2Δ* (3.0 and 4.5-times more than wt, respectively) (Figure 3A,B) and those toward bulk-CuO in the viability test were *cup2Δ* and *gsh1Δ* (3.6 and 2.6-times, respectively) (Figure 3C; Table 2). Interestingly, in the case of some single-gene mutants elevated resistance was observed if compared to the wt: in the cell viability test, *ccs1Δ* was 2-times more resistant toward nano-CuO (Figure 3A), and in the growth inhibition test, *ccs1Δ* and *sod1Δ* were 1.3–1.5-times more resistant than the wt (Figure 3B).

**Toxicity of Copper Ions to *Saccharomyces cerevisiae* BY4741 Wild-Type and Its Single-Gene Deletion Mutants.** Analogously to copper oxides, the toxic effect of Cu-ions to all yeast strains depended on the test medium. For example, in YPD the  $IC_{50}$ -value for wt *S. cerevisiae* was 629-times higher than in DI ( $516 \pm 6.47$  versus  $0.82 \pm 0.32$ , respectively) (Table 2). Similar to the results obtained with both copper oxides, the most sensitive strain in both toxicity assays to Cu-ions was *cup2Δ* ( $IC_{50wt}$  0.23  $\pm$  0.03 mg/L in DI and  $32.8 \pm 0.86 \text{ mg/L}$  in YPD) (Figure 3E,F). Analogously to the experiments with CuO NPs, the *ccs1Δ* strain was phenotypically more resistant to Cu-ions than wild-type in the viability assay (DI) (Figure 3E).

**Toxicity of Menadione and  $H_2O_2$  to *Saccharomyces cerevisiae* BY4741 Wild-Type and Its Single-Gene Deletion Mutants.** Differently from the experiments with copper compounds, the toxicity of menadione to all the yeast strains practically did not depend on the test medium (Figure 3G,H; Table 2). For example, in the case of the wild-type the  $IC_{50}$ -values obtained from the cell viability assay in DI was  $37.1 \pm 2.08$  and in the growth inhibition assay in YPD medium was  $29.0 \pm 4.05 \text{ mg/L}$  (Table 2). In the viability assay, all the tested mutated strains except *gsh1Δ* were more sensitive toward menadione than the wt (Figure 3G), whereas the most sensitive

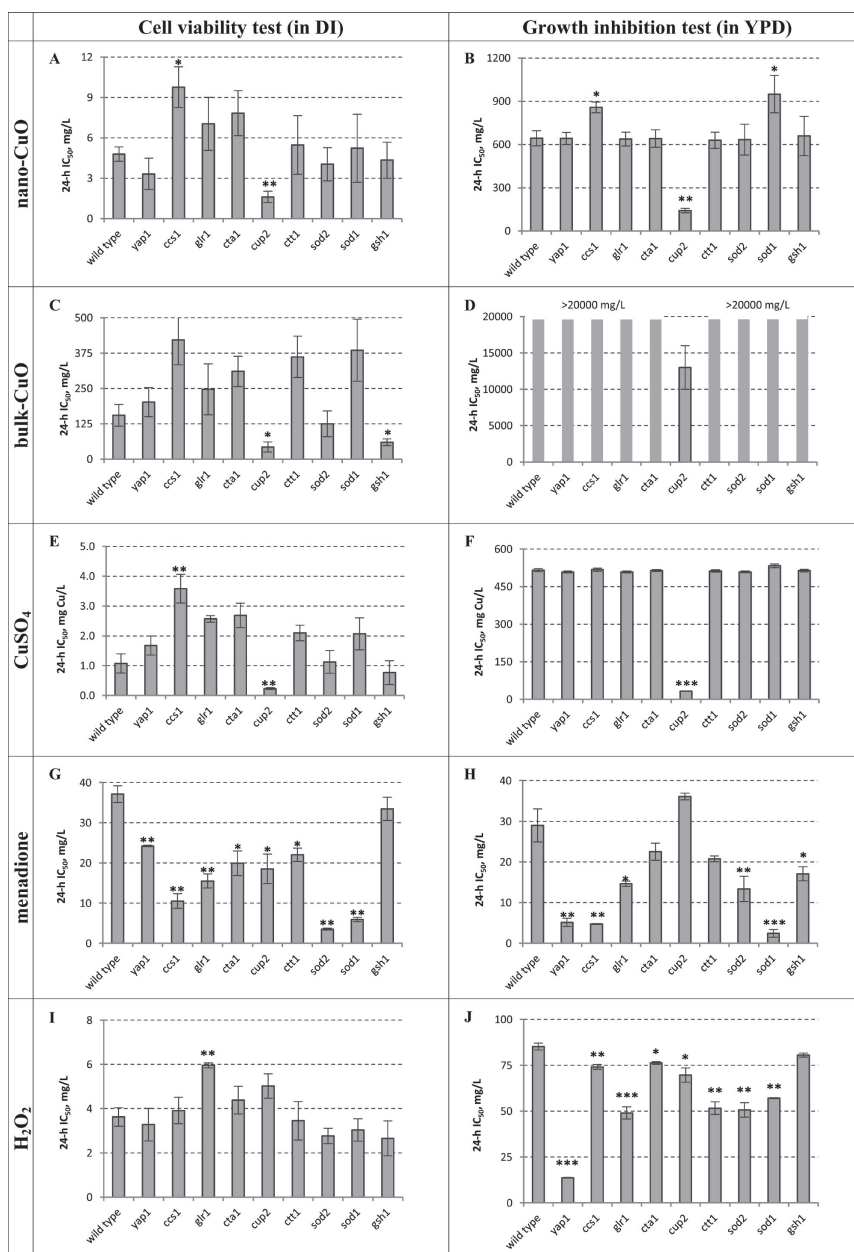


**Figure 3.** Toxicity (24-h  $IC_{50}$ , mg/L) of (A, B) nano-CuO, (C, D) bulk-CuO, (E, F)  $CuSO_4$ , (G, H) menadione, and (I, J)  $H_2O_2$  to *Saccharomyces cerevisiae* BY4741 wild-type and its isogenic single-gene mutants (*yap1Δ*, *ccs1Δ*, *gtr1Δ*, *cta1Δ*, *cup2Δ*, *ctt1Δ*, *sod2Δ*, *sod1Δ*, and *gsh1Δ*); yeast cells were exposed to the tested chemicals during 24 h at 30 °C either in deionized water (DI) (cell viability test) or in YPD medium (growth inhibition test); the mean of two or three independent experiments  $\pm$  range of values is presented; triple, double, and single asterisks denote the difference from wild-type with 99%, 95%, and 90% confidence, respectively. The numerical values of the  $IC_{50}$  are presented in Table 2.

strains (difference with wt was more than 3-times) were *sod2Δ*, *sod1Δ*, and *ccs1Δ* ( $IC_{50}$  of  $3.53 \pm 0.23$ ,  $5.89 \pm 0.53$ , and  $10.5 \pm$

$1.82$  mg/L, respectively). In the growth inhibition assay, the more vulnerable strains compared to the wt were *sod1Δ*, *ccs1Δ*,

**Table 2. Toxicity (24-h IC<sub>50</sub> (mg/L)) of Nano-CuO, Bulk-CuO, Cu<sup>2+</sup> (Tested as CuSO<sub>4</sub>), Menadione, and H<sub>2</sub>O<sub>2</sub> to *Saccharomyces cerevisiae* BY4741 Wild-Type and Respective Isogenic Single-Gene Mutants in Cell Viability and Growth Inhibition Tests**

strain	nano-CuO	bulk-CuO	Cu <sup>2+</sup>	menadione	H <sub>2</sub> O <sub>2</sub>
Cell Viability Test (24-h Exposure in Deionized Water (DI), IC <sub>50</sub> (mg/L))					
wild-type	4.80 ± 0.54	155 ± 38.7	0.82 ± 0.32	37.1 ± 2.08	3.62 ± 0.42
<i>yap1Δ</i>	3.33 ± 1.16	202 ± 51.7	1.68 ± 0.32	24.2 ± 0.17	3.28 ± 0.74
<i>ccs1Δ</i>	9.77 ± 2.28	422 ± 88.2	3.58 ± 0.48	10.5 ± 1.82	3.91 ± 0.60
<i>glr1Δ</i>	7.05 ± 2.47	247 ± 89.9	2.57 ± 0.11	15.5 ± 1.75	5.96 ± 0.11
<i>cta1Δ</i>	7.84 ± 1.67	311 ± 53.7	2.68 ± 0.41	19.9 ± 3.07	4.38 ± 0.62
<i>cup2Δ</i>	1.62 ± 0.85	43.0 ± 17.8	0.23 ± 0.03	18.5 ± 3.66	5.02 ± 0.55
<i>ctt1Δ</i>	5.48 ± 2.18	362 ± 73.1	2.10 ± 0.26	22.0 ± 1.67	3.45 ± 0.87
<i>sod2Δ</i>	4.05 ± 1.23	125 ± 45.6	1.13 ± 0.38	3.53 ± 0.23	2.76 ± 0.34
<i>sod1Δ</i>	5.23 ± 2.54	385 ± 110	2.07 ± 0.54	5.89 ± 0.53	3.03 ± 0.51
<i>gsh1Δ</i>	4.35 ± 1.34	60.2 ± 11.2	0.77 ± 0.40	33.5 ± 2.88	2.65 ± 0.79
Growth Inhibition Test (24-h Exposure in YPD Medium, IC <sub>50</sub> (mg/L))					
wild-type	643 ± 52.0	>20 000	516 ± 6.47	29.0 ± 4.05	85.2 ± 1.89
<i>yap1Δ</i>	642 ± 42.3	>20 000	509 ± 3.91	5.11 ± 1.02	13.8 ± 0.18
<i>ccs1Δ</i>	857 ± 36.8	>20 000	518 ± 6.26	4.70 ± 0.11	74.1 ± 1.28
<i>glr1Δ</i>	637 ± 48.5	>20 000	509 ± 3.76	14.6 ± 0.63	49.0 ± 3.30
<i>cta1Δ</i>	642 ± 61.1	>20 000	514 ± 3.66	22.5 ± 2.11	76.3 ± 0.68
<i>cup2Δ</i>	141 ± 15.6	~13 000	32.8 ± 0.86	36.1 ± 0.80	69.7 ± 3.86
<i>ctt1Δ</i>	630 ± 56.3	>20 000	513 ± 4.43	20.7 ± 0.72	51.6 ± 3.48
<i>sod2Δ</i>	634 ± 107	>20 000	509 ± 3.61	13.4 ± 3.10	50.7 ± 3.95
<i>sod1Δ</i>	950 ± 130	>20 000	533 ± 6.87	2.40 ± 0.90	57.0 ± 0.30
<i>gsh1Δ</i>	660 ± 136	>20 000	514 ± 5.07	17.1 ± 1.74	80.6 ± 1.14

*yap1Δ*, and *sod2Δ* (IC<sub>50</sub> 2.40 ± 0.90, 4.70 ± 0.11, 5.11 ± 1.02, and 13.4 ± 3.10 mg/L, respectively). Differently from the viability assay, in the growth inhibition test the *cup2Δ* strain had sensitivity comparable to that of menadione than wild-type (Figure 3H).

The experiments with H<sub>2</sub>O<sub>2</sub> showed that in the growth inhibition test all the tested mutants, except *gsh1Δ*, were more susceptible to H<sub>2</sub>O<sub>2</sub> than the wild-type and that the most sensitive strain (6-times difference with wt) was *yap1Δ* (Figure 3J). However, in the viability assay in DI there was no difference in the sensitivities between wild-type and single-gene mutants to H<sub>2</sub>O<sub>2</sub>, except for *glr1Δ*, which was more resistant than the wild-type (Figure 3I).

**Spot Test.** At the end of both toxicity tests, treated and not treated yeast cells were examined for their ability to grow/form colonies on the toxicant-free YPD-agar plates. In general, the sensitivity pattern of tested strains in the Spot test was coherent with the cell viability and growth inhibition assays results (Figures 3 and 4). After the exposure to nano-CuO, bulk-CuO, and Cu-ions in cell viability and growth inhibition tests, the most sensitive strain in the spot assay was *cup2Δ* (Figure 4A–F) and to menadione and H<sub>2</sub>O<sub>2</sub> after exposure in the growth inhibition test *sod1Δ* and *yap1Δ*, respectively (Figure 4H,J). Although, the most sensitive strain to menadione in the viability test was *sod2Δ*, in the Spot test the most sensitive strain was *sod1Δ* (Figure 4G).

## DISCUSSION

**Relevance of the Chosen OS-Response Deficient Mutant Strains of *S. cerevisiae* BY4741 for the Evaluation of OS-Inducing Chemicals.** The suitability of the chosen mutant strains for the profiling of OS-inducing chemicals was evaluated by menadione and H<sub>2</sub>O<sub>2</sub>. Compared to the *S. cerevisiae* BY4741 wild-type, the more susceptible mutant strains (up to 12-times) to menadione in both test

formats were *sod1Δ*, *sod2Δ*, *ccs1Δ*, and *yap1Δ* and to H<sub>2</sub>O<sub>2</sub> in the growth inhibition test was *yap1Δ* (Figure 3; Table 2). Thus, these single-gene deletion mutants of *S. cerevisiae* could be used for the phenotype sensitivity based toxicological profiling of chemicals/NPs that are expected to cause oxidative stress via the same mechanisms as menadione and H<sub>2</sub>O<sub>2</sub>. The remarkably increased sensitivity of *sod1Δ*, *sod2Δ*, *ccs1Δ*, and *yap1Δ* to menadione was expected as the cytosolic Sod1p and mitochondrial Sod2p both catalyze the dismutation of the superoxide radicals (O<sup>2•</sup>) to O<sub>2</sub> and H<sub>2</sub>O<sub>2</sub>. Ccs1p is a copper chaperon for Sod1p, and Yap1p is a basic leucine-zipper transcription factor required for oxidative stress response (Table S1 in Supporting Information). Interestingly, only the *gsh1Δ* strain in the cell viability test had sensitivity similar to that of the wild-type to menadione; however, in the growth inhibition test, menadione was more toxic to *gsh1Δ* than to the wild-type strain (Figure 3 G,H). The latter can be explained by the fact that respiro-fermentatively/respiratively growing *S. cerevisiae* cells have energetically functional mitochondria,<sup>35</sup> and it has been shown that the *gsh1Δ* mutant strain exhibits the instability of the mitochondrial genome.<sup>34</sup> The most vulnerable strain to H<sub>2</sub>O<sub>2</sub> in the growth inhibition test was the OS-response transcription factor deficient strain (*yap1Δ*) (differences with wt of more than 6-times) (Figure 3J). Although the role of catalases as peroxide scavengers in the eukaryotic cells have been reported, the catalase-negative strains for cytosolic (*ctt1Δ*) and peroxisomal (*cta1Δ*) catalases were not more sensitive to H<sub>2</sub>O<sub>2</sub> compared to the wt strain in the viability test, and in the growth inhibition assay, only *cta1Δ* was more vulnerable than wt (~1.6-times) (Figure 3L,J; Table 2). These findings refer to the functional redundancy of the genes responsible for the detoxification of H<sub>2</sub>O<sub>2</sub> in the yeast cells. Interestingly, in the viability test the respective H<sub>2</sub>O<sub>2</sub> IC<sub>50</sub> values for *S. cerevisiae* BY4741 wt and mutants (except *yap1Δ*) were ~23-times lower than those in the growth inhibition assay

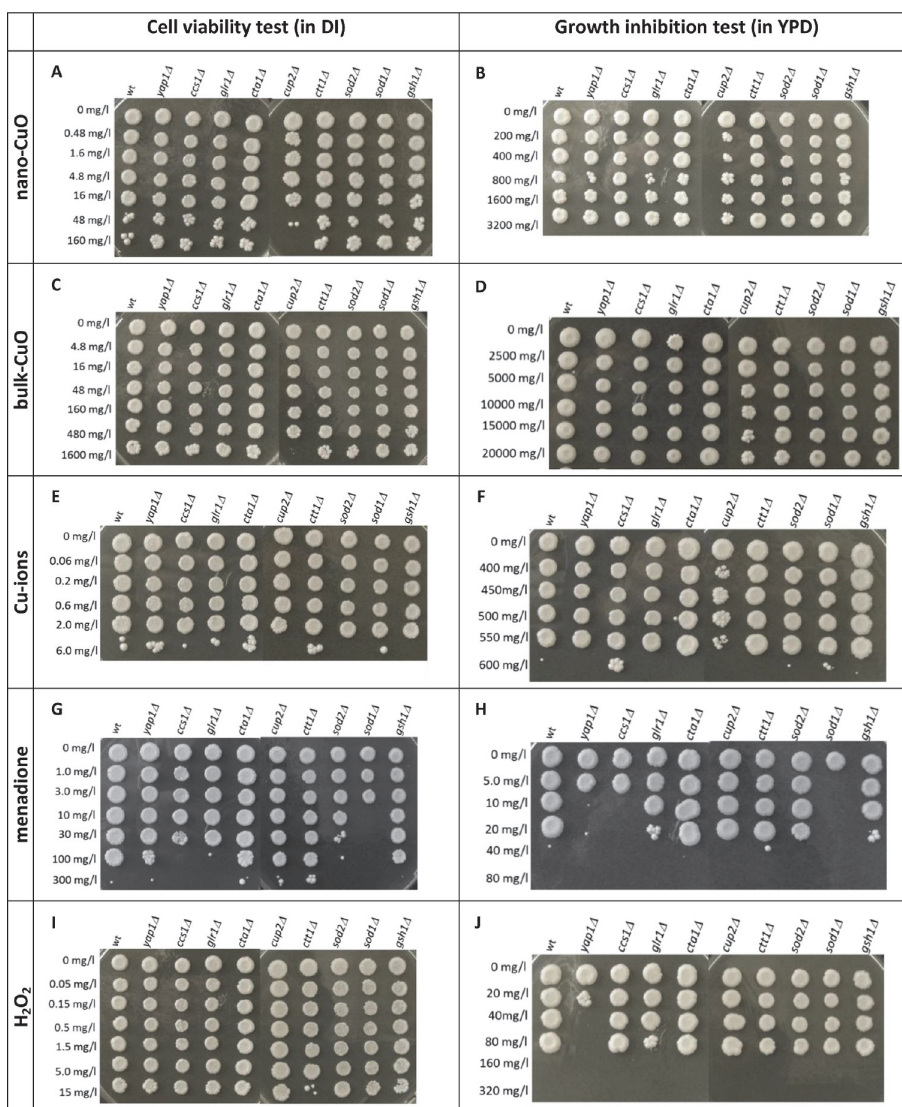


**Figure 4.** Growth of *Saccharomyces cerevisiae* BY4741 wild-type and its single-gene deletion mutants (*yap1Δ*, *ccs1Δ*, *glr1Δ*, *ctal1Δ*, *cup2Δ*, *ct11Δ*, *sod2Δ*, *sod1Δ*, and *gsh1Δ*) after exposure to (A, B) nano-CuO, (C, D) bulk-CuO, (E, F)  $\text{CuSO}_4$ , (G, H) menadione, and (I, J)  $\text{H}_2\text{O}_2$  in the cell viability test in DI or in the growth inhibition test in YPD on 96-well microplates at 30 °C for 24 h; after 24 h of exposure, 2  $\mu\text{L}$  of the culture was pipetted onto the YPD-agar plates and incubated for 72 h at 30 °C.

(Table 2). This phenomenon may be explained by the oxidation of the organics present in the YPD medium by  $\text{H}_2\text{O}_2$ .

**Role of Oxidative Stress in the Toxic Effect of Cu NPs toward Yeast *S. cerevisiae* BY4741.** Surprisingly, the phenotypic sensitivity pattern of the selected mutants upon exposure to nano-CuO, bulk-CuO (size control), and Cu-ions (solubility control) was different from that of menadione and  $\text{H}_2\text{O}_2$ . Namely, the mutant strains with elevated sensitivity to menadione and  $\text{H}_2\text{O}_2$  were not more susceptible than the wild-

type to nano-CuO, bulk-CuO, and to  $\text{CuSO}_4$  (Figure 3A–F; Table 2). These data are not coherent with the studies reporting that copper compounds are prone to induce the oxidative damage of proteins<sup>35</sup> and membrane lipids.<sup>36</sup> Moreover, the dissolution of nano-CuO has been reported as a key factor triggering the OS and DNA damage response in *E. coli*.<sup>11</sup> It has also been shown that the lipid peroxidation byproduct malondialdehyde was more toxic to the *yap1Δ* strain than to wild-type *S. cerevisiae*.<sup>37</sup> However, in the current

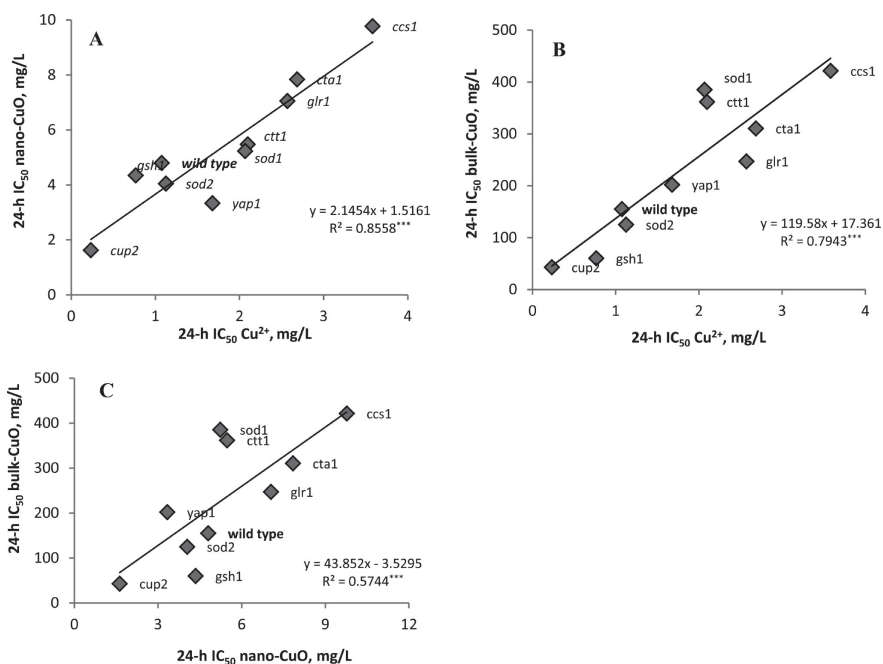


**Figure 5.** Comparison of the cell viability assay toxicity data (24-h  $IC_{50}$ , mg/L) for tested copper compounds for all the studied *S. cerevisiae* BY4741 wild-type and respective single-gene deletion mutants, (A) copper ions versus nano-CuO, (B) copper ions versus bulk-CuO, and (C) nano-CuO versus bulk-CuO. Data are plotted from Table 2. \*\*\*,  $R^2$  values are statistically significant at a 99% confidence level.

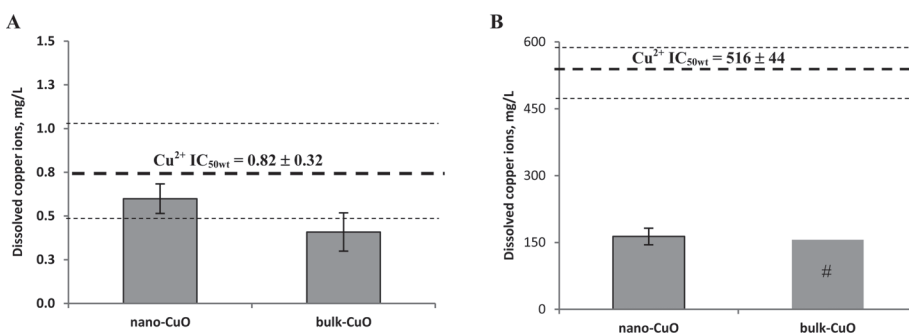


**Figure 6.** Concentration of solubilized copper-ions at the 24-h  $IC_{50}$  values of nano-CuO and bulk-CuO for *S. cerevisiae* BY4741 wild-type strain (A) in the cell viability test (in DI) and (B) in the growth inhibition test (in YPD medium). Concentrations of dissolved Cu-ions at  $IC_{50}$  values (filled bars; C,D) were calculated from the respective dissolution curves of nano-CuO and bulk-CuO (Figure 1). The area between dashed horizontal lines (A,B) represents the 24-h  $IC_{50}$  values  $\pm$  range of values of *S. cerevisiae* BY4741 wild-type for Cu-ions in DI and in YPD medium, respectively. Data are the mean of 2 independent experiments  $\pm$  ranges of values; # concentration of solubilized Cu-ions from 20000 mg/L of bulk-CuO (i.e., below the  $IC_{50}$  value; see Table 2).

experiments the *yap1* $\Delta$  and wild-type yeast had similar sensitivities to the tested copper compounds (Figure 3A–F; Table 2), showing that these compounds probably did not cause the oxidative damage in cellular membranes. Thus, it could be assumed that nano-CuO (but also bulk-CuO and Cu-ions) exerts its toxicity to *S. cerevisiae* by different mechanisms than menadione and  $H_2O_2$ .

**Role of Dissolved Copper in the Toxic Effect of CuO NPs toward Yeast *S. cerevisiae* BY4741.** Upon exposure to nano-CuO, bulk-CuO, and copper ions in both toxicity tests, the most sensitive strain compared to the wild-type was *cup2* $\Delta$ . The Cup2p is a transcription factor, which regulates the expression of metallothioneins encoding genes CUP1–1 and CUP1–2 in yeast as a response to copper stress,<sup>38</sup> and the disruption of the CUP2 gene resulted in elevated sensitivity to

copper compounds.<sup>39</sup> As indicated above, Cu-ions, nano-CuO, and bulk-CuO were remarkably less toxic to yeast cells if tested in rich YPD medium than in deionized water (629-fold in case of Cu-ions; Table 2). The differences in the IC<sub>50</sub>-values in these two media can be explained by copper speciation: in rich media/environment, the organic ligands bind Cu-ions and render Cu-ions as well as nano-CuO and bulk-CuO less bioavailable and thus less toxic.<sup>40–42</sup> Moreover, it could be assumed that upon dispersion of nano-CuO in organics-containing medium (e.g., YPD) two simultaneous processes took place: (i) enhanced dissolution of copper due to the increased dispersion of CuO facilitated by the dissolved organic matter and (ii) dissolved copper complexing by organic matter present in the rich medium.<sup>42</sup> Cronholm et al.<sup>43</sup> have also shown that the serum in the cell medium resulted in less CuO nanoparticle agglomeration and increased Cu release.

On the basis of the *S. cerevisiae* BY4741 wild-type and single-gene mutants' sensitivity profile to nano-CuO, bulk-CuO, and Cu-ions (Figures 3 and 4; Table 2), the toxicity of nano-CuO and bulk-CuO was assumingly caused by Cu-ions. This was supported also by the significant correlation between the IC<sub>50</sub>-values of all tested strains to Cu-ions and nano-CuO, both in the viability assay ( $R^2 = 0.86$ ; Figure 5A) and in the growth inhibition test ( $R^2 = 0.75$ , data not shown) and between Cu-ions and bulk-CuO in the viability test ( $R^2 = 0.79$ ; Figure 5B). Moreover, the correlation ( $R^2 = 0.57$ ) between the viability test IC<sub>50</sub>-values for nano-CuO and bulk-CuO revealed that both CuO formulations had the same mode of action in DI (Figure 5C). The comparison of the concentration of the dissolved fraction of copper in the nano-CuO and bulk-CuO DI- and YPD-suspensions (Figure 6A,B) at IC<sub>50wt</sub> values with the IC<sub>50wt</sub> values for copper ions (Table 2) showed that (i) in the viability assay conducted in DI the toxicity of nano-CuO and bulk-CuO was probably caused by the released Cu-ions (Figure 6A) as there was no statistically significant difference between the concentration of solubilized copper ions ( $0.61 \pm 0.03$  and  $0.43 \pm 0.09$  mg Cu/L at nano-CuO and bulk-CuO concentrations of 4.8 and 155 mg/L, respectively) with IC<sub>50</sub>-values for Cu-ions in DI ( $0.82 \pm 0.32$  mg/L); (ii) in the growth inhibition assay conducted in YPD the solubilized Cu-ions, however, did not explain all the toxicity of nano-CuO as at the nano-CuO concentration of  $643 \pm 52.0$  mg/L, the concentration of dissolved Cu-ions was  $198 \pm 23$  mg/L (Figure 6B), which is 2.6-fold lower than the IC<sub>50wt</sub>-values for copper ions ( $516 \pm 6.47$  mg/L in YPD). The difference was statistically significant at the 95% level. Interestingly, in the bulk-CuO YPD-suspension at the concentration of 20000 mg/L (growth inhibition less than 20%), the solubilized fraction of copper ions ( $201 \pm 32$  mg Cu/L) was quite similar to the dissolved Cu-ions concentration ( $198 \pm 23$  mg Cu/L) in the nano-CuO YPD-suspension ( $643 \pm 52.0$  mg nano-CuO/L) that inhibited the growth of yeast by 50%, but there was no adverse effect on the growth of yeast cells. This interesting observation suggests that upon exposure of yeast cells to CuO NPs in YPD medium, yeast seemed to be affected by other fractions of copper in addition to Cu-ions dissolved in the test medium. This discrepancy, as noted above, was not observed if the yeasts were exposed to CuO NPs in DI. McQuillan et al.<sup>44</sup> have shown that silver NPs enhanced the silver-ion stress response in *E. coli* due to the additional dissolution of NPs in the close vicinity of the cell membrane. One may assume that an analogous mechanism, i.e., additional dissolution of CuO NPs close to the yeast cell wall took place in the growth inhibition

experiments in YPD medium. This is in some contradiction with the fact that in YPD the nano-CuO particles had negative Z-potential ( $-15.6$  mV) but in DI the particles were positively charged ( $31.9$  mV) (Table 1). As the yeast cells were negatively charged in both test media (Z-potential of  $-2.58$  mV in DI and  $-36.2$  mV in YPD), it is possible that nano-CuO particles more efficiently sorbed to yeast cells in DI than in YPD. There is also another possible explanation for the enhanced bioavailability of nano-CuO in YPD medium: as bare nanoparticles in rich growth media immediately acquired a coating of peptides/proteins present in the YPD medium,<sup>45</sup> the protein-coated NPs are better dispersed (hydrodynamic size decreased during 24-h incubation by the dispersion and/or dissolution), and the formed protein corona on the NP surface may enhance the sorption of the NPs onto the yeast surface via specific nutrient-recognizing receptors, e.g., peptide transport system receptors.<sup>46</sup> Thus, the protein-coated NPs even may be misleadingly recognized by yeast as a food, and the sorption may lead to enhanced solubility of the sorbed NPs in the vicinity of the cell wall and enhanced toxic effect. These additionally solubilized Cu-ions, however, were not quantified by the methods used for the analysis of the extracellular solubilized fraction of Cu-ions in the current study. Enhanced effect of adsorbed serum-proteins on the CuO NP uptake by the intestinal Caco-2 cells has been proposed also by Piret et al.<sup>47</sup> As yeast cells have a rigid cell wall and the enhanced uptake due to the NP sorption onto the cells is unlikely, we exclude the Trojan-horse mechanism, i.e., additional release of Cu-ions in the cytosol after the uptake of NPs as described by Limbach et al.<sup>48</sup> for mammalian cells *in vitro*.

## CONCLUSIONS

We conclude that (i) all nine single-gene deletion mutants had practically similar growth patterns as the wild-type strain in toxicant-free YPD medium; (ii) the OS-vulnerable mutants *sod1Δ*, *sod2Δ*, *ccs1Δ*, and *yap1Δ* showed up to 12-fold elevated sensitivity toward OS standard chemicals (menadione and H<sub>2</sub>O<sub>2</sub>) but not to nano-CuO indicating that nano-CuO exerts toxicity to yeast cells via a different mechanism than menadione and H<sub>2</sub>O<sub>2</sub>; (iii) on the basis of copper to all the studied strains the order of the toxicity was as follows: CuSO<sub>4</sub> > nano-CuO > bulk-CuO. The bulk-CuO was about 45-fold less toxic than nano-CuO and about 120-fold less toxic than Cu-ions in the cell viability test (in DI); (iv) as the copper-vulnerable mutant strain *cup2Δ* was up to 16-fold more sensitive to nano-CuO as well to bulk-CuO and Cu-ions, the toxic effect of both copper oxides was exerted via solubilized Cu-ions; (v) the discrepancy between the analysis of solubilized copper and observed toxic effects in the case of assays performed in organics-containing YPD medium may be explained by the stronger sorption of protein-coated NPs onto the cell surface that may facilitate the dissolution of copper in the close vicinity of the cell wall; (vi) because of the complexation of copper ions and decrease in bioavailability, the apparent toxicity of nano-CuO, bulk-CuO, and Cu-ions in organics-rich YPD medium was up to 630-fold lower than in deionized water (DI); (vii) as *S. cerevisiae* cells retained their viability in deionized water even by the 24th hour of incubation, the DI medium is recommended for the profiling of the basal toxicity of chemicals toward yeast; (viii) the mechanism-based phenotypic profiling using *S. cerevisiae* wild-type and single-gene deletion mutants is a promising technique that allows cost-efficient screening of the mode of action of chemicals/NPs.

## ■ ASSOCIATED CONTENT

### ■ Supporting Information

*Saccharomyces cerevisiae* BY4741 single-gene deletion mutants used in this work; dissolution of nano-CuO and bulk-CuO in deionized water and in YPD medium; *Saccharomyces cerevisiae* BY4741 wild-type and its single-gene deletion mutant growth in YPD medium; and growth characteristics of *Saccharomyces cerevisiae* BY4741 wild-type and its single-gene deletion mutants. This material is available free of charge via the Internet at <http://pubs.acs.org>.

## ■ AUTHOR INFORMATION

### Corresponding Author

\*Phone: +372 6398361. Fax: +372 6398382. E-mail: [kaja.kasemets@kbf.i.ee](mailto:kaja.kasemets@kbf.i.ee).

### Funding

This research was supported by the Estonian target funding project SF0690063s08 and the Estonian Science Foundation Grants 7686, 8561, and 9001, and EU 7th Framework Programme under grant agreement no. 263147 (NanoValid).

### Notes

The authors declare no competing financial interest.

## ■ ACKNOWLEDGMENTS

Aleksandr Käkinen is acknowledged for skillful technical assistance.

## ■ REFERENCES

- (1) Kahru, A., and Ivask, A. (2012) Mapping the dawn of nanoecotoxicological research. *Acc. Chem. Res.* [Online early access], DOI: 10.1021/ar3000212, published online Nov 13, 2012.
- (2) Diaz-Ruiz, R., Rigoulet, M., and Devin, A. (2010) The Warburg and Crabtree effects: On the origin of cancer cell energy metabolism and of yeast glucose repression. *Biochim. Biophys. Acta* 1807, 568–576.
- (3) Winzeler, E. A., Shoemaker, D. D., Astromoff, A., Liang, H., Anderson, K., Andre, B., Bangham, R., Benito, R., et al. (1999) Functional characterization of the *Saccharomyces cerevisiae* genome by gene deletion and parallel analysis. *Science* 285, 901–906.
- (4) Wach, A., Brachat, A., Pöhlmann, R., and Philippsen, P. (1994) New heterologous modules for classical or PCR-based gene disruption in *Saccharomyces cerevisiae*. *Yeast* 10, 1793–1808.
- (5) European *Saccharomyces Cerevisiae* Archive for Functional Analysis Website, <http://web.uni-frankfurt.de/fb15/mikro/euroscarf/>
- (6) Higgins, V. J., Alic, N., Thorpe, G. W., Breitenbach, M., Larsson, V., and Dawes, I. W. (2002) Phenotypic analysis of gene deletant strains for sensitivity to oxidative stress. *Yeast* 19, 203–214.
- (7) Ivask, A., Suarez, E., Patel, T., Boren, D., Ji, Z., Holden, P., Telesca, D., Damoiseaux, R., Bradley, K. A., and Godwin, H. (2012) Genome-wide bacterial toxicity screening uncovers the mechanisms of toxicity of a cationic polystyrene nanomaterials. *Environ. Sci. Technol.* 46, 2398–2405.
- (8) Kahru, A., and Savolainen, K. (2010) Potential hazard of nanoparticles: From properties to biological and environmental effects. *Toxicology* 269, 89–91.
- (9) Kahru, A., and Dubourguier, H.-C. (2010) From ecotoxicology to nanoecotoxicology. *Toxicology* 269, 105–119.
- (10) Gabbay, J., Borkow, G., Mishal, J., Magen, E., Zatcoff, R., and Shemer-Avni, Y. (2006) Copper oxide impregnated textiles with potent biocidal activities. *J. Ind. Text.* 35, 323–335.
- (11) Bondarenko, O., Ivask, A., Käkinen, A., and Kahru, A. (2012) Sub-toxic effects of CuO nanoparticles on bacteria: kinetics, role of Cu ions and possible mechanisms of action. *Environ. Pollut.* 169, 81–89.
- (12) Ren, G., Hu, D., Cheng, E. W. C., Vargas-Reus, M. A., Reip, P., and Allaker, R. P. (2009) Characterisation of copper oxide nanoparticles for antimicrobial applications. *Int. J. Antimicrob. Agents* 33, 587–590.
- (13) Baek, Y. W., and An, Y. J. (2011) Microbial toxicity of metal oxide nanoparticles (CuO, NiO, ZnO, and Sb<sub>2</sub>O<sub>3</sub>) to *Escherichia coli*, *Bacillus subtilis* and *Streptococcus aureus*. *Sci. Total Environ.* 409, 1603–1608.
- (14) Heinlaan, M., Ivask, A., Blinova, I., Dubourguier, H.-C., and Kahru, A. (2008) Toxicity of nanosized and bulk ZnO, CuO and TiO<sub>2</sub> to bacteria *Vibrio fischeri* and crustaceans *Daphnia magna* and *Thamnocephalus platyurus*. *Chemosphere* 71, 1308–1316.
- (15) Aruoja, V., Dubourguier, H.-C., Kasemets, K., and Kahru, A. (2009) Toxicity of nanoparticles of CuO, ZnO and TiO<sub>2</sub> to microalgae *Pseudokirchneriella subcapitata*. *Sci. Total Environ.* 407, 1461–1468.
- (16) Kahru, K., Dubourguier, H.-C., Blinova, I., Ivask, A., and Kasemets, K. (2008) Biotests and biosensors for ecotoxicology of metal oxide nanoparticles: A minireview. *Sensors* 8, 5153–5170.
- (17) Golobic, M., Jemec, A., Drobne, D., Romih, T., Kasemets, K., and Kahru, A. (2012) Upon exposure to Cu nanoparticles, accumulation of copper in the isopod *Porcellio scaber* is due to the dissolved Cu ions inside the digestive tract. *Environ. Sci. Technol.* 46, 12112–12119.
- (18) Mortimer, M., Kasemets, K., Vodovnik, M., Marinšek-Logar, R., and Kahru, A. (2011) Exposure to CuO nanoparticles changes the fatty acid composition of protozoa *Tetrahymena thermophila*. *Environ. Sci. Technol.* 45, 6617–6624.
- (19) Heinlaan, M., Kahru, A., Kasemets, K., Arbeille, B., Prensier, G., and Dubourguier, H. C. (2011) Changes in the *Daphnia magna* midgut upon ingestion of copper oxide nanoparticles: a transmission electron microscopy study. *Water Res.* 45, 179–190.
- (20) Shi, J., Abid, A. D., Kennedy, I. M., Hristova, K. R., and Wendy, K. (2011) To duckweeds (*Landoltia punctata*), nanoparticulate copper oxide is more inhibitory than soluble copper in the bulk solution. *Environ. Pollut.* 159, 1277–1282.
- (21) Nel, A., Xia, T., Mädler, L., and Li, N. (2006) Toxic potential of materials at the nanoscale level. *Science* 311, 622–627.
- (22) Karlsson, H. L., Cronholm, P., Gustafsson, J., and Möller, L. (2008) Copper oxide nanoparticles are highly toxic: a comparison between metal oxide nanoparticles and carbon nanotubes. *Chem. Res. Toxicol.* 21, 1726–1732.
- (23) Karlsson, H. L., Gustafsson, J., Cronholm, P., and Moller, L. (2009) Size-dependent toxicity of metal oxide particles: a comparison between nano- and micrometer size. *Toxicol. Lett.* 188, 112–118.
- (24) Wang, Z., Li, N., Zhao, J., White, J. C., Qu, P., and Xing, B. (2012) CuO nanoparticles interaction with human epithelial cells: Cellular uptake, location, export, and genotoxicity. *Chem. Res. Toxicol.* 25, 1512–1521.
- (25) Kasemets, K., Ivask, A., Dubourguier, H.-C., and Kahru, A. (2009) Toxicity of nanoparticles of ZnO, CuO and TiO<sub>2</sub> to yeast *Saccharomyces cerevisiae*. *Toxicol. in Vitro* 23, 1116–1122.
- (26) Jamieson, D. J. (1998) Oxidative stress responses of the yeast *Saccharomyces cerevisiae*. *Yeast* 14, 1511–1527.
- (27) Jo, W. J., Loguinov, A., Chang, M., Wintz, H., Nislow, C., Arkin, A. P., Giaver, G., and Vulpe, C. D. (2008) Identification of genes involved in the toxic response of *Saccharomyces cerevisiae* against iron and copper overload by parallel analysis of deletion mutants. *Toxicol. Sci.* 101, 140–151.
- (28) Kasemets, K., Kahru, A., Laht, T.-M., and Paalme, T. (2006) Study of the toxic effect of short- and medium-chain monocarboxylic acids on the growth of *Saccharomyces cerevisiae* using the CO<sub>2</sub>-auxo-accelerator fermentation system. *Int. J. Food Microbiol.* 111, 206–215.
- (29) REGTOX, Copyright(C) 2001, Eric Vindimian, <http://eric.vindimian9online.fr/>.
- (30) Ivask, A., Rõlova, T., and Kahru, A. (2009) A suite of recombinant luminescent bacterial strains for the quantification of bioavailable heavy metals and toxicity testing. *BMC Biotechnol.* 9, 41.
- (31) Leedjärvi, A., Ivask, A., Virta, M., and Kahru, A. (2006) Analysis of bioavailable phenols from natural samples by recombinant luminescent bacterial sensors. *Chemosphere* 64, 1910–1919.

- (32) Tsao, T. M., Wang, M. K., and Huang, P. M. (2009) Automated ultrafiltration device for efficient collection of environmental nanoparticles from aqueous suspensions. *Solid. Sci. Soc. Am. J.* 73, 1808–1616.
- (33) Kasemets, K., Nisamedtinov, I., Laht, T.-M., Abner, K., and Paalme, T. (2007) Growth characteristics of *Saccharomyces cerevisiae* S288C in changing environmental conditions: auxo-accelerostat study. *Antonie Leeuwenhoek* 92, 109–128.
- (34) Ayer, A., Tan, S.-X., Grant, C. M., Meyer, A. J., Dawes, I. W., and Perrone, G. G. (2010) The critical role of glutathione in maintenance of the mitochondrial genome. *Free Radical Biol. Med.* 49, 1956–1968.
- (35) Shanmuganathana, A., Avery, S. V., Willetts, S. A., and Houghton, J. E. (2004) Copper-induced oxidative stress in *Saccharomyces cerevisiae* targets enzymes of the glycolytic pathway. *FEBS Lett.* 556, 253–259.
- (36) Howlett, N. G., and Avery, V. (1997) Induction of lipid peroxidation during heavy metal stress in *Saccharomyces cerevisiae* and influence of plasma membrane fatty acid unsaturation. *Appl. Environ. Microbiol.* 63, 2971–2976.
- (37) Turton, H. E., Dawes, I. W., and Grant, C. M. (1997) *Saccharomyces cerevisiae* exhibits a  $\gamma$ AP-1-mediated adaptive response to malondialdehyde. *J. Bacteriol.* 4, 1096–1101.
- (38) Yasokawa, D., Murata, S., Kitagawa, E., Iwahashi, Y., Nakagawa, R., Hashido, T., and Iwahashi, H. (2008) Mechanisms of copper toxicity in *Saccharomyces cerevisiae* determined by microarray analysis. *Environ. Toxicol.* 23, 555–606.
- (39) Jo, W. J., Loguinov, A., Chang, M., Wintz, H., Nislow, C., Arkin, A. P., Giaver, G., and Vulpe, C. D. (2008) Identification of genes involved in the toxic response of *Saccharomyces cerevisiae* against iron and copper overload by parallel analysis of deletion mutants. *Toxicol. Sci.* 101, 140–151.
- (40) Hughes, M. N., and Poole, R. K. (1991) Metal speciation and microbial growth: the hard (and soft) facts. *J. Gen. Microbiol.* 137, 725–734.
- (41) Blinova, I., Ivask, A., Mortimer, M., and Kahru, A. (2009) Ecotoxicity of nanoparticles of CuO and ZnO in natural water. *Environ. Pollut.* 158, 41–47.
- (42) Käkinen, A., Bondarenko, O., Ivask, A., and Kahru, A. (2011) The effect of composition of different ecotoxicological test media on free and bioavailable copper from CuSO<sub>4</sub> and CuO nanoparticles: Comparative evidence from a Cu-selective electrode and a Cu-biosensor. *Sensors* 11, 10502–10521.
- (43) Cronholm, P., Midander, K., Karlsson, H. L., Elihn, K., Wallinder, I. O., and Möller, L. (2011) Effect of sonication and serum proteins on copper release from copper nanoparticles and toxicity towards lung epithelial cells. *Nanotoxicology* 5, 269–281.
- (44) McQuillan, J. S., Infante, H. G., Stokes, E., and Shaw, A. M. (2012) Silver nanoparticles enhanced silver ion stress response in *Escherichia coli* K12. *Nanotoxicology* 6, 857–866.
- (45) Cedervall, T., Lynch, I., Lindman, S., Berggård, T., Thulin, E., Nilsson, H., Dawson, K. A., and Linse, S. (2007) Understanding the nanoparticle-protein corona using methods to quantify exchange rates and affinities of proteins for nanoparticles. *Proc. Natl. Acad. Sci. U.S.A.* 104, 2050–2055.
- (46) Wiles, A. M., Cai, H., Naider, F., and Becker, J. M. (2006) Nutrient regulation of oligopeptide transport in *Saccharomyces cerevisiae*. *Microbiology* 152, 3133–3145.
- (47) Piret, J.-P., Vankoningsloo, S., Mejia, J., Noël, F., Boilan, E., Lambinon, F., Zouboulis, C. C., Masereel, B., Lucas, S., Saout, C., and Toussaint, O. (2012) Differential toxicity of copper (II) oxide nanoparticles of similar hydrodynamic diameter on human differentiated intestinal Caco-2 cell monolayers is correlated in part to copper release and shape. *Nanotoxicology* 6, 789–803.
- (48) Limbach, L. K., Wick, P., Manser, P., Grass, R. N., Bruinink, A., and Stark, W. J. (2007) Exposure of engineered nanoparticles to human lung epithelial cells: influence of chemical composition and catalytic activity on oxidative stress. *Environ. Sci. Technol.* 41, 4158–4163.

## SUPPORTING INFORMATION

### Toxicity of CuO nanoparticles to yeast *Saccharomyces cerevisiae* BY4741 wild-type and its nine isogenic single-gene deletion mutants

*Kaja Kasemets*<sup>\*,a</sup>, *Sandra Suppi*<sup>a,b</sup>, *Kai Künnis-Beres*<sup>a</sup> and *Anne Kahru*<sup>a</sup>

<sup>a</sup> National Institute of Chemical Physics and Biophysics, Laboratory of Environmental Toxicology, Akadeemia tee 23, Tallinn 12618, Estonia

<sup>b</sup> Department of Chemical and Materials Technology, Tallinn University of Technology, Ehitajate tee 5, Tallinn 19086, Estonia

\*Corresponding author

#### SUMMARY

##### Materials and Methods

**Table S1.** *Saccharomyces cerevisiae* BY4741 single-gene deletion mutants used in this work

Cultivation of *Saccharomyces cerevisiae* BY4741 wild-type and single-gene deletion mutants in YPD

Viability assessment of yeast cells by the fluorescent stain Acridine Orange

##### Results

**Figure S1.** Dissolution of nano-CuO and bulk-CuO in deionized water and in YPD medium

**Figure S2.** *Saccharomyces cerevisiae* BY4741 wild-type and its single-gene deletion mutants growth on 96-well microplates in YPD medium at 30°C during 24 hours

**Table S2.** Growth characteristics of *Saccharomyces cerevisiae* BY4741 wild-type and its single-gene deletion mutants grown on 96-well microplate in YPD at 30°C during 24 hours

##### References

## MASTERIALS AND METHODS

**Table S1.** Single-gene deletion mutants of *Saccharomyces cerevisiae* BY4741 used in the current work. Strains originate from the EUROSCARF collection (Institute of Microbiology, University of Frankfurt, Germany).

Strain	ORF <sup>a</sup>	Cellular role of gene product <sup>b</sup>	Sensitivity phenotype of single-gene deletion mutant <sup>c</sup>
<i>yap1Δ</i>	YML007w	Basic leucine-zipper transcription factor activates the encoding of anti-oxidant genes (e.g. TRR1, TRX2, GSH1 and GLR1) in response to oxidative stress; activated by H <sub>2</sub> O <sub>2</sub> through the multistep formation of disulphide bonds and transit from the cytoplasm to the nucleus.	Sensitive to multiple oxidative stresses, including H <sub>2</sub> O <sub>2</sub> and compounds that alter the redox status in the cell.
<i>sod1Δ</i>	YJR104c	Cytosolic copper-zinc superoxide dismutase, located in both the cytosol and the mitochondrial intermembrane space, catalyses the breakdown of the superoxide radical (O <sub>2</sub> <sup>-</sup> ) to oxygen and H <sub>2</sub> O <sub>2</sub> .	Hypersensitivity to redox-cycling drugs (e.g., menadione, paraquat).
<i>ccs1Δ</i>	YMR038c	Copper chaperone for superoxide dismutase Sod1p.	Sensitive to oxidants because of a deficiency in Sod1p activity. <sup>2</sup>
<i>sod2Δ</i>	YHR008c	Mitochondrial manganese superoxide dismutase, located in the mitochondrial matrix, catalyses the breakdown of the superoxide radical (O <sub>2</sub> <sup>-</sup> ) to oxygen and H <sub>2</sub> O <sub>2</sub> , protects cells against oxygen toxicity.	Sensitive to high concentrations of oxygen <sup>3</sup> , ethanol <sup>4</sup> , oxidants and particularly sensitive to paraquat. <sup>5</sup>
<i>cta1Δ</i>	YDR256c	Catalase A breaks down H <sub>2</sub> O <sub>2</sub> in the peroxisomal matrix formed by acyl-CoA oxidase (Pox1p) during fatty acid beta-oxidation.	Sensitive to H <sub>2</sub> O <sub>2</sub> in stationary phase. <sup>6</sup>
<i>ctl1Δ</i>	YGR088w	Cytosolic catalase T has a role in protection from oxidative damage by H <sub>2</sub> O <sub>2</sub> .	Sensitive to oxidants in stationary phase.
<i>gsh1Δ</i>	YJL101c	Gamma glutamylcysteine synthetase, catalyses the first step in glutathione (GSH) biosynthesis, expression induced by oxidants, Cd and Hg.	Exhibit instability of the mitochondrial genome and increased sensitivity to H <sub>2</sub> O <sub>2</sub> . <sup>7</sup>
<i>gtr1Δ</i>	YPL091w	Cytosolic and mitochondrial glutathione oxidoreductase, converts oxidized glutathione (GSSG) to reduced glutathione; mitochondrial but not cytosolic form has a role in resistance to hyperoxia.	Accumulate an excess of oxidized glutathione and are hypersensitive to oxidants. <sup>8</sup>
<i>cup2Δ</i>	YGL166w	Copper-binding transcription factor; activates the encoding of the metallothionein genes CUP1-1 and CUP1-2 in response to elevated copper concentrations.	Sensitive to copper stress. <sup>9</sup>

<sup>a</sup> Open Reading Frame; <sup>b,c</sup> Cellular role of gene product and sensitivity phenotype of single-gene deletion mutant as indicated in *Saccharomyces Genome Database* (SGD) ([www.yeastgenome.com](http://www.yeastgenome.com)) and/or in the literature.

**Growth curve of *S. cerevisiae* BY4741 wild-type and its single-gene deletion mutants.** The measurements were performed on 96-well microplate (Non-Tissue Culture Treated, Falcon) in YPD medium (150  $\mu$ l per well) at 30°C for 24 h without shaking. The turbidity ( $OD_{600nm}$ ) of the cell suspension was recorded by Multiskan Spectrum microplate spectrophotometer (Thermo Electron Corporation, Finland) at a 1-h interval for 12 h and at 24 hour of growth. Based on the optical density ( $OD_{600nm}$ ) of the culture the maximum specific growth rate ( $\mu_{max}$ ,  $h^{-1}$ ) was calculated from the slope of plot of  $\ln OD$  versus time in the exponential growth period ( $\mu = (\ln OD_2 - \ln OD_1)/(t_2 - t_1)$ ), where  $OD_2$  and  $OD_1$  was culture density at time  $t_2$  and  $t_1$ ). Doubling time of culture ( $t_d$ , h) was calculated as  $t_d = \ln 2/\mu$ .

**Viability assessment of yeast cells by the fluorescent stain Acridine orange.** Acridine Orange (AO) was purchased from Sigma Diagnostics, St. Louis, MO, US. Yeast cells incubated/cultivated in the deionised water or in YPD medium on the flat bottom 24-well microplates (Non-Tissue Cultured Treated, Falcon), 1 mL *per* well, at 30°C for 24 h were filtered onto Nuclepore Track-Etched polycarbonate 0.2  $\mu$ m pore size membrane filter (Whatman). Few drops of AO solution (1  $\mu$ g/mL in deionised water, DI) were pipetted on the yeast cells in the filter funnel; cells were stained for 2 min and then fixed using 30% formaldehyde. Then a vacuum was applied to remove AO and the filter was twice rinsed with filtered (0.2  $\mu$ m) DI water to eliminate background fluorescence. The membrane filter with AO-stained yeast cells was removed and placed, sample side up, on a standard microscope slide (*In vitro* diagnostics). A drop of immersion oil (Olympus, Japan) was placed on the filter and a cover slip was pressed onto the filter surface. AO fluorescence was observed using the Olympus CX41 fluorescence microscope fitted with a filter cassette (CX-DMB-2) containing an excitation filter BP475 (475 nm) and a barrier filter O515IF (515 nm). The microscope was fitted with an Olympus U-CMAD3 real time colour digital camera DP71 (Japan). The pictures were taken using CellB Software (Olympus Soft Imaging Solutions GmbH).

## RESULTS

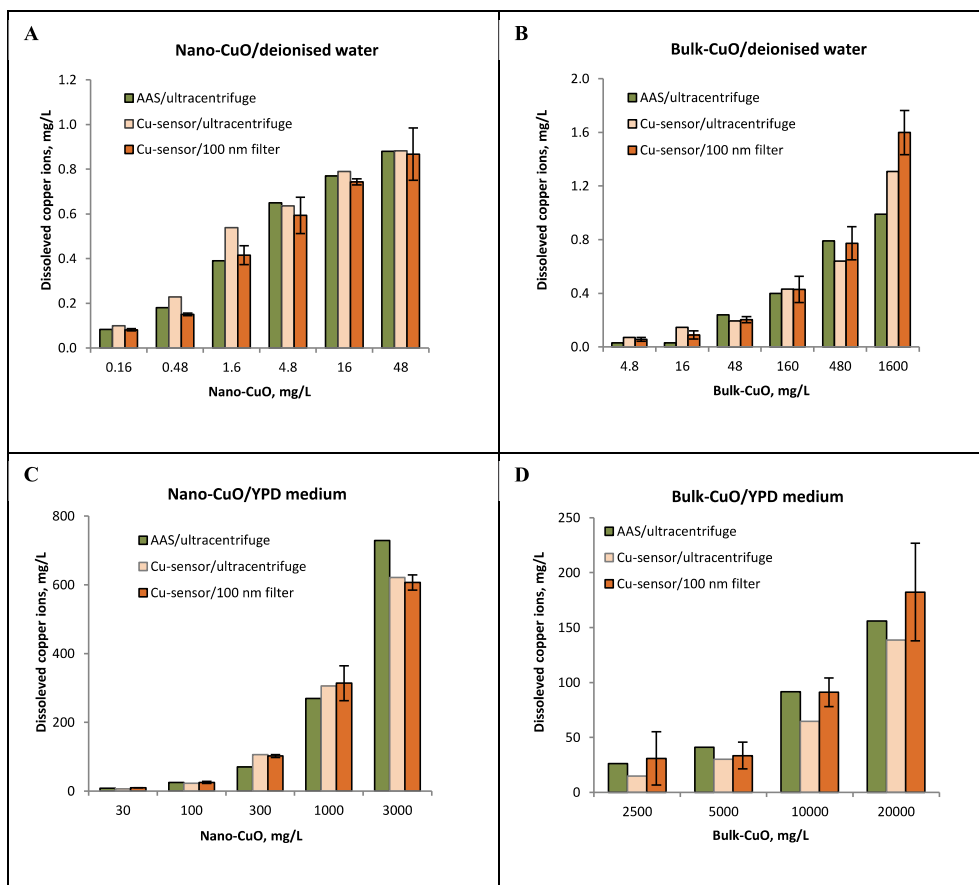


**Figure S1.** Dissolution of nano-CuO and bulk-CuO (A, B) in deionised water and (C, D) in YPD medium after 24-h incubation on 24-well microplates at 30°C; measured by the atomic absorption spectroscopy (AAS) or by Cu-biosensor *Escherichia coli* MC1061 (pSLcueR/pDNPcopAlux). Prior to analysis particulate fraction of the suspensions of nano-CuO and bulk-CuO was removed by ultracentrifugation ( $364\ 326 \times g$  for 30 min) or filtration (Minisart® 100 nm pore size filter, Sartorius). Data on 100-nm filtrates measured by the Cu-sensor are mean of 2 independent experiments  $\pm$  range of value.

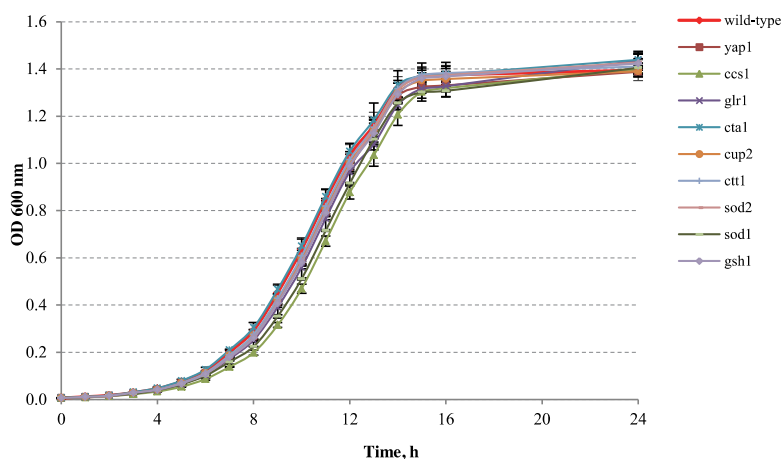


**Figure S2.** The growth curves of *Saccharomyces cerevisiae* BY4741 wild-type and its single-gene deletion mutants grown on 96-well microplates in YPD medium at 30°C for 24 hours without shaking. Optical density (OD<sub>600nm</sub>) of the culture was recorded by Multiskan Spectrum microplate spectrophotometer. Data are mean of 2 independent experiments  $\pm$  range of value.

**Table S2**

The growth characteristics of *Saccharomyces cerevisiae* BY4741 wild-type and its single-gene deletion mutants grown on 96-well microplates in YPD medium at 30°C for 24 hours without shaking, calculated from the respective growth curves (Figure S2).

Strain	Maximum specific growth rate ( $\mu_{\max}$ ) <sup>a</sup> , h <sup>-1</sup>	Doubling time ( $t_d$ ) <sup>b</sup> , h
Wild-type	0.47 $\pm$ 0.03	1.46
<i>yap1</i> $\Delta$	0.47 $\pm$ 0.02	1.47
<i>ccs1</i> $\Delta$	0.44 $\pm$ 0.01	1.56
<i>glr1</i> $\Delta$	0.47 $\pm$ 0.02	1.48
<i>cta1</i> $\Delta$	0.47 $\pm$ 0.02	1.48
<i>cup2</i> $\Delta$	0.48 $\pm$ 0.02	1.45
<i>ctt1</i> $\Delta$	0.48 $\pm$ 0.03	1.44
<i>sod2</i> $\Delta$	0.48 $\pm$ 0.02	1.45
<i>sod1</i> $\Delta$	0.44 $\pm$ 0.00	1.57
<i>gsh1</i> $\Delta$	0.47 $\pm$ 0.02	1.48

<sup>a</sup> Specific growth rate ( $\mu$ , h<sup>-1</sup>) was calculated from the slope of plot of ln OD versus time in the exponential growth phase (between 4–8 hours)

## References

- (1) Kahru, A., Liiders, M., Vanatalu, K., Vilu, R. (1982) Adenylate energy charge during batch culture of *Thermoactinomyces vulgaris*. *Arch. Microbiol.* *133*, 142–144.
- (2) Unlu, E. S., Koc, A. (2007) Effects of deleting mitochondrial antioxidant genes on life span. *Ann. N.Y. Acad. Sci.* *1100*, 505–509, DOI 10.1196/annals.1395.055
- (3) van Loon, A. P. G. M., Pesold-Hurt, B., Schatz, G. A. (1986) Yeast mutant lacking mitochondrial manganese-superoxide dismutase is hypersensitive to oxygen. *Proc. Natl. Acad. Sci. USA* *83*, 3820–3824.
- (4) Costa, V., Reis, E., Quintanilha, A., Moradasferreira, P. (1993) Acquisition of ethanol tolerance in *Saccharomyces cerevisiae*: the key role of the mitochondrial superoxide dismutase. *Arch. Biochem. Biophys.* *300*, 608–614.
- (5) Manfredini, V., Roehrs, R., Peralba, M. C. R., Henriques, J. A. P., Saffi, J., Ramos, A. L. L. P., Benfato, M.S. (2004) Glutathione peroxidase induction protects *Saccharomyces cerevisiae sod1Δsod2Δ* double mutants against oxidative damage. *Braz. J. Med. Biol. Res.* *37*, 159–165.
- (6) Jamieson, D. J. (1998) Oxidative stress responses of the yeast *Saccharomyces cerevisiae*. *Yeast* *14*, 1511–1527.
- (7) Lee, J. C., Straffon, M. J., Jang, T. Y., Higgins, V. J., Grant, C. M., Dawes, I.W. (2001) The essential and ancillary role of glutathione in *Saccharomyces cerevisiae* analysed using a grande *gsh1* disruptant strain. *FEMS Yeast Res.* *1*, 57–65.
- (8) Grant, C. M., Collinson, L. P., Roe, J-H., Dawes, I. W. (1996) Yeast glutathione reductase is required for protection against oxidative stress and is a target for yAP-1 transcriptional regulation. *Mol. Microbiol.* *21*, 171–179.
- (9) Jo, W. J., Loguinov, A., Chang, M., Wintz, H., Nislow, C., Arkin, A. P., Giaever, G., Vulpe, C. D. (2008) Identification of genes involved in the toxic response of *Saccharomyces cerevisiae* against iron and copper overload by parallel analysis of deletion mutants. *Toxicol. Sci.* *101*, 140–151.

## CURRICULUM VITAE

### 1. Personal data

Name Sandra Käosaar (maidenname Suppi)  
Birthday 15/08/1988 (29 y)

### 2. Contact information

Address National Institute of Chemical Physics and Biophysics,  
Akadeemia tee 23, Tallinn 12618  
Telephone +372 6398361  
E-mail sandrakaosaar@gmail.com

### 3. Education

2012-... Tallinn University of Technology, School of Engineering, PhD  
student in chemistry and materials technology  
2010-2012 University of Tartu, Faculty of Science and Technology,  
Master of Science in Natural Sciences (gene technology)  
2007-2010 University of Tartu, Faculty of Science and Technology,  
Bachelor of Science in Natural Sciences (gene technology)

### 4. Employment

2012-... National Institute of Chemical Physics and Biophysics,  
Laboratory of Environmental Toxicology, junior researcher  
and PhD student  
2010-2012 University of Tartu, MSc student

### 5. Additional training

2014 "Practical Course in Advanced Microscopy" (Zurich,  
Switzerland, ETH Zurich and University of Zurich)  
2013 "Implications of Nanomaterials: A hands on course on  
Synthesis, Characterisation, and Ecotoxicology" (Aveiro,  
Portugal, Department of Biology, University of Aveiro)  
2013 "Nanotoxicology - potential risks of engineered  
nanomaterials to human health and the environment" course  
(Stockholm, Sweden, Karolinska Institutet, Institute of  
Environmental Medicine)  
2012 "EUROTOX Advanced Toxicology Course" (Porto, Portugal)

## 6. Publications in peer-reviewed journals

1. Peep, Uudeküll; Jekaterina, Kozlova; Hugo, Mändar; Joosep, Link; Mariliis Sihtmäe; Sandra, Käosaar; Irina, Blinova; Kaja, Kasemets; Anne, Kahru; Raivo, Stern; Tanel, Tätte; Kaupo, Kukli; Aile, Tamm. (2017). Atomic layer deposition of titanium oxide films on As-synthesized magnetic Ni particles: Magnetic and safety properties. *Journal of Magnetism and Magnetic Materials*, 429, 299–304.10.1016/j.jmmm.2017.01.045.
2. Käosaar, S.; Kahru, A., Mantecca, P., Kasemets, K. (2016). Profiling of the toxicity mechanisms of coated and uncoated silver nanoparticles to yeast *Saccharomyces cerevisiae* BY4741 using a set of its 9 single-gene deletion mutants defective in oxidative stress response, cell wall or membrane integrity and endocytosis. *Toxicology in vitro*, 35, 149–162.10.1016/j.tiv.2016.05.018.
3. Suppi, S.; Kasemets, K.; Ivask, A.; Künnis-Beres, K.; Sihtmäe, M.; Kurvet, I.; Aruoja, V.; Kahru, A. (2015). A novel method for comparison of biocidal properties of nanomaterials to bacteria, yeasts and algae. *Journal of Hazardous Materials*, 286, 75–84.
4. Ivask, A.; Kurvet, I.; Kasemets, K.; Blinova, I.; Aruoja, V.; Suppi, S.; Vija, H.; Käkinen, A.; Titma, T.; Heinlaan, M.; Visnapuu, M.; Koller, D.; Kisand, V.; Kahru, A. (2014). Size-dependent Toxicity of Silver Nanoparticles to Bacteria, Yeast, Algae, Crustaceans and Mammalian Cells in Vitro. *PLoS ONE*, 9 (7), e102108.
5. Suppi, S.; Michelson, T; Viigand, K; Alamäe, T. (2013). Repression vs. activation of MOX, FMD, MPP1 and MAL1 promoters by sugars in *Hansenula polymorpha*: the outcome depends on cell's ability to phosphorylate sugar. *FEMS Yeast Research*, 13 (2), 219–232.10.1111/1567-1364.12023.
6. Kasemets, K., Suppi, S., Künnis-Beres, K., Kahru, A. (2013). Toxicity of CuO Nanoparticles to Yeast *Saccharomyces cerevisiae* BY4741 Wild-Type and Its Nine Isogenic Single-Gene Deletion Mutants. *Chemical Research in Toxicology*, 26 (3), 356–367.

## ELULOOKIRJELDUS

1. Isikuandmed
  - Nimi Sandra Käosaar (neiupõlvenimi Suppi)
  - Sünniaeg 15/08/1988 (29 y)
  
2. Kontaktandmed
  - Adress Keemilise ja Bioloogilise Füüsika Instituut, Akadeemia tee 23, Tallinn 12618
  - Telefon +372 6398361
  - E-post sandrakaosaar@gmail.com
  
3. Hariduskäik
  - 2012-... Tallinna Tehnikaülikool, Inseneriteaduskond, keemia- ja materialitehnoloogia doktorant
  - 2010-2012 Tartu Ülikool, Loodus- ja tehnoloogiateaduskond, loodusteaduste magister geenitehnoloogia erialal
  - 2007-2010 Tartu Ülikool, Loodus- ja tehnoloogiateaduskond, loodusteaduste bakalaureus geenitehnoloogia erialal
  
4. Teenistuskäik
  - 2012-... Keemilise ja Bioloogilise Füüsika Instituut, Keskkonnatoksikoloogia laboratoorium, nooremteadur ja doktorant
  - 2010-2012 Tartu Ülikool, magistrant
  
5. Täiendkoolitused
  - 2014 mikroskoopia kursus edasijõudnutele "Practical Course in Advanced Microscopy" (Zürich, Šveits, ETH Zürich ja Zürichi ülikool)
  - 2013 kursus nanoosakeste sünteesi, iseloomustamise ja ökotoksilisuse kohta "Implications of Nanomaterials: A hands on course on Synthesis, Characterisation, and Ecotoxicology" (Aveiro, Portugal, Bioloogia teaduskond, Aveiro ülikool)
  - 2013 nanotoksikoloogia kursus "Nanotoxicology - potential risks of engineered nanomaterials to human health and the environment" course (Stockholm, Rootsi, Karolinska Institutet, Keskkonnameditsiini instituut)
  - 2012 toksikoloogia edasijõudnute kursus "EUROTOX Advanced Toxicology Course" (Porto, Portugal)

6. Publikatsioonid eelretsenseeritud ajakirjades

1. Peep, Uudeküll; Jekaterina, Kozlova; Hugo, Mändar; Joosep, Link; Mariliis Sihtmäe; Sandra, Käosaar; Irina, Blinova; Kaja, Kasemets; Anne, Kahru; Raivo, Stern; Tanel, Tätte; Kaupo, Kukli; Aile, Tamm. (2017). Atomic layer deposition of titanium oxide films on As-synthesized magnetic Ni particles: Magnetic and safety properties. *Journal of Magnetism and Magnetic Materials*, 429, 299–304.10.1016/j.jmmm.2017.01.045.
2. Käosaar, S.; Kahru, A., Mantecca, P., Kasemets, K. (2016). Profiling of the toxicity mechanisms of coated and uncoated silver nanoparticles to yeast *Saccharomyces cerevisiae* BY4741 using a set of its 9 single-gene deletion mutants defective in oxidative stress response, cell wall or membrane integrity and endocytosis. *Toxicology in vitro*, 35, 149–162.10.1016/j.tiv.2016.05.018.
3. Suppi, S.; Kasemets, K.; Ivask, A.; Künnis-Beres, K.; Sihtmäe, M.; Kurvet, I.; Aruoja, V.; Kahru, A. (2015). A novel method for comparison of biocidal properties of nanomaterials to bacteria, yeasts and algae. *Journal of Hazardous Materials*, 286, 75–84.
4. Ivask, A.; Kurvet, I.; Kasemets, K.; Blinova, I.; Aruoja, V.; Suppi, S.; Vija, H.; Käkinen, A.; Titma, T.; Heinlaan, M.; Visnapuu, M.; Koller, D.; Kisand, V.; Kahru, A. (2014). Size-dependent Toxicity of Silver Nanoparticles to Bacteria, Yeast, Algae, Crustaceans and Mammalian Cells in Vitro. *PLoS ONE*, 9 (7), e102108.
5. Suppi, S.; Michelson, T; Viigand, K; Alamäe, T. (2013). Repression vs. activation of MOX, FMD, MPP1 and MAL1 promoters by sugars in *Hansenula polymorpha*: the outcome depends on cell's ability to phosphorylate sugar. *FEMS Yeast Research*, 13 (2), 219–232.10.1111/1567-1364.12023.
6. Kasemets, K., Suppi, S., Künnis-Beres, K., Kahru, A. (2013). Toxicity of CuO Nanoparticles to Yeast *Saccharomyces cerevisiae* BY4741 Wild-Type and Its Nine Isogenic Single-Gene Deletion Mutants. *Chemical Research in Toxicology*, 26 (3), 356–367.

